HHS Public Access

Author manuscript

Chem Rev. Author manuscript; available in PMC 2018 August 09.

Published in final edited form as:

Chem Rev. 2017 August 09; 117(15): 10043–10120. doi:10.1021/acs.chemrev.7b00042.

Mitochondria-Targeted Triphenylphosphonium-Based Compounds: Syntheses, Mechanisms of Action, and Therapeutic and Diagnostic Applications

Jacek Zielonka[1,2,3,*], **Adam Sikora**[4], **Micael Hardy**[5], **Olivier Ouari**[5], **Jeannette Vasquez-Vivar**[1,2], **Gang Cheng**[1,2], **Marcos Lopez**[6,7], and **Balaraman Kalyanaraman**[1,2,3,*]

[1]Department of Biophysics, Medical College of Wisconsin, 8701 Watertown Plank Road, Milwaukee, WI 53226, United States [2]Free Radical Research Center, Medical College of Wisconsin, 8701 Watertown Plank Road, Milwaukee, WI 53226, United States [3]Cancer Center, Medical College of Wisconsin, 8701 Watertown Plank Road, Milwaukee, WI 53226, United States [4]Institute of Applied Radiation Chemistry, Lodz University of Technology, ul. Wroblewskiego 15, 93-590 Lodz, Poland [5]Aix Marseille Univ, CNRS, ICR, UMR 7273, 13013 Marseille, France [6]Translational Biomedical Research Group, Biotechnology Laboratories, Cardiovascular Foundation of Colombia, Carrera 5a No. 6-33, Floridablanca, Santander, Colombia, 681003 [7]Graduate Program of Biomedical Sciences, Faculty of Health, Universidad del Valle, Calle 4B No. 36-00, Cali, Colombia, 760032

Abstract

Mitochondria are recognized as one of the most important targets for new drug design in cancer, cardiovascular, and neurological diseases. Currently, the most effective way to deliver drugs specifically to mitochondria is by covalent linking a lipophilic cation such as an alkyltriphenylphosphonium moiety to a pharmacophore of interest. Other delocalized lipophilic cations, such as rhodamine, natural and synthetic mitochondria-targeting peptides, and nanoparticle vehicles, have also been used for mitochondrial delivery of small molecules. Depending on the approach used, and the potentials of cell and mitochondrial membranes, more than 1000-fold higher mitochondrial concentration can be achieved. Mitochondrial targeting has been developed to study mitochondrial physiology and dysfunction and the interaction between mitochondria and other subcellular organelles and for treatment of a variety of diseases such as neurodegeneration and cancer. In this review, we discuss efforts to target small-molecule compounds to mitochondria for probing mitochondria function, as diagnostic tools and potential therapeutics. We describe the physicochemical basis for mitochondrial accumulation of lipophilic cations, synthetic chemistry strategies to target compounds to mitochondria, mitochondrial probes and sensors, and examples of mitochondrial targeting of bioactive compounds. Finally, we review

*To whom correspondence should be addressed: B. Kalyanaraman or J. Zielonka, Department of Biophysics, Medical College of Wisconsin, 8701 Watertown Plank Road, Milwaukee, WI 53226, United States; balarama@mcw.edu (B.K.), jzielonk@mcw.edu (J.Z.); Tel: (414) 955-4000 (B.K.), (414) 955-4789 (J.Z.); Fax: (414) 955-6512.

Notes

The authors declare no competing financial interests.

published attempts to apply mitochondria-targeted agents for the treatment of cancer and neurodegenerative diseases.

Graphical Abstract

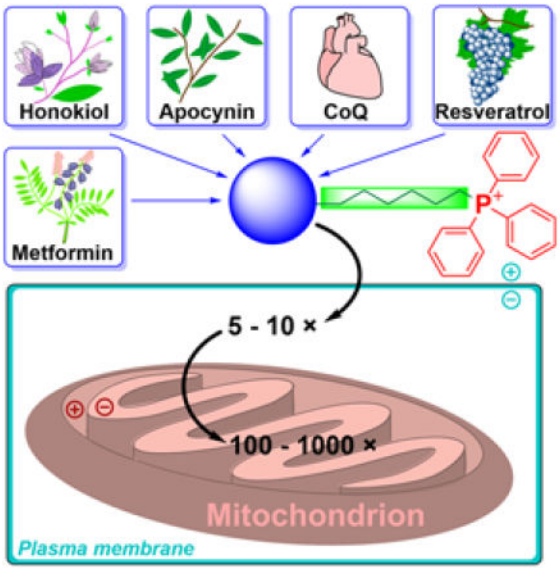

1. INTRODUCTION

Mitochondria, which are generally considered the cellular powerhouse, are small subcellular organelles that generate most cellular energy in the form of adenosine triphosphate (ATP).[1,2] Over the last two decades, research focusing on mitochondria-dependent cellular signaling and cell death has flourished.[3–5] Mitochondrial defects or dysfunctions are associated with the onset of several neurological and cardiovascular diseases.[6–11] Development of therapeutic drugs capable of restoring mitochondrial function is highly significant and critically needed.[1,12,13] Also, specific mitochondrial targeting leads to more-precise and effective drugs. Current thinking is partly based on the premise that mitigation of reactive oxygen species (ROS) by mitochondria-targeted antioxidants or agents (MTAs) inhibit cellular death, and prevent aging and development of chronic diseases.[14,15] Another school of thought is based on the ability of MTAs to alter bioenergetics and energy-sensing mechanisms in cancer and possibly other cells.[16–18] Emerging research in cancer therapy is focused on exploiting the selective targeting and accumulation of mitochondria-targeted cations (MTCs) and their ability to alter ROS-mediated redox signaling and antiproliferative pathways in cancer cells.[17,19,20] Although the exact mechanisms with which MTAs or MTCs affect mitochondrial function are not yet understood, recent publications reveal new and interesting redox-signaling mechanisms induced by this class of compounds in neuronal and cancer cells.[18,21] New interpretations of mechanisms, albeit counterintuitive, will likely infuse new understanding and help advance the field of mitochondrial medicine. The purpose of this review is to provide a critical overview of targeting approaches, plausible molecular mechanisms of action, biological effects, and therapeutic applications of

triphenylphosphonium (TPP^+)-based mitochondria-targeted compounds. Selected examples of mitochondria-targeted compounds, based on approaches other than the TPP^+-targeting moiety are also discussed.

First, we provide an overview of the strategies and physicochemical foundations for targeting and transporting the compounds to mitochondria, as well as examples of mitochondria-selective indicators and mitochondrial membrane potential probes. Next, we discuss the most common synthetic approaches for mitochondrial delivery of chemicals, strategies to develop modulators and sensors of mitochondrial oxidants and redox status as well as development and applications of mitochondria-targeted bioactive molecules, and applications of mitochondria-targeted compounds for the development of new therapeutics in the fields of cancer and neurodegenerative diseases. This includes discussion of possible mechanisms of action of the potential anticancer and neuroprotective drugs, and examples of their successful use in the in vivo models, whether alone or in combination with other drugs or treatments. Finally, we review the application of mitochondria-targeted probes for in vivo imaging of myocardial function and tumors.

We hope this review captures and facilitates the "unmet" need for preclinical and clinical development of mitochondria-targeted compounds in treating various diseases.

2. APPROACHES TO TARGET COMPOUNDS TO MITOCHONDRIA

Over the last decade, the covalent modification of compounds to mitochondria-targeting "vehicles" has gained much traction, due to straightforward chemical synthesis and the high targeting efficiency.[22–39] Because of the negative membrane potential of the mitochondrial inner membrane, positively charged compounds accumulate in the mitochondrial matrix against their concentration gradient. Various lipophilic cations, including alkyltriphenylphosphonium cations, rhodamine, cyanine cations, and cationic peptides, can be attached to the bioactive compound of interest to improve its mitochondrial uptake. Lipophilic cations, which accumulate inside mitochondria according to the Nernst equation, originally were used to investigate the principles of the coupling between mitochondrial electron transport and ATP production, and as a tool to monitor mitochondrial membrane potential.

2.1. Linking to TPP^+

Triphenylphosphonium-based modification of molecules facilitating mitochondria targeting is not a totally new concept as abundant literature already exists with regard to the potent biological effects exhibited by small molecules containing TPP^+.[28,32,33,40–44] Alkylated triphenylphosphonium cations initially were used as probes to study the mechanism of coupling of the mitochondrial membrane potential with oxidative phosphorylation (OXPHOS) and subsequently were used to determine mitochondrial membrane potential.[45–57] The use of TPP^+-conjugated bioactive molecules in mitochondrial biology was reinvented and refined by Murphy and coworkers.[22,58–61] TPP^+ cations were utilized to deliver the probes, antioxidants, and pharmacophores to mitochondria. Murphy's and several other laboratories synthesized novel mitochondria-targeted cationic compounds that were fine-tuned to sequester into the mitochondrial matrix and membranes.[21,62–64] Figure 1

shows the anatomy of a typical molecule with a different functional group conjugated to the TPP^+ cation.

As indicated, the "business end" of the molecule (shown in blue) is a parent "untargeted" molecule containing a nitroxide group (-N-O•) that exhibits a superoxide dismutase (SOD) mimetic activity and a paramagnetic relaxation mechanism, a phenolic hydroxyl group (-OH) with a chain-breaking radical scavenging ability, a radiolabeled technetium group for use in metabolic imaging, or a hydroethidine (HE) moiety that can form a specific marker product upon reaction with superoxide radical anion ($O_2^{\bullet-}$). The "business end" is tethered to a lipophilic, delocalized cation (shown in red) through an alkyl chain or other linker (shown in green). Depending on the length of the linker alkyl chain (typically n = 2–10), the lipophilicity, cellular uptake, and site of mitochondrial sequestration (matrix versus membrane) may be modulated. Representative examples are Mito-CP and Mito-TEMPOL (carboxyPROXYL or TEMPOL nitroxides tethered to TPP^+), Mito-Vit-E or Mito-chromanol (α-tocopherol or vitamin-E analog, based on a chromanol ring conjugated with TPP^+), Mito-^{99m}Tc-MAG3 (^{99m}Tc radionuclide-MAG3 complex linked to TPP^+), Mito-HE (also known as MitoSOX Red, an HE probe linked to TPP^+), MitoQ (ubiquinone attached to TPP^+), Mito-Met (metformin conjugated with TPP^+), Mito-Apo (apocynin linked to TPP^+), Mito-DIPPMPO (DIPPMPO spin trap conjugated with TPP^+) and others (Figure 2).

The advantages of TPP^+-based mitochondrial targeting over other approaches for mitochondrial delivery of small molecules include the stability of the TPP^+ moiety in biological systems, a combination of lipophilic and hydrophilic property, the relatively simple synthesis and purification, the low chemical reactivity toward cellular components, and their lack of light absorption or fluorescence in the visible or near infrared (NIR) spectral region. Most importantly, MitoQ (Figure 2) was shown to be relatively safe in humans, thereby enhancing the potential clinical and translational significance of this class of molecules.

The idea of using the TPP^+ moiety to target various pharmacophores, probes, and imaging agents to mitochondria led to numerous patent applications. By searching the term "triphenylphosphonium AND mitochondria AND targeting" in the Google Patents database, we identified 246 patent applications. Of those, more than 100 applications have already been granted. Examples of granted US patents for selected mitochondria-targeted compounds shown in Figure 2 are included in Table 1.

2.2. Linking to Heterocyclic Aromatic Cations

Many small molecule lipophilic cations (e.g., rhodamine, pyridinium, and cyanine derivatives) have been shown to accumulate in cell mitochondria.[65–71] Rhodamine- and cyanine-based cationic fluorophores have been extensively used as research tools as mitochondrial stains and for monitoring mitochondrial membrane potential, as discussed below, based on the extent of their total cellular uptake or the ratio of mitochondrial to cytosolic concentration of the cationic probe.[72–81] Small molecule heterocyclic cations were also used as vehicles to deliver other compounds to mitochondria.[82–92] The heterocyclic cations have been conjugated with quinone, spin traps, or thiol-reactive moieties to specifically localize those compounds in cell mitochondria. It was demonstrated that the

uptake of rhodamine-linked compounds can be further increased by the addition of the lipophilic tetraphenylborate anion.[93] Some examples of heterocyclic compounds used as mitochondria-targeting vehicles include berberin, rhodamine, benzoindolinium, pyridinium, and guanidinium cations (Chart 1).[63,94–111]

2.3. Mitochondria-Targeted Peptides

Mitochondria-targeted peptides were proposed as the alternative to delocalized lipophilic cations for delivering bioactive compounds to mitochondria. Among these are peptides based on natural amino acid sequences targeting mitochondria and synthetic peptides, typically carrying hydrophobic (phenylalanine, tyrosine, isoleucine) and positively charged (arginine, lysine) amino acids.[112–116] Grafting the molecules of interest is possible through a peptide bond formation, making them easily tunable for diverse a range of cargo to target mitochondria for various applications. Examples of such peptides include a series of compounds known as Szeto-Schiller (SS) peptides, which are designed to deliver dimethyltyrosine (Dmt) as an antioxidant motif to mitochondria.[117–123] However, DMT, as a phenolic compound is not expected to exhibit significant direct scavenging ability toward the superoxide radical anion or hydroperoxides. Thus, other mechanisms of the protective activity of SS peptides may be in play, including their interaction with opioid receptors.[124–127] To fully understand the antioxidant mechanisms of Dmt-containing peptides, it will be important to compare the effects of SS peptides with analogous compounds containing dimethylphenylalanine in place of Dmt.[128]

To protect the peptides from enzymatic cleavage, the D-isomer of arginine was incorporated. The structural requirements (the amino acid sequence, hydrophobicity, and a charge of the peptide) for efficient mitochondria-penetrating peptides (MPP, Chart 2) were subsequently studied.[113,115,129] The exact mechanism of the transfer of MPP into mitochondria, however, is yet to be determined. The ability of the MPP to deliver specific cargo into the mitochondria was confirmed experimentally.[116,129,130] Another class of mitochondria-targeted peptides is based on the partial sequence of the gramicidin S antibiotic (Chart 2).[131,132] Also, short peptides composed of two functional domains, a homing domain for cellular uptake and a proapoptotic domain targeting mitochondrial membranes, were reported and proposed for anticancer therapy.[133–138]

Another strategy to target molecules of interest to mitochondria is the use of the cellular mechanisms of mitochondrial protein delivery using the mitochondria-targeting sequences (MTS), typically composed of 20–30 amino acids reaching mitochondria through the translocase of the outer membrane and translocase of the inner membrane (TOM/TIM) complexes.[33,139,140]

2.4. Mitochondria-Targeted Vesicles

With a few exceptions, the above-mentioned targeting approaches included 1:1 stoichiometry of the cargo to vehicle molecules, with a covalent bond linking the molecule of interest to the carrier. Another approach is based on the use of vesicular drug carriers, in which the cargo molecules are embedded in or conjugated with a small particle targeting mitochondria. Mitochondrial targeting is typically accomplished by “decorating” the

particles with the TPP^+ moiety(ies). Mitochondriotropic liposomes were proposed as efficient carriers of both small molecules and macromolecules to mitochondria. Again, the mitochondrial specificity is obtained by the presence of the delocalized positive charge in the liposomes, with the early example of dequalinium-based liposomes capable of delivering molecules of very different sizes such as DNA and paclitaxel.[141–144] More recently, TPP^+-modified liposomes were used for mitochondrial delivery of the bioactive compounds.[142–148] The major advantage of using liposome-based drug delivery is the possibility of delivering a whole range of chemical moieties with different hydrophobicities and different sizes, from simple molecules to whole proteins. The mitochondrial accumulation of TPP^+-modified liposomes was verified using liposomes, where phospholipids were covalently linked to a fluorescent label. The colocalization of the fluorescence of the label with that of MitoTracker confirmed the mitochondrial localization of the TPP^+-linked liposomes.[143]

To target the intra-mitochondrial compartment, the MITO-Porter concept was introduced, using a nanocarrier liposome-based mitochondrial delivery operating system via membrane fusion.[139,149,150] The structure of this system is composed of a drug-loaded core particle coated with envelope membranes (inner and outer membranes, Figure 3A). The cytosolic and mitochondrial targeting moiety, an octaarginine (R8) peptide, is present on both membranes for internalization into the cell and for mitochondrial uptake.

Another approach is the use of biodegradable polymer nanoparticles, based on the TPP^+-conjugated polymer, PLGA-b-PEG-TPP^+ (Figure 3B), and the mitochondrial accumulation in intact cells has been confirmed by colocalization of the fluorescence of the fluorophore-labeled nanoparticles with that of MitoTracker.[151] Jung et al. prepared mitochondria-targeted coumarin-iron oxide (Mito-CIO, Figure 4A), a coumarin-based fluorescent iron oxide nanoparticle containing TPP^+, which induces cell hyperthermia upon NIR.[152] Again, the mitochondrial uptake in intact cells has been verified by monitoring the colocalization of the fluorescence of the Mito-CIO particles with that of MitoTracker dye. Superparamagnetic iron oxide nanoparticle (SPION) derivatives were used for their capacity to interfere with electron transport chain (ETC) of mitochondria in cancer cells.[153–155]

Polymeric dendrimers conjugated to TPP^+ have also been used to improve drug delivery into mitochondria.[156–158] The main advantage of these structures is their ability to functionalize the peripheral groups by various moieties, making them versatile nanocarriers. Bielski et al. developed TPP^+-conjugated to polyamidoamine (PAMAM) dendrimers, G4-NH_2 for nanocarrier purposes (Figure 4B).[156] It was shown that 10 TPP^+ groups conjugated to the dendrimer *via* a PEG linker yield a good mitochondrial accumulation, as verified by fluorescence colocalization with MitoTracker dye, and low toxicity.

3. TRANSPORT OF SMALL CATIONIC COMPOUNDS AND BIOMOLECULES TO MITOCHONDRIA: BIOPHYSICAL RATIONALE

3.1. Accumulation of Lipophilic Cations in the Mitochondria of Intact Cells

The selective uptake of lipophilic cations by mitochondria in cells is based on the mitochondrial-membrane-potential-driven accumulation of the positively charged ion. The extent of accumulation of any charged species across the membrane occurs against the concentration gradient and is driven by the membrane potential, $\Delta\Psi$. At equilibrium, the concentrations of the ion on both sides of the charged membrane can be described by the Nernst equation:

$$\Delta\Psi = \frac{RT}{nF} \ln \frac{c_{in}}{c_{out}}$$

Where R is the universal gas constant, T is temperature (K), n is the valence of the charged species, F is the Faraday's constant, and c_{out} and c_{in} are the concentrations of the species on both sides (outer and inner) of the charged membrane with the potential $\Delta\Psi$. For a single-charged cationic species accumulating in a space surrounded by a membrane with a potential $\Delta\Psi$, that is negative inside and at the temperature of 37 °C, the Nernst equation can be simplified as follows:

$$\Delta\Psi\,(\mathrm{mV}) = 61.5 \times \log_{10} \frac{c_{in}}{c_{out}}$$

To reach the mitochondria of intact cells, the compound must cross both the plasma and mitochondrial membranes. Fortunately, in both cases, the membrane potential is negative inside, allowing stepwise accumulation of the cationic compounds initially in the cell cytosol and then inside the mitochondria. As shown in Figure 5, the plasma membrane potential, typically 30–40 mV, leads to a three–five-fold increase in the cytosolic concentration of cations when compared with the extracellular medium. Mitochondrial membrane potential in the range of 120–180 mV further increases the concentration of the cation in the mitochondrial matrix by a factor of 100 to 1000.

Thus, when compared with the extracellular medium, cationic compounds can be 100-to 1000-fold concentrated in the mitochondrial matrix. For example, an alkyltriphenylphosphonium cation added extracellularly at the concentration of 1 μM could reach an intramitochondrial concentration in the range of 0.1–2 mM.

The passage of a lipophilic cation through the mitochondrial inner membrane is a multistep process: First, it binds to the intermembrane space (IMS) side of the membrane. Then, remaining within the phospholipid membrane, it transfers to the matrix side of the membrane. Finally, it dissociates from the matrix side of the membrane. The passage of an MTC through a membrane is shown schematically in Figure 6, consisting of the cargo (blue), linker (green), and lipophilic cation moiety (red).[55,160,161]

As shown in Figure 6, upon binding to the mitochondrial membrane, the cationic targeting moiety is localized on the membrane surface, due to an electrostatic interaction with the negatively charged phosphates. The position of the linker and location of the cargo will depend on their physicochemical properties. Hydrophobic linkers and cargo will locate toward the center of the membrane, whereas hydrophilic cargo may position toward the aqueous cytosolic phase. With a positively charged hydrophilic cargo or linker, it is possible that the molecule will "lie" on the surface of the membrane. The energy barrier for the transfer of the lipophilic cations via the phospholipid bilayer typically is related to the transfer of the membrane-bound compound from one to the other side of the membrane (Step 2 in Figure 6). [55,161] Lipophilic cations can more easily permeate the mitochondrial membrane than the plasma membrane. Thus, once internalized into the cell, lipophilic compounds will rapidly accumulate in the mitochondria.

3.2. Structure of the Mitochondrial Membrane

Mitochondria are the only cellular organelles possessing both outer and inner membranes, each composed of the phospholipid bilayer. These two membranes define separate aqueous spaces inside the mitochondria: the IMS and the mitochondrial matrix. Both membranes differ significantly in their permeability to small molecules and macromolecules. The outer membrane contains large pores, enabling diffusion of molecules with molecular weights below ~5–10 kDa. Thus, unrestricted equilibration of small molecules, but not large proteins (> 10 kDa), is allowed between the cytosol and the IMS. Transport via the inner membrane is restricted, even for small particles (e.g., protons), enabling formation of the proton gradient during the electron transfer from the substrates to oxygen.

3.3. Effect of Charge and Hydrophobicity of the Compound

Although the force driving the accumulation of lipophilic cations in mitochondria is the charge of the molecule and mitochondrial membrane potential, the dynamics of the equilibration process are significantly dependent on the lipophilicity of the cation. The energy barrier for some hydrophilic compounds may be so high that even conjugation to the TPP^+ moiety is not sufficient to drive them to mitochondria, as was demonstrated for selected cell-penetrating peptides.[162] On the other hand, increasing the hydrophobicity by elongating the alkyl chain was demonstrated to lead to faster mitochondrial uptake of simple alkylated TPP^+. For example, TPP^+-C_1 reaches a steady-state level in Jurkat T-lymphocytes in six–eight h, whereas TPP^+-C_{10} or $MitoQ_{10}$ (Chart 3) reach a steady-state level in 10 and 30 minutes, respectively.[163]

Improved uptake kinetics is accompanied by an increased lipophilic cation efflux rate, supporting the assumption of a lower energy barrier for the transfer of more lipophilic compounds via the phospholipid bilayer. Higher cation lipophilicity/hydrophobicity is also accompanied by increased membrane-potential-independent uptake and increased partition into the membrane phase, rather than crossing the barrier and accumulating in the mitochondrial matrix.[55,160,163] In fact, the electron paramagnetic resonance (EPR) spectrum of Mito-CP accumulated in the mitochondrial fraction indicates significant immobilization of the nitroxide moiety, and the membrane-potential dependence of $MitoQ_{10}$ accumulation in isolated mitochondria suggests that >90% of the compound is bound to the mitochondrial

membrane.[163,164] Even for the simplest alkyl-TPP^+, TPP^+-C_1, it was shown that, though its accumulation is fully dependent on the membrane potential, ~50% of the compound is bound to the mitochondrial membrane.[55,56,163] However, the cellular uptake and retention of TPP^+-linked compounds is mostly dependent on mitochondrial membrane potential, as it was shown that release of membrane potential by the addition of a mitochondrial uncoupler, FCCP (carbonyl cyanide 4-(trifluoromethoxy)phenylhydrazone), leads to a significantly lower (an ~80% decrease) steady-state level of $MitoQ_{10}$, TPP^+-C_1, or TPP^+-C_{10} in intact cells.[163] Conversely, the FCCP-induced release of $MitoQ_{10}$ and $MitoQ_{15}$ from isolated mitochondria was significantly less efficient when compared to shorter-chain analogs ($MitoQ_3$ and $MitoQ_5$, Chart 3). Clearly, the total amount of the TPP^+-linked compound inside the mitochondrial matrix is a sum of the pools of unbound and of membrane-adsorbed compound on the matrix side of the inner mitochondrial membrane. The higher octanol/water partition coefficient of the lipophilic cation, the greater the accumulation of the compound on the matrix side of mitochondria. As the ratio of the membrane-bound and unbound pools of the compound is defined by the partition constant, the total accumulation at equilibrium is still controlled by the membrane potential, as predicted by the Nernst equation, with correction due to membrane/cytosol or matrix partitioning.

Based on the Nernst equation, double-charged lipophilic cations would be expected to exhibit significantly improved mitochondrial accumulation. Experiments on isolated mitochondria indicate Nernstian accumulation of lipophilic dications.[165] However, this occurs only at relatively low mitochondrial membrane potentials (<100 mV). At higher potentials, the extent of accumulation increases only modestly and can no longer be described by the Nernst equation. Furthermore, the accumulation of lipophilic dications is lower than that of TPP^+-C_1, probably due to a higher energy barrier for the transport of dicationic species through the plasma membrane.[165] This suggests that conjugation to a single lipophilic cation using a long-chain hydrophobic linker is an efficient strategy for mitochondrial delivery. Note that, even for cations exhibiting relatively slow uptake due to a large energy barrier for transport through the lipid bilayer, the rate of uptake can be increased when paired with the lipophilic tetraphenylborate anion (TBB^-, Chart 4). TBB^- was reported to facilitate the transfer of cations through lipid membranes by absorption to the membranes and lowering the energy barrier for the transport, and by forming ion pairs with the lipophilic cations.[166,167] For example, the rate of mitochondrial uptake of the neurotoxin 1-methyl-4-phenylpyridinium cation was shown to increase 20-fold in the presence of TBB^-.[67,69]

3.4. Effect of the Protonation Equilibria of Weak Acids and Bases on Their Mitochondrial Accumulation

Many probes and drugs targeted to mitochondria are weak acids or bases that may undergo differential protonation in the cytosolic and mitochondrial compartments due to differences in their pH. This will affect the extent of their accumulation, as demonstrated for the model compounds, TPP^+-linked aliphatic carboxylic acid and TPP^+-linked aliphatic amine.[168] In such cases, uptake of the compound into mitochondria is controlled not only by the mitochondrial membrane potential but also by the cytosolic and mitochondrial pH values (Figure 7A). In the case of TPP-linked carboxylic acid, upon deprotonation the zwitterionic

product should exhibit low permeability via the membrane due to the lack of a net charge and the high energy barrier for transport through the lipid bilayer, as discussed above for multicharged compounds. Therefore, the protonated form should be that which equilibrates between both sides of the membrane and for which dependence of the extent of accumulation (accumulation ratio [ACR]) on the membrane potential ($\Delta\Psi$) and the pH values on both sides of the membrane can be expressed as follows:

$$ACR = \frac{[MTC]_{mito}}{[MTC]_{cyto}} = 10^{\frac{F \cdot \Delta\Psi}{2.3 \cdot RT}} \times \frac{1+10^{pH_{mito}-pK_a}}{1+10^{pH_{cyto}-pK_a}}$$

Where $[MTC]_{mito}$ and $[MTC]_{cyto}$ describe the total concentration of the MTC in mitochondrial and cytosolic compartments, respectively, and pK_a relates to the acidity constant of the compound.

For weak bases, such as aliphatic amines, protonation will increase the energy barrier for the transfer through the lipid bilayer, so the species responsible for equilibration between the cytosolic and mitochondrial compartment may be expected to be a deprotonated base. In this case, the extent of accumulation of the compound in the mitochondrial matrix can be expressed using the following equation:

$$ACR = \frac{[MTC]_{mito}}{[MTC]_{cyto}} = 10^{\frac{F \cdot \Delta\Psi}{2.3 \cdot RT}} \times \frac{1+10^{pK_a-pH_{mito}}}{1+10^{pK_a-pH_{cyto}}}$$

The effect of the pK_a of weak acids and bases on the extent of their mitochondrial accumulation for typical conditions (T = 37°C, $\Delta\Psi$ = 180 mV, pH_{mito} = 8.0; pH_{cyto} = 7.2) is shown in Figure 7B. For comparison, the ACR value for TPP^+-alkyl cations not bearing additional ionizable groups is indicated by a dotted line. Deprotonation of acids clearly provides an additional driving force for their accumulation in mitochondria, whereas protonation of amines has an inverse effect.

3.5. Mitochondria-Labeling Compounds and Membrane Potential Indicators

Because mitochondria are characterized by the most negative membrane potential, most probes used to label mitochondria are lipophilic cations, which also were used to monitor the changes in mitochondrial membrane potential.[51,73,169–172] Membrane permeable anions also were used to monitor membrane potential, although these are typically used in isolated organelles and membranes rather than in intact cells.[169,170] Cationic indicators of mitochondrial membrane potential accumulate in mitochondria following equilibration across a membrane in a Nernstian fashion (i.e., in response to membrane potential) and, in most cases, can translocate back into cytosol and extracellular medium once the membrane potential is dissipated. Distribution of the radioactive inorganic membrane-permeable cation ^{86}Rb between mitochondrial matrix and extramitochondrial space (reaction medium) was used for the absolute determination of mitochondrial membrane potential in isolated mitochondria.[171,173] Also, TPP^+-C_1 (known as triphenylmethylphosphonium cation [TPMP], Chart 3) and TPP^+-Ph (tetraphenylphosphonium cation [TPP]) were used

extensively to monitor the mitochondrial membrane potential, either with a TPP^+-selective electrode or using a radioactive derivative [^{3}H]TPP^+-C_1 or [^{3}H]TPP^+-Ph.[52–55,57,67,72,171] These compounds are still used as a reference when studying the binding mechanism of lipophilic cations, including mitochondria-targeted compounds.[56,58–60,162,174,175] In contrast, mitochondrial indicators, while responding to the mitochondrial membrane potential for organelle-specific accumulation, form strong, typically covalent bonds with mitochondrial proteins for persistent staining/labeling. Examples of such indicators include the probes of the MitoTracker series (Chart 5). MitoTracker probes, which are used extensively for mitochondrial staining and are based on rosamine or cyanine scaffold, with the thiol-reactive chloromethyl moiety serving as an anchor to mitochondrial proteins.[172,176–180]

The use of mitochondrial labels and membrane potential indicators has some drawbacks and limitations, because these compounds exhibit respiration-inhibitory activity in a concentration- and incubation-time-dependent manner.[50,181–184] For example, MitoTracker Orange (chloromethyltetramethylrosamine) was reported to induce mitochondrial permeability transition and complex I inhibition at low micromolar concentrations.[177] Numerous lipophilic cations were used as metabolic inhibitors, for example in anticancer strategies, as discussed later. Therefore, typically submicromolar or low micromolar concentrations of the probes should be used, and their effect on cellular respiration should be tested. Phototoxicity of the fluorescent probes should be also considered. Even at a concentration of 100 nM, chloromethyl-X-rosamine (MitoTracker Red) was shown to exhibit significant phototoxicity toward osteosarcoma cells.[176] In addition, when working with intact cells, another consideration is that the plasma membrane potential is an additional parameter controlling the extent of probe uptake.[78]

Among different probes for mitochondrial membrane potential, cyanine- and rhodamine-based lipophilic cations are most widely used in cultured cells, mostly due to their intrinsic fluorescence and relatively fast equilibration.

Cyanines—Cyanines are a class of the lipophilic ionic compounds that has been used for optical measurement of membrane potential, due to their intrinsic fluorescence properties that are affected by the accumulation of dye in cells or subcellular organelles.[52,169,170,185] Currently, the green fluorescent JC-1 probe (Chart 6) is the most widely used cyanine-based probe for mitochondrial membrane potential.[186,187]

The probe, when present at micromolar concentrations, forms J-aggregates, leading to a shift in fluorescence from the green to red spectral region. This enables ratiometric analysis of the membrane potential. The major limitations of the JC-1 probe are the potential phototoxicity and the slow kinetics of the potential-dependent equilibration of the aggregate form of the dye.[78] Another popular cyanine-based probe, $DiOC_6(3)$ (Chart 6), although previously used as a mitochondrial stain, was demonstrated to also localize in other cellular organelles, including the endoplasmic reticulum.[73,75,187,188]

Rhodamines—Rhodamine 123 (Rh-123, Chart 7) is one of the first fluorescence indicators used to stain mitochondria in intact, living cells.[71] It is rapidly taken up and

equilibrated in mitochondria and exhibits relatively low cytotoxicity.[78] It was used to monitor mitochondrial membrane potential in isolated mitochondria.[70,74] Rhodamine 123 and its more hydrophobic analogs, tetramethylrhodamine methyl and ethyl esters (TMRM and TMRE, respectively, Chart 7), are the most widely used fluorescent sensors for determination of mitochondrial membrane potential in intact cells.[76,79,189]

N-Nonyl acridine orange—N-Nonyl acridine orange (NOA, Chart 8) is another fluorescent lipophilic cation that was shown to accumulate in cell mitochondria and proposed as a mitochondrial stain.[190] Because cardiolipins were recognized as the primary target of NAO accumulation, the dye was also used to stain mitochondrial cardiolipins.[191–193] Different alkyl chain lengths were tested for such purpose, and the conclusion is that the efficiency of cellular staining is increased with a longer alkyl chain but the target selectivity is compromised.[194,195] Because the probe is cationic, its cellular accumulation was demonstrated to be a function not only of mitochondrial mass and cardiolipin content but also of the mitochondrial membrane potential.[172,196]

Mitochondria-targeted probes with aggregation-induced emission (AIE-mito probes)—Aggregation-induced emission (AIE) is a phenomenon of nonluminescent molecules in solutions becoming luminescent upon aggregate formation. [197–199] A mitochondria-targeted AIE fluorescent probe, TPE-TPP, was synthesized by conjugation of the tetraphenylethene (TPE) moiety, an archetypal AIE luminogen, with two triphenylphosphonium groups (Chart 9).[200]

TPE-TPP exhibits typical AIE properties: In a solution, it is almost nonfluorescent, whereas in the solid state, strong fluorescence is observed (λ_{emi} = 466 nm). In aqueous solutions, the TPE-TPP probe aggregates form fluorescent particles and, upon incubation with HeLa cells, an intense aggregation-induced fluorescence from TPE-TPP was reported. The co-staining experiment using TPE-TPP (5 μM) and MitoTracker Red (50 nM) indicated mitochondrial localization of the TPE-TPP aggregates.[200] Another TPE-based dye, TPE-Py (Chart 9), was synthesized by linking a pyridinium cationic unit with TPE AIE-luminogen through vinyl functionality.[201] TPE-Py was shown to be weakly luminescent in solution but a strong emitter in the solid state.[201] TPE-Py is a good fluorescent imaging agent for specific staining of mitochondria in living cells with high photostability. A mitochondria-targeted AIE-based probe was also designed to monitor mitochondrial membrane potential.[202] Other mitochondrial AIE probes, AIE-MitoGreen-1 and AIE-mito-TPP, were reported for mitochondrial staining (Chart 9).[203,204] The AIE-MitoGreen-1 probe exhibits high cell permeability, good mitochondrial retention, a large Stokes shift, and low toxicity.[203] The AIE-mito-TPP probe was shown to quickly and selectively accumulate in the mitochondria in cancer cells, lighting them up. Accumulation of the probe in the mitochondria of cancer cells led to decrease their membrane potential, induce ROS generation, and inhibit ATP production.[204] Though these effects confound the interpretation of the results when the probe is used to monitor mitochondrial membrane potential, they can be used in the design of new chemotherapeutics. In fact, the synthesis and chemotherapeutic properties of two mitochondria-targeted TPE-based AIE probes, TPECM-1TPP and TPECM-2TPP, which possess one and two TPP^+ groups, respectively (Chart 9), have been reported. Both probes

were designed as potential chemotherapeutic agents.[205] More recently, the chemotherapeutic properties of another TPE-based mitochondria-targeted AIE probe, TPP-TPE-NQO1, were reported.[206] TPP-TPE-NQO1 is activated by NAD(P)H:quinone oxidoreductase-1 (NQO1), an enzyme that is overexpressed in various cancerous tissues. The crucial dependence of the self-aggregation process and the associated cytotoxicity of TPP-TPE-NQO1 on the expression levels of NQO1 was demonstrated both in vitro and in vivo by modulation of NQO1 expression. Also, TPP-TPE-NQO1 treatment in vivo reduced tumor growth by ~80%, a result that is highly dependent on the expression of NQO1 because a gene knockdown resulted in a significantly attenuated growth inhibition effect (~30% growth reduction) in A549 tumor xenografts.[206]

Click-chemistry-based mitochondrial probes—The significant ACR of cationic compounds in energized mitochondria was utilized for delivery of the mitochondria-targeted cyclooctyne as a probe for azide-labeled analytes. The copper-free click-chemistry-based reaction between azide on the target molecule and cyclooctyne groups on the TPP^+-linked MitoOct probe (Chart 10A) leads to formation of the TPP^+-labeled target molecule in the mitochondrial matrix, which can be qualitatively and quantitatively determined by mass spectrometry.[207] This approach was proposed to monitor mitochondrial delivery of molecules of interest, including bioactive compounds. As a proof of concept, the occurrence of the click-chemistry-based reaction was demonstrated between azide-labeled cargo attached to an MTS peptide and a MitoOct probe that was inhibited if the mitochondrial membrane potential was dissipated by the mitochondrial uncoupler, FCCP.[207]

This approach was further extended for monitoring mitochondrial membrane potential by simultaneous use of the TPP^+-linked cyclooctyne (MitoOct) and the TPP^+-linked azidyl group (MitoAzido, Chart 10B).[208] Upon accumulation of both probes in the mitochondrial matrix, they react to form the product called MitoClick, which bears two TPP^+ moieties and can be conveniently measured using liquid chromatography mass spectrometry. Because both reactants accumulate in mitochondria in a membrane-potential-dependent manner, the relative rate of the product (MitoClick) formation is very sensitive to even small changes in mitochondrial energization. The feasibility of this approach was demonstrated in isolated mitochondria, intact cells, and in vivo mouse models.[208]

3.6. Effect of Mitochondria-Targeted Compounds on Mitochondrial Respiration

The accumulation of the lipophilic cations in the mitochondrial matrix can modulate mitochondrial membrane potential and affect mitochondrial function. Early studies reported that cyanine dyes, used for determination of the mitochondrial membrane potential, inhibited mitochondrial complex I and uncoupled the OXPHOS.[50,169,181] Rhodamine was shown to inhibit ADP-stimulated mitochondrial respiration, and the site of inhibition was identified as F_0F_1-ATPase.[74,209] The mitochondrial membrane potential was shown to decrease as a function of the concentration and mitochondrial accumulation of the redox probe, thiobutyltriphenylphosphonium (TBTP).[58] Simple alkylated TPP^+ cations have also been shown to inhibit mitochondrial respiration, and the potency is correlated with increasing hydrophobicity of the cation.[210]

To differentiate the cellular effects of the "cargo" molecule targeted to mitochondria from nonspecific effects of the alkyl-TPP^+ moiety, one should use a "control" TPP^+-linked compound of very similar chemical structure and physicochemical properties but lacking the assumed activity of the "cargo" molecule. As an example, to understand the role of nitroxide redox chemistry in the antiproliferative effects of TPP^+-linked nitroxides (mito-CP), we synthesized an analogous, redox inactive compound, Mito-CP-acetamide (Chart 11), and compared their effects on cancer cell proliferation, as discussed later.[17] A similar strategy can be applied to other TPP^+-linked compounds. For example, to understand the importance of the redox reactions of Mito-Q and Mito-Vit E in their cellular effects, the O-methylated analogs, Mito-$Q(Me)_2$ and Mito-Vit E-Me (Chart 11), should be tested in parallel experiments. This also applies to mitochondria-targeted enzyme inhibitors, donors, etc. It should be emphasized, that the "control" compounds must be as close structurally to the parent compound as possible, including having linker chains of the same length, to make sure cellular and mitochondrial uptake are similar.

4. SYNTHETIC APPROACHES TO MITOCHONDRIA-TARGETED COMPOUNDS

4.1. Synthesis of the TPP^+ Cationic Moiety

Triphenylphosphonium salts are usually synthesized by nucleophilic substitution of a leaving group such as a halide, mesylate, or tosylate from an appropriate alkyl or benzyl precursors (Chart 12).[58,211–214] In most reports, the substitution occurs on primary carbon atoms with good to high yields and is performed at reflux in a solvent such as toluene, acetonitrile, and or acetone for a period of 2–20 h. The method was shown to be efficient and compatible with many functional groups. A number of phosphonium derivatives bearing a reactive group such as an amino, hydroxyl, sulfhydryl, bromo, iodo, carboxylic, alkyl, or azido in ω position were prepared successfully using this method.[21,58,64,163,215–222] Phosphonium salts bearing aryl, cyclohexyl, and ethyl groups were also prepared according to this procedure and yields were good to excellent.

The free radical addition of triphenylphosphonium tetrafluoroborate to nonactivated olefins was reported to be another effective method of preparing alkylated triphenylphosphonium cations (Chart 13). Choosing the counter ion and the initiator is an important parameter, and the best results are obtained using the noncoordinating BF_4^- anion and 1,1′-azobis(cyclohexanecarbonitrile), respectively. The reaction also may be performed under photochemical conditions at room temperature using one additional equivalent of triphenylphosphine.[223]

The reaction of triphenylphosphine with 1,3-propane and 1,4-butane sulfones was reported in toluene at reflux to produce the respective zwitterions with nearly quantitative yields (Chart 14).[224–226]

The direct arylation of triphenylphosphine using the palladium (Pd)-catalyzed coupling reaction was shown to be a valuable method to prepare phosphonium salts bearing four aryl

groups. The reaction was reported to give moderate to high yields on various aryl derivatives using tris(dibenzylideneacetone)dipalladium, $Pd_2(dba)_3$, as a catalyst (Chart 15).[227]

Examples introducing a difluoromethylene group in the α position of the phosphonium moiety were reported (Chart 16) by reacting triphenylphosphine, (bromodifluoromethyl)trimethylsilane (Me_3SiCF_2Br) and ketones or nitro alkenes as electrophiles in the presence of 1,3-dimethylpropyleneurea (DMPU).[228] Aromatic, heteroaromatic, vinyl methyl ketones and nitro alkenes provided the respective corresponding compounds in moderate to good yields. Further treatment with potassium hydroxide (KOH) enables the protodephosphorylation.

Acetylated and vinylether phosphonium salts were prepared by a reaction of acetyl-stabilized phosphonium ylides with electrophiles, such as 2-bromomethyl acetate, in refluxing benzene (Chart 17).[229] It is interesting to note the ambivalent reactivity of the stabilized ylides, yielding the O- or C-alkylated products depending on the electrophiles and the reaction conditions (thermodynamic versus kinetic control).

4.2. Conjugation of the TPP^+ Cations to Functional Moieties

In many cases, TPP^+-derivatization of chemical agents is achieved during the quaternization step of the phosphorus atom of the triphenylphosphine, as described above. This approach has the advantage of relatively easy purification, due to the differences in solubility of triphenylphosphine and TPP^+-bearing compounds in diethyl ether. Triphenylphosphonium cationic compounds are typically not soluble in diethyl ether, allowing the precipitation of the pure product from the reaction mixture. In other cases, however, purification may be more difficult and low-pressure column- or high performance liquid chromatography (HPLC)-based purification of the crude is required to obtain pure product. Moreover, in many cases, it is more practical to first synthesize the TPP^+-alkyl cation bearing a functional group and subsequently couple to the compound of interest via this functional group. The examples include the formation of ester, amide, or ether bonds, and require preparation of TPP^+-bearing alkylamine, carboxylic acid, alcohol, bromoalkyl, alkyne, or azide, as shown in Chart 18.

4.3. Examples of the Approaches to Synthesize Mitochondria-Targeted Agents

A few examples of the synthesis of TPP^+-conjugated probes and bioactive compounds, along with helpful hints are given in the subsequent sections.

Mitochondria-targeted cyclic nitrone spin traps—To obtain mitochondria-targeted cyclic nitrone spin traps based on DEPMPO (5-(diethoxyphosphoryl)-5-methyl-1-pyrroline-N-oxide) and DIPPMPO (5-(diisopropoxyphosphoryl)-5-methyl-1-pyrroline-N-oxide) moieties, we had to meet two major goals: (i) The phosphoryl group and the TPP^+ moiety should be in the cis position enabling the trans-addition of $O_2^{\bullet-}$ for proper assignment of the identity of radicals trapped. (ii) The TPP^+ moiety should be in position four of the nitrone ring, increasing the stability of the superoxide adduct.[230] An additional challenge was to find an activating group allowing further modifications of the trap without degrading the nitrone moiety.[231] In this synthetic pathway, the key step was the DIBAL-H (diisobutylaluminum

hydride)-mediated reduction where the nature of the substrate, the number of equivalents of reactant, the temperature of the reaction, and the conditions of quenching were carefully optimized. An advantage was the use of disuccinimidyl (DSC) chemistry to selectively activate the hydroxyl group and convert the N-hydroxysulfosuccinimide (NHS) derivatives into useful precursors for post-functionalization applications.[64,232,233] The TPP^+-conjugated cyclic nitrones were prepared in a five-steps synthetic sequence (Chart 19).[64,231,234] The Michael addition of the anion of the nitrophosphonate on the 2(5H)-furanone afforded the nitrofuranones, reduced by DIBAL-H to obtain the hemiacetal derivatives. The subsequent reductive cyclization in the presence of zinc and ammonium chloride afforded a mixture of cis/trans nitrones substituted in position four. The cis isomers conjugated with NHS reacted with the appropriate aminophosphonium moieties, yielding the designed mitochondria-targeted spin traps. The synthesis of various spin-trap derivatives illustrates the versatility of the post-functionalization step.

Cyclic Nitrones, DEPMPO and DIPPMPO. Reagents and conditions: i, PBu_3, C_6H_{12}/CH_2Cl_2, rt, 70–80%; ii, DIBAL-H, CH_2Cl_2, −78°C, 40–75%; iii, Zn/NH_4Cl, H_2O/THF, rt, 60–65%; iv, DSC, Et_3N, CH_3CN, rt, 95–100%; v, R_1R_2NH, TEA, CH_2Cl_2, 50–90%.

Mito-Metformin derivatives—The Mito-metformin derivatives were prepared in a three-step synthetic sequence (Chart 20).[21] After the nucleophilic substitution of bromide in phthalimide alkyl bromide by PPh_3 followed by the deprotection of the amino groups, the targeted compounds were conjugated to dicyanamide by neat reactions.

The challenging step in this sequence was the coupling of dicyanamide with the aminophosphonium moiety. To make the reaction feasible and maximize the yield, it is essential to optimize the neat reaction conditions and control the time of the reaction.[21]

^{99m}Mito-MAG$_3$—Mito-MAG_3 was obtained in a two-step synthesis by reacting NHS-MAG_3 with (10-aminodecyl) triphenylphosphonium bromide followed by radiolabeling with ^{99m}Tc (Chart 21).[235]

5. MITOCHONDRIA-TARGETED PROBES AND SENSORS FOR REACTIVE OXYGEN, NITROGEN, AND SULFUR SPECIES: DETECTION, DETOXIFICATION, AND DONOR MOLECULES

Mitochondria are one of the major sources and targets of ROS and reactive nitrogen species (RNS) within cells.[236,237] $O_2^{\bullet-}$, formed upon one-electron reduction of molecular oxygen, was proposed as a by-product of normal respiration in mitochondria.[236] $O_2^{\bullet-}$ either dismutates to hydrogen peroxide (H_2O_2) spontaneously or in reaction catalyzed by superoxide dismutase. It can also react with nitric oxide to form peroxynitrite, a strong oxidizing and nitrating agent. Peroxynitrite formation inside mitochondria is likely to occur, as nitric oxide diffuses easily into mitochondria where it may react with superoxide.[237,238] Increased reactive species formation (superoxide, peroxynitrite, H_2O_2, hydroxyl radical, etc.) was proposed to contribute to mitochondrial damage. The development of reliable

methods for rigorous ROS detection and quantitation is essential to understand their role in redox signaling and pathophysiological processes.[239,240]

5.1. Mitochondria-Targeted Redox Probes

Due to the short lifetime of ROS in biological systems, their detection and quantitation still remain a challenging task.[241–247] In general, rigorous characterization of specific products generated from either biomolecules (proteins, DNA, or lipids) or exogenous probes (exomarkers) is required to completely understand the redox processes.[248–250] This methodology can provide specific detection but does not provide real-time monitoring. The latter is possible with the use of fluorescent techniques. The most informative methodology combines both approaches—the real-time measurements of ROS/RNS production with the use of appropriate fluorogenic probes and the quantitation of the species-specific products using the HPLC-mass spectrometry (HPLC-MS) technique.[251,252] It should be emphasized, that the molecular probes (fluorogenic probes, spin traps, exomarkers) used to detect ROS in biological systems are not present in sufficient concentrations in cells to effectively compete with other cellular targets of superoxide, H_2O_2, or peroxynitrite, and they may trap only a fraction of the total amount of the oxidant produced.

5.1.1. Probes for Superoxide Radical Anion—A generally problematic aspect in discerning production of $O_2^{\bullet-}$ from mitochondria in tissues, cells, and intact mitochondria is the limited specificity and sensitivity of available probes. Although spin trapping seems to be an ideal technique for detecting superoxide in isolated mitochondria, its application was only partially successful so far, as discussed subsequently. In intact cells, the situation is even more complicated, and, in an attempt to measure mitochondrial superoxide production, several probes were conjugated to TPP^+ to gain site specificity. These probes, including Mito-HE, Mito-TEMPO-H, MF-DBZH, and HKSOX-1m (Chart 22), are discussed in the subsequent sections.

MitoSOX Red: Mitochondria-targeted HE (MitoSOX Red or Mito-HE) is a fluorogenic probe in which HE is conjugated to a triphenylphosphonium group via a $-(CH_2)_6-$ alkyl chain.[253–256] During the last 10 years, that probe was widely used in biological studies to detect mitochondrial superoxide (more than 250 citations and 6,000 records are retrieved when “MitoSOX” is queried in the PubMed and Google Scholar databases, respectively). The reactivity pattern of MitoSOX is very similar to that of HE.[257] Due to the positive charge of the probe, it reacts slightly faster with $O_2^{\bullet-}$ than with HE ($k = 1.6 \times 10^4\ M^{-1}s^{-1}$ for Mito-HE versus $6.2 \times 10^3\ M^{-1}s^{-1}$ for HE), and the red fluorescent product 2-hydroxy-mitoethidium (2-OH-Mito-E^+) is formed.[256,258] 2-OH-Mito-E^+ is the only product formed in vitro in pure superoxide-generating systems (e.g., xanthine/xanthine oxidase), and it is specific for $O_2^{\bullet-}$ (Chart 23).

In the presence of trace metal ions, or peroxidases, the nonspecific oxidation product mitoethidium (Mito-E^+) is also formed. 2-OH-Mito-E^+ and Mito-E^+ have overlapping fluorescence spectra and both products are usually formed in cells.[257] As a result, the increase in red fluorescence derived from MitoSOX oxidation cannot be used as a measure of $O_2^{\bullet-}$ production in mitochondria because the red fluorescence can arise both from the

formation of 2-OH-Mito-E^+ and Mito-E^+. In all studies using the MitoSOX probe, the fluorescence measurements should be accompanied by HPLC or LC/MS analyses quantitating the amounts of 2-OH-Mito-E^+ and Mito-E^+.[259] Based on the redox chemistry of HE, we proposed that the oxidative conversion of MitoSOX into 2-OH-Mito-E^+ induced by superoxide involves a radical mechanism. In the first step, the HE moiety in the MitoSOX molecule is oxidized to its radical cation in the reaction with the hydroperoxyl radical ($HO_2^{\bullet}$), the protonated form of $O_2^{\bullet-}$ and a relatively strong one-electron oxidant ($E^{\circ}(HO_2^{\bullet}/H_2O_2) = 1.46 \pm 0.01$ V).[260] In the subsequent reaction, the one-electron oxidation product of MitoSOX combines rapidly with superoxide to form the product, 2-OH-Mito-E^+. The MitoSOX-derived radical cation can also disproportionate or dimerize to form Mito-E^+ and Mito-HE-Mito-HE, respectively, with further oxidation of the dimeric product to Mito-HE-Mito-E^+ and Mito-E^+-Mito-E^+.[256] It is reasonable to assume that various oxidizing agents, including both strong and mild one-electron oxidants (e.g., peroxynitrite-derived radicals, $^{\bullet}NO_2$, $^{\bullet}OH$, $CO_3^{\bullet-}$), are able to oxidize MitoSOX to its radical cation, leading to the formation of Mito-E^+ and dimeric oxidation products. It was shown that the same oxidation products (including Mito-E^+ and the dimers) are also formed in the reaction of MitoSOX with cytochrome c^{3+} (cyt c^{3+}), which is present in mitochondria at a relatively high concentration.[256] In the presence of H_2O_2, the observed rate of MitoSOX oxidation is much faster, due to the peroxidatic activity of cyt c^{3+}.[256] Though MitoSOX is expected to be localized mostly in the mitochondrial matrix, while cytochrome c in the intermembrane space, it has been demonstrated that depletion of cytochrome c in isolated mitochondria significantly increases the stability of the probe, pointing to the importance of the reaction of MitoSOX with cyt c in mitochondria. Recent results suggest that MitoSOX affects mitochondrial bioenergetic function due to the mitochondrial uncoupling and inhibition of complex IV.[183,261] Thus, in order to obtain useful and reliable information using MitoSOX, its effects must be tested on the cellular respiratory function, and the superoxide-specific product, 2-OH-Mito-E^+, and other products, must be monitored. Before using MitoSOX as a probe for detecting superoxide, it is important to determine the optimal concentration at which the probe does not affect the bioenergetic function in a given biological system. The chromatographic techniques (HPLC, LC-MS/MS) are currently the only way for simultaneous determination of probe uptake, profiling, and specific quantification of the oxidation products formed from MitoSOX and other probes.[247,259,262]

Mito-TEMPO-H: Cyclic hydroxylamines can be easily oxidized to the corresponding EPR-detectable, stable nitroxides, and it was proposed that this reaction can be used to monitor the production of $O_2^{\bullet-}$ in cell cultures and tissues using EPR spectrometry.[263] Mito-TEMPO-H (Chart 22) is a hydroxylamine EPR probe in which the TEMPO-H molecule is conjugated to a TPP^+ group via an acetamido ($-CH_2C(O)NH-$) linker. The estimated value of the rate constant of the Mito-TEMPO-H reaction with superoxide is equal to $(7.8 \pm 0.6) \times 10^3$ $M^{-1}s^{-1}$ and is typical for cyclic hydroxylamines.[263]

It was shown that, after the addition of Mito-TEMPO-H to mitochondria isolated from bovine aortic endothelial cells, the intensity of the measured EPR signal is significantly increased, and, in the presence of rotenone or antimycin A, the rate of signal increase is further enhanced. Supplementation of SOD only partially inhibited antimycin A-induced

nitroxide accumulation and did not affect rotenone-induced nitroxide formation.[263] These results suggest that Mito-TEMPO-H accumulates in mitochondria and can be oxidized by superoxide to the corresponding Mito-TEMPO nitroxide. However, the oxidative conversion of cyclic hydroxylamines to nitroxides is not specific for superoxide as other oxidants can also react with cyclic hydroxylamines to yield the EPR signal. It was shown that TPP^+-linked hydroxylamine, Mito-TEMPOL-H, is oxidized by Fe^{3+} and peroxyl radicals to form Mito-TEMPO.[264] In addition, the nitroxide formed may be rapidly reduced back to EPR-silent hydroxylamine by mitochondrial ETC.[265] Therefore, the increase in EPR signal from Mito-TEMPO-H cannot be equated to mitochondrial superoxide.

MF-DBZH: Recently, the novel mitochondria-targeted probe, 9-butyltriphenylphosphoniumacylamino-2,7-dibenzothiazolinefluorene (MF-DBZH, Chart 22), was proposed for the detection of $O_2^{\bullet -}$.[266] The probe consists of a dibenzothiazoline-substituted fluorene fluorophore linked to the TPP^+ cationic moiety. Oxidation of the probe by $O_2^{\bullet -}$ leads to the remarkable increase of fluorescence (λ_{exc} = 483 nm, λ_{emi} = 512 nm).[266] The probe was oxidized to the fluorescent product also in HepG2 cells stimulated with phorbol 12-myristate 13-acetate (PMA).[266] Despite claims that the probe is selective toward superoxide, the possibility of oxidation of the probe by biologically relevant, strong one-electron oxidants should be considered.

HKSOX-1m: A novel, mitochondria-targeted probe was reported for $O_2^{\bullet -}$ detection, (HKSOX-1m, Chart 22), based on superoxide-induced deprotection of the hydroxyl groups. The probe is a 5-carboxy-2′,4′,5′,7′-tetrafluorofluorescein fluorophore linked to the TPP^+ cation and masked by the protection of phenolic OH groups with the trifluoromethanesulfonate group.[267] The non-redox reaction with superoxide leads to the deprotection of –OH groups and the release of fluorophore. However, the oxidizing $CF_3SO_2OO^{\bullet}$ radical is formed during this reaction and may interfere with the redox systems being investigated.

Mitochondria-targeted nitrones as spin traps: EPR spin trapping of free radicals is regarded as one of the most rigorous techniques for characterization of free radicals both in chemical and biological systems (Chart 24).

For the purpose of specific detection of free radicals in mitochondria, several spin traps were conjugated to the triphenylphosphonium cation. The first reported mitochondria-targeted spin trap was TPP^+-linked α-phenyl-N-tert-butyl nitrone (Mito-PBN, Chart 25).[268] Mito-PBN was reported to trap carbon-centered radicals in model chemical systems and to bind to energized isolated mitochondria blocking superoxide-induced activation of uncoupling proteins (UCPs) and mitochondrial lipid peroxidation. As Mito-PBN is not an efficient scavenger of superoxide, these effects were attributed to the ability of Mito-PBN to scavenge carbon-centered radicals.[268] However, no EPR spectra of the radical adducts formed in isolated mitochondria were reported. Thus, the effects observed cannot be attributed solely to radical trapping.

To specifically detect mitochondrial superoxide, the superoxide-reactive spin trap, DEPMPO, was conjugated to the TPP^+ moiety via a short linker to form the mitochondria-

targeted analog, Mito-DEPMPO-C_2 (Chart 25).[231] The spin adducts of different radicals were characterized, and the superoxide spin adduct to Mito-DEPMPO was reported to exhibit a 2.5-fold longer half-life than that of DEPMPO.[234] Further increase in the superoxide adduct lifetime was achieved by replacing the DEPMPO moiety with the DIPPMPO moiety.[64] The addition of the Mito-DEPMPO-C_2 spin trap to isolated mitochondria resulted in the appearance of the EPR signal, with the spectrum attributable to the mixture of the superoxide, hydroxyl radical, and alkyl radical spin adducts. Interestingly, the superoxide adduct was not detected when the "nontargeted" analog, DEPMPO, was used.[231,234]

The analysis of mitochondrial uptake of Mito-DEPMPO analogs indicated that elongation of the linker aliphatic chain improves the uptake and that the analog-bearing 10-carbon linker was optimal for mitochondrial free radical trapping.[64] The cyclic nitrone carrying two TPP^+ moieties, Mito-bis-DIPPMPO (Chart 25), did not show improved mitochondrial uptake, in agreement with the previous report on the uptake of simple lipophilic dications.[165] In assays with energized isolated mitochondria, Mito-bis-DIPPMPO failed to produce any detectable EPR signal. An EPR signal was only detected upon inhibition of mitochondrial respiration with antimycin A.[269] The Mito-bis-DIPPMPO-OH adduct signal detected indicated the fast reduction of the Mito-bis-DIPPMPO-OOH adduct in the mitochondrial compartment, a conclusion that was supported by the lack of radical detection with a non-membrane-permeable spin trap, cyclodextrin-complexed DEPMPO (CD-DEPMPO), and a lack of inhibitory effects of catalase on the signal detected.[270] The oxygen consumption experiments revealed, however, that Mito-bis-DIPPMPO is a potent inhibitor of oxygen consumption. Strong inhibitory activity of complex IV and less potent inhibition of complex III and complex I activities were demonstrated at low micromolar concentrations of the spin trap.[269] The mechanisms of mitochondrial complex inhibition by TPP^+-DIPPMPO and DIPPMPO are not yet fully understood.

Other spin traps targeted to mitochondria, Mito-BMPO, Mito-Spin (Chart 25), and pyridinium cation-linked nitrones were also reported, but their applicability for trapping radicals in mitochondria remains to be tested.[271–273]

The limitations of mitochondrial spin trapping include the strongly reducing environment, which leads to a fast reduction of the EPR-active nitroxides into EPR-silent hydroxylamines.[265] Another limitation is the requirement of a relatively high concentration of the spin trap to efficiently intercept free radicals, as high concentrations of the TPP^+-conjugated spin trap will affect mitochondrial function, as discussed above.

5.1.2. Probes for Hydrogen Peroxide and Peroxynitrite—As discussed, once formed superoxide is rapidly dismutated to hydrogen peroxide. Most studies on the generation of superoxide by isolated mitochondria used the Amplex Red probe, which is oxidized by horseradish peroxidase (HRP)/H_2O_2 to generate the fluorescent product resorufin. Thus, the Amplex Red-based assay for mitochondrial superoxide production is based on the assumption that superoxide quantitatively undergoes dismutation to H_2O_2, which then diffuses out of mitochondria to oxidize the probe. Because of its high sensitivity, this assay is commonly used to infer redox reactions occurring in both mitochondrial intermembrane

and matrix space. A significant drawback of this assay is its sensitivity to light, which amplifies the fluorescence signal and confuses quantitative analyses.[274] It was also shown that Amplex Red can be converted into resorufin on a H_2O_2-independent pathway, catalyzed by mitochondrial carboxylesterase.[275] In addition, the Amplex Red assay cannot distinguish the sites of $O_2^{\bullet-}$ in intact mitochondria, and the amount of H_2O_2 diffusing out of mitochondria may be affected by competitive reactions of $O_2^{\bullet-}$ and H_2O_2 with other scavengers, including MnSOD, peroxiredoxins, or glutathione peroxidase. Therefore, mechanistic interpretations based only on the Amplex Red-based assay are difficult and prone to misinterpretation. To detect H_2O_2 directly, boronate-based probes were linked to the TPP^+ moiety.

Mitochondria-targeted boronate probes: Arylboronates are organic compounds containing a boron atom substituted with one aryl group and two hydroxyl or ester groups in a trigonal planar geometry. The trivalent, sp^2-hybridized boron atom possesses an orthogonal vacant p orbital and can easily coordinate anionic nucleophiles, which makes boronates highly reactive toward acidic hydroperoxides and hypohalous anions.[246,276,277] More than a decade ago, it was proposed that boronate-based fluorogenic probes (non- or weakly fluorescent derivatives of fluorescent dyes) could be used as probes for H_2O_2.[278,279] Subsequently, several boronate-based probes were developed to study oxidants in specific subcellular localizations, including mitochondria.[277,280]

The first mitochondria-targeted boronate probe was a derivative of a hybrid fluorescein/rhodamine dye linked to a TPP^+ moiety, called "Mitochondria-targeted Peroxy Yellow 1" (MitoPY1, Chart 26).[281,282] The mechanism of MitoPY1 action is based on the oxidative deboronation forming a strongly fluorescent product, MitoPY1ox (λ_{abs} = 510 nm; λ_{emi} = 528 nm, Φ = 0.405).[281] At physiological pHs, the reaction between arylboronates and H_2O_2 is rather slow (typically $k \sim 1–2\ M^{-1}s^{-1}$) and the second order rate constant of the MitoPY1 reaction with H_2O_2 was estimated to be 0.2 $M^{-1}s^{-1}$.[276,281] It should be emphasized that oxidants other than H_2O_2 (e.g., hypohalous ions and nucleophilic peroxides) can also oxidize boronates to corresponding phenols so reaction is not specific for H_2O_2 (Chart 27).[246,276,283]

We have demonstrated that arylboronates react rapidly with hypochlorite and peroxynitrite anions ($k \sim 10^4$ and $10^6\ M^{-1}s^{-1}$, respectively).[276] Moreover, boronate probes also can be oxidized by aliphatic and aromatic hydroperoxides.[283,284] The reaction between boronates and peroxynitrite is of special interest because it leads to the formation of peroxynitrite-specific products.[252,276,284–286] We described in detail the mechanism of this reaction for simple aryl boronic acids (Chart 28).[284] The first step is the formation of the anionic adduct of peroxynitrite to the boronate moiety that undergoes either the heterolytic cleavage of the O-O bond forming the major, phenolic product or the homolytic cleavage (~10–20%) of the peroxide bond forming the $PhB(OH)_2O^{\bullet-}$ radical anion, which undergoes spontaneous fragmentation to the corresponding phenyl radical ($Ph^{\bullet}$) and leads to formation of peroxynitrite-specific products.[284]

The next mitochondria-targeted boronate-based probe, 3-(dihydroxyboronyl)benzyltriphenylphosphonium bromide, known as MitoB, or *m*-

MitoPhB$(OH)_2$ (Chart 29), was reported for in vivo measurements of mitochondrial H_2O_2.[287,288] This mass spectrometric probe was used to assess changes in H_2O_2 production in mitochondria of *Drosophila* via the exomarker approach.[287,288]

In general, in this exomarker strategy, the exogenous probe is administered to the organism, where it is modified by the reactive species to form an exomarker. After administration to a living organism, MitoB accumulates rapidly within mitochondria where it is oxidized to the phenolic product (3-hydroxybenzyl)triphenylphosphonium bromide (MitoP, or *m*-MitoPhOH). The extent of MitoB oxidation can be expressed as a ratio of MitoP/MitoB to correct for changes in the distribution of probe and exomarker in the tissue under consideration. The amount of MitoP and MitoB in tissue samples can be determined with the use of liquid chromatography-tandem mass spectrometry, in relation to deuterated internal standards.[248,289] This methodology was successfully applied in several studies on the production/levels of mitochondrial H_2O_2.[290–294]

Later, it was shown that MitoB (or *m*-MitoPhB$(OH)_2$) and its *para* and *ortho* isomers (Chart 29) react rapidly with peroxynitrite.[295] The rate constants of the reaction of peroxynitrite with MitoPhB$(OH)_2$ isomers, determined at pH 7.4, are equal to $(3.5 \pm 0.5) \times 10^5$, $(1.0 \pm 0.1) \times 10^6$, and $(1.0 \pm 0.1) \times 10^6$ $M^{-1}s^{-1}$ for *ortho*, *meta*, and *para* isomers, respectively, and those values are several orders of magnitude higher than those reported for the reaction of *m*-MitoPhB$(OH)_2$ (MitoB) with H_2O_2 ($k = 3.8$ $M^{-1}s^{-1}$ at pH 8).[287,295] All three isomers react with peroxynitrite to form additional, diagnostic marker products via the minor, radical pathway (Chart 30).[295]

In the case of the *ortho* isomer, the transient phenyl radical o-MitoPh$^{\bullet}$ undergoes rapid intramolecular cyclization to form a peroxynitrite-specific *cyclo*-*o*-MitoPh product (9,10-dihydro-9,9-diphenyl-9-phosphoniaphenanthrene) with a relatively high yield.[286] The quantitative analysis of the oxidation reaction of *o*-MitoPhB$(OH)_2$ by $ONOO^-$ indicated 63 that yields of *cyclo*-*o*-MitoPh and *o*-MitoPhNO_2 (the minor, peroxynitrite-specific products), are $10.5 \pm 0.5\%$ and $0.5 \pm 0.1\%$, respectively.[286] Quantitation of the peroxynitrite-derived oxidation products formed from MitoPhB$(OH)_2$ isomers also gives information about the kinetic parameters of both nonradical and radical pathways. The ratio of the rate constants of the radical and nonradical pathways k_{rad}/k_{nonrad} can be estimated from the plot of sum of the minor products versus the amount of MitoPhOH that is formed; these ratios equal 0.1, 0.1, and 0.07 for *ortho*, *meta*, and *para* isomers, respectively.[295] Formation of phenyl radicals during in the reaction of MitoPhB$(OH)_2$ isomers with $ONOO^-$ was confirmed using the spin trapping technique by detection of the MNP(2-methyl-2nitrosopropane)-phenyl radical spin adducts by EPR, similar to simple arylboronates (Figure 8).[252,284] The spin adduct was detected after mixing peroxynitrite with solutions containing *meta* and *para* but not from the *ortho* isomer of MitoPhB$(OH)_2$ because of the steric hindrance and rapid intramolecular cyclization of the phenyl radical (Figure 8).

The generation of peroxynitrite-specific products was proposed and used for specific detection of peroxynitrite in cell-free and cellular systems.[246,252,284–286,295,296] Use of the *o*-MitoPhB$(OH)_2$ probe should allow the production of peroxynitrite and H_2O_2 inside mitochondria of living animals systems to be monitored, by measuring the amounts of *o*-

MitoPhOH and *cyclo*-*o*-MitoPh products with LC-MS/MS.[286] In addition, hypohalous (HOCl) or hypobromous (HOBr)-specific products also can be formed (Chart 31). Thus, a complete profiling of the oxidation products of the *o*-MitoPhB$(OH)_2$ probe will help identify the oxidant(s) formed, whether H_2O_2, peroxynitrite, or hypohalous acids.

Several other mitochondria-targetable boronate-based fluorescent probes were reported for the imaging of H_2O_2, peroxynitrite, and so-called "highly reactive ROS," including SHP-Mito, Mito-H_2O_2, and pep3-NP1 (Chart 32). The SHP-Mito probe and the product of its oxidation exhibit absorption maxima at 342 nm and 383 nm, and the fluorescence emission maxima at 470 nm ($\Phi = 0.13$) and 545 nm ($\Phi = 0.12$), respectively.[297,298] The main drawback of the SHP-Mito probe seems to be its low solubility in aqueous solution (3 μM at pH 7.4). The estimated value of the rate constant of the SHP-Mito reaction with H_2O_2 is equal to 1.0–1.2 $M^{-1}s^{-1}$. SHP-Mito accumulates in cell mitochondria and is oxidized upon treating cells with H_2O_2 (at a high, non-physiological concentration of 200 μM) or after stimulating cells with PMA to produce $O_2^{\bullet-}$.

Mito-H_2O_2 is a fluorogenic chinolinium-based mitochondria-targeted probe for H_2O_2 (Chart 32).[299] Upon oxidation by H_2O_2, a product exhibiting bright green fluorescence ($\lambda_{emi} = 527$ nm, $\Phi = 0.47$) is formed. Treatment of probe-preloaded HeLa cells with 100 μM H_2O_2 or stimulation with PMA resulted in appearance of a strong green fluorescence signal.

The pep3-NP1 probe containing boronate-masked 1,8-naphthalimide fluorophore (Chart 32) was designed and synthesized based on the NP1 probe, previously described in the literature.[300,301] The boronate reporter was linked to a DNA-binding peptide and a positively charged styryl fluorophore. The probe showed a colocalization with MitoTracker Green (500 nM) indicating accumulation of the probe in mitochondria in HeLa cells. Oxidation of the boronate moiety led to a significant increase of green fluorescence ($\lambda_{exc} = 455$ nm, $\lambda_{emi} = 555$ nm, $\Phi \sim 0.06$). The reported value of the rate constant of pep3-NP1 reaction with H_2O_2 is equal to 0.49 $M^{-1}s^{-1}$. Treatment of the pep3-NP1-loaded (5 μM) HeLa cells with 200 μM H_2O_2, or pretreatment of the cells with paraquat (1 mM), resulted in probe oxidation, measured as an increase of green fluorescence signal.

Other probes designed to detect peroxynitrite: Several probes were designed to measure peroxynitrite and/or other oxidants, based on rhodamine or cyanine cations, serving as both mitochondria-targeting moieties and fluorophores. These include MitoAR, MitoHR, and methyl-(4-hydroxyphenyl)amino-substituted pyronin (rhodamine-based probes, Chart 33) and PNCy3Cy5 and Cy-NTe (cyanine-based probes, Chart 34).[302–305] Typically, these probes were shown to respond to peroxynitrite in cell-free systems and in macrophages stimulated with lipopolysaccharide (LPS) and interferon γ (IFN γ) to induce cellular $ONOO^-$ production. Interestingly, the oxidized form of the probe Cy-NTeO can be easily reduced by thiols, such as glutathione or cysteine, back to the Cy-NTe probe, providing a potential tool for dynamic monitoring of the cellular redox environment.

Recently, the TPP^+-conjugated boron-dipyrromethene (BODIPY)-based fluorogenic probe Mito-A2 (Chart 35) was reported for detecting peroxynitrite, based on $ONOO^-$-induced oxidation and nitrosation of the aromatic amine moiety in the probe.[306] However, the

mechanism of the reaction, and the factors controlling distribution of the products remain unestablished.

5.1.3. Probes for Other Oxidants in Mitochondria

Singlet oxygen: A mitochondria-targeted far-red fluorescent probe, Si-DMA (Chart 36), was reported for detecting singlet oxygen during photodynamic therapy.[307] This probe is composed of 9,10-dimethylantracene (DMA), reactive toward $^1O_2$, and a cationic silicon-containing rhodamine fluorophore (Si-rhodamine). The excited state of the Si-rhodamine moiety is quenched via photoinduced electron transfer from the DMA moiety in the probe, resulting in a low fluorescence yield ($\Phi = 0.01$ in methanol). Upon the reaction of the probe with singlet oxygen, the DMA endoperoxide is formed on the center ring of DMA, converting the Si-DMA into a fluorescent Si-DMEP ($\Phi = 0.17$, $\lambda_{exc1} = 405$ nm, $\lambda_{exc2} = 640$ nm, $\lambda_{emi} = 680$ nm).

Lipid peroxides: A ratiometric, fluorescent probe, MitoPerOx (Chart 37), was introduced for assessing mitochondrial lipid peroxidation.[308] MitoPerOx was derived from the C11-BODIPY probe and similarly contains a BODIPY fluorophore conjugated via a diene to a phenyl group. Probe peroxidation results in a fluorescence emission maximum shift from ~ 590 nm (red) to ~ 520 nm (green). Although the products of probe oxidation have not yet been identified, the presence of the TPP^+ cationic moiety should facilitate their structural characterization by mass spectrometry.

Hypochlorous acid: HOCl is potent oxidant and chlorinating agent produced by neutrophils and monocytes in vivo in the reaction catalyzed by myeloperoxidase (MPO). This enzyme is reported to also be present in mitochondria.[309] During the last 10 years, several different probes for mitochondrial HOCl were reported. The probes MitoAR and MitoHR, discussed above, can be oxidized by HOCl, to the fluorescent product HMTMR (Chart 33).[302] Also, mitochondria-targeted profluorescent probes based on hybrid cyanine-phenothiazine (PTZ-Cy2) or pyridinium-phenothiazine (PZ-Py) platforms were reported for detecting hypochlorite (Chart 38).[310,311] In the reaction with HOCl, the phenothiazine moiety is oxidized to the corresponding S-oxide, leading to an increase in fluorescence intensity.

Two other mitochondria-targeted probes for HOCl, based on hemicyanine oxidation, were also described in the literature: CMCY and HPQ-Cy2 (Chart 39).[312,313] It should be emphasized, however, that such hemicyanine probes were also proposed as selective probes for H_2S and HSO^{3-}, bringing into question their selectivity. The specificity of the assay may be potentially gained by monitoring the specific products formed by HOCl.

Also, the BODIPY-based probe conjugated with the TPP^+ moiety was reported for detecting mitochondrial HOCl (MitoClO, Chart 40).[314] In the presence of HOCl, the aldoxime group is oxidized to the corresponding carboxyl (–COOH) group with a concomitant increase in green fluorescence intensity. The mechanism of oxidation is not fully understood, however, as for complete oxidative conversion of the probe, a large excess of HOCl (40–50 equiv) is required.

Another strategy for HOCl detection is based on the oxidation of rhodamine hydrazide derivatives, accompanied by the liberation of rhodamine fluorophore.[315] Four different mitochondria-targeted probes belong to this class: Rh-TPP, Rh-Py, RMClO-1, and RMClO-2 (Chart 41).[107,316]

It should be noted that, in many of the cases described above, DMSO was used as a probe solvent. However, DMSO is an efficient HOCl and $^{\bullet}$OH scavenger (k_{HOCl} = 349 ±38, $k^{\bullet}_{OH}$ = 7×10^9 $M^{-1}s^{-1}$, respectively); even when present at a 0.1% (~ 14 mM) concentration, it will efficiently compete for those oxidants with the probe present at low micromolar concentrations. Thus, the selectivity of these probes for HOCl is questionable.[320,321]

5.1.4. Probes for Mitochondrial Thiols Redox Status—TPP^+-linked butylthiol (TBTP, Chart 43) was the first probe designed and synthesized to study the redox environment of mitochondria.[58] This probe accumulates in the energized isolated mitochondria but does not significantly affect the mitochondrial function up to a concentration of 50 μM. The redox state of the mitochondrial proteins was monitored by using ^{14}C-labeled TBTP and observing its binding to mitochondrial proteins by measuring the radioactivity of the mitochondrial pellet. Oxidation of mitochondrial protein thiols by diamide (1,1′-azobis(N,N-dimethylformamide)) or tert-butylhydroperoxide was shown to lead to increased binding of the TBTB probe, which was reversed by subsequent incubation with thiol reductants, DTT or $NaBH_4$.[58]

TBTB was also used to monitor the redox status of mitochondrial proteins in intact cells.[59] For that purpose, the thiol moiety was acetylated to prevent oxidation in the extracellular medium. The probe was readily hydrolyzed (Chart 43) in cell cytosol and accumulated in cell mitochondria in a membrane-potential-dependent manner. As a proof of concept, it was shown that exposing hepatocytes to oxidizing (diamide, tert-BuOOH) or redox cycling (menadione) agents led to increased retention of the probe in cell mitochondria.[59]

5.1.5. Mitochondria-Targeted Probes for H_2S and Polysulfides—Hydrogen sulfide (H_2S) is recognized as an important signaling molecule and is produced endogenously, mainly from L-cysteine and/or L-homocysteine by cystathionine β-synthase and cystathionine γ-lyase.[322–324] Several methods were developed to detect hydrogen sulfide, and, during recent years, several probes were designed to detect H_2S within mitochondria.[325]

Mitochondria-targeted ratiometric probes for H_2S, SHS-M1 and SHS-M2 (Chart 44), were reported.[326] The mechanism of their action is based on the reduction of the azidyl group to the corresponding amine. The reported second-order rate constants for the reaction of SHS-M1 and SHS-M2 with H_2S are equal 5.8 and 7.0 $M^{-1}s^{-1}$, respectively. The main disadvantage of these probes for in vivo application is that they also react with low molecular thiols, forming the same products as in the reaction with H_2S. The other mitochondria-targeted H_2S probe, Mito-HS (Chart 44), which has a similar mechanism of action based on the azide reduction to amine, was recently described.[327]

The other detection mechanism is based on the nucleophilic addition of HS^- anion to the cyanine moiety of the probe. This mechanism was utilized in the cationic ratiometric probe CouMC (Chart 45) and is constructed by connecting a coumarin fluorophore and the indolenium moiety through an ethylene linker.[328] The indolenium C-2 atom is a target for a nucleophilic HS^- attack; that reaction turns off the merocyanine emission but retains the emission of the coumarin fluorophore. The reaction of CouMC with HS^- leads to a decrease of the CouMC ICT absorption band (at 588 nm) and an increase of the fluorescence F_{510}/F_{652} ratio. However, the selectivity of that probe for H_2S is questionable because it was also applied for detecting hypochlorite, peroxynitrite, and sulfite.[312,329–331]

Another merocyanine-based cationic probe with a similar detection mechanism was recently reported.[332] Due to the high reactivity of cationic merocyanine probes toward different nucleophiles, their use is not presently recommended, pending additional studies. An interesting tandem nucleophilic addition-cyclization strategy was used to detect H_2S with the use of the HS-Cy near-infrared cationic cyanine probe (Chart 45).[333] In that probe, 2-carboxybenzaldehyde was used as an H_2S sensing group linked to a heptamethine cyanine moiety by an ester group. The nucleophilic addition of HS^- anion to the aldehyde group of the HS-Cy probe leads to the formation of a transient nonfluorescent product, qHS-Cy, that slowly undergoes conversion to the red-fluorescent final product keto-Cy (Chart 45).[333] Another H_2S detection mechanism was described recently and is based on the thiolysis of the 7-nitro-1,2,3-benzodiazole amine moiety linked to the TPP^+-linked naphthalimide fluorophore (Chart 46).[334] The reaction with H_2S results in the formation of green-fluorescent piperazine-naphthalimide and 7-nitro-1,2,3-benzodiazole-4-thiol. However, the estimated rate constant value of the reaction of this probe with Na_2S at pH 7.4 is low and equal to *ca.* 20 $M^{-1}s^{-1}$.

In addition to the probes for H_2S, recently, a mitochondria-targeted probe, Mito-ss (Chart 47), was reported for near-infrared fluorescence imaging of hydrogen polysulfides.[335]

5.1.6. Probe for Mitochondrial Glyoxals and Other Electrophiles—Glycation of proteins and nucleotides by glyoxal and methylglyoxal is potentially damaging to the proteome and genome, and a large body of evidence indicates this process plays an important role in disrupting cell function in a range of pathologies, such as diabetes, neurodegeneration, and aging.[336] The glyoxal and methylglyoxal-induced glycation processes may also cause mitochondrial damage related to hyperglycemia.[337] To evaluate the importance of dicarbonyl-related glycation processes to mitochondrial function, a mitochondria-targeted mass spectrometry probe for glyoxals, MitoG (Chart 48), was developed by linking the TPP^+ cation with alkoxy-substituted o-phenylenediamine.[338]

This probe reacts with glyoxal and methylglyoxal, forming specific quinoxaline products.[338] The MitoG probe can be used to determine relative mitochondrial levels of methylglyoxal and glyoxal under hyperglycemia.[338] Although the proposed methodology of dicarbonyl detection reports on mitochondrial glyoxal and methylglyoxal exposure, it cannot indicate the source of those dicarbonyls, as they may be produced in the cytosol with subsequent diffusion into mitochondria. The MitoG probe was used to assess the changes in glyoxal and methylglyoxal production in a mouse model of type I diabetes.[338]

5.2. Modulators of Mitochondrial Redox Status

5.2.1. Mitochondria-Targeted Macrocyclic SOD Mimetics—Manganese-containing porphyrins were used as efficient catalytic scavengers of superoxide and as radioprotecting agents. Not surprisingly, these agents were targeted to mitochondria, for selective scavenging of mitochondrial superoxide. The first reported approach to target manganese porphyrin complex, 5,10,15,20-tetrakis(N-methyl-4-pyridyl)porphinatomanganese ($MnMPy_4P$), to mitochondria involved the MTS peptide attached to the porphyrin ring (Chart 49).[339] The resulting compound exhibited both superoxide and peroxynitrite-scavenging properties, similar to the parent compound, $MnMPy_4P$, but with slower kinetics. The $MnMPy_3P$-MTS construct reportedly exhibits protection against LPS-induced cell death in activated macrophages superior to $MnMPy_4P$.[339]

Another approach to targeting the manganese-based SOD mimetic to mitochondria included conjugating the TPP^+ moiety to manganese macrocyclic complexes. For example, the EUK-134 Mn-salen complex was double-conjugated to the TPP^+ moieties (Chart 49).[340] Although conjugation to the TPP^+ moieties did not improve the protective effects of the compound, it is not clear if the double-substituted analog was able to accumulate in cell mitochondria. Synthesis of a mono-TPP^+-substituted pentaaza macrocyclic Mn(II) SOD mimetic M40403 was reported (Chart 49).[341] This compound, called MitoSOD, was shown to dismutate superoxide with the catalytic rate constant $k = 2.5 \times 10^6\ M^{-1}s^{-1}$, bind to energized mitochondria, and inhibit PQ-induced mitochondrial aconitase inactivation.[341] The superoxide-scavenging mechanism of protection against paraquat-induced aconitase activation, however, has been questioned, because the catalytic rate constant is more than two orders of magnitude lower than that of SOD and the effect of MitoSOD on mitochondrial paraquat uptake was not tested.[342]

Some Mn-porphyrin complexes displaying SOD-like activity and carrying net positive charge possess sufficient lipophilicity to accumulate in mitochondria.[343] For example, Mn(III) meso-tetrakis(N-ethylpyridinium-2-yl)porphyrin ($Mn^{III}TE\text{-}2\text{-}PyP^{5+}$, Chart 49) was shown to accumulate in heart mitochondria in vivo.[344] After a single intraperitoneal injection of the compound in mice at a dose of 10 mg/kg, the intramitochondrial concentration of $Mn^{III}TE\text{-}2\text{-}PyP^{5+}$ was estimated to be ca. ~5 μM, which is high enough to contribute to the scavenging of mitochondrial oxidants.[344] Another lipophilic analog, $MnTnHex\text{-}2\text{-}PyP^{5+}$, was reported to accumulate 20-fold higher in mouse heart mitochondria than $Mn^{III}TE\text{-}2\text{-}PyP^{5+}$.[343,345,346] These compounds also exhibit peroxynitrite-and H_2O_2-scavenging properties and can act as redox cycling prooxidants in the presence of electron donors (e.g., ascorbate).[347,348]

5.2.2. Mitochondria-Targeted Redox Cyclers: Site-Specific Generation of ROS/RNS

Mito-paraquat: One of the most popular one-electron redox cyclers, PQ (also known as methyl viologen), was linked to the TPP^+ moiety for site-specific generation of superoxide in mitochondria.[349] Mitochondria-targeted paraquat (MitoPQ, Chart 50) was shown to induce H_2O_2 production in isolated mitochondria, and this redox cycling activity was dependent on the mitochondrial membrane potential. Also, MitoPQ induced MitoSOX

oxidation, aconitase inactivation, and cell death of C2C12 myoblasts at concentrations ~1000-fold lower than observed for PQ.[349] However, the identity(ies) of the species responsible for MitoSOX oxidation and the importance of the redox cycling activity of MitoPQ in the stimulation of MitoSOX oxidation and inhibition of aconitase activity in intact cells has yet to be determined.

To prove that MitoPQ does redox cycle in mitochondria, the MitoPQ radical cation, which should be sufficiently stable under anaerobic conditions, must be demonstrated and detected by spectrophotometry or EPR. In addition, mitochondrial targeting of other viologens with more positive one-electron reduction potential may result in more efficient redox cycling, with more superoxide produced at the same concentration of the redox cycler. It has been shown that diquat (one-electron reduction potential: −0.33 V) is more potent in stimulating mitochondrial H_2O_2 production than paraquat (one-electron reduction potential: −0.45 V).[350]

5.2.3. Mitochondria-Targeted Donors of Nitric Oxide and Related Species

MitoSNO: Mitochondria-targeted S-nitrosothiol (MitoSNO, Chart 51) was introduced as a potential cardioprotective agent.[351] Stability studies indicate that MitoSNO decays about two-fold faster than the nontargeted analog, S-nitroso-N-acetylpenicillamine, and that the decay is significantly increased in the presence of glutathione, probably due to the transnitrosation reaction.[351]

Significant membrane-potential-dependent mitochondrial uptake of MitoSNO occurs due to the presence of the lipophilic TPP^+ cation.[351] MitoSNO reversibly inhibits mitochondrial respiration at low O_2 concentrations. This mechanism may be significant in hypoxia, as S-nitrosation of mitochondrial complex I is plausible. MitoSNO also exhibits protective effects during the reperfusion after ischemia (I/R). It was proposed that this protection is a consequence of the persistent S-nitrosation of complex I. MitoSNO was most protective when administered during reperfusion, whereas most cardioprotective agents must be administered before I/R injury. The study on MitoSNO-derived S-nitrosation identified a small number of mitochondrial proteins that were persistently S-nitrosated by MitoSNO.[352] Three selected enzymes were identified as mitochondrial targets of S-nitrosation: mitochondrial aconitase, α-KGDH, and mitochondrial ALDH2. Their activities were significantly and reversibly inhibited by MitoSNO.[352] Later, the observed inhibition of complex I was shown to be a result of the selective S-nitrosation of Cys39 on the ND3 complex I subunit, which becomes susceptible to S-nitrosation during ischemia.[353] It was proposed that the reversible S-nitrosation of Cys39 slows the reactivation of mitochondria during the first minutes of the reperfusion, decreasing ROS production, oxidative damage, and cardiac tissue necrosis. It was also shown that intravenous (iv) administration of MitoSNO improves the long-term recovery of the heart following I/R injury.[354]

2-hydroxyamino-vinyl-TPP: A mitochondria-targeted nitric oxide ($^\bullet NO$)-donating prodrug (2-hydroxyamino-vinyl)-triphenylphosphonium (HVTP, Chart 51), was reported to liberate $^\bullet NO$ within mitochondria upon one-electron oxidation.[355] HVTP undergoes cytochrome c (cyt c)-cardiolipin (CL) complex-catalyzed oxidation in the presence of H_2O_2,

liberating •NO that inhibits CL-cyt c peroxidase activity. Because the formation of cytochrome c-cardiolipin complex (CL-cyt c) peroxidative activity is an early event in mitochondrial apoptosis, application of CL-cyt c inhibitors may be a promising antiapoptotic strategy to inhibit mitochondrial apoptosis.[356] HVTP was shown to be able to protect mouse embryonic cells against radiation-induced apoptosis.[357]

5.2.4. Mitochondria-Targeted Ascorbate—Ascorbic acid (vitamin C [Vit. C]) is one of the major and best-characterized hydrophilic, small-molecule antioxidants in biological systems. To direct ascorbic acid to mitochondria, Vit. C was linked to the TPP^+ moiety via a thioalkyl linker.[358] To target hydrophilic ascorbate ($pK_a = 4.4$), different alkyl linker chains were tested, and the number of methylene group ranged from 3 to 21 (Chart 52). While $MitoVitC_3$ seemed too hydrophilic for mitochondrial uptake, $MitoVitC_{11}$ accumulated in response to the mitochondrial membrane potential. The more hydrophobic analogs were also binding but were deemed too hydrophobic to handle easily. $MitoVitC_{11}$ displayed a pK_a similar to that of ascorbic acid ($pK_a = 4.3$), and its binding to mitochondria can be described, as discussed above for TPP^+-conjugated weak acids, with the involvement of the protonated form as the actual species crossing the phospholipid bilayer. Superoxide, peroxyl radicals, and Fe^{3+}, but not H_2O_2, were shown to oxidize $MitoVitC_{11}$. Glutathione or thioredoxin was demonstrated to recycle the oxidized form of $MitoVitC_{11}$. $MitoVitC_{11}$ was shown to prevent mitochondrial lipid peroxidation and protect mitochondrial aconitase from inactivation by superoxide.[358]

5.2.5. Mitochondria-Targeted Glutathione Peroxidase Mimetics—Hydroperoxides (e.g., H_2O_2) are regarded as important redox signaling and oxidative damage intermediates. Small molecule mimetics of glutathione peroxidases (GPx) were used as tools to remove both aliphatic and aromatic hydroperoxides and protect the cells from oxidative insults.[359] To selectively remove and probe the role of mitochondrial hydroperoxides, the GPx mimetic, ebselen, was linked to the TPP^+ moiety.[360] Mito-Ebselen (Chart 53) was shown to bind to energized mitochondria and be reduced by mitochondrial glutathione, a prerequisite for its peroxidase-like activity. Mito-Ebselen protected mitochondria from oxidative damage, but its activity was similar to the "untargeted" ebselen. This was explained by the significant but reversible binding of Mito-Ebselen to mitochondrial protein thiols, which limits its availability to react with hydroperoxides.

Subsequently, a new Mito-Ebselen analog was synthesized, Mito-Ebselen-2 (Chart 53), which was expected to have a lower affinity to cellular thiols.[361] Compared to Mito-Ebselen, the new analog was shown to be less toxic to cells and exhibit better radioprotective effects in vitro. Mito-Ebselen-2 also significantly extended the survival of mice exposed to γ-radiation, even when it was administered 24 h after the exposure.[361]

5.2.6. Mitochondria-Targeted Fullerene—Fullerenes are spherical molecules, typically made of 60 carbon atoms. They have applications in many fields of science, such as material engineering, nanotechnology, and biology.[362,363] For example, fullerenes were reported to interfere with the replication of HIV.[364] Fullerene derivatives exhibit a free-radical scavenging property that is attributed to its hollow spherical moiety.[365–367] However, one of the drawbacks of the fullerene moiety is its low solubility in water. In order to overcome its

low solubility and take advantage of its scavenging properties, mitochondria-targeted, monofunctionalized C_{60}-TPP^+ (TPP-C_{60}, Chart 54) was synthesized.[174]

Unfortunately, TPP-C_{60} did not accumulate in mitochondria.[174] While there seems to be no apparent reason for the lack of mitochondrial accumulation of C_{60}-TPP^+, no further attempts to target fullerenes to mitochondria were reported so far.

5.2.7. Mitochondria-Targeted Electrophiles—During pathophysiological conditions, increased oxidative insults derived from increased ROS and RNS generation can lead to oxidation of lipids or sugars producing weak electrophiles that, in turn, can react with key nucleophilic targets such as thiol groups present in cysteine residues of proteins or glutathione (GSH). These weak electrophiles, which are usually eicosanoids, modify proteins regulating biological function and pathological events such as cancer and inflammation.[368–370]

Mitochondria are organelles rich in electrophile-modifiable, cysteine-containing proteins and are an important target for electrophile-mediated cell signaling processes.[369–373] The cyclopentenone-like eicosanoid electrophile, 15-deoxy-$\Delta^{12,14}$-prostaglandin J_2 (15d-PGJ2), was reported to localize in mitochondria and is responsible for inducing ROS formation in endothelial cells.[374] However, previous work has shown that protein targets of 15d-PGJ2 are found in different sites in the cell, including the cytosol and mitochondria, evidencing the pleiotropic nature of the cyclopentenone.[373–375] In order to study the antiapoptotic effects of 15d-PGJ2 in mitochondria, two novel mitochondria-targeted derivatives of 15d-PGJ2 and prostaglandin E_2 were synthesized using the TPP^+ moiety: electrophilic Mito-15d-PGJ2 and non-electrophilic Mito-PGE2 (Chart 55).[371–375]

Mitochondrial targeting made 15d-PGJ2 less effective in targeting cytosolic pathways normally activated by this electrophile. Mito-15d-PGJ2 profoundly affected mitochondria bioenergetics and membrane potential, and it increased apoptosis in breast cancer cells, in contrast to nontargeted (15d-PGJ2) and nonelectrophilic, targeted (Mito-PGE2) analogs.[373]

Another class of mitochondria-targeted electrophiles is based on iodine-containing compounds (e.g., (4-iodobutyl)triphenylphosphonium [IBTP], Chart 55) that initially were developed as probes for labeling and quantification of mitochondrial protein cysteine residues.[376] Terminal iodine renders an electrophilic character to the adjacent carbon atom in the butyl chain, making it susceptible to nucleophilic attack by mitochondrial protein thiols. This enabled the development of a novel procedure to mass tag mitochondrial thiol proteins using IBTP that, in combination with proteomics, will help detect cysteine residues sensitive to post-translational modifications. This approach was applied to study ethanol-induced oxidation of mitochondrial protein thiols. Ethanol-fed rats were shown to have a significantly lower level of tagged protein thiols, specifically in mitochondrial matrix proteins.[377] Mitochondria-targeted soft electrophiles (MTSE) based on iodoalkyl-TPP^+ cations (Chart 55) were also tested for the treatment of breast cancer cells.[378] Compounds with an alkyl chain from 3–6 carbon atoms were shown to form adducts with mitochondrial proteins in a time-dependent fashion in MDA-MB-231 cells. Based on this observation, IBTP was selected as an optimal MTSE for further studies. IBTP is toxic to MDA-MB-231

breast cancer cells but not to nontumorigenic MCF-10A epithelial cells. IBTP was shown to inhibit cell migration and mitochondrial respiration, demonstrating that this class of mitochondria-targeted soft electrophiles may be potentially useful for treating breast cancer.

5.2.8. Mitochondria-Targeted Donors of Hydrogen Sulfide—Hydrogen sulfide (H_2S), long known for its toxic effects, is now recognized as a signaling molecule that exhibits protective effects against oxidative injury.[322–324] Thus, slow-releasing H_2S donors were used to protect cells from oxidative damage.[379] Because mitochondria were proposed as both the source and target of biological oxidants, the mitochondria-targeted H_2S donor, AP39, was synthesized by linking the TPP^+ moiety to the dithiolethione H_2S donor, DTA-OH (Chart 56).[380]

Using a nontargeted fluorescent probe for H_2S, 7-azido-4-methylcoumarin, and co-staining with MitoTracker Red, it was shown that the H_2S produced was at least partially localized in the mitochondria. AP39 protected endothelial cells from various oxidative insults at a concentration 1000-fold lower than did the nontargeted donor, GYY4137.[380,381] AP39 also protected rat kidney epithelial cells in vitro and partially prevented acute renal injury in rats in vivo.[382] Interestingly, although AP39 exerted protective effects in a mouse model of burn injury, similar effects were observed using an inhibitor of endogenous H_2S biosynthesis.[383] Another mitochondria-targeted H_2S donor, AP123, was recently synthesized by linking the hydroxythiobenzamide H_2S donor, HTB, to the TPP^+ moiety via a long alkyl chain (Chart 56).[384] Both AP39 and AP123 donors were shown to protect endothelial cells from hypoglycemia-induced oxidative damage and were proposed as potential protective agents against diabetic vascular complications.[384] AP39 was also reported to provide protection in vivo in mice subjected to cardiac arrest and cardiopulmonary resuscitation or to left anterior descending coronary ligation.[385,386] A major limitation of these donors is that the actual mechanism of intracellular H_2S release is still unknown.[387]

5.2.9. Mitochondria-Targeted Thiols—Cellular thiols provide a first-line small-molecule defense system against oxidants and electrophiles. Lipoic acid was shown to protect mitochondria from oxidative damage. Although lipoic acid is an intramolecular disulfide, inside the cells it is rapidly reduced to dithiol, dihydrolipoic acid (Chart 57), which may exhibit antioxidant activity in both direct (chemical scavenging of oxidants and electrophiles) and indirect (interaction with antioxidant enzymatic systems) mechanisms.[388] Therefore, to enhance the mitochondrial thiol-based antioxidant system, lipoic acid was conjugated to the TPP^+ moiety.[213] Both mitochondria-targeted lipoic acid, MitoL (Chart 57), and its reduced form, $MitoLH_2$, can bind to energized mitochondria; however, the compounds failed to protect cells from oxidative insults. This observation was explained by inefficient reduction of MitoL in cells and rapid S-methylation of the compound, blocking its redox activity.[213] Whether other mitochondria-targeted dithiols would suffer from similar limitations has not been tested.

An alternative approach proposed for mitochondrial delivery of lipoic acid included a reversible derivatization of lipoic acid with the TPP^+ moiety via an ester bond.[389] Incubation of isolated mitochondria with revMitoLipAc (Chart 57) induced hydrolysis of the ester bond with the formation of lipoic acid and TPP^+-linked alcohol. At a 1 μM concentration,

revMitoLipAc, but not lipoic acid or the "irreversible" analog, irrevMitoLipAc (MitoL), was shown to protect cells from organic hydroperoxide-induced damage.[389]

6. MITOCHONDRIA-TARGETED BIOACTIVE COMPOUNDS AS POTENTIAL THERAPEUTICS

6.1. Mitochondria-Targeted Quinones

Mitochondrial injury disrupts normal cell function, leading to alterations in tissue and organ function. Under certain circumstances, production of $O_2^{\bullet-}$ by mitochondria is anticipated to occur at rates high enough to circumvent the arsenal of specific antioxidant defenses (such as superoxide dismutase [MnSOD], glutathione peroxidases, and peroxiredoxins), promoting membrane lipid peroxidation and protein oxidation with ensuing loss of function. Accumulation of oxidative damage to specific mitochondrial structures leads to the progressive impaired tissue repair functions and disruption energy homeostatic mechanisms that contribute to senescence in whole organisms. Further, selective and localized damage is associated with the onset of a variety of chronic diseases, such as Alzheimer's, Parkinson's, amyotrophic lateral sclerosis (ALS), and cancer. A viable approach that could significantly reverse mitochondrial dysfunction is to increase the antioxidant potential through targeted delivery of antioxidant molecules.[15]

The therapeutic potential of coenzyme Q_{10} (CoQ_{10} or ubiquinone, Chart 58), which helps to normalize mitochondrial functions in several neuropathologies associated with genetic mitochondrial deficiencies, was recognized for a number of years.[390,391] In addition, CoQ_{10} is a naturally occurring lipid soluble antioxidant, the reduced form of which has a well-characterized lipid peroxidation-inhibitory activity.[392] This antioxidant activity is due to inhibition of the initiation step by direct scavenging of the oxidizing species; also, it likely involves direct reduction of the lipid alkoxyl and peroxyl radicals to a less reactive hydroxyl and hydroperoxide derivatives, breaking the chain of lipid peroxidation. The effective regeneration mechanism of the oxidized product ubiquinone is a key aspect in its antioxidant potential. Under normal conditions, cells produce significant amounts of CoQ to fulfill their specific requirements and, though CoQ is found in blood, its uptake into different tissues is limited. This characteristic limited uptake may be due to specific receptors being required to uptake CoQ into cells.[393] The regulation of CoQ levels in different tissues in heath and disease is not well characterized, and the specific analysis of CoQ concentrations in the mitochondria in different diseases is still fragmentary.

Mitoquinone ($MitoQ_{10}$), a TPP^+-linked analog of ubiquinone (Chart 58), was developed to improve mitochondrial antioxidant potential and limit mitochondrial lipid peroxidation.[211] MitoQ was shown to rapidly accumulate in mitochondria, as discussed previously, and undergo fast reduction to the hydroquinone form (mitoquinol, $MitoQ_{10}H_2$, Chart 59).

MitoQ inhibited mitochondrial lipid peroxidation induced by Fenton's reagent, and the effects were attributed to the radical scavenging activity of $MitoQH_2$.[211] In fact, pulse radiolysis studies indicated that $MitoQH_2$ is a good scavenger of peroxyl radicals, with the rate constant of 1.5×10^8 $M^{-1}s^{-1}$ determined for the $HOCH_2OO^{\bullet}$ radical in methanol.[394]

Interestingly, MitoQ was reported to redox cycle in cell-free systems and increase superoxide production in intact endothelial and breast cancer cells, although it is not clear if these two observations are linked.[19,395] The chemical equilibrium between MitoQ and superoxide (Chart 60) was studied by pulse radiolysis in water and methanol as a less polar solvent.[394]

MitoQ (but not $MitoQH_2$) was shown to react rapidly with superoxide, with the rate constant of 2×10^8 $M^{-1}s^{-1}$ and 4×10^8 $M^{-1}s^{-1}$ in aqueous and methanolic solutions, respectively. The rate constant of the reverse reaction of the semiquinone radical with oxygen to form superoxide was lower, equal to 2.9×10^7 $M^{-1}s^{-1}$ and 7.3×10^6 $M^{-1}s^{-1}$ in aqueous and methanolic solutions, respectively.[394] This indicates that, depending on the experimental conditions, MitoQ may act both as an efficient superoxide scavenger and superoxide generator via redox cycling, and in less polar environment superoxide scavenging may be predominant. In fact, the good safety profiles of MitoQ in the in vivo preclinical models and in humans, as discussed subsequently, indicate that even if the redox cycling of MitoQ occurs in vivo, it does not overwhelm the cellular antioxidant systems. A pharmaceutical-grade composition of MitoQ, as methanosulphonate and mesylate salts, is now available for human use. Several clinical trials testing the effects of MitoQ on cognitive, vascular, and motor performance in middle-aged adults and in the treatment of nonalcoholic fatty liver disease are underway. Also, MitoQ was tested to treat hepatitis c, specifically the decrease in aminotransferases activity, which is an index of tissue necrosis. If proven effective, MitoQ will be the first antioxidant therapeutic agent to effectively delay organ dysfunction and link oxidant production with the cause of disease. Moreover, the membrane permeability of MitoQ enhances its uptake in the brain and opens up the possibility of treating neurological degenerative diseases that have been connected with cell death mediated by oxidative injury.[159]

Another mitochondria-targeted quinone, 10-(6′-plastoquinonyl) decyltriphenylphosphonium bromide (SkQ1), an analog of plastoquinone (Chart 58), has shown potent antioxidant activity, has lower prooxidant activity than MitoQ, and presents a partition coefficient comparable to that of MitoQ.[82] SkQ1 forms complexes with the cardiolipin anion in the mitochondria and undergoes the oxidation-reduction reactions that prevent lipid peroxidation, which indicates its antioxidant activity.[63] Both prevention of the peroxidation of cardiolipin and the mild uncoupling and inhibition of $O_2^{\bullet-}$ formation in mitochondria via fatty acid cycling appear to be important in the mechanisms explaining cellular effects of SkQ1.[82] The antioxidant effects were observed at very low concentrations of the compound; however, at higher concentrations, it became a prooxidant. The range of effective "antioxidant" activity of SkQ1 is larger than that of MitoQ, which represents a potential significant advantage of SkQ1 applications in the clinics. The reported rate constant for scavenging lipid peroxyl radicals for the reduced form of SkQ1 ($SkQ1H_2$, $k = 2.2 \times 10^5$ $M^{-1}s^{-1}$) is *ca.* four-fold higher than that of the reduced form of MitoQ ($MitoQ_{10}H_2$, $k = 0.58 \times 10^5$ $M^{-1}s^{-1}$) and three-fold-higher than of α-tocopherol ($k = 0.7 \times 10^5$ $M^{-1}s^{-1}$).[63,396] Thus far, SkQ1 has been tested and has provided promising results in diverse disease models including stroke, autoimmune arthritis, and neurobehavioral disorders.[91,397,398] Moreover, clinical trials of SkQ1 to treat dry eye syndrome were successfully completed.[399–401] SkQ1 currently is prescribed as drops of 0.25 μM solution for the treatment of this common

condition that develops with age. This is the first clinically used, mitochondria-targeted ocular drug.[402]

6.2. Mitochondria-Targeted Nitroxides

Stable nitroxides have been long known for their protective effects against oxidative stress injury.[403,404] Nitroxides can undergo both one-electron oxidation and one-electron reduction, forming a three-component redox system, including hydroxylamine, nitroxide, and the oxoammonium cation (Chart 61).

In cells, both nitroxides and oxoammonium cations are assumed to undergo reduction to hydroxylamines; however, the kinetics of the reduction is structure-dependent, with five-membered cyclic nitroxides being more resistant than six-membered analogs. The proposed mechanisms of cytoprotection by nitroxides include superoxide scavenging (superoxide dismutase-like activity), and scavenging of carbon-centered alkoxyl and peroxyl radicals.[404] Nitroxides have also been shown to switch peroxidase activity into the catalase-like activity of heme proteins.[405,406] To protect mitochondria from oxidative damage, various nitroxides were linked to mitochondria-targeting moieties (e.g., TPP^+) and evaluated for their efficiency of cell protection in different models of oxidative injury.[407]

Mito-carboxyPROXYL (Mito-CP)—Although TPP^+-linked analogs of nitroxides were synthesized almost 40 years ago in order to measure transmembrane potentials by EPR, Mito-CP was the first mitochondria-targeted nitroxide developed as an antioxidant agent and mitochondria-targeted mimetic of superoxide dismutase.[164,408] EPR analyses of subcellular fractions were used to demonstrate that Mito-CP is cell permeable and rapidly accumulates in the mitochondria of endothelial cells (Figure 9). On the other hand, untargeted CP slowly enters the cells but no nitroxide EPR signal can be detected in mitochondrial fractions. This demonstrates that derivatization of CP by conjugation with the TPP^+ cation via a long alkyl chain improves the kinetics of cellular uptake and targets it to mitochondria. This also shows that, even after prolonged incubation (> 8 h), the compound remains at least partially present in the oxidized (nitroxide), EPR active redox form.

Mito-CP protects endothelial cells from oxidative injury induced by cell exposure to a steady-state flux of H_2O_2 or lipid peroxides.[164] Mito-CP was subsequently used as a probe to study the role of mitochondrial superoxide in cancer cell proliferation. Significant antiproliferative effects of Mito-CP against cancer cells suggest that mitochondrially generated superoxide plays an important role in cancer growth.[409] However, this interpretation was later challenged by the use of a Mito-CP analog lacking the nitroxide moiety (Mito-CP-Ac, Figure 10A).[17] Spin trapping experiments show that, whereas Mito-CP displays superoxide-scavenging activity, Mito-CP-Ac does not (Figure 10B). Furthermore, Mito-CP-Ac remains intact inside the cells (Figure 10C), excluding the possibility of being metabolized to redox-active Mito-CP inside the cells. Thus, although Mito-CP-Ac lacks the superoxide-scavenging activity of Mito-CP, both compounds exhibit similar antiproliferative activities in cancer cells (Figure 10D).[17]

It was proposed that the ability of Mito-CP and Mito-CP-Ac to modulate cellular bioenergetic status was the predominant mechanism of their antiproliferative activities.

Mito-CP was shown to prevent the oxidative injury and preserve hepatic function in the hepatic ischemia-reperfusion in vivo model.[410] New Mito-CP analogs, with a short-chain linker between the TPP^+ and PROXYL moieties, have recently been reported and shown to exhibit antihypertensive properties.[411] While the SOD-like activity of these compounds may be important, other mechanisms, including catalase-like activity of nitroxide/heme systems and scavenging of radical species other than superoxide, should also be considered.[403–406] As discussed above, the redox-inactive analogs should be tested in parallel, to understand the importance of the redox reactions of the nitroxide moiety in the effects of this class of compounds.

Hemigramicidin-TEMPO conjugates—To target TEMPO (2,2,6,6-tetramethylpiperidine-N-oxyl) to mitochondria, 4-amino-TEMPO was conjugated to fragments of the gramicidin S cyclopeptide antibiotic, which is characterized by a high affinity to bacterial membranes.[131,132] The synthetic peptide, XJB-5-131 (Chart 2), accumulates in cell mitochondria and prevents oxidant-induced cell death.[132] Intracellularly, the nitroxide underwent partial reduction to EPR-inactive hydroxylamine. In rats subjected to hemorrhagic shock, XJB-5-131 protected the mucosal barrier function, decreased the extent of cardiolipin peroxidation, and extended the animals' survival.[132] Hemigramicidin S-TEMPO conjugates possess radioprotective effects in vitro and in vivo.[412–416] Preventing the oxidation of mitochondrial lipids by hemigramicidin S-TEMPO conjugates was shown to protect cells from ferroptosis, the oxidative, nonapoptotic form of cell death characterized by an iron-dependent accumulation of lipid peroxides.[417]

Triphenylphosphonium-conjugated TEMPO derivatives—In the late 1970s and 1980s, TPP^+-linked derivatives of TEMPO were synthesized to study the transport of hydrophobic ions through membranes.[160,408,418] More recently, in an attempt to introduce nitroxide as a potent antioxidant to mitochondria, several groups have synthesized structurally similar mitochondria-targeted TEMPO analogs via attachment to the TPP^+ moiety using linkers of a different chemical nature, various alkyl chain lengths, and, thus, different hydrophobicity (Chart 62).[265,340,419,420]

Mito-TEMPOL was shown to be able to scavenge superoxide, oxidize EDTA-complexed reduced iron, and inhibit lipid peroxidation in the chemical systems.[264] Mito-TEMPOL was taken up rapidly by energized mitochondria, where it underwent a rapid reduction to hydroxylamine, mediated by ubiquinol. The hydroxylamine form of Mito-TEMPOL was concluded to be the predominant form present is cells and is the major form responsible for the antioxidant effects observed.[265] A series of TPP^+-linked TEMPO and CP derivatives were tested for their radioprotective effects in cultured cells in vitro.[419] Interestingly, in the model used, the analogs containing the linker amide bond next to the TEMPOL or PROXYL moiety did not show protection, while 4-imino-TEMPO derivative (TPEY-Tempo) prevented radiation-induced cardiolipin oxidation and cell apoptosis.[419] TPEY-Tempo was subsequently shown to exert radioprotective effects in the in vivo models.[421] Also, antihypertensive activity of Mito-$TEMPO_2$ (Chart 62) in mice was reported.[422] Mito-$TEMPOL_4$ was shown to exhibit cardioprotective and chemotherapeutic effects in a syngeneic breast tumor preclinical rat model, as discussed in a subsequent section.[420]

6.3. Mitochondria-Targeted Tocopherols

Vitamin E comprises several tocopherols and tocotrienols that have long been known to provide protection from lipid peroxidation. In addition, new roles and mechanisms of vitamin E in cell protection and signaling are emerging.[423,424] To provide site-specific antioxidant protection to mitochondria, an analog of α-tocopherol was synthesized by linking the chromanol part of α-tocopherol to the TPP^+ moiety via a two-carbon aliphatic linker.[60] $MitoVit_2$ E (Chart 63) was shown to bind to energized mitochondria and protect them from oxidative damage in a concentration-dependent manner. Treatment of the cells with $MitoVit_2$ E led to its accumulation in the mitochondria and did not show toxic effects after a 24-h incubation period at a maximum concentration of 10 μM.[60]

$MitoVit_2$ E, but not "untargeted" α-tocopherol, was shown to protect endothelial cells from H_2O_2-induced iron uptake, inactivation of mitochondrial complex I, and apoptosis.[425] A series of MitoVit E analogs were synthesized varying the length of the alkyl linker, and with the hydroxyl group of the chromanol moiety esterified with a succinic acid (Chart 63).[426,427] The homolog bearing 11 carbon atoms in the linker, called $MitoVE_{11}S$, was shown to induce apoptosis in cancer cells in vitro and suppress tumor growth in vivo. The proposed mechanism involved inhibition of the electron transfer between mitochondrial complexes II and III, leading to increased production of mitochondrial superoxide.[426,427] At a low micromolar concentration, $MitoVE_{11}S$ was reported to act as mitochondrial uncoupler, both in isolated mitochondria and intact cells.[428] The antitumor effects of $MitoVE_{11}S$ were also linked to its antiangiogenic activity, and inhibition of mitochondrial DNA transcription and mitogenesis were observed both in vitro and in vivo.[429,430] Interestingly, $MitoVE_{11}S$ efficiently blocked the proliferation of both VES-sensitive and VES-resistant cell lines.[431] Although it was assumed that the succinate moiety was important for interaction with mitochondrial complex II, the susceptibility of mitochondria-targeted vitamin E succinate (MitoVES) to intracellular hydrolysis, and the anticancer effects of $MitoVE_{11}S$ were not compared with its hydrolyzed analog, $MitoVE_{11}$. However, another report demonstrated that $MitoVit_{11}$ E (Mito-ChM, Chart 63) and its acetate ester (Mito-ChMAc) were capable of inducing cell death in several lines of breast cancer cells.[432] As the acetate ester undergoes rapid intracellular hydrolysis, the stability of MitoVES in cells and tissues and the importance of the succinate moiety in its antiproliferative effects have yet to be demonstrated. Another MitoVit E analog was prepared using the solid-phase synthesis, with a lysine linker between the chromanol and TPP^+ moieties.[433] It was reported that the compound decreases oxidative stress in endothelial cells in vitro and accumulates in mouse heart mitochondria in vivo. Recently, a new general synthetic pathway to MitoVit E homologs, which have alkyl chain lengths ranging from 2 to 11 carbon atoms, was reported.[434] In the cell-free system, $MitoVit_2$ E and $MitoVit_{10}$ E showed similar protective effects against lipid peroxidation in rat liver mitochondria, significantly stronger than the "untargeted" chromanol analog. α-tocopheryl succinate (VES) was also delivered to mitochondria using TPP^+-tagged nanoparticles as a vehicle.[151] VES-loaded mitochondria-targeted nanoparticles were shown to be more cytotoxic toward neuroblastoma cells than free VES or VES-loaded "untargeted" nanoparticles.

Although many mitochondria-targeted analogs of α-tocopherol were synthesized as described above, no attempts to synthesize other forms of vitamin E were reported. For example, γ-tocopherol was shown to exhibit superior antioxidative reactivity, so it would be of interest to compare its mitochondria-targeted analog with the MitoVit E structures described above in protecting mitochondria from oxidative insults.

6.4. Mitochondria-Targeted Uncouplers

The protonmotive force generated during the electron transfer from mitochondrial substrates to oxygen is used to synthesize ATP (OXPHOS) or is dissipated by proton leak into the mitochondrial matrix with the generation of heat (thermogenesis). While complete uncoupling of substrates oxidation from ATP production may be detrimental to cell bioenergetic status, it was proposed that "mild uncoupling" may be a viable therapeutic strategy for obesity through mitochondrial oxidation of excess fatty acids.[435,436] TPP^+ cations bearing long alkyl chains efficiently promote the mitochondrial uncoupling activity of fatty acids, 2,4-dinitrophenol (DNP) and FCCP, possibly via formation of ion pairs to decrease the energy barrier for transport.[437,438] Interestingly, a similar effect was observed for hydrophobic rhodamine-, berberine-, and palmatine-based cations.[63,439] Hydrophobic membrane-penetrating cations may be used to treat obesity by increasing the uncoupling activity and oxidation of endogenous fatty acids and to lower the effective concentrations of the therapeutically relevant mitochondrial uncouplers.[437] In fact, TPP^+-C_{12} was shown to combat high-fat-diet-induced obesity in mice.[440] Several attempts were made to covalently conjugate uncoupling agents to the mitochondria-targeting moiety, in order to improve their efficiency and selectivity and decrease the potential toxicity.

Mitochondria-targeted DNP—The DNP uncoupler was linked to the TPP^+ moiety to generate the mitochondria-targeted uncoupler, Mito-DNP (Chart 64).[441] It was postulated that, by using the TPP^+ moiety, the mitochondrial uptake of the uncoupler would be dependent on the mitochondrial membrane potential, and, thus, would be self-limiting, avoiding complete uncoupling of mitochondria and mitigating its cytotoxicity. Whereas Mito-DNP was shown to bind to mitochondria in a membrane-potential-dependent manner, it failed to act as a protonophore (or proton shuttle), possibly due to the inefficient efflux of its deprotonated form from the mitochondrial matrix to the medium.[441]

An interesting approach to target DNP to mitochondria was reported using a trifunctional compound bearing the "caged" DNP moiety, mitochondria-targeting TPP^+, and the H_2O_2- (and $ONOO^-$-) reactive boronate moiety for DNP activation (MitoDNP-SUM, Chart 64).[442] The compound was shown to release "free" DNP in mitochondria under the conditions of H_2O_2 production. A similar strategy was also proposed for mitochondria-targeted "caged" DNP, activatable by light (MitoPhotoDNP, Chart 64).[443] Here, instead of using the boronate moiety as the oxidant sensor, the DNP and TPP^+ moieties are linked via the ortho-nitrobenzyl moiety, which acts as a photocleavable group. Upon light exposure, DNP is released, leading to mitochondrial uncoupling of smooth muscle cells.[443] Potentially, both approaches can also be used for mitochondrial delivery of therapeutics, activatable by mitochondrial H_2O_2 or light.[442,443]

Also, DNP was delivered to cell mitochondria using TPP^+-tagged nanoparticles.[151] Mitochondria-targeted nanoparticles loaded with DNP led to a significant decrease in the accumulation of lipids during the differentiation of preadipocytes into adipocytes. Significantly higher concentrations of free DNP or DNP-loaded untargeted nanoparticles had to be used to obtain similar effects.[151]

MitoFluo—A TPP^+-linked derivative of fluorescein called mitoFluo (10-[2-(3-hydroxy-6-oxo-xanthen-9-yl)benzoyl]oxydecyl-triphenylphosphonium bromide, Chart 64) was also reported as a mitochondria-targeted protophoric uncoupler because it facilitates proton transfer across the mitochondrial membrane and stimulates mitochondrial respiration.[444] Similar effects were observed previously for the dodecyl and octyl esters of fluorescein.[445] The fluorescent properties of mitoFluo enabled the study on the uptake of the probe from medium to mitochondria. The energization of mitochondria with succinate resulted in the probe uptake.[444] The study on mitoFluo cytotoxicity showed a decrease in the viability of L929 fibrosarcoma cells, starting with 2 μM mitoFluo.[444] Recently, the protonophoric and uncoupling properties of mitoFluo were compared with those of the newly synthesized analog C_4-mitoFluo, which has a butyl spacer.[446] Contrary to mitoFluo, C_4-mitoFluo was unable to induce the collapse of the mitochondrial-membrane potential or to stimulate mitochondrial respiration. The observed differences in the uncoupling activity of both compounds were correlated with the differences in their protonophoric activity on a lipid membrane.[446] MitoFluo was shown to attenuate kidney injury after ischemia/reperfusion in rats. It was also effective in preventing the consequences of brain trauma in rats.[446]

6.5. Mitochondria-Targeting Dichloroacetate

Dichloroacetate (DCA) is an orally available small molecule inhibitor of pyruvate dehydrogenase kinase (PDK) currently undergoing clinical trials for a variety of cancers. Phosphorylation of pyruvate kinase by PDK inhibits the pyruvate utilization by mitochondrial OXPHOS and promotes glycolysis leading to the Warburg phenotype. DCA, by inhibiting PDK, re-routes pyruvate into mitochondrial metabolism, leading to decreased glycolytic function and increased mitochondrial respiration, which induces apoptotic signaling in cancer cells sensitizing them to other treatments.[447,448] To improve the bioavailability and increase the mitochondrial accumulation of DCA, it was linked to the TPP^+ moiety.[449] Interestingly, two analogs were synthesized, one with a TPP^+ moiety linked to a single DCA molecule via an alkyl chain (TPP-DCA, Chart 65), and the second with three DCA molecules attached via a tris(hydroxymethyl)aminomethane (Tris) linker to a single TPP^+ moiety (Mito-DCA, Chart 65). Both compounds induced mitochondrial metabolism and downregulated glycolysis, as determined by observation of increased mitochondrial membrane potential and intracellular ATP levels, along with decreased intracellular levels of lactic acid.

In all these assays mitochondria-targeted dichloroacetate (Mito-DCA) was more efficient than the TPP-DCA analog. Mito-DCA was *ca.* 100- to 1000-fold more potent than DCA in inhibiting the viability of several prostate cancer cell lines without affecting the viability of human mesenchymal stem cells.[449] An additional approach for the mitochondrial delivery of DCA is based on the conjugation of DCA with tris(aminoethyl)amine.[219] The product was

10-fold more potent in inhibiting proliferation of various cancer cell lines, although its mitochondrial delivery was not ascertained. In both approaches the intracellular/intramitochondrial release of free DCA molecules has yet to be demonstrated.

6.6. Mitochondrial-Targeted Metformin

Metformin is currently a first-line orally available glucose-lowering drug and is also the most prescribed antidiabetic drug in the world.[450] Although metformin is not metabolized itself, its efficacy is attributed to the modulation of cellular metabolic pathways.[451–454] Epidemiological studies recently have shown an association between metformin use and decreased incidence of cancer and cardiovascular diseases.[455–458] It is assumed that mitochondria are the major target of metformin, as metformin inhibits mitochondrial respiration, leading to AMPK activation and bioenergetic reprogramming.[454,459,460] As metformin is a hydrophilic cationic compound, its cellular and mitochondrial uptake is limited mostly to specific cationic transporters rather than via passive diffusion through the membranes. Thus, for mitochondrial delivery of metformin, it was linked to TPP^+ cation via alkyl linkers of various lengths (Chart 66). Increasing the linker length improved the ability of mito-metformins to inhibit mitochondrial respiration and proliferation of pancreatic cancer cells.[21,461] The mechanistic aspects of the antiproliferative effects of mito-metformins are discussed later.

6.7. Mitochondria-Targeted Hsp90 Inhibitors

90 kDa heat shock proteins (Hsp90) are a family of homodimeric ATPases serving as molecular chaperones responsible for correct folding of many newly synthesized polypeptides and misfolded proteins.[462,463] Because many Hsp90 client proteins are in oncogenic signaling pathways, Hsp90 was proposed as a therapeutic target for anticancer strategies.[464] Geldanamycin is a naturally occurring antibiotic, with Hsp90 identified as its molecular target. Although geldanamycin displays unfavorable pharmacokinetic and toxicity profiles, one of its derivatives, tanespimycin, was the first Hsp90 inhibitor, which progressed into clinical trials. To selectively target mitochondrial Hsp90 proteins, geldanamycin was derivatized to target the mitochondria (Chart 67).

Two strategies were tested: (i) attachment to multiple (n = 1–4) cationic cyclic guanidinium moieties ($G\text{-}G_n$), and (ii) attachment to the TPP^+ moiety (G-TPP).[110] These compounds, called gamitrinibs, bind to mitochondria isolated from HeLa cells and induce the release of cytochrome c. Both TPP^+- and cyclic guanidinium-linked derivatives of geldanamycin were shown to be significantly more potent than the underivatized parent molecule, when tested for their effect on cancer cell viability.[110] In a broad spectrum of different cancer cell lines, the derivative carrying four cyclic guanidinium moieties was at least 10-fold more potent than the parent compound. All mitochondria-targeted derivatives exhibit stronger antitumor effects than geldanamycin in in vivo xenograft models.[110,465]

One of the members of Hsp90 family of molecular chaperones is mitochondrial tumor necrosis factor receptor-associated protein-1 (Trap-1).[466] To efficiently and selectively inhibit Trap-1 in mitochondria, the Hsp90 inhibitor, PU-H71, was linked to the TPP^+ moiety (SMTIN-P01, Chart 67).[467] Derivatization with TPP^+ significantly enhanced mitochondrial

accumulation of the inhibitor. Similar to the gamitrinibs inhibitors described above, SMTIN-P01 was able to induce mitochondrial membrane depolarization, and showed stronger cytotoxicity toward cancer cells when compared with the "untargeted" parent inhibitor.[467]

6.8. Mitochondria-Targeted Polyphenolic Compounds

Plant polyphenols continue to be the object of intense research, due to their low toxicity and relevance to multiple pathophysiological conditions from cardiovascular dysfunction, via neurodegeneration to cancer. Polyphenols were shown to act as very efficient free-radical scavengers in chemical systems; initially, direct oxidant scavenging activity was assumed to be the major mechanism of their protective effects. However, it is now clear that, due to their physicochemical properties and rapid metabolism in vivo, the mechanism of action must involve interaction with specific proteins/receptors. Polyphenolic compounds were shown to affect cell metabolism and mitochondrial function, e.g., via inhibition of hexokinase activity, modulation of the activity of thioredoxin reductases, depletion of cellular the glutathione level, and inhibition of mitochondrial ETC complexes.[468,469] As many anticancer effects reported for plant polyphenols were attributed to their effects on cancer cell mitochondria, several mitochondria-targeted derivatives were designed and tested for their anticancer effects.

Resveratrol—Attachment of the TPP^+ moiety to resveratrol (Mito-resveratrol, R = H, Chart 68) significantly increased its antiproliferative activity against colon tumor cells, regardless of the acetylation status of the hydroxyl groups.[470] Subsequently, more analogs of mito-resveratrol were synthesized (Chart 68), and it was shown that methylation of the hydroxyl groups increased the cytotoxic effects of mito-resveratrol.[471] The mechanism involved was postulated to increase formation of H_2O_2, as the exogenously added PEG-catalase, but not PEG-SOD, attenuated the antiproliferative effects of the compounds. The mitochondria-targeted resveratrol analogs were concluded to exhibit anticancer effects via mitochondrial generation of H_2O_2, formed from dismutation of superoxide.[471]

Further research led to the identification of mitochondrial complexes I and III as possible sources of superoxide. Interestingly, mito-resveratrol behaves as a mitochondrial uncoupler, regardless of the methylation status of the hydroxyl groups.[20] Mitochondrial delivery of resveratrol was also achieved with the use of dequalinium-based mitochondria-targeted liposomes, leading to anticancer effects against resistant lung cancer cells.[472]

Quercetin—Similar to resveratrol, another polyphenol, quercetin, was conjugated to the TPP^+ moiety to increase its mitochondrial accumulation (Chart 69).[473]

Mito-quercetin was shown to inhibit ATPase in permeabilized rat liver mitochondria and inhibit proliferation of colon tumor cells more efficiently than quercetin. Mito-quercetin (and its analog carrying acetylated hydroxyl groups) induced mitochondrial permeability transition and behaved like an uncoupler in isolated mitochondria.[474] In intact cells, mito-quercetin induced mitochondrial depolarization and oxidation of the MitoSOX Red probe, suggesting generation of mitochondrial oxidants.[474,475] In contrast to mitochondria-targeted resveratrol, mito-quercetin cytotoxic effects were attenuated by both PEG-SOD and PEG-

catalase. Also, methylation of free hydroxyl groups led to attenuation of its cytotoxic effects.[476]

Curcumin—Although curcumin was shown to exhibit antiproliferative effects against cancer cells in vitro, its anticancer efficacy in vivo was limited due to low bioavailability. Mitochondria-targeted analogs of curcumin were synthesized by derivatization of one or both hydroxyl groups of curcumin with the alkyl-TPP^+ moiety (Chart 70).[477] It was shown that mito-curcumins exhibit significant antiproliferative effects in vitro in various cancer cell lines, but not in nontumorigenic MCF-10A cells. The proposed mechanism of action involved induction of mitochondrial superoxide generation, inhibition of STAT3 and Akt phosphorylation, enhanced ERK phosphorylation, and upregulation of proapoptotic BNIP3 expression.[477]

The mitochondria-targeted, TPP^+-linked oxovanadium complex of curcumin (Cur-V-TPP, Chart 70) was reported as a phototoxic complex for photodynamic therapy.[478] While the synthesized complex was cytotoxic even in the dark, exposure to light significantly increased cytostatic and cytotoxic effects against MCF-7 and HeLa cancer cells.

Also, curcumin-loaded mitochondria-targeted nanoparticles were reported to exhibit protective effects in human neuroblastoma cells against the cytotoxic effects of amyloid β.[151]

7. MITOCHONDRIA-TARGETED THERAPEUTICS IN THE PRE-CLINICAL MODELS

7.1. In Vivo Biodistribution and Pharmacokinetics of Mitochondria-Targeted Compounds

In view of the potential use of selected mitochondria-targeted compounds in preclinical and clinical in vivo studies, the whole organism distribution and pharmacokinetic properties of the selected compounds were investigated. In addition, in vivo studies of radiotracers for positron emission tomography (PET) imaging also resulted in the data on distribution and pharmacokinetics of the mitochondria-targeted compounds. As discussed below, the compounds proposed for PET imaging indicated a significant uptake of the lipophilic compounds in heart and tumor tissues. This enabled the use of such compounds for noninvasive imaging of myocardium and tumors in vivo. Among other organs commonly labeled with the lipophilic compounds were the kidney, liver, and gut. Below are some data on the biodistribution of selected mitochondria-targeted compounds.

TPP^+-linked to alkyl chain, phenyl or benzyl ring: Administration of TPMP intraperitoneally (ip) to mice results in rapid accumulation in the liver, followed by redistribution to the heart within 16 h and clearance after 24 h.[159] TPMP was shown to exhibit low permeability and no accumulation in brains of healthy mice.[159,479] Brain accumulation of TPMP was dependent on the route of administration. No brain accumulation was detected upon ip injection but levels were detectable upon iv injection or feeding mice the compound in drinking water.[159] More hydrophobic analog, TPP^+-C_{10}, rapidly accumulated in mouse liver and kidney after iv injection, with almost complete

clearance within 24 h.[480] TPP accumulated in mouse heart and liver within 5 min after administration. No significant accumulation in the brain was observed.[481,482] ^{18}F-fluorobenzyltriphenylphosphonium accumulated in the kidney, gallbladder, heart, and liver of dogs after administration via a femoral vein.[483] In mice, the probe accumulated mostly in the kidney, heart, and liver.[484] ^{18}F-fluorophenyltriphenylphosphonium accumulated in rat kidney and heart.[485]

MitoQ: It was reported that feeding mice with $MitoQ_{10}$ (Chart 58) in drinking water led to its accumulation in the liver, kidney, skeletal muscles, heart, and brain, with the liver exhibiting the highest and brain the lowest accumulation.[159] Single iv administration led to a rapid uptake by the kidney and liver; accumulation in the heart was significantly lower and accumulation in brain was negligible.[486] Whereas MitoQ was cleared from most organs within 24 h, low but detectable amounts were detected in the mouse heart even 48 h after an iv injection. While showing similar pharmacokinetic behavior, absolute levels of $MitoQ_{10}$ tissue accumulation were more than one order magnitude higher than that of corresponding TPP^+-C_{10} after an iv injection.[486] MitoQ, in the form of tablets containing its mesylate (methanesulfonate) salt, was also tested in humans (in phase 1 and 2 clinical trials), at the doses of 40 and 80 mg/day (0.5 and 1 mg/kg).[487,488] Administration of 80 mg of MitoQ led to maximal plasma concentration of 33 ng/ml (~50 nM) measured 1 hr after single oral intake.[36] Continuous daily administration of MitoQ tablets for up to 1 month led to average plasma concentrations of 3 and 6 ng/mL (~5 and 10 nM) for the doses of 40 and 80 mg per day, respectively.[487]

Mito-Vit-E: Although several forms of mitochondria-targeted vitamin E (Chart 63) were reported, the kidney was one of the common and major targets.[159,432] Other target organs included the heart, liver, and brain. Interestingly, Mito-$VitE_2$ accumulated in those organs 10-fold higher than $MitoQ_{10}$.[159]

Mito-CP: After iv administration, Mito-CP (Figure 9) is absorbed from rat blood within minutes, as determined by in vivo EPR.[489] Mito-CP underwent reduction in vivo and was present as both nitroxide and hydroxylamine in both mouse blood and kidney tissue.[490] Within 12 h, the compound was completely cleared from both mouse blood and kidney tissue.[490]

7.2. Potential Toxicity of the Mitochondria-Targeted Agents

—Although only few papers report results of the toxicity studies of the mitochondria-targeted compounds, the dosage of the compounds that do not lead to apparent toxicity can often be inferred from in vivo preclinical studies. Based on the dosage required for acute toxicity for different TPP^+-containing compounds, the toxicity of the TPP^+-conjugated compounds is postulated to be mainly due to the TPP^+ moiety itself, rather than the side chain.[159] In case of human studies, only MitoQ and SkQ1 (Chart 58) were introduced to clinical trials, with neither compound showing signs of systemic toxicity when used at pharmacologically relevant doses.

MitoQ and SkQ1: The most data on *in vivo* toxicity were obtained for MitoQ (Chart 58), as it was approved for clinical trials.[487,488] MitoQ is now available in health food stores for enhancing energy, although it has not undergone an extensive clinical trial for this purpose. Results obtained so far in humans indicate that MitoQ can be safely administered daily for one year at a dosage (1 mg/kg) high enough to decrease liver damage in patients bearing the hepatitis C virus.[487,488,491] The reported adverse effects of MitoQ administration included headache, mild nausea, and vomiting.[487,488] It was reported that MitoQ did not show any toxicity in rats at the dosage of 0.5 g/kg per day.[492] In mice, the highest tolerable dosage of MitoQ was reported as 20 mg/kg following a single iv administration, and 230 mg/kg per day when fed a liquid diet supplemented with the compound.

The other TPP^+-linked quinone tested in clinical trials is SkQ1, which was administered locally to humans, in the form of eye droplets. At the effective doses of 0.155 and 1.55 μg/mL (0.25 and 2.5 μM, respectively) the compound did not show local or systemic toxicity, when administered as one to two drops, two times per day for a period of 4 weeks.[400,401]

MitoVit E: The maximal tolerated dose of Mito-$VitE_2$ (Chart 63) upon a single *iv* administration was reported as 6 mg/kg in mice.[159] Mito-$VitE_2$ was shown to be well tolerated in mice fed with Mito-$VitE_2$ in drinking water at the dosage of 60 mg/kg per day.[159] Similarly, treatment of mice *via* oral gavage with another mitochondria-targeted analog of Vit E bearing the 10-carbon alkyl linker, Mito-ChM, at the dosage of 60 mg/kg five times per week for four weeks did not lead to any apparent toxic effects.[432]

Mito-apocynin: When administered via oral gavage three times per week for 12 months at the dosage of 3 mg/kg or for 24 weeks at the dosage of 10 mg/kg, high enough to exhibit neuroprotective effects, Mito-Apo_{11} (Figure 2) was shown to be nontoxic in mice models.[493,494] Also, the short-chain homolog, Mito-Apo_2, was shown to be safe and neuroprotective in mice treated daily via oral gavage for 12 days at the dosage of 3 mg/kg.[495]

Mito-metformin: Mito-Met_{10} (Chart 64) did not show any apparent toxicity when administered daily *via* ip for two weeks at the dosage of 1 mg/kg.[21] The maximal tolerated dosage for daily ip administration was reported to be 4.4 μmol/kg, which corresponds to ~2.5 mg/kg.[461]

Other compounds: TPP^+-C_1 was shown to be well tolerated in mice when fed in drinking water at the dosage of 35 mg/kg per day, while the maximum tolerable dose upon single iv injection was determined to be 4 mg/kg.[159] For Rh-123 dye, the maximal tolerable dose was reported as ~10–15 mg/kg in mice when administered every other day.[496] No toxicity was observed in mice treated with dequalinium chloride when administered ip daily at the dosage of 2 mg/kg or every other day at the dosage of 4 mg/kg.[66]

The acute maximal tolerated dose (MTD) of tri(dimethylaminophenyl)phosphonium linked to iodo- or chloropropane (APPI and APPCL, respectively) was 25 mg/kg ip in mice, while the LD_{50} value was estimated for both compounds to be 50 mg/kg. The study of cumulative

toxicity of the compounds indicated the cumulative MTD of 5 mg/kg per injection, for eight ip injections administered every other day. The acute hepatotoxicity is proposed to be the limiting factor for dose escalation.[497]

7.3. Antiproliferative and Antitumor Effects of Mitochondria-Targeted Compounds

—Most tumor cells or tissues metabolize glucose to lactate even under aerobic conditions (the Warburg effect).[498–501] The reason why cancer cells choose to pursue the less efficient aerobic glycolytic pathway for energy production is not fully understood. Cancer cell mitochondria are hypothesized to be dysfunctional, forcing the cells to rely on glycolysis for their energetic needs. Later studies showed that cancer cells have functional mitochondria due to their ability to perform mitochondrial respiration.[502–504] More recent studies clarified the functional role of mitochondria in cancer cells with the help of mitochondria-targeted nitroxide, Mito-CP (Figure 9). To our knowledge, this study is one of the first that provides experimental evidence showing that repressed respiration in cancer cells results in decreased cell proliferation.[409] Using ρ0 cells, the role of mitochondria was demonstrated clearly.[409] It was suggested that Mito-CP, a superoxide dismutase mimetic and a nonspecific radical scavenger, decreases the mitochondrial ROS responsible for stimulating cell proliferation. As was discussed, this mechanism appears to be unlikely. However, the original idea concerning the signaling role of mitochondria-generated ROS in cancer cell proliferation is still a viable mechanism.[505,506]

Overcoming drug resistance and microenvironmental issues using mitochondria-targeted drugs?: Multidrug transporter p-glycoprotein (MDR-1) induces chemotherapeutic drug resistance by pumping out positively charged drugs from cancer cells.[507,508] Conventional standard-of-care chemotherapeutic drugs (doxorubicin and cisplatin) induce multidrug resistance through elevated expression of MDR-1. P-glycoprotein (Mdr1a/1b) and breast cancer resistance protein (Bcrp) were shown to decrease the uptake of hydrophobic alkyl triphenylphosphonium cations, such as MitoQ and MitoF, in the brain.[509] Another mitochondria-targeted quinone, SkQR1, was reported to be the substrate of multidrug resistance pump P-glycoprotein (Pgp 170) and to selectively protect Pgp 170-negative cells against oxidative stress.[510] Conversely, SkQR1 did not protect Pgp170-positive K562 subline against DNA damage induced by gamma radiation. The selective radioprotection of normal Pgp 170-negative cells by mitochondria-targeted antioxidants could be a promising strategy to increase the efficiency of radiotherapy for multidrug-resistant tumors.[511] SkQR1 was pumped out of the chemotherapy resistant cells by p-glycoprotein. [512,513] It was also shown that SkQR1 pumping is neutralized by p-glycoprotein inhibitors (verapamil and pluronic L61).[513]

MDR-1 uses ATP as a cofactor to enable the pumping mechanism. Reports indicate that ATP regulates chemoresistance in colon cancer cells.[514] Mitochondria-targeted agents (Mito-CP, Mito-chromanol) could hinder the pump activity of MDR-1 due to depletion of intracellular ATP levels. Although mitochondria-targeted agents such as MitoQ are relatively less effective in resistant cancer cells, other compounds (Mito-CP-acetate) exerted potent antiproliferative effects.[17] Mito-VES was shown to overcome ABCA1-dependent resistance of lung carcinoma to α-tocopheryl succinate, and attaching the TPP^+ moiety to doxorubicin

was reported to overcome doxorubicin resistance in breast cancer cells, as discussed subsequently.[431,515] Also, loading the drug, paclitaxel, into mitochondria-targeting liposomes was shown to improve its cytotoxic effects in paclitaxel-resistant human ovarian carcinoma cells.[516]

Solid tumors harbor a microenvironment around tumor tissue that is hypoxic and provides a limited availability of nutrients such as glucose.[517–519] This is due to the lack of adequate blood supply to tumors caused by the abnormal vascularization of solid tumors.[520] Consequently, cells residing in such environments grow slowly and have altered phenotypic characteristics.[517,519] The phenotypic alterations make the cells in the microenvironment resistant to chemotherapeutic agents that rely on DNA replication and cell division as an antitumor mechanism. Mitochondria-targeted drugs that inhibit OXPHOS in tumor cells in a metabolically compromised environment (a low glucose environment, for example) may be more effective in inhibiting proliferation.

7.3.1. Selectivity of Lipophilic Cations Toward Cancer Cells—Lipophilic, delocalized cationic compounds (e.g., Figure 2, Chart 70) were used to target tumor mitochondria because of higher (more negative inside) plasma membrane and mitochondrial membrane potentials in tumor cells compared to normal cells.[496,497,521–525] Rh-123 is a lipophilic, cationic fluorescent dye that was used as an indicator of transmembrane potential. Rh-123 is shown to be retained longer (two–three days) in the mitochondria of tumor-derived cells than in the mitochondria of normal epithelial-derived cells.[72,526–529] The increased uptake and retention of Rh-123 in cancer cells correlates well with its selective and enhanced toxicity in cancer cells.[209,496,524,530]

7.3.2. Lipophilic Cations Other than TPP^+—Due to increased uptake by cancer cells, numerous lipophilic cations (Chart 71) were designed for selective targeting of tumors, providing new diagnostic tools (as discussed subsequently) and potential novel, less toxic anticancer agents. Below are examples of lipophilic cations exhibiting anticancer properties that accumulate in mitochondria and do not need to be conjugated to a mitochondria targeting moiety (e.g., TPP^+). These compounds are typically used at higher concentrations than those reported for triphenylphosphonium-conjugated compounds.

Rhodamine 123: Rhodamines, rosamines, and rhodocyanines are delocalized lipophilic cations that accumulate selectively in cancer cell mitochondria and were shown to possess selective anticancer activity, both in vitro and in vivo, either when used alone or in combination with other anticancer agents. The mitochondria of a variety of carcinomas retain Rh-123 for prolonged periods (two–five days), whereas normal epithelial cells release it within a few hours.[526,528] The increased uptake and retention of Rh-123 was attributed to elevated mitochondrial and plasma membrane potentials in cancer cells (MCF-7).[72] The differences in mitochondrial membrane potential between normal and cancer cells contribute to the selective cytotoxicity exhibited by Rh-123.[209] Rh-123 was shown to exhibit selective toxicity towards several carcinoma cells in vitro and in bone marrow cells and to accumulate selectively in vivo in glioma tumor tissue when compared with normal brain tissue.[529–532] Also, it was reported to inhibit mitochondrial ATP synthesis.[533,534] Further, Rh-123 was shown to compromise mitochondrial bioenergetic function by inhibition of F_0F_1-ATPase and

to inhibit colony formation by committed hematopoietic progenitor cells and ovarian cancer cells in vitro.[209,532,535–537]

Rhodacyanine MKT-077: Similar to Rh-123, MKT-077 (also known as FJ-776, Chart 71) was reported to preferentially accumulate in the mitochondria of cancer cells, inhibit mitochondrial respiration, and inhibit cell proliferation. However, the mechanism of mitochondrial toxicity of the rhodacyanine, MKT-077, is believed to be different than that of Rh-123. The toxicity of MKT-077 stems from a general perturbation of mitochondrial membranes and consequent nonspecific inhibition of the activity of membrane-bound mitochondrial respiratory enzymes. This compound also appears to have a slight degradative effect on mitochondrial DNA. The FDA approved clinical trials testing MKT-077 for the treatment of carcinoma. However, the trials were discontinued during phase II, because MKT-077's efficacy in killing tumor cells was not demonstrated at the approved dosage.[538–540]

Dequalinium cation: Dequalinium chloride (DQ, Chart 71) is a lipophilic dication composed of two cationic quinolinium moieties linked via a 10-carbon alkyl chain. It shows antiproliferative activity against several cancer lines in vitro and antitumor effects in vivo.[66] Dequalinium dication localizes in cancer cell mitochondria and exhibits antiproliferative properties against bladder and colon cancers in the in vivo mouse models.[528] Results have shown that dequalinium can prolong the survival of tumor-bearing mice, inhibit tumor growth in vivo, and has synergistic effects with cisplatin in mouse model.[528] Dequalinium demonstrated 100-fold greater inhibition of the clonal growth of carcinoma versus control epithelial cells in culture, showed the anticarcinoma activity against human colon adenocarcinoma cells injected subcutaneously in nude mice, and led to a significant regression of tumors in rats carrying in situ mammary adenocarcinomas induced by 7,12-dimethylbenzanthracene (DMBA).[66,541] The proposed mechanism of anticancer effects of dequalinium chloride included a decrease in the mitochondrial respiration rate by inhibiting NADH-ubiquinone reductase activity in respiratory complex I.[542,543]

AA1: A monovalent lipophilic cation, 2,6-bis(4-amino-phenyl)-4-[4-(dimethylamino)phenyl]thiopyrylium chloride (AA1, Chart 71), was reported to have anticarcinoma activity both in vitro and in vivo, identified based on screening more than 1000 different lipophilic cations.[535] AA1 was shown to be 10 times more toxic to cancer cell line CX-1 than to normal epithelial cell line CV-1 and to prolong survival of tumor-bearing mouse. AA1 inhibited mitochondrial ATPase at low μM concentrations and was shown to be significantly more potent in vivo than other lipophilic cations, such as Rh-123 or dequalinium.

F16: Another delocalized lipophilic cation, F16 (Chart 71), was discovered during a high throughput screening of a chemical library for antiproliferative compounds against neu-expressing mammary epithelial cells.[544] F16 is a small molecule that selectively inhibits proliferation of a variety of mouse mammary tumor and human breast cancer cell lines. F16 belongs to a group of structurally similar molecules with a delocalized positive charge and has very low binding to mitochondrial membranes, which results in an almost complete

accumulation in the mitochondrial matrix in response to elevated mitochondrial membrane potential. The accumulation of F16 in the mitochondrial matrix was shown to lead to membrane depolarization, opening of the permeability transition pore (PTP) with the loss of mitochondrial structural integrity, release of cytochrome *c*, arrest of the cell cycle, and death of the target cells.[544] Also, a fluorescent derivative of the F16 compound was obtained by conjugating F16 to the BODIPY fluorescent tag using a phenylethynyl linker.[545] It was shown that the compound selectively accumulates in cancer cell mitochondria and induces cell death. The compound was shown to be ~2–20 times more potent toward gastric cancer cells (SGC-7901) than normal gastric epithelium cells (GES-1) due to different uptake in cancer and normal cells.

7.3.3. TPP$^+$-Based Mitochondria-Targeting Anticancer Agents—Compared to rhodamine-like lipophilic cations, TPP$^+$-based cations are typically more efficient in inhibiting cancer cell proliferation, and numerous TPP$^+$-linked compounds are currently being developed to selectively target cancer cells. Interestingly, more than 10,000 small-molecule drug-like compounds underwent high-throughput screening against a panel of cancer cells in order to identify their antiproliferative effects, and TPP$^+$-bearing compounds were found to be promising anticancer agents.[546] All three identified phosphonium cations inhibited cell proliferation, induced cell cycle arrest independent of the p53 status in various of cancer cells, and significantly decreased tumor growth in a human breast cancer xenograft mouse model.[546]

Tetraphenylphosphonium: Similar to other lipophilic cations, the TPP$^+$ cation was shown to selectively accumulate in cancer cells.[524] Based on the results obtained with the TPP$^+$ cation and other TPP$^+$ derivatives, the compounds in this class were proposed as mitochondria-targeting agents exhibiting selective inhibition of tumorigenic cell proliferation.[521]

TPP$^+$ alkyl derivatives: Several derivatives of the alkyl-TPP$^+$ cation were reported to selectively inhibit proliferation of carcinoma cells via inhibition of mitochondrial respiration and ATP synthesis.[522] The mitochondrial effects of alkyl-TPP$^+$ cationic compounds were recently studied in detail, and the compounds were shown to inhibit respiratory chain complexes and decrease mitochondrial membrane potential and ATP synthesis.[210] These negative effects on mitochondrial function correlate with the increasing hydrophobicity of TPP$^+$ compounds by increasing the length of the alkyl chain. The extent of mitochondrial function disruption by the TPP$^+$-linked antioxidant was shown to depend mostly on the TPP$^+$-linker part of the molecules, rather than on the antioxidant moiety.[547] However, modulation of specific mitochondrial targets and selectivity of the TPP$^+$-linked compounds may depend on the chemical nature of the molecule conjugated to the TPP$^+$ cation.

Mitochondria-targeted chromanol: Chromanols are a family of phenolic compounds that contain a chromanol ring system and an aliphatic side chain. Tocopherols, including vitamin E and tocotrienols, consist of a chromanol ring and a 16-carbon side chain (Chart 63). Isomers of tocopherol and tocotrienol exhibit antiproliferative and proapoptotic antitumor activity in tumor models.[548] Mito-ChM is a synthetic compound containing a naturally

occurring chromanol ring system conjugated to an alkyl TPP^+ via a side chain carbon-carbon linker sequence (Chart 63).[432] Thus, Mito-ChM is also referred to as Mito-Vitamin-E or Mito-E, and various chemical forms of mitochondria-targeted vitamin E analogs were synthesized and reported, as discussed previously. Because chromanols are active components of naturally occurring antioxidants (e.g., tocopherols and tocotrienols), investigating the antitumor effects of Mito-ChM is of particular interest. Previous reports indicate that mitochondria-targeted α-tocopheryl succinate is a more potent antiproliferative agent than α-tocopherol.[426,427] However, it remained unclear whether succinylation of the phenolic hydroxyl group is a critical requirement for observing the antitumor potential of mitochondria-targeted vitamin E analogs.[549]

The dose-dependent cytotoxicity of Mito-ChM and its acetate, Mito-ChMAc, in nine breast cancer cells and non-cancerous control cells, MCF-10A, was monitored for 24 h and the real-time cell death curves (Figure 11A) indicate a dose-dependent increase in cytotoxicity in MCF-7 and MDA-MB-231 cells treated with Mito-ChM. In contrast, very little cell death is noticeable in MCF-10A control cells treated under the same conditions. Figure 11B shows the titration of nine different breast cancer cells and the noncancerous control cell, MCF-10A, with Mito-ChM. The EC_{50} values (concentration inducing 50% of cell death) for Mito-ChM were estimated to be below 10 μM in eight of the nine breast cancer cells and 20 μM in MCF-7 cells. In MCF-10A, Mito-ChM did not induce detectable toxicity under these conditions.[432]

Analysis of the cellular concentrations of Mito-ChM indicated that the intracellular level of Mito-ChM was about 2.7-fold higher in MCF-7 cells than in MCF-10A cells.[432] Treatment of these cells for an additional 24 h caused a six-fold difference in intracellular concentration of Mito-ChM in MCF-7 cells. Enhanced accumulation of Mito-ChM was observed in MDA-MB-231 breast cancer cells as well.

Oral administration of Mito-ChM in mice breast cancer xenograft experiments resulted in a significant decrease in the bioluminescence signal intensity (or tumor growth) when compared with the control mice breast cancer xenografts (Figure 12).[432] This was verified by measuring the tumor weight (Figure 12). As discussed previously, Mito-ChM accumulated selectively in breast tumor tissue and in kidney tissue but not in heart or liver tissue (Figure 12). Thus, Mito-ChM selectively accumulates in tumor tissue, probably in tumor mitochondria as demonstrated in breast cancer cells.

Mitochondria-targeted vitamin E succinate: α-Tocopherol succinate (VES) selectively induces apoptosis in cancer cells and suppresses tumor growth in vivo. To increase the potency of VES, the chromanol-succinate moiety of VES was linked to TPP^+ via a long alkyl chain (Chart 63). Mito-VES was shown to kill breast tumor-initiating cells (TICs) in a mitochondrial complex II-dependent manner.[550] MitoVES was reported to cause apoptosis in malignant mesothelioma cells by mitochondrial destabilization, resulting in the loss of mitochondrial membrane potential, generation of ROS, and destabilization of respiratory supercomplexes, leading to inhibition of mitochondrial complex II activity. MitoVES also suppressed mesothelioma growth in nude mice.[551] Further research indicated that MitoVES suppresses proliferation of cancer cells at subapoptotic doses by affecting the mitochondrial

DNA (mtDNA) transcripts. This led to the inhibition of mitochondrial respiration, depolarization of mitochondrial membrane, and generation of ROS. In addition, exposure of cancer cells to MitoVES led to decreased expression of mitochondrial transcription factor A and diminished mitochondrial biogenesis. The inhibition of mitochondrial transcription was replicated in vivo in a mouse model of $HER2^{high}$ breast cancer.[430] MitoVES stimulated basal respiration and ATP hydrolysis but inhibited net state 3 (ADP-stimulated) respiration and Ca^{2+} uptake by collapsing the membrane potential. Respiratory complex II was proposed to be the most sensitive MitoVES target.[428] MitoVES induced considerably more robust apoptosis in cancer cells with a 1–2 log gain in anticancer activity compared to the unmodified counterpart, while maintaining selectivity for malignant cells. MitoVES was proposed to induce generation of ROS that subsequently trigger mitochondria-dependent apoptosis, involving a transcriptional modulation of the Bcl-2 family proteins.[427]

MitoVES was also shown to cause apoptosis and induce production of oxidants in mitochondrial complex II-proficient malignant cells but not their complex II-dysfunctional counterparts. MitoVES inhibited the succinate dehydrogenase activity of complex II with IC_{50} of 80 μM, whereas the electron transfer from CII to CIII was inhibited with an IC_{50} of 1.5 μM. Reportedly, MitoVES does not affect the enzymatic activity of mitochondrial complex I or the electron transfer from complex I to complex III. MitoVES was proposed to interact with the proximal UbQ-binding (Q_P) site of complex II, which endows it with greater activity for inducing cancer cell apoptosis.[426]

MitoVES was also found to efficiently kill proliferating endothelial cells (ECs) but not contact-arrested ECs or ECs deficient in mitochondrial DNA; it also was found to suppress angiogenesis in vitro by inducing accumulation of ROS and induction of apoptosis in proliferating/angiogenic ECs. MitoVES was found to suppress HER2-positive breast carcinomas in a transgenic mouse as well as inhibit tumor angiogenesis.[429] It appears that mitochondrial bioenergetics in cancer cells is altered differently by MitoVES (complex II inhibition) when compared with other mitochondria-targeted compounds (complex I inhibition), as discussed below.

Mitochondria-targeted metformin: Metformin (Chart 66) is currently being repurposed as a potential drug in cancer treatment.[451–453,456,457] Approved for antidiabetic treatment more than 20 years ago, metformin is now the most prescribed antidiabetic drug in the world.[454,458] Metformin is relatively safe, with minimal side effects. However, it is poorly bioavailable, and patients with type 2 diabetes mellitus take several grams of metformin daily to decrease blood glucose levels. Metformin is mostly excreted out unchanged, without being metabolized. However, its efficacy is attributed to the many metabolic pathways it induces or alters in the.[454,460] Epidemiological studies have shown that metformin use is related to decreased incidence of pancreatic cancer in diabetic patients taking metformin.[455–457] Other lipophilic analogs of metformin, such as phenformin, have increased bioavailability and exhibit more potent antitumor effects.[552–554] However, phenformin was discontinued in the United States due to enhanced acidosis.[555,556]

Metformin is a highly hydrophilic cation at physiological pH and targets mitochondria somewhat poorly. Recently several metformin analogs (e.g., Mito-Met_2, Mito-Met_6, etc.)

conjugated to a TPP^+ moiety via alkyl linker chains of varying lengths were synthesized and characterized (Chart 66). Mito-Met_{10}, synthesized by attaching TPP^+ to metformin through a 10-carbon aliphatic side chain, was nearly 1,000 times more potent than metformin at inhibiting pancreatic ductal adenocarcinoma cell proliferation.[21] Mito-Met_2 and Mito-Met_6 were relatively less potent than Mito-Met_{10}, suggesting that fine-tuning alkyl side chain length is necessary to achieve optimal antiproliferative potency with this type of compounds. Importantly, at the concentrations shown to inhibit proliferation of cancer cells, Mito-Met_{10} exhibited no effect on nontransformed control cells.

Recent studies have shown that inhibiting mitochondrial complex I in cancer cells decreases cell proliferation.[21,557] Metformin's inhibitory effects on tumorigenesis and cancer progression were partly attributed to its ability to inhibit mitochondrial complex I.[18,454,459,557] The complex I activity was determined by monitoring oxygen consumption in pancreatic cancer cells treated with varying concentrations of metformin and Mito-Met with different alkyl side chain lengths. As shown in Figure 13, the extent of complex I inhibition was dependent on the alkyl chain length with Mito-Met_{10} being the most potent (IC_{50} = 0.4 μM) against pancreatic cancer cells. When compared with metformin, Mito-Met_{10} was nearly 250-fold more potent than metformin at inhibiting mitochondrial complex I.[21] However, the molecular mechanism by which Mito-Met analogs inhibit complex I has yet to be determined.

One of the consequences of mitochondrial complex I inhibition is stimulation of superoxide and other ROS.[236,558] Using state-of-the-art probes and fluorescence-based assays, superoxide and H_2O_2 were detected in pancreatic cancer cells treated with Mito-Met_{10}.[21] The levels of superoxide-specific product, 2-hydroxyethidium (2-OH-E^+), derived from the interaction between HE (cell-permeable fluorescent dye) and superoxide were increased in pancreatic cancer cells treated with Mito-Met_{10}. A mitochondria-targeted boronate probe, *o*-MitoPhB$(OH)_2$ was used to detect H_2O_2 generated in Mito-Met_{10}-treated cells. As discussed previously, the reason for using o-MitoPhB$(OH)_2$ instead of m-MitoPhB$(OH)_2$ (known as the MitoB probe) is that the ortho-substituted probe allows distinguishment between H_2O_2 or peroxynitrite oxidants (Chart 30, Chart 31). Treatment of pancreatic cancer cells with Mito-Met_{10} leads to a significant increase in the oxidation of the *o*-MitoPhB$(OH)_2$ probe, without the formation of peroxynitrite-specific products, suggesting that H_2O_2 is the oxidant detected.

Mito-Met_{10} activated adenosine monophosphate (AMP)-activated protein kinase (AMPK) phosphorylation at micromolar concentrations whereas metformin activated AMPK at millimolar concentrations.[21] It was postulated that Mito-Met_{10} exerts antiproliferative effects in pancreatic cancer cells by targeting the energy-sensing bioenergetics pathway (Figure 14). H_2O_2 generated in mitochondria (formed from the dismutation of superoxide arising from complex I inhibition by Mito-Met_{10}) is likely contributing to AMPK activation, leading to antiproliferative effects (Figure 14). Thus, mitochondria-targeted compounds could induce a novel redox-signaling mechanism in which H_2O_2 may play a critical role in the antiproliferative effects in cancer cells.

Mitochondria-targeted carboxyPROXYL: Mitochondria-targeted nitroxide, Mito-CP (Figure 9), was developed as a mitochondria-targeted superoxide dismutase mimetic, as described previously.[164] The inhibitory effect of Mito-CP on the anchorage-independent growth in colon cancer cells HCT-116 was used as a proof of principle that mitochondria-derived ROS are critical for anchorage-independent growth.[409] The same group has also reported that Mito-CP and MitoQ, as antioxidants, can diminish adipocyte differentiation, which can be rescued by adding exogenous H_2O_2.[559]

Later, the antiproliferative effects of Mito-CP, exhibiting SOD-like activity, were compared to the effects of its acetamide analog (Mito-CP-Ac, Figure 10), which lacks the nitroxide moiety responsible for SOD activity. Results indicated that both Mito-CP and Mito-CP-Ac potently inhibited the proliferation of various cancer cells, apparently via a mechanism independent of superoxide dismutation in mitochondria, and that these compounds alter the bioenergetics pathways in tumor cells, leading to the inhibition of cancer cell proliferation.[17]

Mito-CP was also reported to suppress medullary thyroid carcinoma cell survival in vitro and in vivo by inducing caspase-dependent apoptosis.[560] These effects were accompanied by mitochondrial membrane depolarization, decreased oxygen consumption, and increased oxidative stress in cells. Mito-CP was proposed to mediate tumor-suppressive effects via redox-dependent and -independent mechanisms. Mitochondria-targeted nitroxides (Mito-CP and Mito-TEMPOL) were shown to inhibit FOXM1 and peroxiredoxin-3 expression by inducing marked mitochondrial fragmentation and increased production of mitochondrial oxidants, a phenotypic response that appears distinct from mitochondrial fission in malignant mesothelioma cells.[561]

Mitochondria-targeted quinones: Major applications have been found for MitoQ (Chart 58) as a protecting agent against mitochondrial redox stress in a wide range in vitro and in vivo disease models. However, MitoQ is also reported to exhibit selective toxicity toward cancer cells.[19] MitoQ was shown to inhibit proliferation of breast cancer cells but not nontumorigenic cells, with concomitant induction of autophagy, cellular oxidants, and activation of the oxidant-sensitive Nrf2 antioxidant transcription factor. The structurally similar SkQ1 molecule (Chart 58) was shown to suppress spontaneous tumorigenesis in $p53^{-/-}$ mice as well as HCT116/$p53^{-/-}$ tumor xenograft growth in athymic mice.[512]

Mitochondria-targeted polyphenols: As discussed previously, many naturally occurring polyphenolic compounds were shown to alter mitochondrial metabolism and modulate OXPHOS.[468,469] Mitochondria-targeted derivatives of resveratrol (Chart 68) are cytotoxic in vitro, selectively inducing mostly necrotic death of fast-growing and tumorigenic cells when used in the low μM concentration range. Cytotoxicity of mito-resveratrol was attributed to induction of H_2O_2 generation and mitochondrial depolarization upon accumulation of the compounds into mitochondria.[471] The proposed mechanism underlying ROS generation included inhibition of the respiratory chain, especially complexes I and III, causing superoxide production, and inhibition of ATPase in mouse colon cancer CT-26 cells.[20] Similarly, quercetin was conjugated to the TPP^+ to target it to mitochondria and increase its anticancer potency.[473] Similar to mito-resveratrol, mito-quercetin (Chart 69) showed selective toxicity toward fast-growing cells. Mitochondria-targeted quercetin derivatives

were shown to induce mitochondrial permeability transition and uncouple isolated mitochondria.[474] In intact cells, mitochondria-targeted quercetins were shown to depolarize mitochondria and induce production of cellular oxidants. Both superoxide and H_2O_2 were implicated in the mechanism of antiproliferative effects of the compounds.[476]

3-Chloropropyltris(4-dimethylaminophe-nyl)phosphonium chloride (APPCL) and 3-iodopropyltris(4-dimethylaminophenyl)phosphonium iodide (APPI): The tri(dimethylaminophenyl)phosphonium linked to iodo- or chloropropane (APPI and APPCL, respectively, Chart 72) were reported to exert anticancer effects against ovarian cancer cells in vitro, at submicromolar concentrations.[497]

Due to the presence of the haloalkyl moieties, the compounds were assumed to possess protein alkylating capabilities. The treatment led to the damage of mitochondrial membranes, attenuation of cellular accumulation of Rh-123, and a decreased number of mitochondria per cell. The analysis of the survival in the in vivo ovarian cancer xenograft mouse model indicated the disease-free survival of 12.5% mice treated with APPI and 37.5% of mice treated with APPCL after 180 days, while all untreated mice died within the first 50 days of the study. Both compounds were effective against cancer cells resistant to the standard-of-care drugs, Taxol and cisplatin.[497]

Mitochondria-targeted dichloroacetate: As discussed previously, DCA (Chart 65) is an inhibitor of PDK, a key enzyme controlling the activity of pyruvate dehydrogenase and pyruvate-dependent tricarboxylic acid (Kreb's) cycle activity and mitochondrial function. Inhibition of PDK by DCA leads to a metabolic switch from glycolysis to mitochondrial OXPHOS, which is accompanied by the inhibition of cancer cell proliferation. Typically, DCA needs to be used in a millimolar concentration to show efficiency. To improve the potency of DCA, it was linked to the TPP^+ moiety, thus increasing the uptake and mitochondrial accumulation of the agent.[449] It was reported that Mito-DCA (Chart 65), with three orders of magnitude enhanced potency and cancer cell specificity compared with DCA, is very effective in highly glycolytic cancer cells, and causes a switch from glycolysis to OXPHOS and subsequent cell death via apoptosis.[449] Mito-DCA treatment led to reduced glycolytic functions, reduced basal cellular respiration, suppressed the ATP synthesis, and attenuated spare respiratory capacity in prostate cancer cells. Not only can Mito-DCA modulate the tumor cell glycolysis efficiently, it also has the potential to alter the immunosuppressive environment modulated by lactic acid.

Mitochondria-targeted Hsp90 inhibitors: The mitochondrial pool of Hsp90 chaperones plays an important role in regulating mitochondrial integrity, protecting against oxidative stress, and inhibiting cell death, as discussed previously. Pharmacological inactivation of the chaperones induced mitochondrial dysfunction and concomitant cell death selectively in cancer cells, suggesting they can be target proteins for the development of cancer therapeutics.[562]

An Hsp90 inhibitor, geldanamycin, was linked to different mitochondria-targeting moieties to increase its mitochondrial accumulation and target organelle-specific Hsp90 function. Gamitrinibs (geldanamycin mitochondrial matrix inhibitors) were reported as mitochondria-

targeted Hsp90 inhibitors (Chart 67). In the National Cancer Institute 60-cell line screening, gamitrinibs were active against all tumor cell types tested, and they efficiently killed metastatic, hormone-refractory, and multidrug-resistant prostate cancer cells. Gamitrinibs induced acute mitochondrial dysfunction in prostate cancer cells with loss of organelle membrane potential, release of cytochrome c, and caspase activity, independently of proapoptotic Bcl-2 proteins, Bax and Bak.[465] A structurally different mitochondria-accumulating Hsp90 inhibitor, SMTIN-P01 (a conjugate of PU-H71 and TPP^+, Chart 67), shows stronger cytotoxic activity against cancer cells than the parental Hsp90 inhibitor PU-H71 and slightly improved cytotoxicity over gamitrinibs in selected types of cancer cells, including 22Rv1, A172, H460, and MDA-MB-231 cells.[467]

Mitochondria-targeted soft electrophiles: A series of MTSEs was designed that selectively accumulates within the mitochondria of highly energetic breast cancer cells and modify mitochondrial proteins.[378] A prototype MTSE, iodobutyl-TPP^+ (IBTP, Chart 55), significantly inhibits mitochondrial OXPHOS, resulting in decreased breast cancer cell proliferation, cell attachment, and migration in vitro, while nontumorigenic MCF10A cells remain relatively insensitive.

Mitochondria-targeted terpenoids: Naturally occurring lupane triterpenoids, including betulinic acid, exhibit antitumor properties, and mitochondria were proposed as the target of betulinic acid.[563,564] A series of mitochondria-targeted analogs of betulinic acid were synthesized and tested for cytotoxic effects against cancer cells (Chart 73).[565] Mitochondria-targeted betulinic acids were shown to exhibit enhanced antitumor activity in mastocytoma P-815 and Ehrlich carcinoma cell lines.[565] Also, TPP^+-conjugated diterpenoid isosteviol analogs were reported to exhibit antimitotic activity, with a potential application as anticancer agents.[566]

Also, sclareol, a natural diterpene alcohol, known for its anticancer effects against leukemia and colon cancer cells, was targeted to mitochondria using TPP^+-functionalized liposomes.[144,567] Sclareol-loaded mitochondria-targeted liposomes were significantly more cytotoxic to colon carcinoma (COLO205) cells than free sclareol or sclareol-loaded untargeted liposomes.

Mitochondrial delivery of ceramide: Ceramides are a family of sphingolipid signaling molecules shown to mediate the proapoptotic effects of many extracellular stimuli. Accumulation of ceramide in the mitochondrial membrane was proposed to result in the formation of ceramide channel, enabling the release of cytochrome c from mitochondria into the cytosol, an important step in apoptosis. Ceramide was loaded into TPP^+-conjugated liposomes for enhanced mitochondrial delivery of the compound.[568] Ceramide-loaded mitochondria-targeted liposomes were shown to induce apoptosis in COLO205 cancer cells to a significantly higher extent than empty mitochondria-targeted liposomes, or ceramide loaded into untargeted liposomes. The ceramide-loaded mitochondria-targeted liposomes, but not empty liposomes, significantly reduced the rate of tumor growth in the in vivo mouse xenograft breast cancer model.[568]

Targeting 3-bromopyruvate to mitochondria: 3-Bromopyruvate (3-BP, Chart 74) was proposed as a potential anticancer drug, targeting cancer bioenergetic pathways.

To target 3-BP to mitochondria, 3-BP was incorporated into mitochondria-targeted gold nanoparticles decorated with the TPP^+ moieties.[569] In vitro studies demonstrated enhanced anticancer activity of the 3-BP-loaded nanoparticles (T-3-BP-AuNP, Chart 74), as compared to the nontargeted construct or free 3-BP. Both glycolytic and mitochondrial functions were inhibited upon treatment. The anticancer activity of the 3-BP-loaded mitochondria-targeted gold nanoparticles was further enhanced by simultaneous releasing of a glycolytic inhibitor (3-BP) and photothermal ablation (AuNP) as a combination effect.[569]

Mitochondrial targeting of 2-methoxyestradiol: 2-Methoxyestradiol (2-ME) is a potent anticancer drug candidate that was shown to possess antiproliferative, proapoptotic, antiangiogenic, and antimetastatic effects in various types of cancer cells.[570] Because 2-ME was reported to inhibit superoxide dismutase, it was loaded into mitochondria-targeted mesoporous silica nanocarriers to selectively induce oxidative stress in HeLa cancer cell mitochondria. Mitochondrial targeting was achieved by conjugating the particles to mitochondria-targeting sequence peptide; to further increase selectivity toward cancer cells, the particles were also decorated with folic acid. The mitochondria-targeted nanoparticles carrying 2-ME were shown to induce mitochondrial oxidants and to exhibit higher efficiency in initiating cell apoptosis when compared with free 2-ME. Finally, taking advantage of magnetic guiding was reported to further increase the HeLa cells' killing efficacy of the constructed nanoparticles.[571]

Mitochondria-targeted gold(I) N-heterocyclic carbene complexes: Increased activities of thioredoxin and thioredoxin reductase antioxidant enzymes were observed in numerous cancer cells. To selectively inhibit thioredoxin reductase in cancer cells, cationic and lipophilic gold (I) complexes were synthesized.[572] The synthesized Au(I) complexes selectively induced apoptosis in cancer cells but not in normal cells and allowed selective targeting of mitochondrial selenoproteins, such as TrxR.[572]

7.3.4. Mitochondrial Targeting of Standard-of-Care Therapeutics: Defying Drug Resistance?

Mitochondrial targeting of doxorubicin: Doxorubicin (DOX) is an anticancer drug, the potency of which is limited by acquired resistance of cancer cells. To overcome the resistance, DOX was linked to the TPP^+ cation (TPP-DOX, Chart 75) and tested for its toxicity against MDA-MB-453 breast cancer cells and their DOX-resistant derivative.[515] TPP-DOX was shown to accumulate to a significantly higher extent than DOX in DOX-resistant cells. While there was no significant difference in sensitivity to DOX versus TPP-DOX in wild-type breast cancer cells, TPP-DOX was much more potent in DOX-resistant cells. TPP-DOX induces cleavage of caspase-3 and PARP, and apoptosis in DOX-resistant cancer cells.

In addition to direct linking DOX to the TPP^+ cation, targeting this drug to mitochondria was accomplished using mitochondria-targeted vesicles. The first approach was based on loading DOX into liposomes carrying folic acid and TPP^+ ligands for selective delivery of

DOX into mitochondria of cancer cells, taking advantage of increased expression of folate receptors in a variety of human carcinomas.[573] Dual targeting of DOX-loaded liposomes was shown to be most efficient in inhibiting proliferation of human oral carcinoma KB cells, as compared to single-labeled (TPP^+ or folic acid) or untargeted liposomes.[573] DOX was also encapsulated in TPP^+-functionalized poly(ethylene imine)-based nanoparticles, for site-specific cellular delivery.[574] It was reported that loading DOX into mitochondria-targeted nanoparticles results in rapid and severe cytotoxicity in prostate carcinoma cells DU145.[574] Another approach was based on incorporation of DOX into TPP^+-functionalized mesoporous silica nanoparticles.[575] Such prepared DOX-loaded mitochondria-targeted nanoparticles exhibited enhanced cytotoxicity, reduced ATP production, and decreased mitochondrial membrane potential in HeLa cancer cells. A similar approach was also tested using TPP^+-conjugated poly(ε-caprolactone)-based nanoparticles.[576] Compared with free DOX, DOX-loaded mitochondria-targeted nanoparticles exhibited an approximately two- to seven-fold higher mitochondria-to-nucleus preference and resulted in superior (approximately 7.5–18-fold compared with free DOX) cytotoxicity towards HeLa and HepG2 cancer cells.[576] Also, TPP^+-modified cerasomes were proposed to deliver DOX to mitochondria for enhanced anticancer potency.[577] The prepared cerasomes showed good stability, excellent biocompatibility, and sustainable drug release behavior. Although the TPP^+-modified cerasomes led to greater drug accumulation in mitochondria, and tended to exhibit stronger cytotoxic effects when compared with non-targeted DOX-loaded cerasomes, free DOX was more toxic toward the cancer cells tested, which brings into question the advantages of loading the drug into the cerasomes.[577] DOX was also encapsulated in TPP^+-conjugated fluorescent polymersomes.[578] Although mitochondrial accumulation of the particles was confirmed, only very modest improvement in the cytotoxic effects against BxPC-3 spheroids, when compared with free DOX or DOX-loaded untargeted polymersomes, was observed.

Mitochondrial targeting of cisplatin: Cisplatin (Chart 76) is one of the most widely used anticancer agents for solid tumors, whose mechanism of action includes binding to nuclear DNA and inducing DNA crosslinking. One of the mechanism of cisplatin resistance is based on the DNA repair mechanism involving nucleotide excision repair (NER), which operates in the nucleus but not in mitochondria.[579] Thus, it was proposed that targeting the alkylating agents to mitochondrial genome may overcome the cancer cell resistance. To divert the drug from nuclear to mitochondrial DNA, cisplatin was linked to mitochondria-penetrating peptide (mtPt, Chart 76).[580] MPP-linked cisplatin targets mitochondrial DNA without significant effects on nuclear DNA. Cisplatin-MPP conjugate was shown to overcome cisplatin tolerance in ovarian cancer cells. Similar effects on cisplatin-resistant neuroblastoma cells were observed using cisplatin conjugated covalently to TPP^+ (Platin M, Chart 76) and embedded in TPP^+-linked, mitochondria-targeted nanoparticles.[581] Interestingly, Platin-M-containing mitochondria-targeted nanoparticles significantly accumulated in the mouse brain, while free Platin-M or Platin-M embedded in nontargeted nanoparticles accumulated mostly in liver, spleen, and kidney tissues.[581]

Mitochondria-targeted chlorambucil: Chlorambucil (Chart 77) is another potent alkylating agent of clinically relevant anticancer activity. To overcome the limitations of

chlorambucil-based therapy, it was conjugated to mitochondria-penetrating peptide (mt-Cbl, Chart 77).[582] Mitochondrial targeting of the drug was shown to lead to its increased anticancer activity even in the cells resistant to chlorambucil.[582] It was found that, due to its high reactivity, mt-Clb induces a necrotic type of cell death via rapid nonspecific alkylation of mitochondrial proteins.

By tuning the alkylating activity of the chlorambucil moiety via chemical modification, the rate of generation of protein adducts can be reduced, resulting in a shift of the cell death mechanism from necrosis to a more controlled apoptotic pathway.[583] Another approach to "reroute" chlorambucil to mitochondria involved conjugation with the TPP^+ moiety (Mito-Chlor, Chart 77).[584,585] TPP^+-linked chlorambucil was shown to be 80-fold more potent than the parent compound in inducing cell death of breast and pancreatic cancer cells in vitro.[584] Linking of chlorambucil either to the mitochondria-penetrating peptide or to the TPP^+ moiety enhances its in vivo antitumor potency against leukemia and pancreatic cancer in mouse models.[584,585]

Mitochondrial targeting of paclitaxel: Paclitaxel (Chart 78) is an anticancer drug used to treat ovarian, breast, pancreatic, and other cancers. To target the drug to mitochondria, paclitaxel was loaded into dequalinium-based liposomes (DQAsomes) and tested for possible modulation of its proapoptotic effects.[142] Loading paclitaxel into DQAsomes was shown to significantly improve its proapoptotic effects. A similar approach, but using liposomes carrying Rh-123 as the mitochondria-targeting motif, was also reported.[586] Rh-123-modified liposomes loaded with paclitaxel were shown to be significantly more toxic to HeLa cancer cells than free paclitaxel or untargeted liposomes carrying the drug.

In the subsequent research, the liposomes modified with the TPP^+ moiety were tested as a vehicle for paclitaxel in the in vitro and in vivo models.[141] Paclitaxel-loaded TPP^+-linked liposomes exhibited enhanced cytotoxic effects against HeLa cancer cells in vitro and tumor growth inhibitory activity against breast cancer xenografts in mice in vivo. A similar approach using TPP^+-conjugated liposomes for mitochondrial delivery of paclitaxel was reported to result in improved mitochondrial localization and enhanced cytotoxicity in a paclitaxel-resistant cell line.[516] The improvement in cytotoxicity was attributed not only to the increased accumulation of paclitaxel in the mitochondria but also to the specific toxicity of STPP toward the resistant cell line by decreasing the mitochondrial membrane potential.

Also, mitochondrial delivery of the synthetic analog of paclitaxel, fluorinated docetaxel, via covalent conjugation to cationic rhodamine B was reported (4FDT-RhB, Chart 78).[587] The rhodamine B (RhB) moiety served not only as the targeting agent but also as a fluorescent label, enabling tracking of the pro-drug localization. The mitochondria-targeted docetaxel was shown to undergo intracellular hydrolysis to release the active drug and exhibit enhanced cytotoxic effects against HepG2 cells upon drug release. It is possible that an approach similar to rhodamine-based derivatization can be applied to conjugate the drug with the TPP^+ moiety to further improve its mitochondrial uptake and potency against cancer cells.

7.3.5. Mitochondria-Targeted Radiosensitizers and Photosensitizers—Tumor hypoxia is a major hindrance for successful implementation of both radiation and photodynamic therapy (PDT). Tumor hypoxia results from an imbalance between oxygen delivery and oxygen utilization.[517–520] Published reports suggest that decreasing oxygen consumption by inhibiting respiration with pharmacologic agents is an effective way to increase tumor oxygenation (i.e., decreased hypoxia) and radiosensitivity.[588,589] Several inhibitors of mitochondrial respiration, including metformin, enhanced tumor radiosensitivity by improving tumor oxygenation.[590–595]

Mitochondria-targeted agents inhibit respiration at much lower concentrations.[16,17,21,210,432,547] Thus, the compounds within this class likely will act as much more potent radiosensitizers. As shown previously, Mito-Met_{10} (Chart 66) inhibited mitochondrial complex I activity and pancreatic cancer cell respiration at micromolar levels, whereas metformin inhibited respiration to a similar extent at millimolar level.[21] Mito-Met_{10} was shown to be significantly more effective than metformin in inhibiting proliferation of pancreatic cancer cells subjected to X-radiation.[21] Mito-Met_{10}, at concentrations 1,000-fold lower than metformin, inhibited mitochondrial respiration, induced AMPK activation, and decreased Forkhead Box M1 (FOXM1), a redox-responsive transcription factor. It is possible that two or more mechanisms operate. AMPK-activating drugs increase tumor radiosensitivity.[592,593,596] The suppression of FOXM1 was shown to enhance the radiosensitivity of different human cancer cells.[597,598] Mito-Met_{10} and other mitochondria-targeted metformin analogs can be considered as potential radiosensitizers. Other mitochondria-targeted agents, including derivatives of TEMPOL, were shown to protect against radiation-induced oxidative damage in normal cells and radiosensitize the glioma cells.[412,413,419,421]

Mitochondria-targeting lipophilic cations, by their ability to inhibit mitochondrial respiration, may increase steady-state concentration of intracellular oxygen and sensitize cells to PDT and ionizing radiation, especially under a limited supply of oxygen. It was suggested that the MKT-077 cation, by decreasing the rate of oxygen consumption, may increase tumor oxygen levels and radiosensitivity.[599]

Photodynamic therapy is considered as safe, efficient, and minimally invasive cancer treatment.[600] Mitochondria have been reported to play a major role in photodynamic cell death.[601] One of the limitations of PDT involves a lack of tumor selectivity of the photosensitizer, leading to injury of normal tissue upon exposure to light. To overcome this limitation and to accumulate the PDT agents in mitochondria, which is an important organelle in the induction of apoptosis, numerous attempts have been made to target photosensitizers to cancer cell mitochondria, as discussed below.

Linking porphyrin to guanidines: In an attempt to target the porphyrin photosensitizer to cancer cell mitochondria, it was conjugated to guanidine, biguanidine, and the mitochondrial localization sequence (MLS) peptide (Chart 79).[602] Though all three porphyrin derivatives displayed low dark toxicity, they showed significant phototoxicity, and the guanidine-linked porphyrin was the most potent photosensitizer. Interestingly, the guanidine and bisguanidine

derivatives were reported to localize in mitochondria, lysosomes, and endoplasmic reticulum (ER), and the MLS derivative was reported to localize mostly in lysosomes.[602]

Linking porphyrin to lipophilic cations: Two lipophilic cations, RhB and acridine orange (AO), were linked via a short alkyl chain to porphyrin (Porphyrin-RhB and Porphyrin-AO, Chart 79) to deliver it to mitochondria.[84] AO and AO-porphyrin conjugate were shown to exhibit significant dark toxicity and, therefore, were deemed unsuitable for PDT. Conversely, RhB-porphyrin exhibited low dark toxicity but significantly increased cellular uptake and mitochondrial localization of porphyrin, which translated into potent phototoxic activity of the conjugate.[84] Also, porphyrin conjugated to the TPP^+ moiety (Porphyrin-TPP^+, Chart 79) was synthesized and showed mitochondrial localization and enhanced photosensitizing activity against breast cancer cells.[603]

Linking core-modified porphyrin to lipophilic cations: Core-modified porphyrins have been extensively studied as a second-generation of photosensitizers. To target dithiaporphyrin to cancer cell mitochondria, it was selected for derivatization by conjugation to RhB or TPP^+ cations (Chart 80).[89] All compounds synthesized displayed low dark toxicity. It was reported that linking dithiaporphyrin to a single TPP^+ led to the highest cellular uptake and the strongest phototoxic efficacy. Derivatization with two TPP^+ moieties or RhB led to lower, but still significant, cellular accumulation of the compounds and phototoxic effects. Interestingly, it was observed that, though the RhB conjugate accumulated in cell mitochondria, the TPP^+ conjugates were less efficient in mitochondrial localization.[89]

Linking protoporphyrin IX with mitochondria-targeted proapoptotic peptide: To improve tumor selectivity and efficiency of the PDT, the photosensitizer protoporphyrin IX (PpIX) was conjugated with a mitochondria-targeted peptide $(KLAKLAK)_2$ using a short PEG linker.[604] $(KLAKLAK)_2$ peptide previously was reported to target cancer cells and induce apoptosis by disrupting mitochondrial membranes and inducing mitochondrial swelling.[133] The PpIX-peptide conjugate was shown to be a significantly more potent photosensitizer than PpIX or peptide alone.[604] In addition, the conjugate exhibited superior accumulation in tumor tissue in vivo and was more potent than PpIX or the peptide in inhibiting tumor growth in the mouse hepatoma H22-tumor-bearing mouse model. It was also reported that the conjugate can self-assemble, and this feature was used to combine PDT with mitochondrial delivery of DOX.[605] Cells incubated with DOX-loaded PpIX-peptide nanoparticles were shown to be most sensitive to PDT. The proposed approach also enabled accumulation of DOX in DOX-resistant MCF-7/ADR cells.

Mitochondria-targeted Pt(II) porphyrin: Platinum (II)-porphyrin complexes are being developed as phosphorescent probes for monitoring oxygen levels in biological systems. Because the same complexes are also capable of producing singlet oxygen, they were proposed for use as theranostic (therapeutic-diagnostic) agents in PDT.[606] TPP^+-conjugated nanoparticles were doped with Pt(II)-meso-tetra(pentafluorophenyl)porphine (PtTFPP) and delivered to cancer cell mitochondria for improved phototherapy and monitoring of cancer cell respiratory activity in response to phototherapy. Irradiating cells with short wavelength

light (405 nm) induced cell death, which was attributed to singlet oxygen, $^1O_2$. By monitoring the lifetime of the phosphorescent nanoparticles, the changes in intramitochondrial oxygen concentration were determined. In response to PDT, a significant increase in the intramitochondrial oxygen level was observed, which corresponds to decreased mitochondrial respiration, as a result of light-induced cytotoxicity.[606]

Mitochondrial targeting of Zn(II) phthalocyanine: Phthalocyanines (Pc, Chart 81) are widely studied photosensitizers with an intense absorption band in the 650–800 nm spectral region. To target Zn(II)-Pc complex to mitochondria, the Pc core was conjugated with methylimidazolium cations.[607] Intracellular distribution of the mitochondria-targeted Zn-Pc complex (ZnPc1) indicated its mitochondrial accumulation. Remarkable photocytotoxicity but low dark cytotoxic properties were observed for ZnPc1 in four different cancer cell lines. PDT with ZnPc1 resulted in a collapse of the mitochondrial membrane potential and chromatin condensation, all important hallmarks of apoptosis.[607]

Mitochondrial delivery of the ZnPc photosensitizer was also achieved by using mitochondria-targeted TPP^+-conjugated nanoparticles, based on a biodegradable polymer. It was proposed that mitochondrial localization of ZnPc could help boost host immune defense against cancer cells upon photoirradiation.[608,609] Breast cancer cells loaded with mitochondria-targeted nanoparticles carrying ZnPc and exposed to light were shown to generate tumor antigens that activated dendritic cell (DC) to produce high levels of interferon-gamma, an important cytokine considered to be a product of T-cells, and natural killer cells, the key players in the defense against cancer cells.[608] Thus, by targeting photosensitizers to mitochondria, the direct killing of cancer cells by PDT would be accompanied by the stimulation of host immune response, with a potentially improved therapy outcome.

Mitochondrial delivery of chlorin e6: Similar to porphyrin-based photosensitizers, chlorin e6 (Ce6, Chart 81) was targeted to mitochondria to improve the PDT efficiency. Ce6 was encapsulated with the NIR dye IR780 in TPP^+-conjugated liposomes.[610] In addition to being a potential agent for photothermal therapy (PTT), IR780 dye served as an acceptor of the Ce6 fluorescence via the fluorescence resonance energy transfer (FRET) mechanism, effectively acting as an “off switch” for PDT and controlling the Ce6 phototoxicity. NIR light-induced photodegradation of IR780 acted as an “on switch,” enabling Ce6 fluorescence and singlet oxygen generation. It was shown that prepared liposomes accumulate in the mitochondria of HeLa cells and sensitize the cells to PDT after photodegradation of IR780.[610] Mitochondrial targeting significantly enhanced the killing efficiency in the proposed irradiation regimen.

Oxovanadium (IV) complexes of curcumin: An oxovanadium (IV) complex of curcumin, a nonporphyrin PDT agent, was conjugated to the TPP^+ moiety to target it to mitochondria and induce site-specific photodamage.[478] The TPP^+-linked complex (Cur-V-TPP, Chart 70) induced significant phototoxicity and led to cell cycle arrest at sub-G1/G0 phase cell-cycle.[478] The limitation of the proposed approach was the significant dark toxicity of the compound, possibly due to presence of the TPP^+ moiety.

Mitochondrial targeting of iridium (III) complexes: Iridium (III) complexes are another class of potential nonporphyrin PDT agents. Similar to Pt(II)-porphyrin, iridium (III) complexes exhibit long-lived, oxygen-sensitive phosphorescence, and thus can also be potentially used as theranostic agents. Iridium (III) complex has been linked to the TPP^+ moiety to target it to cancer cell mitochondria (Chart 82).[611]

Mitochondrial targeting led to significantly higher phototoxic effects, when compared with analogous compound targeted to lysosomes, both at 21% and 5% oxygen (O_2). It should be noted that at 5% O_2, the lysosome-targeted probe did not show phototoxic effects. This was explained by the requirement of O_2 for PDT, and a low steady-state intracellular oxygen level due to cellular respiration and a low O_2 supply. In contrast, the TPP^+-linked photosensitizer inhibited mitochondrial respiration, leading to higher steady-state levels of O_2, sufficient for PDT. Thus, the TPP^+ moiety not only served as a targeting agent, but also sensitized cells by raising the intracellular/intramitochondrial O_2 concentration.

Mitochondrial targeting of ruthenium (II) complexes: Four ruthenium (II) complexes (RuL1–RuL4, Chart 83) were designed and developed to act as mitochondria-targeted two-photon photodynamic anticancer agents. Two of them were conjugated to the TPP^+ moiety via alkyl chain linkers of different lengths.[612]

The homolog with the longer linker, RuL4, was shown to possess the highest affinity to mitochondria and the highest phototoxic potency. These Ru(II) complexes were shown to generate sufficient singlet oxygen under one- and two-photon irradiation to trigger cell death in both monolayer cells and 3D HeLa multicellular spheroids (MCSs). RuL4 is an order of magnitude more toxic than cisplatin in 3D MCSs.[612]

Cyanine-based NIR photosensitizers: Cyanine dyes are lipophilic compounds that may act as the mitochondria-targeting moiety, NIR fluorophore, as well as PDT and PTT agents. A series of heptamethine cyanine dyes were tested for their accumulation in tumor tissue in vivo, and the cyanines showing preferential localization in tumor were tested for their PTT/PDT efficacy.[613] The compound exhibiting the highest potential as an efficient PTT and PDT agent was shown to localize in cell mitochondria and enabled highly efficient phototherapy in multiple cancer cells and animal xenograft models.[613]

Mitochondria-targeted triphenylamine derivatives: Triphenylamines (TPAs) represent a new class of potential photosensitizers. TPAs, functionalized with pyridinium (TP2Py) or benzimidazolium (TP3Bzim) cationic groups, were synthesized and tested for their phototoxic effects via two-photon NIR irradiation (Chart 84).[614]

The TPA cationic derivatives were shown to accumulate in cell mitochondria, and upon NIR irradiation trigger the mitochondrial apoptotic pathway. It was concluded that mitochondrial localization, together with large two-photon absorption cross-section in the 760–860 spectral region, makes the compounds promising for in vivo PDT using NIR irradiation.

Mitochondria-targeted aggregation-induced emission fluorophores: As discussed previously, Mito-AIEs exhibit anticancer properties. However, it was shown that this class of

compounds may be also used in PDT.[205] By linking the AIE fluorophore to one or two TPP^+, the compound was targeted to mitochondria, and exhibited significant improvement in phototoxic potency. While the double-TPP^+-substituted analog also displayed dark toxicity, the mono-substituted analog was relatively nontoxic in the dark. Because the compounds can fluoresce upon accumulation in mitochondria, they can also act as theranostic agents and be used to monitor tumor growth.[205]

Mitochondria-targeted UCNPs: Upconversion nanoparticles (UCNPs) possess the capacity to emit short-wavelength (higher energy) light upon exposure to longer wavelength (typically NIR) excitation. This feature makes them ideal for bioimaging and for combination with PDT agents. UCNPs were recently functionalized with transcriptional activator (TAT) peptides as targeting moieties.[615] Upon functionalization, the particles were reported to localize in cell mitochondria. Upon loading with the pyropheophorbide a photosensitizer, the particles exhibited significant cellular uptake and dramatically elevated photocytotoxicity. It was proposed that UCNPs can serve as both nanoprobes and carriers of photosensitizers toward mitochondria for PDT.

7.3.6. Combination of Mitochondria-Targeted Compounds with Antiglycolytic or Other Treatments—

The chemotherapies and cocktail chemotherapies currently available often are associated with significant morbidity and enhanced side effects.[616–618] A major objective in cancer chemotherapy is to enhance tumor cell cytotoxicity without exerting undue cytotoxicity in normal cells. One way to achieve this objective is to combine the standard-of-care chemotherapies and/or radiation with relatively nontoxic cationic mitochondria-targeted synthetic compounds containing a naturally occurring component that can selectively inhibit cancer cell energy metabolism and promote antiproliferative effects. If this modality were to selectively and synergistically enhance cytostatic and cytotoxic effects in cancer cells, it may be possible to decrease the toxic side effects of chemotherapy.

The combination of mitochondria-targeted lipophilic cations with other anticancer agents targeting cancer cell metabolism was proposed soon after discovery of selective anticancer effects of Rh-123. In fact, it was demonstrated that Rh-123's anticancer activity (prolongation of survival) was potentiated by glycolysis inhibitor, 2-deoxy-D-glucose (2-DG), in vitro and in tumor-bearing mice.[496,530] Rh-123 was found to hypersensitize osteosarcoma cells to glycolysis inhibitors, such as 2-DG and oxamate, by inhibiting mitochondrial OXPHOS and increasing lactic acid amounts, which make tumors more anaerobic.[619]

The chemotherapeutic efficacies of Mito-CP and MitoQ in combination with glycolysis inhibitor, 2-DG were reported in breast cancer cells. Both Mito-CP and MitoQ synergized with 2-DG to decrease ATP levels (Figure 15). However, with time, the cellular bioenergetic function and clonogenic survival were largely restored in MCF-10A but not in MCF-7 cells. Also, the combined treatment of Mito-CP and 2-DG led to a significant tumor regression without causing any major morphological changes in kidney, liver, and heart tissue in a breast cancer xenograft mice model.[16] Similar results of this combination were also reported in liver cancer cells.[620] In addition, Mito-CP was reported to significantly enhance

fluvastatin-mediated cytotoxicity in MCF-7 cells and have only a minimal effect on MCF-10A cells, which are nontumorigenic mammary epithelial cells.[621]

Another cationic rhodacyanine-based anticancer agent, MKT-077, was reported to enhance the cytotoxic effect of 3′-azido-3′-deoxythymidine (AZT) through inhibition of mitochondrial energy metabolism and DNA synthesis due to limited deoxythymidine monophosphate availability.[622]

Enhancing the therapeutic index using MitoQ to protect against DOX-induced cardiotoxicity and exacerbate DOX-induced cytotoxicity in cancer cells: DOX, or Adriamycin, an anthracycline quinone antibiotic, is currently being used alone and in combination therapy to treat a wide variety of cancers, including breast and testicular cancers, Hodgkin's disease, and leukemia.[623–626] The clinical use of DOX in adult breast cancer patients is associated with a dose-dependent increase in cardiotoxicity (cardiomyopathy or congestive heart failure).[627,628] This problem manifests in patients long after the cessation of chemotherapy. Implications of delayed cardiotoxicity are much worse in pediatric patients. Children treated with DOX for acute lymphoblastic leukemia are eight times more susceptible to develop cardiac problems (e.g., impaired left ventricular contractility and late congestive heart failure) many years later in their adulthood.[629] Clearly, prophylactic cardioprotective treatment post-chemotherapy is critically needed. The exact mechanism of DOX-induced delayed cardiomyopathy still remains unknown, although multiple mechanisms were proposed, including oxidative stress, mitochondrial DNA damage, intracellular calcium overload, and release of inflammatory cytokines.[630–632]

Previously, coenzyme-Q (Co-Q) administration was shown to prevent the onset and progression of DOX-induced cardiomyopathy.[633] Co-Q administration improved EKG changes and survival rates. Although numerous antioxidant therapies previously were developed to combat DOX toxicity, most of them were not particularly effective.[634] In addition, these antioxidants were not specifically targeted to mitochondria in cardiomyocytes.

Cardiac mitochondria are the target organ of DOX toxicity. DOX was shown to accumulate into mitochondria over time. The intramitochondrial concentration of DOX was reported to be 100 times higher than its extracellular concentration. The selective toxicity of DOX to the heart is attributed to the selective damage to cardiac mitochondria.[635,636] Thus, MitoQ_{10}, a triphenylphosphonium-conjugated analog of coenzyme Q, was chosen as a potential cardioprotective agent.[637]

MitoQ exhibits selective antiproliferative activity against breast cancer cells (Figure 16A).[19] However, opposite results were seen in cardiomyocytes (Figure 16B).[638] Treatment of primary cardiomyocytes and cultured H9c2 cells with DOX induced apoptosis, as shown by caspase-3 and −8 activation. However, coincubation of these cells with MitoQ completely prevented DOX-induced caspase-3/8 activation.

MitoQ-mediated cardioprotection was demonstrated in a DOX-induced cardiomyopathy model.[637] Low doses of DOX were chronically administered to rats once a week and 2D

echocardiography was performed to assess the morphologic and functional changes in the left ventricle.[637] There was a progressive reduction in the global strain (also cardiac function) starting at eight weeks after DOX treatment. Coadministration of MitoQ prevented the progressive decline in cardiac function (Figure 17).

Using low-temperature ex vivo EPR analyzes, a time-dependent decrease in the heme signal, characteristic of the exchange interaction between cytochrome *c* oxidase (CcO)-Fe(III) heme a3 and CuB, was detected in heart tissues isolated from rats administered a cumulative dose of DOX. The EPR data suggest that a prolonged treatment with DOX uncouples the heme a3/CuB dinuclear active center of subunit 1 of cytochrome *c* oxidase that is involved in oxygen binding. In agreement with the EPR data, the CcO activity and the expressions of CcO subunits that were restored by MitoQ decreased.[637] These findings suggest a novel cardioprotection mechanism (not related to oxidative stress) by MitoQ during DOX-induced cardiomyopathy involving cytochrome *c* oxidase.

MitoQ effectively protected against cardiotoxicity induced by DOX in a rat model of cardiomyopathy and without mitigating its antitumor potency. Given the safety profile of MitoQ in humans established so far in PD studies, MitoQ could prove to be a favorable drug candidate for combination therapy with DOX in breast cancer treatment and/or as a long-term cardioprotective drug post DOX chemotherapy.

Mito-TEMPOL: The separate monitoring of cancer therapeutic and cardioprotective effects of the experimental drugs is one of the limitations of most preclinical models in cardio-oncology. The more physiologically relevant models are being developed for monitoring cardioprotective effects of the potential drugs in animals bearing the tumor, so that the effect of the compound on both cardiac function and tumor growth can be simultaneously monitored, when used alone or in combination with standard-of-care chemotherapeutics. Mito-TEMPOL-C_4 was tested alone and in combination with DOX in a syngeneic breast tumor rat model.[420] It was demonstrated that the compound accumulated both in tumor and in cardiac tissues. Mito-TEMPOL-C_4 was shown to ameliorate doxorubicin-induced cardiomyopathy without altering the antitumor activity, independently or in combination with doxorubicin. (Figure 18).[420]

Dual targeting of mitochondrial bioenergetics and glycolytic metabolism: New combinatorial therapeutic usage of MTAs

Antiproliferative and cytotoxic effects: As discussed previously, one of the fundamental changes that occurs in most malignant tumor cells is the metabolic reprogramming mechanism—the shift in energy metabolism from OXPHOS to aerobic glycolysis to generate ATP.[498,500,501] However, glycolytic inhibition using 2-DG (an antiglycolytic agent) did not prove to be a viable chemotherapeutic strategy due the lack of efficiency when used as a monotherapy at a clinically relevant dosage.[639] Recent studies suggest a novel dual-targeting approach utilizing both mitochondria-targeted compounds and antiglycolytic agents as a plausible route to increase the anticancer potency of 2-DG.[16,496,619,620,640] Rh-123, which accumulates in mitochondria and inhibits cellular respiration, was shown to sensitize cancer cells to 2-DG both in vitro and in vivo.[496,530] Similarly, synergistic effects

of combination of the TPP^+ cation and 2-DG on proliferation of FaDu carcinoma cells were reported.[522]

The Seahorse Bioscience Extracellular Flux Analyzer (Agilent Technologies, Santa Clara, CA) is suitable for monitoring changes in mitochondrial bioenergetics (OXPHOS and glycolysis) caused by mitochondria-targeted agents alone and in combination with antiglycolytics.[16,21,641] Using this technique, the basal or baseline oxygen consumption rate (OCR) and extracellular acidification rate in cancer cells exposed to different concentrations of drugs, treatment time, and drug washout can be monitored in real time. From these measurements, indices of mitochondrial function and mitochondrial complexes in the ETC can be determined.

Below, we briefly summarize the synergistic antiproliferative effects of Mito-CP or MitoQ and 2-DG (Figure 19) detected in breast cancer cell lines (MCF-7 and MDA-MB-231) but not in the noncancerous control cell line (MCF-10A).[16]

One of the hallmarks of tumor cells is their ability to form colonies. As shown in Figure 19, the addition of varying levels of 2-DG alone did not significantly decrease the colony formation in these cells. In contrast, colony formation in MCF-7 cells decreased when treated with 2-DG in the presence of 1 μM Mito-CP or MitoQ, although Mito-CP was more potent in inhibiting the colony formation (Figure 19). Figure 19B shows the survival fractions of MCF-7, MDA-MB-231, and MCF-10A calculated from the clonogenic survival assay. Both MitoQ and Mito-CP more potently decreased the survival fraction in MCF-7 and MDA-MB-231 cells when compared with MCF-10A cells in the presence of 2-DG. Under these conditions, incubation with TPP^+-C_{10} and different 2-DG levels did not significantly decrease the survival fraction in either cancer cell line (Figure 19). Incubation with the untargeted nitroxide CP or TPP^+-C_1 alone and together with different 2-DG levels did not significantly affect cell survival. When using MTAs of this type, it is always important to combine the parent compound with alkyl-TPP^+ cation to rule out nonspecific effects.

ATP measurements: Mitochondria-targeted cationic agents deplete intracellular ATP selectively in cancer cells.[432]. Although redox-based chemotherapeutics cause depletion of intracellular ATP through increased oxidative stress, these drugs also induce oxidative mechanism in normal cells resulting in depletion of ATP.[642,643] It appears that selective inhibition of ATP-linked respiration in tumor cells by mitochondria-targeted agents is responsible for ATP depletion.[16,17,432] The inhibitory effect is prolonged and permanent in breast cancer cells but not in control, noncancerous cells.[432] This is an interesting finding that links the selective cytotoxic effects of mitochondria-targeted cationic agents to the inhibition of intracellular energy metabolism. A representative example (Figure 20) shows a heat map representation of intracellular ATP levels in MCF-7 and MDA-MB-231 breast cancer cells and MCF-10A nontumorigenic cells (colored areas from brown to purple indicate a progressive decrease in ATP from 100% to 0%).[432] Intracellular ATP levels were measured using a luciferase-based assay. The same approach can be used to monitor changes in ATP in tumor xenografts based on luciferase-expressing cancer cells, using biophotonic imaging.

Rh-123 treatment alone (up to 100 μM) did not cause significant intracellular ATP depletion in MCF-7 cells; however, the combined treatment of Rh-123 (30 μM) and 2-DG induced a rapid loss of ATP in MCF-7 cells.

Mitochondrial bioenergetic function: To accurately mimic and correlate bioenergetics results with clonogenic survival measurements, we used the experimental protocol shown in Figure 21. Both MCF-7 and MCF-10A cells were treated with Mito-CP or MitoQ in combination with 2-DG for six h, followed by washout, and then were returned to fresh culture media.[16] After 36 h, the OCR was measured in the absence and presence of added metabolic modulators (oligomycin to inhibit ATP synthase, FCCP to uncouple the mitochondria and yield maximal OCR, and antimycin A to inhibit complex III and mitochondrial oxygen consumption). Interestingly, Mito-CP exerted the most dramatic effect on basal OCR and the OCR-linked to ATP production. It is evident that inhibition of OCR was persistent 36 h after removal of Mito-CP in MCF-7 cells but not in MCF-10A cells. MitoQ had a similar effect, although slightly lower. The inhibitory effect of these compounds was significantly lower in MCF-10A cells. This suggests that either MCF-10A cells are more adept at recovering from inhibition of mitochondrial function than MCF-7 cells or these compounds (MitoQ and Mito-CP) accumulate to a higher level in MCF-7 cells than MCF-10A cells. The inhibition of OCR persisted even up to 60 h after washout of Mito-CP or MitoQ in MCF-7 but not in MCF-10A cells (Figure 21). Similar effects were also observed for the mitochondria-targeted vitamin E analog, Mito-ChM.[432] Collectively, these results indicate that MTDs and 2-DG cause synergistic inhibition of proliferation of MCF-7 breast cancer cells through irreversible mitochondrial inhibition.[16]

Mito-CP prevents cisplatin-induced nephropathy: An anti-inflammatory agent?: Cisplatin is a widely used antineoplastic agent. Cisplatin arrests DNA synthesis in rapidly dividing cancer cells.[644,645] A major limitation of cisplatin chemotherapy is the development of a dose-dependent nephrotoxicity in 30% of patients, thus restricting its continued use in chemotherapy. Enhanced oxidative and nitrative damage and inflammation were implicated in cisplatin-induced renal tubular cell injury.[646,647] In addition to enhancing renal oxidative/nitrative stress (as measured by formation of 3-nitrotyrosine, HNE/carbonyl adducts, malondialdehyde, and 8-OH-dG), cisplatin caused deterioration of mitochondrial structure and function, an intense inflammatory response, histopathological injury, and renal dysfunction. Mitochondria-targeted antioxidants (Mito-CP or MitoQ) dose-dependently prevented cisplatin-induced renal function and inhibited oxidative and nitrative stress.[490] One of the major findings of this study is that Mito-CP mitigates cisplatin-induced acute and late inflammatory response. Cisplatin markedly increased the proinflammatory cytokines, MCP-1 and MIP1α/2; the tumor necrosis factor, TNF-alpha; the adhesion molecule, ICAM-1; and MPO activity (an indicator of leukocyte infiltration, Figure 22).[490]

Mito-CP also inhibited the second wave of inflammatory damage and ROS formation following enhanced leukocyte infiltration. The secondary wave of ROS formation induced by cisplatin probably involves the phagocyte nicotinamide adenine dinucleotide phosphate (NADPH) oxidase isoform, gp91phox/NOX2 and NOX4/renox, and the expression of these enzymes was significantly increased in the kidneys the day after cisplatin administration.

Mito-CP inhibited the late/secondary expression of mRNA and protein levels of ROS-generating enzymes, NOX2/4.[490] These findings indicate a novel signaling role for mitochondria-targeted antioxidants (Mito-CP and MitoQ), which downregulate the expression of proinflammatory processes induced by chemotherapeutics such as cisplatin in normal tissues. Mito-CP, however, augmented the cytotoxicity induced by cisplatin in bladder cancer cells. Thus, it appears that Mito-CP can enhance the therapeutic index of cisplatin.

7.4. Mitochondria-Targeted Neuroprotective Agents

Several lines of evidence implicate that PD is a free radical disease involving mitochondrial dysfunction leading to failure of energy production.[648–650] Increased oxidative damage, dopamine depletion, protein nitration, iron accumulation, protein aggregation, and apoptosis were shown to be characteristic hallmarks of PD.[651,652] Numerous antioxidants and iron chelators alone and in combination were used in PD treatment and PD clinical trials with little or limited success.[653–655] MitoQ was used in a clinical trial conducted in New Zeland.[488] MitoQ was shown to be relatively safe but prolonged administration of MitoQ in PD patients did not halt the progression of this disease.[488] The proposed mechanism was that MitoQ would detoxify superoxide in a reaction involving the recycling of MitoQ and its reduced form.[394,488] Clearly, PD is a multifactorial disease involving several mechanisms, and it is likely that a combinatorial therapy involving various mitochondria-targeted agents is essential to restore the extensive neuronal damage and dopamine depletion that has already occurred in patients showing PD symptoms. MitoQ treatment partially restored the neurobehavioral deficit and mitochondrial aconitase inactivation in the 1-methyl-4-phenyl-1,2,3,6-tetrahydropyridine (MPTP) mice model of PD.[656] In order to obtain a better understanding of the anti-inflammatory effects of mitochondrial antioxidants, in-depth investigation of other mitochondria-targeted agents using several preclinical models of PD is essential.

Investigators showed the beneficial effects of subchronic infusion of very low levels of a cationic compound, diphenyleneiodonium (DPI), in multiple PD models.[657] Although DPI was used as a nonspecific inhibitor of mitochondrial complex I, NADPH oxidase, and other flavoprotein enzymes, at the ultra-low subpicomolar concentrations (10^{-14} to 10^{-13} M) used in that study, the investigators concluded that DPI selectively inhibited microglia-induced chronic inflammation by selectively inhibiting the superoxide-generating enzyme, NADPH oxidase.[657,658] Activation of resident immune cells in the brain (called microglia) by inflammatory mediators or molecules generated during inflammation contribute to the death or degeneration of neurons.[659–661] It was suggested that ultra-low-dose DPI could be used as a promising neuroprotective therapy in patients with PD.[657] Prior research in PD has also implicated a role for NADPH oxidase activation and ROS/RNS formation in PD model systems.[658,662,663] Thus, there is a critical unmet need to develop nontoxic drugs that can permeate the blood-brain barrier and inhibit microglial activation, inhibit NOX-192 induced oxidant formation, mitigate neuroinflammation, and afford long-term dopaminergic neuroprotection.

Apocynin (4-hydroxy-3-methoxyacetophenone) is a naturally occurring methoxy-substituted catechol that was reported to inhibit NADPH-oxidase in several model systems, although the mechanism of inhibition seems to be indirect.[664,665] Diapocynin, formed by dimerization of two molecules of apocynin, was shown to inhibit neuroinflammation in microglial cell culture models, MPTP and LRRK2^{R1441G} models of neuroinflammation and PD.[666,667] Both apocynin and diapocynin were used at high doses (300 mg/kg body weight), although they are not toxic even at these high concentrations.[666–668] Based on MitoQ's ability to cross the blood-brain barrier, it was surmised that mitochondrial targeting of apocynin would provide more effective neuroprotection. To this end, mitochondria-targeted apocynins (Mito-Apo$_n$, Chart 85) were synthesized by conjugating the apocynin moiety with a TPP$^+$ cation. Both short-chain and long-chain Mito-Apo compounds (Mito-Apo$_2$ and Mito-Apo$_{11}$) were synthesized and characterized.[493,495] These compounds are orally available and target mitochondria.

In recent studies, Mito-Apos were shown to be effective in preventing both early PD-like symptoms and neuroinflammation in preclinical animal models of PD.[493,495] Decreased olfactory function is an early indication of PD in human patients. The lucine-rich repeat kinase 2 (LRRK2^{R1441G}) transgenic mouse was used as a genetic model of 193 human PD.[493] LRRK2 transgenic mice display deficits in sense of smell in both the hidden treat test and a radial arm maze test.[666] Treatment with Mito-Apo$_{11}$ prevented the loss of smell as evidenced by the animals' ability to identify either a scented treat or a food pellet as well as the wild-type littermates (Figure 23).[493] In addition, Mito-Apo$_{11}$ treatment for 15 months significantly restored the loss of motor function in the LRRK2 transgenic wild-type littermates. These improvements were noticed in LRRK2 mice treated with doses of Mito-Apo$_{11}$ lower than those required for diapocynin.

Mito-apocynin-C$_2$ treatment afforded neuroprotection in the MPTP mouse model of PD.[495] Mito-Apo$_2$ restored the behavioral performance of MPTP-treated mice. Oral administration of Mito-Apo$_2$ significantly attenuated MPTP-induced glial cell activation, proinflammatory cytokine upregulation, inducible nitric oxide synthase, and NOX2 components (gp91^{phox}). Mito-Apo$_2$ also decreased nitrotyrosine and 4-hydroxynonenal formation in the substantia nigra.[495] These results are consistent with the ability of mitochondria-targeted compounds to decrease the expression of NOX2, inducible NOS, and other proinflammatory mediators, as shown for Mito-CP. To our knowledge, this is one of the first reports on the anti-neuroinflammatory effects of mitochondria-targeted drugs of this class.

In a more recent work, investigators reported a polyanhydride, nanoparticle-based, mitochondria-targeted approach to treat neurodegenerative diseases.[669] In particular, nano-formulated mitochondria-targeted apocynin was synthesized, and this nano-formulated Mito-Apo afforded excellent protection against mitochondrial dysfunction and neuronal damage in a variety of neuronal cell lines.[669]

8. MITOCHONDRIA-TARGETED AGENTS IN IMAGING

8.1. Mitochondria-Targeted MRI Contrast Agents

Noninvasive imaging of tissues and organs is an indispensable tool in neurological, cardiovascular, and cancer research.[670] The most widely used noninvasive tomographic imaging modality that offers soft tissue contrast is magnetic resonance imaging (MRI). MRI is based on the ability to capture the intrinsic nuclear magnetic moment of hydrogen nuclei, mainly from water (^1H in H_2O) and lipid molecules. Radiofrequency irradiation of nuclei exposed to a static magnetic field causes a perturbation of the steady-state equilibrium, and with time- and space-dependent modulation of the magnetic field. Nuclei relax after that perturbation by two related relaxation mechanisms, which are the T_1 (spin-lattice relaxation) and T_2 (spin-spin relaxation) times. However, in many cases, in order to enhance the resolution of specific tissues, it is necessary to employ contrast agents. In MRI, contrast agents (which are usually paramagnetic substances) modify the T_1 and T_2 relaxation times, altering the contrast of the image. The use of contrast agents has greatly enhanced the scope of MRI and enabled probing of different tumors.[671]

The paramagnetic nitroxides have long been proposed as potential contrast agents.[672] However, their modest relaxivity when compared with gadolinium (Gd)-based contrast agents hindered their translation into clinical use.[673] Recent advances and enhancements in MRI instrumentation, including more powerful magnets, coupled with bioreduction-resistant nitroxides and the fact that nitroxide metabolism in tissue could be used as a tool for probing tumor metabolism, have again opened the potential for their use in biomedical research.[674–677]

Mitochondria-targeted nitroxides—One of the first mitochondria-targeted nitroxides used for the specific purpose of tumor tissue imaging was Mito-CP. As a proof of concept, Mito-CP was tested in tubes containing suspended isolated mitochondria, in the presence of succinate as a substrate (Figure 24).[678] By imaging spin echo inversion recovery, the sedimenting mitochondrial pellet is clearly seen in the tubes containing Mito-CP, but not in the control (or CP-containing) tubes. This proves that Mito-CP binds to mitochondria and can be used for MRI visualization of mitochondria.

Targeting CP to mitochondria allowed for labeling tumor tissue in vivo (Figure 25) and resulted in an enhancement of the longitudinal relaxivity.[489,678–680] The in vivo systemic concentration studies showed that Mito-CP but not CP was reduced/cleared completely after 30 mins of bolus injection. A dynamic T_1-weighted time course obtained from a breast tumor indicated the uptake of the Mito-CP contrast agent. The reduction rate of Mito-CP in MCF7 cells was 20.8 times higher than that of the parent compound CP.[679,680]

As nitroxides undergo rapid reduction to the diamagnetic hydroxylamines, they were used to probe the redox status of tissues.[672,675,677,681–685] Studies have demonstrated that the ratio of the nitroxide/hydroxylamine is dependent on the redox environment of the tissue.[683–685] Increased capabilities of newer MRI instruments may help overcome the limitations of nitroxides for clinical diagnostic use.[672,675,677,681,682]

Recently, two reports have employed Mito-TEMPO (Chart 62) as a contrast agent for MRI-based redox probing.[686,687] Mito-TEMPO was used to monitor the redox status of the dopaminergic sector of the brain in the MPTP-based mouse model of PD.[687] A weak and short-lived nitroxide-enhanced signal was observed in the brain of healthy animals. In contrast, MPTP-treated mice brain tissue displayed a long-lived and strong nitroxide-enhanced signal indicative of the highly oxidative environment, especially in the dopaminergic areas. In the second report, the role of superoxide/H_2O_2 production, presumably from mitochondria and/or NADPH oxidases, in controlling the nitroxide-enhanced MRI signal was evaluated.[686,687] The MRI signal was monitored in Mito-TEMPO-loaded cultured cells upon inhibition of mitochondrial function in order to induce aberrant superoxide production. Results obtained suggest that mitochondria-derived superoxide is responsible for enhanced T_1-weighted MRI contrast in cells. However, the other possible interpretation is that, by inhibiting mitochondrial electron transfer, the cellular reduction of the nitroxide was slower, leading to an increased steady-state concentration of the Mito-TEMPO nitroxide and increased MRI contrast effect.

Mitochondria-targeted Gd(III)-DOTA and Gd(III)-DTPA and other MRI contrast agents—Currently, the metal chelates most widely used in MRI are Gd(III) ions complexed by 1, 4, 7, 10-tetraazacyclododecane -N, N, N, N-tetraacetic acid (DOTA) or diethylenetriaminepentaacetic acid (DTPA). Several analogs of these complexes were synthesized to target specific tissues or cell receptors.[688] Following the same rationale taken with Mito-CP nitroxide, mitochondria-targeted Gd(III) metal complexes were designed and synthesized by conjugating both Gd(III)-DTPA and Gd(III)-DOTA to an alkylene-TPP^+ moiety (Chart 86).[679]

Both Mito-Gd(III)-DOTA and Mito-Gd(III)-DTPA are feasible for use as in vivo MRI contrast agents. Mito-Gd(III)-DOTA accumulates in rat brain tumors, with the uptake different than that of the parent contrast agent, Gd(III)-DOTA.[678,689] This opens up the possibility of translating mitochondria-targeted Gd-complexes into the clinic for diagnosis and monitoring of brain cancer.

A novel DO3A-based Gd^{3+} chelate conjugated to a 2-(diphenylphosphoryl)-ethyldiphenylphosphonium cation was also reported as a lipophilic and cationic MRI contrast agent for tumor imaging.[690] Preparation of this novel compound was based on the translation to MRI of previous research results obtained by the group in the development of the novel TPP^+-conjugated analog compounds linked to ^{64}Cu as tumor-selective PET imaging radiotracers (see below).[691–694] Gd(DO3A-xy-$TPEP)^+$ exhibited a relatively low toxicity, with IC_{50} values in the low millimolar range in both normal and tumor cells. In vivo imaging studies in C57BL/6 mice showed a significant accumulation of Gd(DO3A-xy-$TPEP)^+$ in liver and kidney tissue even at five h post injection, attributed to the possible binding of the probe to membranes. Xenograft studies on SCID (severe combined immunodeficiency) female mice bearing A498 kidney carcinoma tumors showed that Gd(DO3A-xy-$TPEP)^+$ accumulates in both tumor and normal tissue, but with higher signal enhancement in tumor tissue.[690]

Recently, novel, bifunctional Gd^{3+} complexes using the DO3A moiety targeted to the mitochondria with arylphosphonium cations were reported (Chart 87).[695,696] An in vitro study performed in human glioblastoma multiforme (T98G) cells and primary human carotid artery endothelial cells (HCtAEC) demonstrated low cytotoxicity and selectivity for tumor cells, a feature that was previously reported for some other TPP^+-targeted agents.[16,17,21,679,680,697–699] Cell loading of these novel complexes in tumor cells exceeds an impressive 10^{10} Gd atoms per cell. Therefore, these compounds are potential candidates for novel cutting-edge cancer therapies such as neutron capture therapy and photon activation therapy due to their capacity to transport high quantities of Gd(III) ion selectively to tumors with low peripheral toxicity.[695]

8.2. Mitochondria-Targeted Radiopharmaceuticals as Imaging Agents

In the field of nuclear medicine, patients are administered a compound labeled with a gamma ray- or positron-emitting radionuclide. The emitted radiation can be detected with high sensitivity to construct an image of the distribution of the radionuclide in the body. Nuclear medicine imaging has two distinct modalities: 1) the tomographic imaging technique, single-photon emission computed tomography (SPECT) for gamma emitting probes, and 2) the PET for positron-emitting radionuclides. In contrast with other imaging modalities such as MRI or computer tomography, nuclear medicine imaging techniques provide anatomic and metabolic/functional information of a tissue or even a biological process using ultrasensitive nano- or picomolar concentrations of the radiotracers.

Unlike MRI probes, PET and SPECT radiotracers are not synthesized to enhance the contrast of an image, but to target a specific tissue, cell, or process for monitoring. Conjugation of molecules with known features to radiolabeled monoclonal antibodies or site-specific radiopharmaceuticals directed at molecular targets is feasible and currently under development.

Phosphonium cations—In nuclear medicine, mitochondria have been a target for radiotracer development mainly for cancer and myocardial perfusion imaging. [^{3}H]-TPP and [^{3}H]-TPMP (Chart 88) were initially used to measure mitochondrial and plasma membrane potentials in tissues, cells, and subcellular fractions/particles.[47,52,53,72,524,700–708] [^{3}H]-TPP was tested in a Lewis lung carcinoma and compared to ^{99m}Tc-MIBI.[481] Results demonstrated that the uptake in tumors of [^{3}H]-TPP in lung carcinomas was orders of magnitude greater than that of ^{99m}Tc-MIBI. These results suggest that [^{3}H]-TPP can be used for in vivo tumor staging and to investigate tumor evolution. [^{3}H]-TPP was also tested in an in vivo mice melanoma model in comparison with [^{18}F]-FDG. Results evidenced that [^{3}H]-TPP accumulation was similar to the uptake of [^{18}F]-FDG. In inflammatory tissues, accumulation of [^{3}H]-TPP was lower than ^{18}F-FDG, rendering [^{3}H]-TPP another choice for tumor imaging in PET.

Following previous reports on radioiodinated cations, the [(E)-1-[^{123}I]Iodo-1-penten-5-yl]triphenylphosphonium cation ([^{123}I]-IPenTPP, Chart 88) was synthesized and tested for heart imaging in vivo.[709–713] Experiments demonstrated a high myocardial uptake of the probe in rats and dogs. Later, authors investigated the effects of alkyl and aryl substitution,

and the use of arsonium and ammonium cations instead of phosphonium, on the heart specificity of these radioiodinated compounds.[714] Replacement of phosphorus with arsenic atom or changing phenyl for cyclohexyl groups had no significant effect on heart uptake. On the other hand, the change of cyclic groups for alkyl dramatically decreased the uptake.

Another TPP^+-based probe reported is ^{11}C-triphenylmethylphosphonium ([^{11}C]-TPMP, Chart 88).[715] [^{11}C]-TPMP was first evaluated in vivo in mice and rats for estimation of the membrane potential in the heart using PET. Biodistribution studies revealed a sustained accumulation of the tracer in the heart tissue of the rat within minutes of its injection. Results concluded that [^{11}C]-TPMP was a suitable probe for in vivo tomographic mapping of heart membrane potential.[715] Another study reported the use of [^{11}C]-TPMP for myocardial perfusion experiments in mongrel dogs using PET.[716] The probe was also used for a PET study in a canine brain tumor model.[479] PET imaging in combination with histology indicated that [^{11}C]-TPMP had enhanced uptake and a long retention period in brain tumors.[479] Also, ^{18}F-labeled TPP^+-bearing probes were developed and tested for PET imaging applications in vivo, including 3-[^{18}F]fluoropropyl-([^{18}F]-FPrTP), 4-[^{18}F]fluorobenzyl-triphenylphosphonium (^{18}F-FBnTP) and 4-[^{18}F]fluorobenzyltris-4-dimethylaminophenylphosphonium (4-[^{18}F]-FBnTDMAPP) cations (Chart 89).[717]

^{18}F-FBnTP undergoes rapid blood clearance and myocardial accumulation in dogs, with a heart-to-lung ratio of 15:1. In a breast carcinoma model in mice, the same compound showed a 45% reduced uptake of the compound after 48 h of injection of Taxotere, with no effect in heart, liver, or kidney uptake.[717] Another ^{18}F-bearing probe, 4-[^{18}F]fluorophenyltriphenylphosphonium ([^{18}F]-TPP, Chart 89), was synthesized and evaluated as a myocardial blood flow agent for PET.[485,718,719] Subsequently, a myriad of other analogs, varying the hydrophobicity of the alkyl linker connecting the fluorine-18 atom and the TPP^+ were synthesized and tested in heart models.[214,485,720–729] Results showed a preferential uptake of the TPP^+-based PET agents in the heart with enhanced heart-to-lung ratios in mice one h after injection.[729]

Mitochondria-targeted ^{64}Cu complexes—Another class of TPP^+-based radiopharmaceuticals developed as PET radiotracers for tumor imaging are the mitochondria-targeted ^{64}Cu complexes. Although ^{11}C- and ^{18}F-labeled TPP^+ cations have shown great utility for cancer applications, they may be not the best choice.[691–694,730] Using bifunctional chelators, several TPP^+-based mitochondria-targeted ^{64}Cu complexes were synthesized and tested in vivo.[691–694] The effects of the linker, targeting moiety, bifunctional chelator, and molecular charge were studied in order to select the best candidates for tumor imaging. In that series of publications, various mitochondria-targeted TPP^+ or TPEP-based ^{64}Cu complexes (Chart 90) were evaluated in vivo for tumor imaging and monitoring of the multidrug resistance transport function in tumors of different origin. The prepared ^{64}Cu complexes have the advantage of having a half-life of 12.7 h, which makes their preparation and transport for clinical applications for PET feasible. Of all of the analogs tested, based on high tumor uptake and high T/B ratios ^{64}Cu(DO3A-xy)TPEP (Chart 90), was selected as the most promising candidate for tumor imaging.[88,691,693,694,730–732] ^{64}Cu(DO3A-xy)TPEP was found to have a better tumor selectivity than ^{99m}Tc-MIBI (Chart 91).

Mitochondria-targeted ^{99m}Tc-MAG3 (Mito-^{99m}Tc-MAG3—^{99m}Tc-MAG3 is a widely used agent to assess renal function clinically. This technetium-based compound was designed for replacement of omicron-iodohippurate [^{131}I]OIH.[733] Nowadays, ^{99m}Tc-MAG3 is the agent of choice for renograms over ^{99m}Tc-DTPA. For tumor imaging purposes, ^{99m}Tc-MAG3 was conjugated with the TPP^+ moiety.[734] Mito-^{99m}Tc-MAG3 (Chart 91) was tested in vivo in rats using a DMBA-induced breast cancer model.

Biodistribution studies performed in comparison with ^{99m}Tc-MIBI demonstrated that myocardial uptake of Mito-^{99m}Tc-MAG3 was orders of magnitude lower than that of ^{99m}Tc-MIBI. Results obtained with a gamma camera indicated, apart from the known tumor sites at mammary glands, the presence of other well-defined focal uptake areas, and subsequent histology confirmed the presence of papillary carcinoma. Findings from this study demonstrate that Mito-^{99m}Tc-MAG3 enables the detection of breast cancer tumors one week earlier than they were evident by palpation. (Figure 26).

9. SUMMARY AND OUTLOOK

In this review, we discuss the potential applications of TPP^+-based mitochondria-targeted probes for detecting, detoxifying, and releasing reactive oxygen, nitrogen, and sulfur species and electrophiles in mitochondria; the anticancer and antimetastatic properties of mitochondria-targeted, naturally occurring bioactive compounds and their effect on mitochondrial bioenergetics and the mitochondria-dependent signaling mechanism; the cardioprotective effects of mitochondria-targeted therapeutics in chemotherapy; the neuroprotective effects of TPP^+-based mitochondria-targeted compounds; and the possibility of imaging mitochondrial metabolism and function using mitochondria-targeted paramagnetic agents and radiopharmaceuticals. This review reveals the therapeutic potency of several TPP^+-modified bioactive compounds in preclinical models.

Going forward, it is important to carefully consider the most likely clinical applications of mitochondria-targeted compounds. Much is already known concerning the clinical safety and toxicity, oral bioavailability, and pharmacokinetics of MitoQ in humans. Several clinical trials using MitoQ and SkQ1 compounds have been completed or are underway (Table 2). The therapeutic efficacy of MitoQ to alleviate liver damage in patients afflicted with the hepatitis C virus is already well established. MitoQ is currently available in health-food stores and is used to enhance mitochondrial function and energy, although it has not undergone extensive clinical-trial analyses for this purpose.

Preclinical studies have shown that mitochondria-targeted agents including MitoQ protect against doxorubicin-induced cardiotoxicity and cisplatin-mediated nephropathy in animal models.[490,637] Thus, it would be prudent to initially test the efficacy of MitoQ for alleviating DOX-induced cardiotoxicity and cisplatin-induced nephrotoxicity in patients. Cancer patients treated with doxorubicin alone and in combination with other chemotherapeutics develop cardiac problems many years after the cessation of chemotherapy. Currently, no effective prophylactic treatment for mitigating cardiotoxicity exists. It is reasonable to test MitoQ as a potential cardioprotective drug in a well-controlled clinical trial designed to mitigate cardiotoxicity in cancer patients post-chemotherapy.

Cisplatin is a widely used antineoplastic drug. Its clinical efficacy is compromised by a dose-dependent nephrotoxicity. In preclinical models, mitochondria-targeted drugs, including MitoQ, inhibited the second wave of inflammatory damage and oxidative/nitrative stress induced by NOX enzymes.[490] It seems logical to test whether MitoQ mitigates the proinflammatory processes in the kidneys of cancer patients treated with cisplatin.

Mito-Apo has shown promise as an anti-neuroinflammatory compound in multiple preclinical models PD.[493–495,669] Mito-Apo effectively inhibited early PD-like symptoms and neuroinflammation. Because MitoQ failed to reverse or slow the progression of PD in humans, it is obvious that the potential therapeutic efficacy of Mito-Apo in PD treatment should be questioned. Studies indicate that Mito-Apo, unlike MitoQ, inhibits neuroinflammation through a novel mechanism inhibiting glial cell activation. Based on preclinical studies, any clinical trial using Mito-Apo should be designed to primarily prevent the early PD-like symptoms (e.g., loss of smell) and neuroinflammation.

With regard to possible diagnostic applications, mitochondria-targeted probes could serve as valuable tools if used with caution. Mitochondria-targeted boronate modified with TPP^+ could be used to detect hydrogen peroxide, peroxynitrite, or hypochlorous acid generated in mitochondria by identifying the specific products formed from the reaction between boronates and these oxidants.[286,295,296] One of the assays most frequently used to detect mitochondrial superoxide is based on monitoring MitoSOX-derived red fluorescence. However, as discussed earlier, MitoSOX-derived red fluorescence cannot be equated to mitochondrial superoxide.[257] It is essential to separate and identify the superoxide-specific and nonspecific oxidation products formed from the MitoSOX probe. More importantly, prior to using any mitochondria-targeted probes, the optimal concentration of the probe that does not affect the mitochondrial function must be established.

Finally, it has been known for more than three decades that cancer cells exhibit increased uptake and retention of lipophilic cations.[525] Mitochondria-targeted compounds (e.g., Mito-metformin) are a new class of relatively nontoxic compounds that target mitochondrial bioenergetics to inhibit tumor growth in vivo in several types of cancer in rodent models. The increased uptake and retention of lipophilic cations provides a rationale not only for development of new, more selective anticancer drugs, but also for the imaging agents allowing for early detection and localization of tumors using a variety of imaging modalities, including MRI, PET, and fluorescence. TPP^+-linked imaging agents show the potential for imaging early tumors that are not detectable by palpation in animal models.[235] This provides an opportunity to use such probes for in vivo studies of tumor growth in animal models with the potential translation into new cancer cell imaging tools in humans.

Acknowledgments

The authors would like to thank all the collaborators on the therapeutic applications of mitochondria-targeted compounds, whose names are shown in the references cited, including Narayan G. Avadhani (University of Pennsylvania), Michael B. Dwinell (Medical College of Wisconsin), Anumantha G. Kanthasamy (Iowa State University), Raymond Q. Migrino (College of Medicine – Phoenix), Pal Pacher (NIAAA, NIH), V. Ashutosh Rao (FDA), and Ming You (Medical College of Wisconsin).

This work was supported by NIH National Cancer Institute grants U01 CA178960 and R01 CA152810 to B.K., a grant from the Polish National Science Centre (NCN) within the SONATA BIS 5 program (Grant No. 2015/18/E/

ST4/00235) to A.S. and grants from the French National Research Agency (ANR-09-BLAN-0193-02, ANR-15-CE29-0022-01 and ANR-16-CE07-0023-01) to O.O. and M.H. The authors wish to thank Renata Smulik-Izydorczyk for preparing the selected figures and Lydia Washechek for copy editing the manuscript.

References

1. Milane L, Trivedi M, Singh A, Talekar M, Amiji M. Mitochondrial Biology, Targets, and Drug Delivery. J Control Release. 2015; 207:40–58. [PubMed: 25841699]
2. Nunnari J, Suomalainen A. Mitochondria: In Sickness and in Health. Cell. 2012; 148:1145–1159. [PubMed: 22424226]
3. Chandel NS. Evolution of Mitochondria as Signaling Organelles. Cell Metab. 2015; 22:204–206. [PubMed: 26073494]
4. Willems PH, Rossignol R, Dieteren CE, Murphy MP, Koopman WJ. Redox Homeostasis and Mitochondrial Dynamics. Cell Metab. 2015; 22:207–218. [PubMed: 26166745]
5. Chouchani ET, Pell VR, James AM, Work LM, Saeb-Parsy K, Frezza C, Krieg T, Murphy MP. A Unifying Mechanism for Mitochondrial Superoxide Production During Ischemia-Reperfusion Injury. Cell Metab. 2016; 23:254–263. [PubMed: 26777689]
6. Lin MT, Beal MF. Mitochondrial Dysfunction and Oxidative Stress in Neurodegenerative Diseases. Nature. 2006; 443:787–795. [PubMed: 17051205]
7. Cadonic C, Sabbir MG, Albensi BC. Mechanisms of Mitochondrial Dysfunction in Alzheimer's Disease. Mol Neurobiol. 2016; 53:6078–6090. [PubMed: 26537901]
8. Bose A, Beal MF. Mitochondrial Dysfunction in Parkinson's Disease. J Neurochem. 2016; 139(Suppl 1):216–231. [PubMed: 27546335]
9. Ballinger SW. Mitochondrial Dysfunction in Cardiovascular Disease. Free Radic Biol Med. 2005; 38:1278–1295. [PubMed: 15855047]
10. Rosca MG, Hoppel CL. Mitochondrial Dysfunction in Heart Failure. Heart Fail Rev. 2013; 18:607–622. [PubMed: 22948484]
11. Vasquez-Trincado C, Garcia-Carvajal I, Pennanen C, Parra V, Hill JA, Rothermel BA, Lavandero S. Mitochondrial Dynamics, Mitophagy and Cardiovascular Disease. J Physiol. 2016; 594:509–525. [PubMed: 26537557]
12. Picard M, Wallace DC, Burelle Y. The Rise of Mitochondria in Medicine. Mitochondrion. 2016; 30:105–116. [PubMed: 27423788]
13. Viscomi C, Bottani E, Zeviani M. Emerging Concepts in the Therapy of Mitochondrial Disease. Biochim Biophys Acta. 2015; 1847:544–557. [PubMed: 25766847]
14. Rocha M, Apostolova N, Herance JR, Rovira-Llopis S, Hernandez-Mijares A, Victor VM. Perspectives and Potential Applications of Mitochondria-Targeted Antioxidants in Cardiometabolic Diseases and Type 2 Diabetes. Med Res Rev. 2014; 34:160–189. [PubMed: 23650093]
15. Murphy MP. Understanding and Preventing Mitochondrial Oxidative Damage. Biochem Soc Trans. 2016; 44:1219–1226. [PubMed: 27911703]
16. Cheng G, Zielonka J, Dranka BP, McAllister D, Mackinnon AC Jr, Joseph J, Kalyanaraman B. Mitochondria-Targeted Drugs Synergize with 2-Deoxyglucose to Trigger Breast Cancer Cell Death. Cancer Res. 2012; 72:2634–2644. [PubMed: 22431711]
17. Cheng G, Zielonka J, McAllister D, Hardy M, Ouari O, Joseph J, Dwinell MB, Kalyanaraman B. Antiproliferative Effects of Mitochondria-Targeted Cationic Antioxidants and Analogs: Role of Mitochondrial Bioenergetics and Energy-Sensing Mechanism. Cancer Lett. 2015; 365:96–106. [PubMed: 26004344]
18. Kalyanaraman B, Cheng G, Hardy M, Ouari O, Sikora A, Zielonka J, Dwinell M. Mitochondria-Targeted Metformins: Anti-Tumour and Redox Signalling Mechanisms. Interface Focus. 2017; 7:20160109. [PubMed: 28382202]
19. Rao VA, Klein SR, Bonar SJ, Zielonka J, Mizuno N, Dickey JS, Keller PW, Joseph J, Kalyanaraman B, Shacter E. The Antioxidant Transcription Factor Nrf2 Negatively Regulates Autophagy and Growth Arrest Induced by the Anticancer Redox Agent Mitoquinone. J Biol Chem. 2010; 285:34447–34459. [PubMed: 20805228]

20. Sassi N, Mattarei A, Azzolini M, Szabo I, Paradisi C, Zoratti M, Biasutto L. Cytotoxicity of Mitochondria-Targeted Resveratrol Derivatives: Interactions with Respiratory Chain Complexes and ATP Synthase. Biochim Biophys Acta. 2014; 1837:1781–1789. [PubMed: 24997425]
21. Cheng G, Zielonka J, Ouari O, Lopez M, McAllister D, Boyle K, Barrios CS, Weber JJ, Johnson BD, Hardy M, et al. Mitochondria-Targeted Analogues of Metformin Exhibit Enhanced Antiproliferative and Radiosensitizing Effects in Pancreatic Cancer Cells. Cancer Res. 2016; 76:3904–3915. [PubMed: 27216187]
22. Murphy MP. Selective Targeting of Bioactive Compounds to Mitochondria. Trends Biotechnol. 1997; 15:326–330. [PubMed: 9263481]
23. Armstrong JS. Mitochondrial Medicine: Pharmacological Targeting of Mitochondria in Disease. Br J Pharmacol. 2007; 151:1154–1165. [PubMed: 17519949]
24. Horobin RW, Trapp S, Weissig V. Mitochondriotropics: A Review of Their Mode of Action, and Their Applications for Drug and DNA Delivery to Mammalian Mitochondria. J Control Release. 2007; 121:125–136. [PubMed: 17658192]
25. Hoye AT, Davoren JE, Wipf P, Fink MP, Kagan VE. Targeting Mitochondria. Acc Chem Res. 2008; 41:87–97. [PubMed: 18193822]
26. Smith RA, Hartley RC, Murphy MP. Mitochondria-Targeted Small Molecule Therapeutics and Probes. Antioxid Redox Signal. 2011; 15:3021–3038. [PubMed: 21395490]
27. Weissig V. From Serendipity to Mitochondria-Targeted Nanocarriers. Pharm Res. 2011; 28:2657–2668. [PubMed: 21833792]
28. Heller A, Brockhoff G, Goepferich A. Targeting Drugs to Mitochondria. Eur J Pharm Biopharm. 2012; 82:1–18. [PubMed: 22687572]
29. Murphy MP. Antioxidants as Therapies: Can We Improve on Nature? Free Radic Biol Med. 2014; 66:20–23. [PubMed: 23603661]
30. Sorriento D, Pascale AV, Finelli R, Carillo AL, Annunziata R, Trimarco B, Iaccarino G. Targeting Mitochondria as Therapeutic Strategy for Metabolic Disorders. Sci World J. 2014; 2014:604685.
31. Tabara LC, Poveda J, Martin-Cleary C, Selgas R, Ortiz A, Sanchez-Nino MD. Mitochondria-Targeted Therapies for Acute Kidney Injury. Expert Rev Mol Med. 2014; 16:e13. [PubMed: 25104110]
32. Oyewole AO, Birch-Machin MA. Mitochondria-Targeted Antioxidants. FASEB J. 2015; 29:4766–4771. [PubMed: 26253366]
33. Lu P, Bruno BJ, Rabenau M, Lim CS. Delivery of Drugs and Macromolecules to the Mitochondria for Cancer Therapy. J Control Release. 2016; 240:38–51. [PubMed: 26482081]
34. Biasutto L, Dong LF, Zoratti M, Neuzil J. Mitochondrially Targeted Anti-Cancer Agents. Mitochondrion. 2010; 10:670–681. [PubMed: 20601192]
35. Weissig, V., D'Souza, GGM. Organelle-Specific Pharmaceutical Nanotechnology. D'Souza, VWaGGM., editor. John Wiley & Sons, Inc; Hoboken, NJ, USA: 2010. p. 385-401.
36. Smith RA, Murphy MP. Mitochondria-Targeted Antioxidants as Therapies. Discov Med. 2011; 11:106–114. [PubMed: 21356165]
37. Durazo SA, Kompella UB. Functionalized Nanosystems for Targeted Mitochondrial Delivery. Mitochondrion. 2012; 12:190–201. [PubMed: 22138492]
38. Errico A. Targeted Therapy: Targeting Mitochondria in Pancreatic Cancer. Nat Rev Clin Oncol. 2014; 11:562.
39. Smith RAJ, Adlam VJ, Blaikie FH, Manas ARB, Porteous CM, James AM, Ross MF, Logan A, Cochemé HM, Trnka J, et al. Mitochondria-Targeted Antioxidants in the Treatment of Disease. Ann N Y Acad Sci. 2008; 1147:105–111. [PubMed: 19076435]
40. Ross MF, Kelso GF, Blaikie FH, James AM, Cochemé HM, Filipovska A, Da Ros T, Hurd TR, Smith RAJ, Murphy MP. Lipophilic Triphenylphosphonium Cations as Tools in Mitochondrial Bioenergetics and Free Radical Biology. Biochemistry (Moscow). 2005; 70:222–230. [PubMed: 15807662]
41. Murphy MP, Smith RAJ. Targeting Antioxidants to Mitochondria by Conjugation to Lipophilic Cations. Annu Rev Pharmacol Toxicol. 2007; 47:629–656. [PubMed: 17014364]

42. Skulachev VP. Cationic Antioxidants as a Powerful Tool against Mitochondrial Oxidative Stress. Biochem Biophys Res Commun. 2013; 441:275–279. [PubMed: 24161394]
43. Kezic A, Spasojevic I, Lezaic V, Bajcetic M. Mitochondria-Targeted Antioxidants: Future Perspectives in Kidney Ischemia Reperfusion Injury. Oxid Med Cell Longev. 2016; 2016:2950503. [PubMed: 27313826]
44. Xu W, Zeng Z, Jiang JH, Chang YT, Yuan L. Discerning the Chemistry in Individual Organelles with Small-Molecule Fluorescent Probes. Angew Chem Int Ed Engl. 2016; 55:13658–13699. [PubMed: 27571316]
45. Liberman EA, Topaly VP, Tsofina LM, Jasaitis AA, Skulachev VP. Mechanism of Coupling of Oxidative Phosphorylation and the Membrane Potential of Mitochondria. Nature. 1969; 222:1076–1078. [PubMed: 5787094]
46. Bakeeva LE, Grinius LL, Jasaitis AA, Kuliene VV, Levitsky DO, Liberman EA, Severina II, Skulachev VP. Conversion of Biomembrane-Produced Energy into Electric Form. II. Intact Mitochondria. Biochim Biophys Acta. 1970; 216:13–21. [PubMed: 4250571]
47. Grinius LL, Jasaitis AA, Kadziauskas YP, Liberman EA, Skulachev VP, Topali VP, Tsofina LM, Vladimirova MA. Conversion of Biomembrane-Produced Energy into Electric Form. I. Submitochondrial Particles. Biochim Biophys Acta. 1970; 216:1–12. [PubMed: 4395700]
48. Isaev PI, Liberman EA, Samuilov VD, Skulachev VP, Tsofina LM. Conversion of Biomembrane-Produced Energy into Electric Form. III. Chromatophores of Rhodospirillum Rubrum. Biochim Biophys Acta. 1970; 216:22–29. [PubMed: 4322294]
49. Liberman EA, Skulachev VP. Conversion of Biomembrane-Produced Energy into Electric Form. IV. General Discussion. Biochim Biophys Acta. 1970; 216:30–42. [PubMed: 4250572]
50. Kinnally KW, Tedeschi H. Metabolic Effects of Some Electrofluorimetric Dyes. Biochim Biophys Acta. 1978; 503:380–388. [PubMed: 687611]
51. Kinnally KW, Tedeschi H, Maloff BL. Use of Dyes to Estimate the Electrical Potential of the Mitochondrial Membrane. Biochemistry. 1978; 17:3419–3428. [PubMed: 687593]
52. Lichtshtein D, Kaback HR, Blume AJ. Use of a Lipophilic Cation for Determination of Membrane Potential in Neuroblastoma-Glioma Hybrid Cell Suspensions. Proc Natl Acad Sci U S A. 1979; 76:650–654. [PubMed: 284390]
53. Hoek JB, Nicholls DG, Williamson JR. Determination of the Mitochondrial Protonmotive Force in Isolated Hepatocytes. J Biol Chem. 1980; 255:1458–1464. [PubMed: 7354039]
54. Hiller R, Schaefer A, Zibirre R, Kaback HR, Koch G. Factors Influencing the Accumulation of Tetraphenylphosphonium Cation in HeLa Cells. Mol Cell Biol. 1984; 4:199–202. [PubMed: 6700585]
55. Rottenberg H. Membrane Potential and Surface Potential in Mitochondria: Uptake and Binding of Lipophilic Cations. J Membr Biol. 1984; 81:127–138. [PubMed: 6492133]
56. Brown GC, Brand MD. Thermodynamic Control of Electron Flux through Mitochondrial Cytochrome bc1 Complex. Biochem J. 1985; 225:399–405. [PubMed: 2983670]
57. Holian A, Wilson DF. Relationship of Transmembrane pH and Electrical Gradients with Respiration and Adenosine 5′-Triphosphate Synthesis in Mitochondria. Biochemistry. 1980; 19:4213–4221. [PubMed: 7417402]
58. Burns RJ, Smith RA, Murphy MP. Synthesis and Characterization of Thiobutyltriphenylphosphonium Bromide, a Novel Thiol Reagent Targeted to the Mitochondrial Matrix. Arch Biochem Biophys. 1995; 322:60–68. [PubMed: 7574695]
59. Burns RJ, Murphy MP. Labeling of Mitochondrial Proteins in Living Cells by the Thiol Probe Thiobutyltriphenylphosphonium Bromide. Arch Biochem Biophys. 1997; 339:33–39. [PubMed: 9056230]
60. Smith RA, Porteous CM, Coulter CV, Murphy MP. Selective Targeting of an Antioxidant to Mitochondria. Eur J Biochem. 1999; 263:709–716. [PubMed: 10469134]
61. Coulter CV, Kelso GF, Lin TK, Smith RA, Murphy MP. Mitochondrially Targeted Antioxidants and Thiol Reagents. Free Radic Biol Med. 2000; 28:1547–1554. [PubMed: 10927180]
62. Asin-Cayuela J, Manas AR, James AM, Smith RA, Murphy MP. Fine-Tuning the Hydrophobicity of a Mitochondria-Targeted Antioxidant. FEBS Lett. 2004; 571:9–16. [PubMed: 15280009]

63. Skulachev VP, Antonenko YN, Cherepanov DA, Chernyak BV, Izyumov DS, Khailova LS, Klishin SS, Korshunova GA, Lyamzaev KG, Pletjushkina OY, et al. Prevention of Cardiolipin Oxidation and Fatty Acid Cycling as Two Antioxidant Mechanisms of Cationic Derivatives of Plastoquinone (SkQs). Biochim Biophys Acta. 2010; 1797:878–889. [PubMed: 20307489]
64. Hardy M, Poulhes F, Rizzato E, Rockenbauer A, Banaszak K, Karoui H, Lopez M, Zielonka J, Vasquez-Vivar J, Sethumadhavan S, et al. Mitochondria-Targeted Spin Traps: Synthesis, Superoxide Spin Trapping, and Mitochondrial Uptake. Chem Res Toxicol. 2014; 27:1155–1165. [PubMed: 24890552]
65. Dodin G, Averbeck D, Demerseman P, Nocentini S, Dupont J. Mitochondrial Uptake of Bridged Bis-Methylpyridinium Aldoximes and Induction of the "Petite" Phenotype in Yeast. Biochem Biophys Res Commun. 1991; 179:992–999. [PubMed: 1898417]
66. Weiss MJ, Wong JR, Ha CS, Bleday R, Salem RR, Steele GD Jr, Chen LB. Dequalinium, a Topical Antimicrobial Agent, Displays Anticarcinoma Activity Based on Selective Mitochondrial Accumulation. Proc Natl Acad Sci U S A. 1987; 84:5444–5448. [PubMed: 3474661]
67. Davey GP, Tipton KF, Murphy MP. Uptake and Accumulation of 1-Methyl-4-Phenylpyridinium by Rat Liver Mitochondria Measured Using an Ion-Selective Electrode. Biochem J. 1992; 288(Pt 2): 439–443. [PubMed: 1463448]
68. Davey GP, Tipton KF, Murphy MP. Use of an Electrode Selective for 1-Methyl-4-Phenylpyridinium (MPP+) to Measure Its Uptake and Accumulation by Mitochondria. J Neural Transm Suppl. 1993; 40:47–55. [PubMed: 8294900]
69. Murphy MP, Krueger MJ, Sablin SO, Ramsay RR, Singer TP. Inhibition of Complex I by Hydrophobic Analogues of N-Methyl-4-Phenylpyridinium (MPP+) and the Use of an Ion-Selective Electrode to Measure Their Accumulation by Mitochondria and Electron-Transport Particles. Biochem J. 1995; 306(Pt 2):359–365. [PubMed: 7887889]
70. Bunting JR. Influx and Efflux Kinetics of Cationic Dye Binding to Respiring Mitochondria. Biophys Chem. 1992; 42:163–175. [PubMed: 1567988]
71. Johnson LV, Walsh ML, Chen LB. Localization of Mitochondria in Living Cells with Rhodamine 123. Proc Natl Acad Sci U S A. 1980; 77:990–994. [PubMed: 6965798]
72. Davis S, Weiss MJ, Wong JR, Lampidis TJ, Chen LB. Mitochondrial and Plasma Membrane Potentials Cause Unusual Accumulation and Retention of Rhodamine 123 by Human Breast Adenocarcinoma-Derived MCF-7 Cells. J Biol Chem. 1985; 260:13844–13850. [PubMed: 4055760]
73. Johnson LV, Walsh ML, Bockus BJ, Chen LB. Monitoring of Relative Mitochondrial Membrane Potential in Living Cells by Fluorescence Microscopy. J Cell Biol. 1981; 88:526–535. [PubMed: 6783667]
74. Emaus RK, Grunwald R, Lemasters JJ. Rhodamine 123 as a Probe of Transmembrane Potential in Isolated Rat-Liver Mitochondria: Spectral and Metabolic Properties. Biochim Biophys Acta. 1986; 850:436–448. [PubMed: 2873836]
75. Rottenberg H, Wu S. Quantitative Assay by Flow Cytometry of the Mitochondrial Membrane Potential in Intact Cells. Biochim Biophys Acta. 1998; 1404:393–404. [PubMed: 9739168]
76. Solaini G, Sgarbi G, Lenaz G, Baracca A. Evaluating Mitochondrial Membrane Potential in Cells. Biosci Rep. 2007; 27:11–21. [PubMed: 17497220]
77. Serviddio G, Sastre J. Measurement of Mitochondrial Membrane Potential and Proton Leak. Methods Mol Biol. 2010; 594:107–121. [PubMed: 20072912]
78. Perry SW, Norman JP, Barbieri J, Brown EB, Gelbard HA. Mitochondrial Membrane Potential Probes and the Proton Gradient: A Practical Usage Guide. Biotechniques. 2011; 50:98–115. [PubMed: 21486251]
79. Gerencser AA, Chinopoulos C, Birket MJ, Jastroch M, Vitelli C, Nicholls DG, Brand MD. Quantitative Measurement of Mitochondrial Membrane Potential in Cultured Cells: Calcium-Induced De- and Hyperpolarization of Neuronal Mitochondria. J Physiol. 2012; 590:2845–2871. [PubMed: 22495585]
80. Nicholls DG. Fluorescence Measurement of Mitochondrial Membrane Potential Changes in Cultured Cells. Methods Mol Biol. 2012; 810:119–133. [PubMed: 22057564]

81. Onoe S, Temma T, Shimizu Y, Ono M, Saji H. Investigation of Cyanine Dyes for in Vivo Optical Imaging of Altered Mitochondrial Membrane Potential in Tumors. Cancer Med. 2014; 3:775–786. [PubMed: 24737784]

82. Antonenko YN, Avetisyan AV, Bakeeva LE, Chernyak BV, Chertkov VA, Domnina LV, Ivanova OY, Izyumov DS, Khailova LS, Klishin SS, et al. Mitochondria-Targeted Plastoquinone Derivatives as Tools to Interrupt Execution of the Aging Program. 1. Cationic Plastoquinone Derivatives: Synthesis and in Vitro Studies. Biochemistry (Mosc). 2008; 73:1273–1287. [PubMed: 19120014]

83. Bakeeva LE, Barskov IV, Egorov MV, Isaev NK, Kapelko VI, Kazachenko AV, Kirpatovsky VI, Kozlovsky SV, Lakomkin VL, Levina SB, et al. Mitochondria-Targeted Plastoquinone Derivatives as Tools to Interrupt Execution of the Aging Program. 2. Treatment of Some ROS- and Age-Related Diseases (Heart Arrhythmia, Heart Infarctions, Kidney Ischemia, and Stroke). Biochemistry (Mosc). 2008; 73:1288–1299. [PubMed: 19120015]

84. Ngen EJ, Rajaputra P, You Y. Evaluation of Delocalized Lipophilic Cationic Dyes as Delivery Vehicles for Photosensitizers to Mitochondria. Bioorg Med Chem. 2009; 17:6631–6640. [PubMed: 19692249]

85. Fetisova EK, Avetisyan AV, Izyumov DS, Korotetskaya MV, Chernyak BV, Skulachev VP. Mitochondria-Targeted Antioxidant SkQR1 Selectively Protects MDR (Pgp 170)-Negative Cells against Oxidative Stress. FEBS Lett. 2010; 584:562–566. [PubMed: 19995561]

86. Rokitskaya TI, Sumbatyan NV, Tashlitsky VN, Korshunova GA, Antonenko YN, Skulachev VP. Mitochondria-Targeted Penetrating Cations as Carriers of Hydrophobic Anions through Lipid Membranes. Biochim Biophys Acta. 2010; 1798:1698–1706. [PubMed: 20510172]

87. Antonenko YN, Avetisyan AV, Cherepanov DA, Knorre DA, Korshunova GA, Markova OV, Ojovan SM, Perevoshchikova IV, Pustovidko AV, Rokitskaya TI, et al. Derivatives of Rhodamine 19 as Mild Mitochondria-Targeted Cationic Uncouplers. J Biol Chem. 2011; 286:17831–17840. [PubMed: 21454507]

88. Zhou Y, Kim YS, Yan X, Jacobson O, Chen X, Liu S. 64Cu-Labeled Lissamine Rhodamine B: A Promising PET Radiotracer Targeting Tumor Mitochondria. Mol Pharm. 2011; 8:1198–1208. [PubMed: 21545131]

89. Rajaputra P, Nkepang G, Watley R, You Y. Synthesis and in Vitro Biological Evaluation of Lipophilic Cation Conjugated Photosensitizers for Targeting Mitochondria. Bioorg Med Chem. 2013; 21:379–387. [PubMed: 23245573]

90. Yoong SL, Wong BS, Zhou QL, Chin CF, Li J, Venkatesan T, Ho HK, Yu V, Ang WH, Pastorin G. Enhanced Cytotoxicity to Cancer Cells by Mitochondria-Targeting Mwcnts Containing Platinum(IV) Prodrug of Cisplatin. Biomaterials. 2014; 35:748–759. [PubMed: 24140044]

91. Silachev DN, Plotnikov EY, Zorova LD, Pevzner IB, Sumbatyan NV, Korshunova GA, Gulyaev MV, Pirogov YA, Skulachev VP, Zorov DB. Neuroprotective Effects of Mitochondria-Targeted Plastoquinone and Thymoquinone in a Rat Model of Brain Ischemia/Reperfusion Injury. Molecules. 2015; 20:14487–14503. [PubMed: 26270657]

92. Li X, Yin Y, Du B, Li N, Li Y. The Synthesis and Evaluations of the 68ga-Lissamine Rhodamine B (LRB) as a New Radiotracer for Imaging Tumors by Positron Emission Tomography. Bio Med Res Int. 2016; 2016:8549635.

93. Antonenko YN, Nechaeva NL, Baksheeva VE, Rokitskaya TI, Plotnikov EY, Kotova EA, Zorov DB. Intramitochondrial Accumulation of Cationic Atto520-Biotin Proceeds Via Voltage-Dependent Slow Permeation through Lipid Membrane. Biochim Biophys Acta. 2015; 1848:1277–1284. [PubMed: 25753112]

94. Szulc ZM, Bielawski J, Gracz H, Gustilo M, Mayroo N, Hannun YA, Obeid LM, Bielawska A. Tailoring Structure-Function and Targeting Properties of Ceramides by Site-Specific Cationization. Bioorg Med Chem. 2006; 14:7083–7104. [PubMed: 16919460]

95. Dindo D, Dahm F, Szulc Z, Bielawska A, Obeid LM, Hannun YA, Graf R, Clavien PA. Cationic Long-Chain Ceramide LCL-30 Induces Cell Death by Mitochondrial Targeting in SW403 Cells. Mol Cancer Ther. 2006; 5:1520–1529. [PubMed: 16818511]

96. Beckham TH, Lu P, Jones EE, Marrison T, Lewis CS, Cheng JC, Ramshesh VK, Beeson G, Beeson CC, Drake RR, et al. LCL124, a Cationic Analog of Ceramide, Selectively Induces Pancreatic

Cancer Cell Death by Accumulating in Mitochondria. J Pharmacol Exp Ther. 2013; 344:167–178. [PubMed: 23086228]

97. Bielawska, A., Hannun, Y., Szulc, Z., Obeid, L., Ogretmen, B. Cationic Ceramides, and Analogs Thereof, and Their Use for Preventing or Treating Cancer. Patent WO. 2006050264. 2006.
98. Novgorodov SA, Szulc ZM, Luberto C, Jones JA, Bielawski J, Bielawska A, Hannun YA, Obeid LM. Positively Charged Ceramide Is a Potent Inducer of Mitochondrial Permeabilization. J Biol Chem. 2005; 280:16096–16105. [PubMed: 15722351]
99. Chernyak BV, Antonenko YN, Galimov ER, Domnina LV, Dugina VB, Zvyagilskaya RA, Ivanova OY, Izyumov DS, Lyamzaev KG, Pustovidko AV, et al. Novel Mitochondria-Targeted Compounds Composed of Natural Constituents: Conjugates of Plant Alkaloids Berberine and Palmatine with Plastoquinone. Biochemistry (Mosc). 2012; 77:983–995. [PubMed: 23157257]
100. Plotnikov EY, Chupyrkina AA, Jankauskas SS, Pevzner IB, Silachev DN, Skulachev VP, Zorov DB. Mechanisms of Nephroprotective Effect of Mitochondria-Targeted Antioxidants under Rhabdomyolysis and Ischemia/Reperfusion. Biochim Biophys Acta. 2011; 1812:77–86. [PubMed: 20884348]
101. Wang P, Huang J, Gu Y. Rational Design of a Novel Mitochondrial-Targeted near-Infrared Fluorescent pH Probe for Imaging in Living Cells and in Vivo. RSC Adv. 2016; 6:95708–95714.
102. Zhao X, Li Y, Jin D, Xing Y, Yan X, Chen L. A near-Infrared Multifunctional Fluorescent Probe with an Inherent Tumor-Targeting Property for Bioimaging. Chem Commun (Camb). 2015; 51:11721–11724. [PubMed: 26104217]
103. Chevalier A, Zhang Y, Khdour OM, Kaye JB, Hecht SM. Mitochondrial Nitroreductase Activity Enables Selective Imaging and Therapeutic Targeting. J Am Chem Soc. 2016; 138:12009–12012. [PubMed: 27571326]
104. Han C, Yang H, Chen M, Su Q, Feng W, Li F. Mitochondria-Targeted near-Infrared Fluorescent Off-on Probe for Selective Detection of Cysteine in Living Cells and in Vivo. ACS Appl Mater Interfaces. 2015; 7:27968–27975. [PubMed: 26618279]
105. Yang J, Li K, Hou JT, Li LL, Lu CY, Xie YM, Wang X, Yu XQ. Novel Tumor-Specific and Mitochondria-Targeted near-Infrared-Emission Fluorescent Probe for SO2 Derivatives in Living Cells. ACS Sensors. 2016; 1:166–172.
106. Liu Y, Li K, Wu MY, Liu YH, Xie YM, Yu XQ. A Mitochondria-Targeted Colorimetric and Ratiometric Fluorescent Probe for Biological SO2 Derivatives in Living Cells. Chem Commun (Camb). 2015; 51:10236–10239. [PubMed: 26021301]
107. Hou JT, Li K, Yang J, Yu KK, Liao YX, Ran YZ, Liu YH, Zhou XD, Yu XQ. A Ratiometric Fluorescent Probe for in Situ Quantification of Basal Mitochondrial Hypochlorite in Cancer Cells. Chem Commun (Camb). 2015; 51:6781–6784. [PubMed: 25785927]
108. Maiti KK, Lee WS, Takeuchi T, Watkins C, Fretz M, Kim DC, Futaki S, Jones A, Kim KT, Chung SK. Guanidine-Containing Molecular Transporters: Sorbitol-Based Transporters Show High Intracellular Selectivity toward Mitochondria. Angewandte Chemie-International Edition. 2007; 46:5880–5884. [PubMed: 17607670]
109. Fernandez-Carneado J, Van Gool M, Martos V, Castel S, Prados P, de Mendoza J, Giralt E. Highly Efficient, Nonpeptidic Oligoguanidinium Vectors That Selectively Internalize into Mitochondria. J Am Chem Soc. 2005; 127:869–874. [PubMed: 15656624]
110. Kang BH, Plescia J, Song HY, Meli M, Colombo G, Beebe K, Scroggins B, Neckers L, Altieri DC. Combinatorial Drug Design Targeting Multiple Cancer Signaling Networks Controlled by Mitochondrial Hsp90. J Clin Invest. 2009; 119:454–464. [PubMed: 19229106]
111. Valero J, Van Gool M, Perez-Fernandez R, Castreno P, Sanchez-Quesada J, Prados P, de Mendoza J. Non-Peptidic Cell-Penetrating Agents: Synthesis of Oligomeric Chiral Bicyclic Guanidinium Vectors. Org Biomol Chem. 2012; 10:5417–5430. [PubMed: 22692145]
112. Vestweber D, Schatz G. Mitochondria Can Import Artificial Precursor Proteins Containing a Branched Polypeptide Chain or a Carboxy-Terminal Stilbene Disulfonate. J Cell Biol. 1988; 107:2045–2049. [PubMed: 2848848]
113. Horton KL, Stewart KM, Fonseca SB, Guo Q, Kelley SO. Mitochondria-Penetrating Peptides. Chem Biol. 2008; 15:375–382. [PubMed: 18420144]

114. Rocha M, Hernandez-Mijares A, Garcia-Malpartida K, Banuls C, Bellod L, Victor VM. Mitochondria-Targeted Antioxidant Peptides. Curr Pharm Des. 2010; 16:3124–3131. [PubMed: 20687871]
115. Cerrato CP, Pirisinu M, Vlachos EN, Langel U. Novel Cell-Penetrating Peptide Targeting Mitochondria. FASEB J. 2015; 29:4589–4599. [PubMed: 26195590]
116. Jean SR, Ahmed M, Lei EK, Wisnovsky SP, Kelley SO. Peptide-Mediated Delivery of Chemical Probes and Therapeutics to Mitochondria. Acc Chem Res. 2016; 49:1893–1902. [PubMed: 27529125]
117. Szeto HH. Mitochondria-Targeted Peptide Antioxidants: Novel Neuroprotective Agents. AAPS J. 2006; 8:E521–531. [PubMed: 17025271]
118. Szeto HH. Development of Mitochondria-Targeted Aromatic-Cationic Peptides for Neurodegenerative Diseases. Ann N Y Acad Sci. 2008; 1147:112–121. [PubMed: 19076436]
119. Szeto HH. Mitochondria-Targeted Cytoprotective Peptides for Ischemia-Reperfusion Injury. Antioxid Redox Signal. 2008; 10:601–619. [PubMed: 17999629]
120. Szeto HH, Schiller PW. Novel Therapies Targeting Inner Mitochondrial Membrane-from Discovery to Clinical Development. Pharm Res. 2011; 28:2669–2679. [PubMed: 21638136]
121. Bai L, Li Z, Chen J, Chung NN, Wilkes BC, Li T, Schiller PW. [Dmt(1)]Dalda Analogues with Enhanced Mu Opioid Agonist Potency and with a Mixed Mu/Kappa Opioid Activity Profile. Bioorg Med Chem. 2014; 22:2333–2338. [PubMed: 24602401]
122. Yoshinori, H., Akira, N., Masaru, M. Preparation of a Tetrapeptide Compound and Its Use in the Production of an Antioxidant Peptide. Patent WO. 2015060462. 2015.
123. Schiller PW, Nguyen TM, Berezowska I, Dupuis S, Weltrowska G, Chung NN, Lemieux C. Synthesis and in Vitro Opioid Activity Profiles of Dalda Analogues. Eur J Med Chem. 2000; 35:895–901. [PubMed: 11121615]
124. Fujita Y, Tsuda Y, Motoyama T, Li T, Miyazaki A, Yokoi T, Sasaki Y, Ambo A, Niizuma H, Jinsmaa Y, et al. Studies on the Structure-Activity Relationship of 2′,6′-Dimethyl-L-Tyrosine (Dmt) Derivatives: Bioactivity Profile of H-Dmt-NH-CH(3). Bioorganic & medicinal chemistry letters. 2005; 15:599–602. [PubMed: 15664820]
125. Bryant SD, Jinsmaa Y, Salvadori S, Okada Y, Lazarus LH. Dmt and Opioid Peptides: A Potent Alliance. Biopolymers. 2003; 71:86–102. [PubMed: 12767112]
126. Skulachev VP. How to Clean the Dirtiest Place in the Cell: Cationic Antioxidants as Intramitochondrial ROS Scavengers. IUBMB Life. 2005; 57:305–310. [PubMed: 16036614]
127. Riba P, Ben Y, Nguyen TM, Furst S, Schiller PW, Lee NM. [Dmt(1)]Dalda Is Highly Selective and Potent at Mu Opioid Receptors but Is Not Cross-Tolerant with Systemic Morphine. Curr Med Chem. 2002; 9:31–39. [PubMed: 11860345]
128. Sasaki Y, Ambo A. 2′,6′-Dimethylphenylalanine: A Useful Aromatic Amino Acid Surrogate for Tyr or Phe Residue in Opioid Peptides. International journal of medicinal chemistry. 2012; 2012:498901. [PubMed: 25954528]
129. Horton KL, Pereira MP, Stewart KM, Fonseca SB, Kelley SO. Tuning the Activity of Mitochondria-Penetrating Peptides for Delivery or Disruption. Chem Bio Chem. 2012; 13:476–485.
130. Yousif LF, Stewart KM, Horton KL, Kelley SO. Mitochondria-Penetrating Peptides: Sequence Effects and Model Cargo Transport. Chem Bio Chem. 2009; 10:2081–2088.
131. Fink MP, Macias CA, Xiao J, Tyurina YY, Delude RL, Greenberger JS, Kagan VE, Wipf P. Hemigramicidin-Tempo Conjugates: Novel Mitochondria-Targeted Antioxidants. Crit Care Med. 2007; 35:S461–467. [PubMed: 17713394]
132. Fink MP, Macias CA, Xiao J, Tyurina YY, Jiang J, Belikova N, Delude RL, Greenberger JS, Kagan VE, Wipf P. Hemigramicidin-Tempo Conjugates: Novel Mitochondria-Targeted Anti-Oxidants. Biochem Pharmacol. 2007; 74:801–809. [PubMed: 17601494]
133. Ellerby HM, Arap W, Ellerby LM, Kain R, Andrusiak R, Rio GD, Krajewski S, Lombardo CR, Rao R, Ruoslahti E, et al. Anti-Cancer Activity of Targeted Pro-Apoptotic Peptides. Nat Med. 1999; 5:1032–1038. [PubMed: 10470080]
134. Horton KL, Kelley SO. Engineered Apoptosis-Inducing Peptides with Enhanced Mitochondrial Localization and Potency. J Med Chem. 2009; 52:3293–3299. [PubMed: 19397319]

135. Pennarun B, Gaidos G, Bucur O, Tinari A, Rupasinghe C, Jin T, Dewar R, Song K, Santos MT, Malorni W, et al. Killerflip: A Novel Lytic Peptide Specifically Inducing Cancer Cell Death. Cell Death Dis. 2013; 4:e894. [PubMed: 24176852]

136. Farsinejad S, Gheisary Z, Ebrahimi Samani S, Alizadeh AM. Mitochondrial Targeted Peptides for Cancer Therapy. Tumour Biol. 2015; 36:5715–5725. [PubMed: 26142734]

137. Jang JH, Kim YJ, Kim H, Kim SC, Cho JH. Buforin IIb Induces Endoplasmic Reticulum Stress-Mediated Apoptosis in HeLa Cells. Peptides. 2015; 69:144–149. [PubMed: 25958204]

138. Del Gaizo V, MacKenzie JA, Payne RM. Targeting Proteins to Mitochondria Using Tat. Mol Genet Metab. 2003; 80:170–180. [PubMed: 14567966]

139. Yamada Y, Harashima H. Mitochondrial Drug Delivery Systems for Macromolecule and Their Therapeutic Application to Mitochondrial Diseases. Adv Drug Deliv Rev. 2008; 60:1439–1462. [PubMed: 18655816]

140. Schleiff E, Becker T. Common Ground for Protein Translocation: Access Control for Mitochondria and Chloroplasts. Nat Rev Mol Cell Biol. 2011; 12:48–59. [PubMed: 21139638]

141. Biswas S, Dodwadkar NS, Deshpande PP, Torchilin VP. Liposomes Loaded with Paclitaxel and Modified with Novel Triphenylphosphonium-PEG-PE Conjugate Possess Low Toxicity, Target Mitochondria and Demonstrate Enhanced Antitumor Effects in Vitro and in Vivo. J Control Release. 2012; 159:393–402. [PubMed: 22286008]

142. D'Souza GG, Cheng SM, Boddapati SV, Horobin RW, Weissig V. Nanocarrier-Assisted Sub-Cellular Targeting to the Site of Mitochondria Improves the Pro-Apoptotic Activity of Paclitaxel. J Drug Target. 2008; 16:578–585. [PubMed: 18686127]

143. Weissig V, Boddapati SV, Cheng SM, D'Souza GG. Liposomes and Liposome-Like Vesicles for Drug and DNA Delivery to Mitochondria. J Liposome Res. 2006; 16:249–264. [PubMed: 16952879]

144. Patel NR, Hatziantoniou S, Georgopoulos A, Demetzos C, Torchilin VP, Weissig V, D'Souza GG. Mitochondria-Targeted Liposomes Improve the Apoptotic and Cytotoxic Action of Sclareol. J Liposome Res. 2010; 20:244–249. [PubMed: 19883213]

145. Boddapati SV, Tongcharoensirikul P, Hanson RN, D'Souza GG, Torchilin VP, Weissig V. Mitochondriotropic Liposomes. J Liposome Res. 2005; 15:49–58. [PubMed: 16194927]

146. Malhi SS, Murthy RS. Delivery to Mitochondria: A Narrower Approach for Broader Therapeutics. Expert Opin Drug Deliv. 2012; 9:909–935. [PubMed: 22663303]

147. Benien P, Almuteri MA, Mehanna AS, D'Souza GG. Synthesis of Triphenylphosphonium Phospholipid Conjugates for the Preparation of Mitochondriotropic Liposomes. Methods Mol Biol. 2015; 1265:51–57. [PubMed: 25634266]

148. Benien P, Solomon MA, Nguyen P, Sheehan EM, Mehanna AS, D'Souza GG. Hydrophobized Triphenyl Phosphonium Derivatives for the Preparation of Mitochondriotropic Liposomes: Choice of Hydrophobic Anchor Influences Cytotoxicity but Not Mitochondriotropic Effect. J Liposome Res. 2016; 26:21–27. [PubMed: 25811811]

149. Futaki S, Suzuki T, Ohashi W, Yagami T, Tanaka S, Ueda K, Sugiura Y. Arginine-Rich Peptides. An Abundant Source of Membrane-Permeable Peptides Having Potential as Carriers for Intracellular Protein Delivery. J Biol Chem. 2001; 276:5836–5840. [PubMed: 11084031]

150. Nakase I, Niwa M, Takeuchi T, Sonomura K, Kawabata N, Koike Y, Takehashi M, Tanaka S, Ueda K, Simpson JC, et al. Cellular Uptake of Arginine-Rich Peptides: Roles for Macropinocytosis and Actin Rearrangement. Mol Ther. 2004; 10:1011–1022. [PubMed: 15564133]

151. Marrache S, Dhar S. Engineering of Blended Nanoparticle Platform for Delivery of Mitochondria-Acting Therapeutics. Proc Natl Acad Sci U S A. 2012; 109:16288–16293. [PubMed: 22991470]

152. Jung HS, Han J, Lee JH, Lee JH, Choi JM, Kweon HS, Han JH, Kim JH, Byun KM, Jung JH, et al. Enhanced NIR Radiation-Triggered Hyperthermia by Mitochondrial Targeting. J Am Chem Soc. 2015; 137:3017–3023. [PubMed: 25662739]

153. Zhao L, Yang H, Amano T, Qin H, Zheng L, Takahashi A, Zhao S, Tooyama I, Murakamid T, Komatsu N. Efficient Delivery of Chlorin e6 into Ovarian Cancer Cells with Octalysine

Conjugated Superparamagnetic Iron Oxide Nanoparticles for Effective Photodynamic Therapy. J Mater Chem B. 2016; 4:7741–7748.

154. He C, Jiang S, Jin H, Chen S, Lin G, Yao H, Wang X, Mi P, Ji Z, Lin Y, et al. Mitochondrial Electron Transport Chain Identified as a Novel Molecular Target of SPIO Nanoparticles Mediated Cancer-Specific Cytotoxicity. Biomaterials. 2016; 83:102–114. [PubMed: 26773667]
155. Nagesh PK, Johnson NR, Boya VK, Chowdhury P, Othman SF, Khalilzad-Sharghi V, Hafeez BB, Ganju A, Khan S, Behrman SW, et al. PSMA Targeted Docetaxel-Loaded Superparamagnetic Iron Oxide Nanoparticles for Prostate Cancer. Colloid Surf B Biointerfaces. 2016; 144:8–20. [PubMed: 27058278]
156. Bielski ER, Zhong Q, Brown M, da Rocha SR. Effect of the Conjugation Density of Triphenylphosphonium Cation on the Mitochondrial Targeting of Poly(Amidoamine) Dendrimers. Mol Pharm. 2015; 12:3043–3053. [PubMed: 26158804]
157. Biswas S, Dodwadkar NS, Piroyan A, Torchilin VP. Surface Conjugation of Triphenylphosphonium to Target Poly(Amidoamine) Dendrimers to Mitochondria. Biomaterials. 2012; 33:4773–4782. [PubMed: 22469294]
158. Mkandawire MM, Lakatos M, Springer A, Clemens A, Appelhans D, Krause-Buchholz U, Pompe W, Rodel G, Mkandawire M. Induction of Apoptosis in Human Cancer Cells by Targeting Mitochondria with Gold Nanoparticles. Nanoscale. 2015; 7:10634–10640. [PubMed: 26022234]
159. Smith RA, Porteous CM, Gane AM, Murphy MP. Delivery of Bioactive Molecules to Mitochondria in Vivo. Proc Natl Acad Sci U S A. 2003; 100:5407–5412. [PubMed: 12697897]
160. Flewelling RF, Hubbell WL. Hydrophobic Ion Interactions with Membranes. Thermodynamic Analysis of Tetraphenylphosphonium Binding to Vesicles. Biophys J. 1986; 49:531–540. [PubMed: 3006814]
161. Ono A, Miyauchi S, Demura M, Asakura T, Kamo N. Activation Energy for Permeation of Phosphonium Cations through Phospholipid Bilayer Membrane. Biochemistry. 1994; 33:4312–4318. [PubMed: 8155648]
162. Ross MF, Filipovska A, Smith RA, Gait MJ, Murphy MP. Cell-Penetrating Peptides Do Not Cross Mitochondrial Membranes Even When Conjugated to a Lipophilic Cation: Evidence against Direct Passage through Phospholipid Bilayers. Biochem J. 2004; 383:457–468. [PubMed: 15270716]
163. Ross MF, Prime TA, Abakumova I, James AM, Porteous CM, Smith RA, Murphy MP. Rapid and Extensive Uptake and Activation of Hydrophobic Triphenylphosphonium Cations within Cells. Biochem J. 2008; 411:633–645. [PubMed: 18294140]
164. Dhanasekaran A, Kotamraju S, Karunakaran C, Kalivendi SV, Thomas S, Joseph J, Kalyanaraman B. Mitochondria Superoxide Dismutase Mimetic Inhibits Peroxide-Induced Oxidative Damage and Apoptosis: Role of Mitochondrial Superoxide. Free Radic Biol Med. 2005; 39:567–583. [PubMed: 16085176]
165. Ross MF, Da Ros T, Blaikie FH, Prime TA, Porteous CM, Severina, Skulachev VP, Kjaergaard HG, Smith RA, Murphy MP. Accumulation of Lipophilic Dications by Mitochondria and Cells. Biochem J. 2006; 400:199–208. [PubMed: 16948637]
166. Andersen PS, Fuchs M. Potential Energy Barriers to Ion Transport within Lipid Bilayers. Studies with Tetraphenylborate. Biophys J. 1975; 15:795–830. [PubMed: 1148364]
167. Rokitskaya TI, Murphy MP, Skulachev VP, Antonenko YN. Ubiquinol and Plastoquinol Triphenylphosphonium Conjugates Can Carry Electrons through Phospholipid Membranes. Bioelectrochemistry. 2016; 111:23–30. [PubMed: 27182824]
168. Finichiu PG, James AM, Larsen L, Smith RA, Murphy MP. Mitochondrial Accumulation of a Lipophilic Cation Conjugated to an Ionisable Group Depends on Membrane Potential, pH Gradient and pK(a): Implications for the Design of Mitochondrial Probes and Therapies. J Bioenerg Biomembr. 2013; 45:165–173. [PubMed: 23180142]
169. Waggoner A. Optical Probes of Membrane Potential. J Membr Biol. 1976; 27:317–334. [PubMed: 787526]
170. Bashford CL, Smith JC. The Use of Optical Probes to Monitor Membrane Potential. Methods Enzymol. 1979; 55:569–586. [PubMed: 459857]

171. Rottenberg H. The Measurement of Membrane Potential and ΔpH in Cells, Organelles, and Vesicles. Methods Enzymol. 1979; 55:547–569. [PubMed: 37402]

172. Keij JF, Bell-Prince C, Steinkamp JA. Staining of Mitochondrial Membranes with 10-Nonyl Acridine Orange, Mitofluor Green, and Mitotracker Green Is Affected by Mitochondrial Membrane Potential Altering Drugs. Cytometry. 2000; 39:203–210. [PubMed: 10685077]

173. Murphy MP, Brand MD. Membrane-Potential-Dependent Changes in the Stoichiometry of Charge Translocation by the Mitochondrial Electron Transport Chain. Eur J Biochem. 1988; 173:637–644. [PubMed: 2836195]

174. Coulter CV, Smith RAJ, Murphy MP. Synthesis, Characterization, and Biological Properties of a Fullerene Triphenylphosphonium Salt. Fullerene Science and Technology. 2001; 9:339–350.

175. Severina, Muntyan MS, Lewis K, Skulachev VP. Transfer of Cationic Antibacterial Agents Berberine, Palmatine and Benzalkonium through Bimolecular Planar Phospholipid Film and Staphylococcus Aureus Membrane. IUBMB Life. 2001; 52:321–324. [PubMed: 11895082]

176. Minamikawa T, Sriratana A, Williams DA, Bowser DN, Hill JS, Nagley P. Chloromethyl-X-Rosamine (Mitotracker Red) Photosensitises Mitochondria and Induces Apoptosis in Intact Human Cells. J Cell Sci. 1999; 112(Pt 14):2419–2430. [PubMed: 10381397]

177. Scorrano L, Petronilli V, Colonna R, Di Lisa F, Bernardi P. Chloromethyltetramethylrosamine (Mitotracker Orange) Induces the Mitochondrial Permeability Transition and Inhibits Respiratory Complex I. Implications for the Mechanism of Cytochrome c Release. J Biol Chem. 1999; 274:24657–24663. [PubMed: 10455132]

178. Buckman JF, Hernandez H, Kress GJ, Votyakova TV, Pal S, Reynolds IJ. Mitotracker Labeling in Primary Neuronal and Astrocytic Cultures: Influence of Mitochondrial Membrane Potential and Oxidants. J Neurosci Methods. 2001; 104:165–176. [PubMed: 11164242]

179. Pendergrass W, Wolf N, Poot M. Efficacy of Mitotracker Green and CMX rosamine to Measure Changes in Mitochondrial Membrane Potentials in Living Cells and Tissues. Cytometry A. 2004; 61:162–169. [PubMed: 15382028]

180. Dong H, Cheung SH, Liang Y, Wang B, Ramalingam R, Wang P, Sun H, Cheng SH, Lam YW. "Stainomics": Identification of Mitotracker Labeled Proteins in Mammalian Cells. Electrophoresis. 2013; 34:1957–1964. [PubMed: 23595693]

181. Howard PH Jr, Wilson SB. Effects of the Cyanine Dye 3, 3′-Dipropylthiocarbocyanine on Mitochondrial Energy Conservation. Biochem J. 1979; 180:669–672. [PubMed: 486140]

182. Khailova LS, Nazarov PA, Sumbatyan NV, Korshunova GA, Rokitskaya TI, Dedukhova VI, Antonenko YN, Skulachev VP. Uncoupling and Toxic Action of Alkyltriphenylphosphonium Cations on Mitochondria and the Bacterium Bacillus Subtilis as a Function of Alkyl Chain Length. Biochemistry (Mosc). 2015; 80:1589–1597. [PubMed: 26638684]

183. Roelofs BA, Ge SX, Studlack PE, Polster BM. Low Micromolar Concentrations of the Superoxide Probe MitoSOX Uncouple Neural Mitochondria and Inhibit Complex IV. Free Radic Biol Med. 2015; 86:250–258. [PubMed: 26057935]

184. Polster BM, Nicholls DG, Ge SX, Roelofs BA. Use of Potentiometric Fluorophores in the Measurement of Mitochondrial Reactive Oxygen Species. Methods Enzymol. 2014; 547:225–250. [PubMed: 25416361]

185. Sims PJ, Waggoner AS, Wang CH, Hoffman JF. Mechanism by Which Cyanine Dyes Measure Membrane Potential in Red Blood Cells and Phosphatidylcholine Vesicles. Biochemistry. 2002; 13:3315–3330.

186. Cossarizza A, Baccaranicontri M, Kalashnikova G, Franceschi C. A New Method for the Cytofluorometric Analysis of Mitochondrial Membrane Potential Using the J-Aggregate Forming Lipophilic Cation 5,5′,6,6′-Tetrachloro-1,1′,3,3′-Tetraethylbenzimidazolcarbocyanine Iodide (JC-1). Biochem Biophys Res Commun. 1993; 197:40–45. [PubMed: 8250945]

187. Salvioli S, Ardizzoni A, Franceschi C, Cossarizza A. JC-1, but Not DiOC6(3) or Rhodamine 123, Is a Reliable Fluorescent Probe to Assess Δψ Changes in Intact Cells: Implications for Studies on Mitochondrial Functionality During Apoptosis. FEBS Lett. 1997; 411:77–82. [PubMed: 9247146]

188. Terasaki M, Reese TS. Characterization of Endoplasmic Reticulum by Co-Localization of BiP and Dicarbocyanine Dyes. J Cell Sci. 1992; 101(Pt 2):315–322. [PubMed: 1378452]

189. Nicholls DG. Simultaneous Monitoring of Ionophore- and Inhibitor-Mediated Plasma and Mitochondrial Membrane Potential Changes in Cultured Neurons. J Biol Chem. 2006; 281:14864–14874. [PubMed: 16551630]

190. Maftah A, Petit JM, Ratinaud MH, Julien R. 10-N Nonyl-Acridine Orange: A Fluorescent Probe Which Stains Mitochondria Independently of Their Energetic State. Biochem Biophys Res Commun. 1989; 164:185–190. [PubMed: 2478126]

191. Mileykovskaya E, Dowhan W, Birke RL, Zheng D, Lutterodt L, Haines TH. Cardiolipin Binds Nonyl Acridine Orange by Aggregating the Dye at Exposed Hydrophobic Domains on Bilayer Surfaces. FEBS Lett. 2001; 507:187–190. [PubMed: 11684095]

192. Garcia Fernandez MI, Ceccarelli D, Muscatello U. Use of the Fluorescent Dye 10-N Nonyl Acridine Orange in Quantitative and Location Assays of Cardiolipin: A Study on Different Experimental Models. Anal Biochem. 2004; 328:174–180. [PubMed: 15113694]

193. Kaewsuya P, Danielson ND, Ekhterae D. Fluorescent Determination of Cardiolipin Using 10-N-Nonyl Acridine Orange. Anal Bioanal Chem. 2007; 387:2775–2782. [PubMed: 17377779]

194. Kaewsuya P, Miller JD, Danielson ND, Sanjeevi J, James PF. Comparison of N-Alkyl Acridine Orange Dyes as Fluorescence Probes for the Determination of Cardiolipin. Anal Chim Acta. 2008; 626:111–118. [PubMed: 18790112]

195. Rodriguez ME, Azizuddin K, Zhang P, Chiu SM, Lam M, Kenney ME, Burda C, Oleinick NL. Targeting of Mitochondria by 10-N-Alkyl Acridine Orange Analogues: Role of Alkyl Chain Length in Determining Cellular Uptake and Localization. Mitochondrion. 2008; 8:237–246. [PubMed: 18514589]

196. Jacobson J, Duchen MR, Heales SJ. Intracellular Distribution of the Fluorescent Dye Nonyl Acridine Orange Responds to the Mitochondrial Membrane Potential: Implications for Assays of Cardiolipin and Mitochondrial Mass. J Neurochem. 2002; 82:224–233. [PubMed: 12124423]

197. Liang J, Tang BZ, Liu B. Specific Light-up Bioprobes Based on AIEgen Conjugates. Chem Soc Rev. 2015; 44:2798–2811. [PubMed: 25686761]

198. Luo J, Xie Z, Lam JW, Cheng L, Chen H, Qiu C, Kwok HS, Zhan X, Liu Y, Zhu D, et al. Aggregation-Induced Emission of 1-Methyl-1,2,3,4,5-Pentaphenylsilole. Chem Commun (Camb). 2001:1740–1741. [PubMed: 12240292]

199. Mei J, Leung NL, Kwok RT, Lam JW, Tang BZ. Aggregation-Induced Emission: Together We Shine, United We Soar! Chem Rev. 2015; 115:11718–11940. [PubMed: 26492387]

200. Leung CW, Hong Y, Chen S, Zhao E, Lam JW, Tang BZ. A Photostable AIE Luminogen for Specific Mitochondrial Imaging and Tracking. J Am Chem Soc. 2013; 135:62–65. [PubMed: 23244346]

201. Zhao N, Li M, Yan Y, Lam JWY, Zhang YL, Zhao YS, Wong KS, Tang BZ. A Tetraphenylethene-Substituted Pyridinium Salt with Multiple Functionalities: Synthesis, Stimuli-Responsive Emission, Optical Waveguide and Specific Mitochondrion Imaging. J Mater Chem C. 2013; 1:4640.

202. Zhao N, Chen S, Hong Y, Tang BZ. A Red Emitting Mitochondria-Targeted AIE Probe as an Indicator for Membrane Potential and Mouse Sperm Activity. Chem Commun (Camb). 2015; 51:13599–13602. [PubMed: 26264419]

203. Gao M, Sim CK, Leung CW, Hu Q, Feng G, Xu F, Tang BZ, Liu B. A Fluorescent Light-up Probe with AIE Characteristics for Specific Mitochondrial Imaging to Identify Differentiating Brown Adipose Cells. Chem Commun (Camb). 2014; 50:8312–8315. [PubMed: 24940580]

204. Hu Q, Gao M, Feng G, Liu B. Mitochondria-Targeted Cancer Therapy Using a Light-up Probe with Aggregation-Induced-Emission Characteristics. Angew Chem Int Ed Engl. 2014; 53:14225–14229. [PubMed: 25318447]

205. Zhang CJ, Hu Q, Feng G, Zhang R, Yuan Y, Lu X, Liu B. Image-Guided Combination Chemotherapy and Photodynamic Therapy Using a Mitochondria-Targeted Molecular Probe with Aggregation-Induced Emission Characteristics. Chem Sci. 2015; 6:4580–4586. [PubMed: 28717475]

206. Shin WS, Lee MG, Verwilst P, Lee JH, Chi SG, Kim JS. Mitochondria-Targeted Aggregation Induced Emission Theranostics: Crucial Importance of in Situ Activation. Chem Sci. 2016; 7:6050–6059.

207. Hoogewijs K, James AM, Smith RA, Gait MJ, Murphy MP, Lightowlers RN. Assessing the Delivery of Molecules to the Mitochondrial Matrix Using Click Chemistry. Chem Bio Chem. 2016; 17:1312–1316.

208. Logan A, Pell VR, Shaffer KJ, Evans C, Stanley NJ, Robb EL, Prime TA, Chouchani ET, Cocheme HM, Fearnley IM, et al. Assessing the Mitochondrial Membrane Potential in Cells and in Vivo Using Targeted Click Chemistry and Mass Spectrometry. Cell Metab. 2016; 23:379–385. [PubMed: 26712463]

209. Modica-Napolitano JS, Aprille JR. Basis for the Selective Cytotoxicity of Rhodamine 123. Cancer Res. 1987; 47:4361–4365. [PubMed: 2886218]

210. Trnka J, Elkalaf M, Andel M. Lipophilic Triphenylphosphonium Cations Inhibit Mitochondrial Electron Transport Chain and Induce Mitochondrial Proton Leak. PLoS One. 2015; 10:e0121837. [PubMed: 25927600]

211. Kelso GF, Porteous CM, Coulter CV, Hughes G, Porteous WK, Ledgerwood EC, Smith RA, Murphy MP. Selective Targeting of a Redox-Active Ubiquinone to Mitochondria within Cells: Antioxidant and Antiapoptotic Properties. J Biol Chem. 2001; 276:4588–4596. [PubMed: 11092892]

212. Wendt B, Ha HR, Hesse M. Synthesis of Two Metabolites of the Antiarrythmicum Amiodarone. Helv Chim Acta. 2002; 85:2990–3001.

213. Brown SE, Ross MF, Sanjuan-Pla A, Manas AR, Smith RA, Murphy MP. Targeting Lipoic Acid to Mitochondria: Synthesis and Characterization of a Triphenylphosphonium-Conjugated Alpha-Lipoyl Derivative. Free Radic Biol Med. 2007; 42:1766–1780. [PubMed: 17512456]

214. Kim DY, Kim HJ, Yu KH, Min JJ. Synthesis of [18F]-Labeled (6-Fluorohexyl)Triphenylphosphonium Cation as a Potential Agent for Myocardial Imaging Using Positron Emission Tomography. Bioconjug Chem. 2012; 23:431–437. [PubMed: 22264022]

215. Mehiri M, Caldarelli S, Di Giorgio A, Barouillet T, Doglio A, Condom R, Patino N. A "Ready-to-Use" Fluorescent-Labelled-Cysteine-TBTP (4-Thiobutyltriphenylphosphonium) Synthon to Investigate the Delivery of Non-Permeable Pna (Peptide Nucleic Acids)-Based Compounds to Cells. Bioorg Chem. 2007; 35:313–326. [PubMed: 17368717]

216. Maryanoff BE, Reitz AB, Duhlemswiler BA. Stereochemistry of the Wittig Reaction - Effect of Nucleophilic Groups in the Phosphonium Ylide. J Am Chem Soc. 1985; 107:217–226.

217. Liang B, Shao W, Zhu C, Wen G, Yue X, Wang R, Quan J, Du J, Bu X. Mitochondria-Targeted Approach: Remarkably Enhanced Cellular Bioactivities of TPP2a as Selective Inhibitor and Probe toward TrxR. ACS Chem Biol. 2016; 11:425–434. [PubMed: 26653078]

218. Chhen A, Vaultier M, Carrie R. Stereospecific Synthesis of Z-Olefins Bearing an Omega-Azido Group. Tetrahedron Lett. 1989; 30:4953–4956.

219. Trapella C, Voltan R, Melloni E, Tisato V, Celeghini C, Bianco S, Fantinati A, Salvadori S, Guerrini R, Secchiero P, et al. Design, Synthesis, and Biological Characterization of Novel Mitochondria Targeted Dichloroacetate-Loaded Compounds with Antileukemic Activity. J Med Chem. 2016; 59:147–156. [PubMed: 26653539]

220. Chevalier A, Zhang YM, Khdour OM, Hecht SM. Selective Functionalization of Antimycin a through an N-Transacylation Reaction. Org Lett. 2016; 18:2395–2398. [PubMed: 27168333]

221. Haslop A, Gee A, Plisson C, Long N. Fully Automated Radiosynthesis of [1-(2-[18 F]Fluoroethyl),1H[1,2,3]Triazole 4-Ethylene] Triphenylphosphonium Bromide as a Potential Positron Emission Tomography Tracer for Imaging Apoptosis. J Labelled Comp Radiopharm. 2013; 56:313–316. [PubMed: 24285410]

222. Kolmel DK, Horner A, Ronicke F, Nieger M, Schepers U, Brase S. Cell-Penetrating Peptoids: Introduction of Novel Cationic Side Chains. Eur J Med Chem. 2014; 79:231–243. [PubMed: 24739871]

223. Daeffler CS, Grubbs RH. Radical-Mediated Anti-Markovnikov Hydrophosphonation of Olefins. Org Lett. 2011; 13:6429–6431. [PubMed: 22085313]

224. Bates ED, Mayton RD, Ntai I, Davis JH. CO2 Capture by a Task-Specific Ionic Liquid. J Am Chem Soc. 2002; 124:926–927. [PubMed: 11829599]

225. Vahdat SM, Zolfigol MA, Baghery S. Straightforward Hantzsch Four- and Three-Component Condensation in the Presence of Triphenyl(Propyl-3-

Sulfonyl)Phosphoniumtrifluoromethanesulfonate {[Tppsp]Otf} as a Reusable and Green Mild Ionic Liquid Catalyst. Appl Organomet Chem. 2016; 30:311–317.

226. Song HY, Jin FX, Jin RH, Kang MR, Li Z, Chen J. Functional Ionic Liquids as Efficient and Recyclable Catalysts for the Methylation of Formaldehyde with Aromatics. Catal Lett. 2016; 146:1264–1272.
227. Toda Y, Komiyama Y, Kikuchi A, Suga H. Tetraarylphosphonium Salt-Catalyzed Carbon Dioxide Fixation at Atmospheric Pressure for the Synthesis of Cyclic Carbonates. ACS Catal. 2016; 6:6906–6910.
228. Trifonov AL, Zemtsov AA, Levin VV, Struchkova MI, Dilman AD. Nucleophilic Difluoromethylation Using (Bromodifluoromethyl)Trimethylsilane. Org Lett. 2016; 18:3458–3461. [PubMed: 27336618]
229. Byrne PA, Karaghiosoff K, Mayr H. Ambident Reactivity of Acetyl- and Formyl-Stabilized Phosphonium Ylides. J Am Chem Soc. 2016; 138:11272–11281. [PubMed: 27499510]
230. Hardy M, Chalier F, Finet JP, Rockenbauer A, Tordo P. Diastereoselective Synthesis and ESR Study of 4-Phenyldepmpo Spin Traps. J Org Chem. 2005; 70:2135–2142. [PubMed: 15760197]
231. Hardy M, Chalier F, Ouari O, Finet JP, Rockenbauer A, Kalyanaraman B, Tordo P. Mito-DEPMPO Synthesized from a Novel NH2-Reactive DEPMPO Spin Trap: A New and Improved Trap for the Detection of Superoxide. Chem Commun (Camb). 2007:1083–1085. [PubMed: 17325813]
232. Hardy M, Bardelang D, Karoui H, Rockenbauer A, Finet JP, Jicsinszky L, Rosas R, Ouari O, Tordo P. Improving the Trapping of Superoxide Radical with a Beta-Cyclodextrin-5-Diethoxyphosphoryl-5-Methyl-1-Pyrroline-N-Oxide (DEPMPO) Conjugate. Chemistry (Easton). 2009; 15:11114–11118.
233. Chalier F, Hardy M, Ouari O, Rockenbauer A, Tordo P. Design of New Derivatives of Nitrone DEPMPO Functionalized at C-4 for Further Specific Applications in Superoxide Radical Detection. J Org Chem. 2007; 72:7886–7892. [PubMed: 17880238]
234. Hardy M, Rockenbauer A, Vasquez-Vivar J, Felix C, Lopez M, Srinivasan S, Avadhani N, Tordo P, Kalyanaraman B. Detection, Characterization, and Decay Kinetics of ROS and Thiyl Adducts of Mito-DEPMPO Spin Trap. Chem Res Toxicol. 2007; 20:1053–1060. [PubMed: 17559235]
235. Li Z, Lopez M, Hardy M, McAllister DM, Kalyanaraman B, Zhao M. A (99m)Tc-Labeled Triphenylphosphonium Derivative for the Early Detection of Breast Tumors. Cancer Biother Radiopharm. 2009; 24:579–587. [PubMed: 19877888]
236. Murphy MP. How Mitochondria Produce Reactive Oxygen Species. Biochem J. 2009; 417:1–13. [PubMed: 19061483]
237. Radi R, Cassina A, Hodara R, Quijano C, Castro L. Peroxynitrite Reactions and Formation in Mitochondria. Free Radic Biol Med. 2002; 33:1451–1464. [PubMed: 12446202]
238. Mailloux RJ. Teaching the Fundamentals of Electron Transfer Reactions in Mitochondria and the Production and Detection of Reactive Oxygen Species. Redox Biol. 2015; 4:381–398. [PubMed: 25744690]
239. Dikalov SI, Harrison DG. Methods for Detection of Mitochondrial and Cellular Reactive Oxygen Species. Antioxid Redox Signal. 2014; 20:372–382. [PubMed: 22978713]
240. Dickinson BC, Srikun D, Chang CJ. Mitochondrial-Targeted Fluorescent Probes for Reactive Oxygen Species. Curr Opin Chem Biol. 2010; 14:50–56. [PubMed: 19910238]
241. Wardman P. Fluorescent and Luminescent Probes for Measurement of Oxidative and Nitrosative Species in Cells and Tissues: Progress, Pitfalls, and Prospects. Free Radic Biol Med. 2007; 43:995–1022. [PubMed: 17761297]
242. Murphy MP, Holmgren A, Larsson NG, Halliwell B, Chang CJ, Kalyanaraman B, Rhee SG, Thornalley PJ, Partridge L, Gems D, et al. Unraveling the Biological Roles of Reactive Oxygen Species. Cell Metab. 2011; 13:361–366. [PubMed: 21459321]
243. Kalyanaraman B. Oxidative Chemistry of Fluorescent Dyes: Implications in the Detection of Reactive Oxygen and Nitrogen Species. Biochem Soc Trans. 2011; 39:1221–1225. [PubMed: 21936793]
244. Kalyanaraman B, Darley-Usmar V, Davies KJ, Dennery PA, Forman HJ, Grisham MB, Mann GE, Moore K, Roberts LJ 2nd, Ischiropoulos H. Measuring Reactive Oxygen and Nitrogen Species

with Fluorescent Probes: Challenges and Limitations. Free Radic Biol Med. 2012; 52:1–6. [PubMed: 22027063]

245. Winterbourn CC. The Challenges of Using Fluorescent Probes to Detect and Quantify Specific Reactive Oxygen Species in Living Cells. Biochim Biophys Acta. 2014; 1840:730–738. [PubMed: 23665586]
246. Debowska K, Debski D, Hardy M, Jakubowska M, Kalyanaraman B, Marcinek A, Michalski R, Michalowski B, Ouari O, Sikora A, et al. Toward Selective Detection of Reactive Oxygen and Nitrogen Species with the Use of Fluorogenic Probes - Limitations, Progress, and Perspectives. Pharmacol Rep. 2015; 67:756–764. [PubMed: 26321278]
247. Kalyanaraman B, Hardy M, Podsiadly R, Cheng G, Zielonka J. Recent Developments in Detection of Superoxide Radical Anion and Hydrogen Peroxide: Opportunities, Challenges, and Implications in Redox Signaling. Arch Biochem Biophys. 2017; 617:38–47. [PubMed: 27590268]
248. Logan A, Cocheme HM, Li Pun PB, Apostolova N, Smith RA, Larsen L, Larsen DS, James AM, Fearnley IM, Rogatti S, et al. Using Exomarkers to Assess Mitochondrial Reactive Species in Vivo. Biochim Biophys Acta. 2014; 1840:923–930. [PubMed: 23726990]
249. Wisnovsky S, Lei EK, Jean SR, Kelley SO. Mitochondrial Chemical Biology: New Probes Elucidate the Secrets of the Powerhouse of the Cell. Cell Chem Biol. 2016; 23:917–927. [PubMed: 27478157]
250. Xu Z, Xu L. Fluorescent Probes for the Selective Detection of Chemical Species inside Mitochondria. Chem Commun (Camb). 2016; 52:1094–1119. [PubMed: 26621071]
251. Zielonka J, Zielonka M, Sikora A, Adamus J, Joseph J, Hardy M, Ouari O, Dranka BP, Kalyanaraman B. Global Profiling of Reactive Oxygen and Nitrogen Species in Biological Systems: High-Throughput Real-Time Analyses. J Biol Chem. 2012; 287:2984–2995. [PubMed: 22139901]
252. Zielonka J, Joseph J, Sikora A, Kalyanaraman B. Real-Time Monitoring of Reactive Oxygen and Nitrogen Species in a Multiwell Plate Using the Diagnostic Marker Products of Specific Probes. Methods Enzymol. 2013; 526:145–157. [PubMed: 23791099]
253. Robinson KM, Janes MS, Pehar M, Monette JS, Ross MF, Hagen TM, Murphy MP, Beckman JS. Selective Fluorescent Imaging of Superoxide in Vivo Using Ethidium-Based Probes. Proc Natl Acad Sci U S A. 2006; 103:15038–15043. [PubMed: 17015830]
254. De Biasi S, Gibellini L, Bianchini E, Nasi M, Pinti M, Salvioli S, Cossarizza A. Quantification of Mitochondrial Reactive Oxygen Species in Living Cells by Using Multi-Laser Polychromatic Flow Cytometry. Cytometry A. 2016; 89:1106–1110. [PubMed: 27575554]
255. Kauffman ME, Kauffman MK, Traore K, Zhu H, Trush MA, Jia Z, Li YR. MitoSOX-Based Flow Cytometry for Detecting Mitochondrial ROS. Reactive Oxygen Species. 2016; 2:361–370.
256. Zielonka J, Srinivasan S, Hardy M, Ouari O, Lopez M, Vasquez-Vivar J, Avadhani NG, Kalyanaraman B. Cytochrome c-Mediated Oxidation of Hydroethidine and Mito-Hydroethidine in Mitochondria: Identification of Homo- and Heterodimers. Free Radic Biol Med. 2008; 44:835–846. [PubMed: 18155177]
257. Zielonka J, Kalyanaraman B. Hydroethidine- and MitoSOX-Derived Red Fluorescence Is Not a Reliable Indicator of Intracellular Superoxide Formation: Another Inconvenient Truth. Free Radic Biol Med. 2010; 48:983–1001. [PubMed: 20116425]
258. Michalski R, Zielonka J, Hardy M, Joseph J, Kalyanaraman B. Hydropropidine: A Novel, Cell-Impermeant Fluorogenic Probe for Detecting Extracellular Superoxide. Free Radic Biol Med. 2013; 54:135–147. [PubMed: 23051008]
259. Kalyanaraman B, Dranka BP, Hardy M, Michalski R, Zielonka J. HPLC-Based Monitoring of Products Formed from Hydroethidine-Based Fluorogenic Probes - the Ultimate Approach for Intra- and Extracellular Superoxide Detection. Biochim Biophys Acta. 2014; 1840:739–744. [PubMed: 23668959]
260. Armstrong DA, Huie RE, Lymar S, Koppenol WH, Merényi G, Neta P, Stanbury DM, Steenken S, Wardman P. Standard Electrode Potentials Involving Radicals in Aqueous Solution: Inorganic Radicals. Bio Inorganic Reaction Mechanisms. 2013; 9:59–61.

261. Cheng G, Zielonka J, Kalyanaraman B. Modulatory Effects of MitoSOX on Cellular Bioenergetics: A Cautionary Note. Free Radic Biol Med. 2011; 51:S37–S38.

262. Kalyanaraman B, Hardy M, Zielonka J. A Critical Review of Methodologies to Detect Reactive Oxygen and Nitrogen Species Stimulated by NADPH Oxidase Enzymes: Implications in Pesticide Toxicity. Curr Pharmacol Rep. 2016; 2:193–201. [PubMed: 27774407]

263. Dikalov SI, Kirilyuk IA, Voinov M, Grigor'ev IA. EPR Detection of Cellular and Mitochondrial Superoxide Using Cyclic Hydroxylamines. Free Radic Res. 2011; 45:417–430. [PubMed: 21128732]

264. Trnka J, Blaikie FH, Logan A, Smith RA, Murphy MP. Antioxidant Properties of MitoTEMPOL and Its Hydroxylamine. Free Radic Res. 2009; 43:4–12. [PubMed: 19058062]

265. Trnka J, Blaikie FH, Smith RA, Murphy MP. A Mitochondria-Targeted Nitroxide Is Reduced to Its Hydroxylamine by Ubiquinol in Mitochondria. Free Radic Biol Med. 2008; 44:1406–1419. [PubMed: 18206669]

266. Li P, Zhang W, Li K, Liu X, Xiao H, Zhang W, Tang B. Mitochondria-Targeted Reaction-Based Two-Photon Fluorescent Probe for Imaging of Superoxide Anion in Live Cells and in Vivo. Anal Chem. 2013; 85:9877–9881. [PubMed: 24073893]

267. Hu JJ, Wong NK, Ye S, Chen X, Lu MY, Zhao AQ, Guo Y, Ma AC, Leung AY, Shen J, et al. Fluorescent Probe HKSOX-1 for Imaging and Detection of Endogenous Superoxide in Live Cells and in Vivo. J Am Chem Soc. 2015; 137:6837–6843. [PubMed: 25988218]

268. Murphy MP, Echtay KS, Blaikie FH, Asin-Cayuela J, Cocheme HM, Green K, Buckingham JA, Taylor ER, Hurrell F, Hughes G, et al. Superoxide Activates Uncoupling Proteins by Generating Carbon-Centered Radicals and Initiating Lipid Peroxidation: Studies Using a Mitochondria-Targeted Spin Trap Derived from Alpha-Phenyl-N-Tert-Butylnitrone. J Biol Chem. 2003; 278:48534–48545. [PubMed: 12972420]

269. Sethumadhavan S, Hardy M, Vasquez-Vivar J. Site-Specific Detection of Superoxide from Heart Mitochondria. Free Radic Biol Med. 2012; 53:S28.

270. Beziere N, Hardy M, Poulhes F, Karoui H, Tordo P, Ouari O, Frapart YM, Rockenbauer A, Boucher JL, Mansuy D, et al. Metabolic Stability of Superoxide Adducts Derived from Newly Developed Cyclic Nitrone Spin Traps. Free Radic Biol Med. 2014; 67:150–158. [PubMed: 24161442]

271. Xu Y, Kalyanaraman B. Synthesis and ESR Studies of a Novel Cyclic Nitrone Spin Trap Attached to a Phosphonium Group-a Suitable Trap for Mitochondria-Generated ROS? Free Radic Res. 2007; 41:1–7. [PubMed: 17164173]

272. Quin C, Trnka J, Hay A, Murphy MP, Hartley RC. Synthesis of a Mitochondria-Targeted Spin Trap Using a Novel Parham-Type Cyclization. Tetrahedron. 2009; 65:8154–8160. [PubMed: 19888470]

273. Robertson L, Hartley RC. Synthesis of N-Arylpyridinium Salts Bearing a Nitrone Spin Trap as Potential Mitochondria-Targeted Antioxidants. Tetrahedron. 2009; 65:5284–5292. [PubMed: 19693262]

274. Summers FA, Zhao B, Ganini D, Mason RP. Photooxidation of Amplex Red to Resorufin: Implications of Exposing the Amplex Red Assay to Light. Methods Enzymol. 2013; 526:1–17. [PubMed: 23791091]

275. Miwa S, Treumann A, Bell A, Vistoli G, Nelson G, Hay S, von Zglinicki T. Carboxylesterase Converts Amplex Red to Resorufin: Implications for Mitochondrial H2O2 Release Assays. Free Radic Biol Med. 2016; 90:173–183. [PubMed: 26577176]

276. Sikora A, Zielonka J, Lopez M, Joseph J, Kalyanaraman B. Direct Oxidation of Boronates by Peroxynitrite: Mechanism and Implications in Fluorescence Imaging of Peroxynitrite. Free Radic Biol Med. 2009; 47:1401–1407. [PubMed: 19686842]

277. Zielonka J, Sikora A, Hardy M, Joseph J, Dranka BP, Kalyanaraman B. Boronate Probes as Diagnostic Tools for Real Time Monitoring of Peroxynitrite and Hydroperoxides. Chem Res Toxicol. 2012; 25:1793–1799. [PubMed: 22731669]

278. Lo LC, Chu CY. Development of Highly Selective and Sensitive Probes for Hydrogen Peroxide. Chem Commun (Camb). 2003:2728–2729. [PubMed: 14649832]

279. Chang MC, Pralle A, Isacoff EY, Chang CJ. A Selective, Cell-Permeable Optical Probe for Hydrogen Peroxide in Living Cells. J Am Chem Soc. 2004; 126:15392–15393. [PubMed: 15563161]

280. Lippert AR, Van de Bittner GC, Chang CJ. Boronate Oxidation as a Bioorthogonal Reaction Approach for Studying the Chemistry of Hydrogen Peroxide in Living Systems. Acc Chem Res. 2011; 44:793–804. [PubMed: 21834525]

281. Dickinson BC, Chang CJ. A Targetable Fluorescent Probe for Imaging Hydrogen Peroxide in the Mitochondria of Living Cells. J Am Chem Soc. 2008; 130:9638–9639. [PubMed: 18605728]

282. Dickinson BC, Lin VS, Chang CJ. Preparation and Use of MitoPY1 for Imaging Hydrogen Peroxide in Mitochondria of Live Cells. Nat Protoc. 2013; 8:1249–1259. [PubMed: 23722262]

283. Michalski R, Zielonka J, Gapys E, Marcinek A, Joseph J, Kalyanaraman B. Real-Time Measurements of Amino Acid and Protein Hydroperoxides Using Coumarin Boronic Acid. J Biol Chem. 2014; 289:22536–22553. [PubMed: 24928516]

284. Sikora A, Zielonka J, Lopez M, Dybala-Defratyka A, Joseph J, Marcinek A, Kalyanaraman B. Reaction between Peroxynitrite and Boronates: EPR Spin-Trapping, HPLC Analyses, and Quantum Mechanical Study of the Free Radical Pathway. Chem Res Toxicol. 2011; 24:687–697. [PubMed: 21434648]

285. Smulik R, Debski D, Zielonka J, Michalowski B, Adamus J, Marcinek A, Kalyanaraman B, Sikora A. Nitroxyl (HNO) Reacts with Molecular Oxygen and Forms Peroxynitrite at Physiological pH. Biological Implications. J Biol Chem. 2014; 289:35570–35581. [PubMed: 25378389]

286. Zielonka J, Zielonka M, VerPlank L, Cheng G, Hardy M, Ouari O, Ayhan MM, Podsiadly R, Sikora A, Lambeth JD, et al. Mitigation of NADPH Oxidase 2 Activity as a Strategy to Inhibit Peroxynitrite Formation. J Biol Chem. 2016; 291:7029–7044. [PubMed: 26839313]

287. Cocheme HM, Quin C, McQuaker SJ, Cabreiro F, Logan A, Prime TA, Abakumova I, Patel JV, Fearnley IM, James AM, et al. Measurement of H2O2 within Living Drosophila During Aging Using a Ratiometric Mass Spectrometry Probe Targeted to the Mitochondrial Matrix. Cell Metab. 2011; 13:340–350. [PubMed: 21356523]

288. Cocheme HM, Logan A, Prime TA, Abakumova I, Quin C, McQuaker SJ, Patel JV, Fearnley IM, James AM, Porteous CM, et al. Using the Mitochondria-Targeted Ratiometric Mass Spectrometry Probe MitoB to Measure H2O2 in Living Drosophila. Nat Protoc. 2012; 7:946–958. [PubMed: 22517261]

289. Cairns AG, McQuaker SJ, Murphy MP, Hartley RC. Targeting Mitochondria with Small Molecules: The Preparation of MitoB and MitoP as Exomarkers of Mitochondrial Hydrogen Peroxide. Methods Mol Biol. 2015; 1265:25–50. [PubMed: 25634265]

290. Mackenzie RM, Salt IP, Miller WH, Logan A, Ibrahim HA, Degasperi A, Dymott JA, Hamilton CA, Murphy MP, Delles C, et al. Mitochondrial Reactive Oxygen Species Enhance AMP-Activated Protein Kinase Activation in the Endothelium of Patients with Coronary Artery Disease and Diabetes. Clin Sci (Lond). 2013; 124:403–411. [PubMed: 23057846]

291. Logan A, Shabalina IG, Prime TA, Rogatti S, Kalinovich AV, Hartley RC, Budd RC, Cannon B, Murphy MP. In Vivo Levels of Mitochondrial Hydrogen Peroxide Increase with Age in mtDNA Mutator Mice. Aging Cell. 2014; 13:765–768. [PubMed: 24621297]

292. Chouchani ET, Methner C, Buonincontri G, Hu CH, Logan A, Sawiak SJ, Murphy MP, Krieg T. Complex I Deficiency Due to Selective Loss of Ndufs4 in the Mouse Heart Results in Severe Hypertrophic Cardiomyopathy. PLoS One. 2014; 9:e94157. [PubMed: 24705922]

293. Salin K, Auer SK, Rudolf AM, Anderson GJ, Cairns AG, Mullen W, Hartley RC, Selman C, Metcalfe NB. Individuals with Higher Metabolic Rates Have Lower Levels of Reactive Oxygen Species in Vivo. Biol Lett. 2015; 11:20150538. [PubMed: 26382073]

294. Gallego-Villar L, Rivera-Barahona A, Cuevas-Martin C, Guenzel A, Perez B, Barry MA, Murphy MP, Logan A, Gonzalez-Quintana A, Martin MA, et al. In Vivo Evidence of Mitochondrial Dysfunction and Altered Redox Homeostasis in a Genetic Mouse Model of Propionic Acidemia: Implications for the Pathophysiology of This Disorder. Free Radic Biol Med. 2016; 96:1–12. [PubMed: 27083476]

295. Sikora A, Zielonka J, Adamus J, Debski D, Dybala-Defratyka A, Michalowski B, Joseph J, Hartley RC, Murphy MP, Kalyanaraman B. Reaction between Peroxynitrite and Triphenylphosphonium-Substituted Arylboronic Acid Isomers: Identification of Diagnostic Marker Products and Biological Implications. Chem Res Toxicol. 2013; 26:856–867. [PubMed: 23611338]

296. Zielonka J, Sikora A, Adamus J, Kalyanaraman B. Detection and Differentiation between Peroxynitrite and Hydroperoxides Using Mitochondria-Targeted Arylboronic Acid. Methods Mol Biol. 2015; 1264:171–181. [PubMed: 25631013]

297. Masanta G, Heo CH, Lim CS, Bae SK, Cho BR, Kim HM. A Mitochondria-Localized Two-Photon Fluorescent Probe for Ratiometric Imaging of Hydrogen Peroxide in Live Tissue. Chem Commun (Camb). 2012; 48:3518–3520. [PubMed: 22382302]

298. Kim HM, Cho BR. Mitochondrial-Targeted Two-Photon Fluorescent Probes for Zinc Ions, H2O2, and Thiols in Living Tissues. Oxid Med Cell Longev. 2013; 2013:323619. [PubMed: 23431410]

299. Xu J, Zhang Y, Yu H, Gao X, Shao S. Mitochondria-Targeted Fluorescent Probe for Imaging Hydrogen Peroxide in Living Cells. Anal Chem. 2016; 88:1455–1461. [PubMed: 26695451]

300. Wen Y, Liu K, Yang H, Li Y, Lan H, Liu Y, Zhang X, Yi T. A Highly Sensitive Ratiometric Fluorescent Probe for the Detection of Cytoplasmic and Nuclear Hydrogen Peroxide. Anal Chem. 2014; 86:9970–9976. [PubMed: 25196578]

301. Wen Y, Liu K, Yang H, Liu Y, Chen L, Liu Z, Huang C, Yi T. Mitochondria-Directed Fluorescent Probe for the Detection of Hydrogen Peroxide near Mitochondrial DNA. Anal Chem. 2015; 87:10579–10584. [PubMed: 26399738]

302. Koide Y, Urano Y, Kenmoku S, Kojima H, Nagano T. Design and Synthesis of Fluorescent Probes for Selective Detection of Highly Reactive Oxygen Species in Mitochondria of Living Cells. J Am Chem Soc. 2007; 129:10324–10325. [PubMed: 17672465]

303. Zhang H, Liu J, Sun YQ, Huo Y, Li Y, Liu W, Wu X, Zhu N, Shi Y, Guo W. A Mitochondria-Targetable Fluorescent Probe for Peroxynitrite: Fast Response and High Selectivity. Chem Commun (Camb). 2015; 51:2721–2724. [PubMed: 25575130]

304. Jia X, Chen Q, Yang Y, Tang Y, Wang R, Xu Y, Zhu W, Qian X. FRET-Based Mito-Specific Fluorescent Probe for Ratiometric Detection and Imaging of Endogenous Peroxynitrite: Dyad of Cy3 and Cy5. J Am Chem Soc. 2016; 138:10778–10781. [PubMed: 27517310]

305. Yu F, Li P, Wang B, Han K. Reversible near-Infrared Fluorescent Probe Introducing Tellurium to Mimetic Glutathione Peroxidase for Monitoring the Redox Cycles between Peroxynitrite and Glutathione in Vivo. J Am Chem Soc. 2013; 135:7674–7680. [PubMed: 23621710]

306. Miao J, Huo Y, Liu Q, Li Z, Shi H, Shi Y, Guo W. A New Class of Fast-Response and Highly Selective Fluorescent Probes for Visualizing Peroxynitrite in Live Cells, Subcellular Organelles, and Kidney Tissue of Diabetic Rats. Biomaterials. 2016; 107:33–43. [PubMed: 27606902]

307. Kim S, Tachikawa T, Fujitsuka M, Majima T. Far-Red Fluorescence Probe for Monitoring Singlet Oxygen During Photodynamic Therapy. J Am Chem Soc. 2014; 136:11707–11715. [PubMed: 25075870]

308. Prime TA, Forkink M, Logan A, Finichiu PG, McLachlan J, Li Pun PB, Koopman WJ, Larsen L, Latter MJ, Smith RA, et al. A Ratiometric Fluorescent Probe for Assessing Mitochondrial Phospholipid Peroxidation within Living Cells. Free Radic Biol Med. 2012; 53:544–553. [PubMed: 22659314]

309. de Araujo TH, Okada SS, Ghosn EE, Taniwaki NN, Rodrigues MR, de Almeida SR, Mortara RA, Russo M, Campa A, Albuquerque RC. Intracellular Localization of Myeloperoxidase in Murine Peritoneal B-Lymphocytes and Macrophages. Cell Immunol. 2013; 281:27–30. [PubMed: 23434459]

310. Liu F, Wu T, Cao J, Zhang H, Hu M, Sun S, Song F, Fan J, Wang J, Peng X. A Novel Fluorescent Sensor for Detection of Highly Reactive Oxygen Species, and for Imaging Such Endogenous hROS in the Mitochondria of Living Cells. Analyst. 2013; 138:775–778. [PubMed: 23232359]

311. Xiao H, Xin K, Dou H, Yin G, Quan Y, Wang R. A Fast-Responsive Mitochondria-Targeted Fluorescent Probe Detecting Endogenous Hypochlorite in Living RAW 264.7 Cells and Nude Mouse. Chem Commun (Camb). 2015; 51:1442–1445. [PubMed: 25487031]

312. Zha J, Fu B, Qin C, Zeng L, Hu X. A Ratiometric Fluorescent Probe for Rapid and Sensitive Visualization of Hypochlorite in Living Cells. RSC Adv. 2014; 4:43110–43113.

313. Zhou L, Lu DQ, Wang Q, Hu S, Wang H, Sun H, Zhang X. A High-Resolution Mitochondria-Targeting Ratiometric Fluorescent Probe for Detection of the Endogenous Hypochlorous Acid. Spectrochim Acta A Mol Biomol Spectrosc. 2016; 166:129–134. [PubMed: 27236136]

314. Cheng G, Fan J, Sun W, Sui K, Jin X, Wang J, Peng X. A Highly Specific BODIPY-Based Probe Localized in Mitochondria for HClO Imaging. Analyst. 2013; 138:6091–6096. [PubMed: 23961536]

315. Chen X, Wang X, Wang S, Shi W, Wang K, Ma H. A Highly Selective and Sensitive Fluorescence Probe for the Hypochlorite Anion. Chemistry (Easton). 2008; 14:4719–4724.

316. Hou JT, Wu MY, Li K, Yang J, Yu KK, Xie YM, Yu XQ. Mitochondria-Targeted Colorimetric and Fluorescent Probes for Hypochlorite and Their Applications for in Vivo Imaging. Chem Commun (Camb). 2014; 50:8640–8643. [PubMed: 24870251]

317. Yuan L, Wang L, Agrawalla BK, Park SJ, Zhu H, Sivaraman B, Peng J, Xu QH, Chang YT. Development of Targetable Two-Photon Fluorescent Probes to Image Hypochlorous Acid in Mitochondria and Lysosome in Live Cell and Inflamed Mouse Model. J Am Chem Soc. 2015; 137:5930–5938. [PubMed: 25905448]

318. Li G, Lin Q, Ji L, Chao H. Phosphorescent Iridium(III) Complexes as Multicolour Probes for Imaging of Hypochlorite Ions in Mitochondria. J Mater Chem B. 2014; 2:7918–7926.

319. Li G, Lin Q, Sun L, Feng C, Zhang P, Yu B, Chen Y, Wen Y, Wang H, Ji L, et al. A Mitochondrial Targeted Two-Photon Iridium(III) Phosphorescent Probe for Selective Detection of Hypochlorite in Live Cells and in Vivo. Biomaterials. 2015; 53:285–295. [PubMed: 25890727]

320. Amels P, Elias H, Wannowius KJ. Kinetics and Mechanism of the Oxidation of Dimethyl Sulfide by Hydroperoxides in Aqueous Medium Study on the Potential Contribution of Liquid-Phase Oxidation of Dimethyl Sulfide in the Atmosphere. J Chem Society, Faraday Trans. 1997; 93:2537–2544.

321. Veltwisch D, Janata E, Asmus K-D. Primary Processes in the Reaction of OH·-Radicals with Sulphoxides. J Chem Soc, Perkin Trans. 1980; 2:146–153.doi: 10.1039/p29800000146

322. Kimura H. Signaling Molecules: Hydrogen Sulfide and Polysulfide. Antioxid Redox Signal. 2015; 22:362–376. [PubMed: 24800864]

323. Paul BD, Snyder SH. Modes of Physiologic H2S Signaling in the Brain and Peripheral Tissues. Antioxid Redox Signal. 2015; 22:411–423. [PubMed: 24684551]

324. Polhemus DJ, Lefer DJ. Emergence of Hydrogen Sulfide as an Endogenous Gaseous Signaling Molecule in Cardiovascular Disease. Circ Res. 2014; 114:730–737. [PubMed: 24526678]

325. Lin VS, Chen W, Xian M, Chang CJ. Chemical Probes for Molecular Imaging and Detection of Hydrogen Sulfide and Reactive Sulfur Species in Biological Systems. Chem Soc Rev. 2015; 44:4596–4618. [PubMed: 25474627]

326. Bae SK, Heo CH, Choi DJ, Sen D, Joe EH, Cho BR, Kim HM. A Ratiometric Two-Photon Fluorescent Probe Reveals Reduction in Mitochondrial H2S Production in Parkinson's Disease Gene Knockout Astrocytes. J Am Chem Soc. 2013; 135:9915–9923. [PubMed: 23745510]

327. Wu Z, Liang D, Tang X. Visualizing Hydrogen Sulfide in Mitochondria and Lysosome of Living Cells and in Tumors of Living Mice with Positively Charged Fluorescent Chemosensors. Anal Chem. 2016; 88:9213–9218. [PubMed: 27537069]

328. Chen Y, Zhu C, Yang Z, Chen J, He Y, Jiao Y, He W, Qiu L, Cen J, Guo Z. A Ratiometric Fluorescent Probe for Rapid Detection of Hydrogen Sulfide in Mitochondria. Angew Chem Int Ed Engl. 2013; 52:1688–1691. [PubMed: 23288697]

329. Xu J, Pan J, Jiang X, Qin C, Zeng L, Zhang H, Zhang JF. A Mitochondria-Targeted Ratiometric Fluorescent Probe for Rapid, Sensitive and Specific Detection of Biological SO2 Derivatives in Living Cells. Biosens Bioelectron. 2016; 77:725–732. [PubMed: 26499868]

330. Zhou X, Kwon Y, Kim G, Ryu JH, Yoon J. A Ratiometric Fluorescent Probe Based on a Coumarin-Hemicyanine Scaffold for Sensitive and Selective Detection of Endogenous Peroxynitrite. Biosens Bioelectron. 2015; 64:285–291. [PubMed: 25240128]

331. Xu W, Teoh CL, Peng J, Su D, Yuan L, Chang YT. A Mitochondria-Targeted Ratiometric Fluorescent Probe to Monitor Endogenously Generated Sulfur Dioxide Derivatives in Living Cells. Biomaterials. 2015; 56:1–9. [PubMed: 25934273]

332. Feng X, Zhang T, Liu JT, Miao JY, Zhao BX. A New Ratiometric Fluorescent Probe for Rapid, Sensitive and Selective Detection of Endogenous Hydrogen Sulfide in Mitochondria. Chem Commun (Camb). 2016; 52:3131–3134. [PubMed: 26806758]

333. Wang X, Sun J, Zhang W, Ma X, Lv J, Tang B. A near-Infrared Ratiometric Fluorescent Probe for Rapid and Highly Sensitive Imaging of Endogenous Hydrogen Sulfide in Living Cells. Chem Sci. 2013; 4:2551.

334. Pak YL, Li J, Ko KC, Kim G, Lee JY, Yoon J. Mitochondria-Targeted Reaction-Based Fluorescent Probe for Hydrogen Sulfide. Anal Chem. 2016; 88:5476–5481. [PubMed: 27094621]

335. Gao M, Yu F, Chen H, Chen L. Near-Infrared Fluorescent Probe for Imaging Mitochondrial Hydrogen Polysulfides in Living Cells and in Vivo. Anal Chem. 2015; 87:3631–3638. [PubMed: 25751615]

336. Thornalley PJ. Protein and Nucleotide Damage by Glyoxal and Methylglyoxal in Physiological Systems - Role in Ageing and Disease. Drug Metabol Drug Interact. 2008; 23:125–150. [PubMed: 18533367]

337. Pun PB, Murphy MP. Pathological Significance of Mitochondrial Glycation. Int J Cell Biol. 2012; 2012:843505. [PubMed: 22778743]

338. Pun PB, Logan A, Darley-Usmar V, Chacko B, Johnson MS, Huang GW, Rogatti S, Prime TA, Methner C, Krieg T, et al. A Mitochondria-Targeted Mass Spectrometry Probe to Detect Glyoxals: Implications for Diabetes. Free Radic Biol Med. 2014; 67:437–450. [PubMed: 24316194]

339. Asayama S, Kawamura E, Nagaoka S, Kawakami H. Design of Manganese Porphyrin Modified with Mitochondrial Signal Peptide for a New Antioxidant. Mol Pharm. 2006; 3:468–470. [PubMed: 16889441]

340. Dessolin J, Schuler M, Quinart A, De Giorgi F, Ghosez L, Ichas F. Selective Targeting of Synthetic Antioxidants to Mitochondria: Towards a Mitochondrial Medicine for Neurodegenerative Diseases? Eur J Pharmacol. 2002; 447:155–161. [PubMed: 12151007]

341. Kelso GF, Maroz A, Cocheme HM, Logan A, Prime TA, Peskin AV, Winterbourn CC, James AM, Ross MF, Brooker S, et al. A Mitochondria-Targeted Macrocyclic Mn(II) Superoxide Dismutase Mimetic. Chem Biol. 2012; 19:1237–1246. [PubMed: 23102218]

342. Liochev SI, Fridovich I. Does MitoSOD Protect against the Toxicity of Paraquat toward Mitochondria by Acting as a Superoxide Dismutase Mimic? Free Radic Biol Med. 2013; 65:1534. [PubMed: 23434767]

343. Miriyala S, Spasojevic I, Tovmasyan A, Salvemini D, Vujaskovic Z, St Clair D, Batinic-Haberle I. Manganese Superoxide Dismutase, MnSOD and Its Mimics. Biochim Biophys Acta. 2012; 1822:794–814. [PubMed: 22198225]

344. Spasojevic I, Chen Y, Noel TJ, Yu Y, Cole MP, Zhang L, Zhao Y, St Clair DK, Batinic-Haberle I. Mn Porphyrin-Based Superoxide Dismutase (SOD) Mimic, MnIIITE-2-PyP5+, Targets Mouse Heart Mitochondria. Free Radic Biol Med. 2007; 42:1193–1200. [PubMed: 17382200]

345. Spasojevic I, Miriyala S, Tovmasyan A, Salvemini D, Fan P, Vujaskovic Z, Batinic-Haberle I, Clair DKS. Lipophilicity of Mn(III) N-Alkylpyridylporphyrins Dominates Their Accumulation within Mitochondria and Therefore in Vivo Efficacy: A Mouse Study. Free Radic Biol Med. 2011; 51:S98–S99.

346. Aitken JB, Shearer EL, Giles NM, Lai B, Vogt S, Reboucas JS, Batinic-Haberle I, Lay PA, Giles GI. Intracellular Targeting and Pharmacological Activity of the Superoxide Dismutase Mimics MnTE-2-PyP5+ and Mntnhex-2-Pyp5+ Regulated by Their Porphyrin Ring Substituents. Inorg Chem. 2013; 52:4121–4123. [PubMed: 23551184]

347. Batinic-Haberle I, Rajic Z, Tovmasyan A, Reboucas JS, Ye X, Leong KW, Dewhirst MW, Vujaskovic Z, Benov L, Spasojevic I. Diverse Functions of Cationic Mn(III) N-Substituted Pyridylporphyrins, Recognized as SOD Mimics. Free Radic Biol Med. 2011; 51:1035–1053. [PubMed: 21616142]

348. Batinic-Haberle I, Tovmasyan A, Spasojevic I. An Educational Overview of the Chemistry, Biochemistry and Therapeutic Aspects of Mn Porphyrins - from Superoxide Dismutation to H2O2-Driven Pathways. Redox Biol. 2015; 5:43–65. [PubMed: 25827425]

349. Robb EL, Gawel JM, Aksentijevic D, Cocheme HM, Stewart TS, Shchepinova MM, Qiang H, Prime TA, Bright TP, James AM, et al. Selective Superoxide Generation within Mitochondria by the Targeted Redox Cycler MitoParaquat. Free Radic Biol Med. 2015; 89:883–894. [PubMed: 26454075]

350. Drechsel DA, Patel M. Differential Contribution of the Mitochondrial Respiratory Chain Complexes to Reactive Oxygen Species Production by Redox Cycling Agents Implicated in Parkinsonism. Toxicol Sci. 2009; 112:427–434. [PubMed: 19767442]

351. Prime TA, Blaikie FH, Evans C, Nadtochiy SM, James AM, Dahm CC, Vitturi DA, Patel RP, Hiley CR, Abakumova I, et al. A Mitochondria-Targeted S-Nitrosothiol Modulates Respiration, Nitrosates Thiols, and Protects against Ischemia-Reperfusion Injury. Proc Natl Acad Sci U S A. 2009; 106:10764–10769. [PubMed: 19528654]

352. Chouchani ET, Hurd TR, Nadtochiy SM, Brookes PS, Fearnley IM, Lilley KS, Smith RA, Murphy MP. Identification of S-Nitrosated Mitochondrial Proteins by S-Nitrosothiol Difference in Gel Electrophoresis (SNO-DIGE): Implications for the Regulation of Mitochondrial Function by Reversible S-Nitrosation. Biochem J. 2010; 430:49–59. [PubMed: 20533907]

353. Chouchani ET, Methner C, Nadtochiy SM, Logan A, Pell VR, Ding S, James AM, Cocheme HM, Reinhold J, Lilley KS, et al. Cardioprotection by S-Nitrosation of a Cysteine Switch on Mitochondrial Complex I. Nat Med. 2013; 19:753–759. [PubMed: 23708290]

354. Methner C, Chouchani ET, Buonincontri G, Pell VR, Sawiak SJ, Murphy MP, Krieg T. Mitochondria Selective S-Nitrosation by Mitochondria-Targeted S-Nitrosothiol Protects against Post-Infarct Heart Failure in Mouse Hearts. Eur J Heart Fail. 2014; 16:712–717. [PubMed: 24891297]

355. Stoyanovsky DA, Vlasova, Belikova NA, Kapralov A, Tyurin V, Greenberger JS, Kagan VE. Activation of NO Donors in Mitochondria: Peroxidase Metabolism of (2-Hydroxyamino-Vinyl)-Triphenyl-Phosphonium by Cytochrome c Releases NO and Protects Cells against Apoptosis. FEBS Lett. 2008; 582:725–728. [PubMed: 18258194]

356. Kagan VE, Bayir A, Bayir H, Stoyanovsky D, Borisenko GG, Tyurina YY, Wipf P, Atkinson J, Greenberger JS, Chapkin RS, et al. Mitochondria-Targeted Disruptors and Inhibitors of Cytochrome c/Cardiolipin Peroxidase Complexes: A New Strategy in Anti-Apoptotic Drug Discovery. Mol Nutr Food Res. 2009; 53:104–114. [PubMed: 18979502]

357. Belikova NA, Jiang J, Stoyanovsky DA, Glumac A, Bayir H, Greenberger JS, Kagan VE. Mitochondria-Targeted (2-Hydroxyamino-Vinyl)-Triphenyl-Phosphonium Releases NO(.) and Protects Mouse Embryonic Cells against Irradiation-Induced Apoptosis. FEBS Lett. 2009; 583:1945–1950. [PubMed: 19427865]

358. Finichiu PG, Larsen DS, Evans C, Larsen L, Bright TP, Robb EL, Trnka J, Prime TA, James AM, Smith RA, et al. A Mitochondria-Targeted Derivative of Ascorbate: MitoC. Free Radic Biol Med. 2015; 89:668–678. [PubMed: 26453920]

359. Bhowmick D, Mugesh G. Insights into the Catalytic Mechanism of Synthetic Glutathione Peroxidase Mimetics. Org Biomol Chem. 2015; 13:10262–10272. [PubMed: 26372527]

360. Filipovska A, Kelso GF, Brown SE, Beer SM, Smith RA, Murphy MP. Synthesis and Characterization of a Triphenylphosphonium-Conjugated Peroxidase Mimetic. Insights into the Interaction of Ebselen with Mitochondria. J Biol Chem. 2005; 280:24113–24126. [PubMed: 15831495]

361. Stoyanovsky DA, Jiang J, Murphy MP, Epperly M, Zhang X, Li S, Greenberger J, Kagan V, Bayir H. Design and Synthesis of a Mitochondria-Targeted Mimic of Glutathione Peroxidase, Mitoebselen-2, as a Radiation Mitigator. ACS Med Chem Lett. 2014; 5:1304–1307. [PubMed: 25530831]

362. Bakry R, Vallant RM, Najam-ul-Haq M, Rainer M, Szabo Z, Huck CW, Bonn GK. Medicinal Applications of Fullerenes. Int J Nanomedicine. 2007; 2:639–649. [PubMed: 18203430]

363. Liu Q, Cui Q, Li XJ, Jin L. The Applications of Buckminsterfullerene C60 and Derivatives in Orthopaedic Research. Connect Tissue Res. 2014; 55:71–79. [PubMed: 24409811]

364. Friedman SH, DeCamp DL, Sijbesma RP, Srdanov G, Wudl F, Kenyon GL. Inhibition of the HIV-1 Protease by Fullerene Derivatives: Model Building Studies and Experimental Verification. J Am Chem Soc. 1993; 115:6506–6509.

365. Krusic PJ, Wasserman E, Keizer PN, Morton JR, Preston KF. Radical Reactions of C60. Science. 1991; 254:1183–1185. [PubMed: 17776407]

366. Nakamura E, Isobe H. Functionalized Fullerenes in Water. The First 10 Years of Their Chemistry, Biology, and Nanoscience. Acc Chem Res. 2003; 36:807–815. [PubMed: 14622027]

367. Xiao L, Aoshima H, Saitoh Y, Miwa N. Highly Hydroxylated Fullerene Localizes at the Cytoskeleton and Inhibits Oxidative Stress in Adipocytes and a Subcutaneous Adipose-Tissue Equivalent. Free Radic Biol Med. 2011; 51:1376–1389. [PubMed: 21684329]

368. Wall SB, Oh JY, Diers AR, Landar A. Oxidative Modification of Proteins: An Emerging Mechanism of Cell Signaling. Front Physiol. 2012; 3:369. [PubMed: 23049513]

369. Vasil'ev YV, Tzeng SC, Huang L, Maier CS. Protein Modifications by Electrophilic Lipoxidation Products: Adduct Formation, Chemical Strategies and Tandem Mass Spectrometry for Their Detection and Identification. Mass Spectrom Rev. 2014; 33:157–182. [PubMed: 24818247]

370. Wall SB, Smith MR, Ricart K, Zhou F, Vayalil PK, Oh JY, Landar A. Detection of Electrophile-Sensitive Proteins. Biochim Biophys Acta. 2014; 1840:913–922. [PubMed: 24021887]

371. Martinez B, Perez-Castillo A, Santos A. The Mitochondrial Respiratory Complex I Is a Target for 15-Deoxy-Delta12,14-Prostaglandin J2 Action. J Lipid Res. 2005; 46:736–743. [PubMed: 15654126]

372. Landar A, Shiva S, Levonen AL, Oh JY, Zaragoza C, Johnson MS, Darley-Usmar VM. Induction of the Permeability Transition and Cytochrome c Release by 15-Deoxy-Delta12,14-Prostaglandin J2 in Mitochondria. Biochem J. 2006; 394:185–195. [PubMed: 16268779]

373. Diers AR, Higdon AN, Ricart KC, Johnson MS, Agarwal A, Kalyanaraman B, Landar A, Darley-Usmar VM. Mitochondrial Targeting of the Electrophilic Lipid 15-Deoxy-Delta12,14-Prostaglandin J2 Increases Apoptotic Efficacy Via Redox Cell Signalling Mechanisms. Biochem J. 2010; 426:31–41. [PubMed: 19916962]

374. Landar A, Zmijewski JW, Dickinson DA, Le Goffe C, Johnson MS, Milne GL, Zanoni G, Vidari G, Morrow JD, Darley-Usmar VM. Interaction of Electrophilic Lipid Oxidation Products with Mitochondria in Endothelial Cells and Formation of Reactive Oxygen Species. Am J Physiol Heart Circ Physiol. 2006; 290:H1777–1787. [PubMed: 16387790]

375. Cernuda-Morollon E, Pineda-Molina E, Canada FJ, Perez-Sala D. 15-Deoxy-Delta 12,14-Prostaglandin J2 Inhibition of NF-kappaB-DNA Binding through Covalent Modification of the P50 Subunit. J Biol Chem. 2001; 276:35530–35536. [PubMed: 11466314]

376. Lin TK, Hughes G, Muratovska A, Blaikie FH, Brookes PS, Darley-Usmar V, Smith RA, Murphy MP. Specific Modification of Mitochondrial Protein Thiols in Response to Oxidative Stress: A Proteomics Approach. J Biol Chem. 2002; 277:17048–17056. [PubMed: 11861642]

377. Venkatraman A, Landar A, Davis AJ, Ulasova E, Page G, Murphy MP, Darley-Usmar V, Bailey SM. Oxidative Modification of Hepatic Mitochondria Protein Thiols: Effect of Chronic Alcohol Consumption. Am J Physiol Gastrointest Liver Physiol. 2004; 286:G521–527. [PubMed: 14670822]

378. Vayalil PK, Oh JY, Zhou F, Diers AR, Smith MR, Golzarian H, Oliver PG, Smith RA, Murphy MP, Velu SE, et al. A Novel Class of Mitochondria-Targeted Soft Electrophiles Modifies Mitochondrial Proteins and Inhibits Mitochondrial Metabolism in Breast Cancer Cells through Redox Mechanisms. PLoS One. 2015; 10:e0120460. [PubMed: 25785718]

379. Fox B, Schantz JT, Haigh R, Wood ME, Moore PK, Viner N, Spencer JP, Winyard PG, Whiteman M. Inducible Hydrogen Sulfide Synthesis in Chondrocytes and Mesenchymal Progenitor Cells: Is H2S a Novel Cytoprotective Mediator in the Inflamed Joint? J Cell Mol Med. 2012; 16:896–910. [PubMed: 21679296]

380. Le Trionnaire S, Perry A, Szczesny B, Szabo C, Winyard PG, Whatmore JL, Wood ME, Whiteman M. The Synthesis and Functional Evaluation of a Mitochondria-Targeted Hydrogen Sulfide Donor, (10-Oxo-10-(4-(3-Thioxo-3H-1,2-Dithiol-5-Yl)Phenoxy)Decyl)Triphenylphosphonium Bromide (AP39). Med Chem Comm. 2014; 5:728.

381. Szczesny B, Modis K, Yanagi K, Coletta C, Le Trionnaire S, Perry A, Wood ME, Whiteman M, Szabo C. AP39, a Novel Mitochondria-Targeted Hydrogen Sulfide Donor, Stimulates Cellular Bioenergetics, Exerts Cytoprotective Effects and Protects against the Loss of Mitochondrial DNA Integrity in Oxidatively Stressed Endothelial Cells in Vitro. Nitric Oxide. 2014; 41:120–130. [PubMed: 24755204]

382. Ahmad A, Olah G, Szczesny B, Wood ME, Whiteman M, Szabo C. AP39, a Mitochondrially Targeted Hydrogen Sulfide Donor, Exerts Protective Effects in Renal Epithelial Cells Subjected to Oxidative Stress in Vitro and in Acute Renal Injury in Vivo. Shock. 2016; 45:88–97. [PubMed: 26513708]

383. Ahmad A, Szabo C. Both the H2S Biosynthesis Inhibitor Aminooxyacetic Acid and the Mitochondrially Targeted H2S Donor AP39 Exert Protective Effects in a Mouse Model of Burn Injury. Pharmacol Res. 2016; 113:348–355. [PubMed: 27639598]

384. Gero D, Torregrossa R, Perry A, Waters A, Le-Trionnaire S, Whatmore JL, Wood M, Whiteman M. The Novel Mitochondria-Targeted Hydrogen Sulfide (H2S) Donors AP123 and AP39 Protect against Hyperglycemic Injury in Microvascular Endothelial Cells in Vitro. Pharmacol Res. 2016; 113:186–198. [PubMed: 27565382]

385. Ikeda K, Marutani E, Hirai S, Wood ME, Whiteman M, Ichinose F. Mitochondria-Targeted Hydrogen Sulfide Donor AP39 Improves Neurological Outcomes after Cardiac Arrest in Mice. Nitric Oxide. 2015; 49:90–96. [PubMed: 25960429]

386. Chatzianastasiou A, Bibli SI, Andreadou I, Efentakis P, Kaludercic N, Wood ME, Whiteman M, Di Lisa F, Daiber A, Manolopoulos VG, et al. Cardioprotection by H2S Donors: Nitric Oxide-Dependent and Independent Mechanisms. J Pharmacol Exp Ther. 2016; 358:431–440. [PubMed: 27342567]

387. Zhao Y, Biggs TD, Xian M. Hydrogen Sulfide (H2S) Releasing Agents: Chemistry and Biological Applications. Chem Commun (Camb). 2014; 50:11788–11805. [PubMed: 25019301]

388. Rochette L, Ghibu S, Muresan A, Vergely C. Alpha-Lipoic Acid: Molecular Mechanisms and Therapeutic Potential in Diabetes. Can J Physiol Pharmacol. 2015; 93:1021–1027. [PubMed: 26406389]

389. Ripcke J, Zarse K, Ristow M, Birringer M. Small-Molecule Targeting of the Mitochondrial Compartment with an Endogenously Cleaved Reversible Tag. Chem Bio Chem. 2009; 10:1689–1696.

390. Acosta MJ, Vazquez Fonseca L, Desbats MA, Cerqua C, Zordan R, Trevisson E, Salviati L. Coenzyme Q Biosynthesis in Health and Disease. Biochim Biophys Acta. 2016; 1857:1079–1085. [PubMed: 27060254]

391. Hargreaves IP. Coenzyme Q10 as a Therapy for Mitochondrial Disease. Int J Biochem Cell Biol. 2014; 49:105–111. [PubMed: 24495877]

392. Bentinger M, Brismar K, Dallner G. The Antioxidant Role of Coenzyme Q. Mitochondrion. 2007; (7 Suppl):S41–50. [PubMed: 17482888]

393. Anderson CM, Kazantzis M, Wang J, Venkatraman S, Goncalves RL, Quinlan CL, Ng R, Jastroch M, Benjamin DI, Nie B, et al. Dependence of Brown Adipose Tissue Function on CD36-Mediated Coenzyme Q Uptake. Cell Rep. 2015; 10:505–515. [PubMed: 25620701]

394. Maroz A, Anderson RF, Smith RA, Murphy MP. Reactivity of Ubiquinone and Ubiquinol with Superoxide and the Hydroperoxyl Radical: Implications for in Vivo Antioxidant Activity. Free Radic Biol Med. 2009; 46:105–109. [PubMed: 18977291]

395. Doughan AK, Dikalov SI. Mitochondrial Redox Cycling of Mitoquinone Leads to Superoxide Production and Cellular Apoptosis. Antioxid Redox Signal. 2007; 9:1825–1836. [PubMed: 17854275]

396. Roginsky VA, Tashlitsky VN, Skulachev VP. Chain-Breaking Antioxidant Activity of Reduced Forms of Mitochondria-Targeted Quinones, a Novel Type of Geroprotectors. Aging (Albany NY). 2009; 1:481–489. [PubMed: 20195487]

397. Genrikhs EE, Stelmashook EV, Popova OV, Kapay NA, Korshunova GA, Sumbatyan NV, Skrebitsky VG, Skulachev VP, Isaev NK. Mitochondria-Targeted Antioxidant SkQT1 Decreases Trauma-Induced Neurological Deficit in Rat and Prevents Amyloid-Beta-Induced Impairment of

Long-Term Potentiation in Rat Hippocampal Slices. J Drug Target. 2015; 23:347–352. [PubMed: 25585580]

398. Andreev-Andrievskiy AA, Kolosova NG, Stefanova NA, Lovat MV, Egorov MV, Manskikh VN, Zinovkin RA, Galkin, Prikhodko AS, Skulachev MV, et al. Efficacy of Mitochondrial Antioxidant Plastoquinonyl-Decyl-Triphenylphosphonium Bromide (SkQ1) in the Rat Model of Autoimmune Arthritis. Oxid Med Cell Longev. 2016; 2016:8703645. [PubMed: 27293517]
399. Yani E, Katargina L, Chesnokova N, Beznos O, Savchenko A, Vygodin V, Gudkova E, Zamyatnin A, Skulachev M. The First Experience of Using the Drug Vizomitin in the Treatment of Dry Eyes. Pract Med (Russ). 2012; 4:134–137.
400. Brzheskiy VV, Efimova EL, Vorontsova TN, Alekseev VN, Gusarevich OG, Shaidurova KN, Ryabtseva AA, Andryukhina OM, Kamenskikh TG, Sumarokova ES, et al. Results of a Multicenter, Randomized, Double-Masked, Placebo Controlled Clinical Study of the Efficacy and Safety of Visomitin Eye Drops in Patients with Dry Eye Syndrome. Adv Ther. 2015; 32:1263–1279. [PubMed: 26660938]
401. Petrov A, Perekhvatova N, Skulachev M, Stein L, Ousler G. SkQ1 Ophthalmic Solution for Dry Eye Treatment: Results of a Phase 2 Safety and Efficacy Clinical Study in the Environment and During Challenge in the Controlled Adverse Environment Model. Adv Ther. 2016; 33:96–115. [PubMed: 26733410]
402. Skulachev VP. What Is "Phenoptosis" and How to Fight It? Biochemistry (Mosc). 2012; 77:689–706. [PubMed: 22817532]
403. Wilcox CS. Effects of Tempol and Redox-Cycling Nitroxides in Models of Oxidative Stress. Pharmacol Ther. 2010; 126:119–145. [PubMed: 20153367]
404. Soule BP, Hyodo F, Matsumoto K, Simone NL, Cook JA, Krishna MC, Mitchell JB. The Chemistry and Biology of Nitroxide Compounds. Free Radic Biol Med. 2007; 42:1632–1650. [PubMed: 17462532]
405. Krishna MC, Samuni A, Taira J, Goldstein S, Mitchell JB, Russo A. Stimulation by Nitroxides of Catalase-Like Activity of Hemeproteins. Kinetics and Mechanism. J Biol Chem. 1996; 271:26018–26025. [PubMed: 8824241]
406. Samuni U, Czapski G, Goldstein S. Nitroxide Radicals as Research Tools: Elucidating the Kinetics and Mechanisms of Catalase-Like and "Suicide Inactivation" of Metmyoglobin. Biochim Biophys Acta. 2016; 1860:1409–1416. [PubMed: 27062906]
407. Kagan VE, Wipf P, Stoyanovsky D, Greenberger JS, Borisenko G, Belikova NA, Yanamala N, Samhan Arias AK, Tungekar MA, Jiang J, et al. Mitochondrial Targeting of Electron Scavenging Antioxidants: Regulation of Selective Oxidation vs Random Chain Reactions. Adv Drug Deliv Rev. 2009; 61:1375–1385. [PubMed: 19716396]
408. Cafiso DS, Hubbell WL. Estimation of Transmembrane Potentials from Phase Equilibriums of Hydrophobic Paramagnetic Ions. Biochemistry. 2002; 17:187–195.
409. Weinberg F, Hamanaka R, Wheaton WW, Weinberg S, Joseph J, Lopez M, Kalyanaraman B, Mutlu GM, Budinger GR, Chandel NS. Mitochondrial Metabolism and ROS Generation Are Essential for Kras-Mediated Tumorigenicity. Proc Natl Acad Sci U S A. 2010; 107:8788–8793. [PubMed: 20421486]
410. Mukhopadhyay P, Horvath B, Zsengeller Z, Batkai S, Cao Z, Kechrid M, Holovac E, Erdelyi K, Tanchian G, Liaudet L, et al. Mitochondrial Reactive Oxygen Species Generation Triggers Inflammatory Response and Tissue Injury Associated with Hepatic Ischemia-Reperfusion: Therapeutic Potential of Mitochondrially Targeted Antioxidants. Free Radic Biol Med. 2012; 53:1123–1138. [PubMed: 22683818]
411. Dikalova AE, Kirilyuk IA, Dikalov SI. Antihypertensive Effect of Mitochondria-Targeted Proxyl Nitroxides. Redox Biol. 2015; 4:355–362. [PubMed: 25677087]
412. Jiang J, Belikova NA, Hoye AT, Zhao Q, Epperly MW, Greenberger JS, Wipf P, Kagan VE. A Mitochondria-Targeted Nitroxide/Hemigramicidin S Conjugate Protects Mouse Embryonic Cells against Gamma Irradiation. Int J Radiat Oncol Biol Phys. 2008; 70:816–825. [PubMed: 18262096]
413. Shinde A, Berhane H, Rhieu BH, Kalash R, Xu K, Goff J, Epperly MW, Franicola D, Zhang X, Dixon T, et al. Intraoral Mitochondrial-Targeted Gs-Nitroxide, JP4-039, Radioprotects Normal

Tissue in Tumor-Bearing Radiosensitive Fancd2(-/-) (C57BL/6) Mice. Radiat Res. 2016; 185:134–150. [PubMed: 26789701]

414. Rajagopalan MS, Gupta K, Epperly MW, Franicola D, Zhang X, Wang H, Zhao H, Tyurin VA, Pierce JG, Kagan VE, et al. The Mitochondria-Targeted Nitroxide JP4-039 Augments Potentially Lethal Irradiation Damage Repair. In Vivo. 2009; 23:717–726. [PubMed: 19779106]
415. Rwigema JC, Beck B, Wang W, Doemling A, Epperly MW, Shields D, Goff JP, Franicola D, Dixon T, Frantz MC, et al. Two Strategies for the Development of Mitochondrion-Targeted Small Molecule Radiation Damage Mitigators. Int J Radiat Oncol Biol Phys. 2011; 80:860–868. [PubMed: 21493014]
416. Berhane H, Shinde A, Kalash R, Xu K, Epperly MW, Goff J, Franicola D, Zhang X, Dixon T, Shields D, et al. Amelioration of Radiation-Induced Oral Cavity Mucositis and Distant Bone Marrow Suppression in Fanconi Anemia Fancd2−/− (Fvb/N) Mice by Intraoral GS-nitroxide JP4-039. Radiat Res. 2014; 182:35–49. [PubMed: 24932534]
417. Krainz T, Gaschler MM, Lim C, Sacher JR, Stockwell BR, Wipf P. A Mitochondrial-Targeted Nitroxide Is a Potent Inhibitor of Ferroptosis. ACS Cent Sci. 2016; 2:653–659. [PubMed: 27725964]
418. Cafiso DS, Hubbell WL. Light-Induced Interfacial Potentials in Photoreceptor Membranes. Biophys J. 1980; 30:243–263. [PubMed: 6266528]
419. Jiang J, Stoyanovsky DA, Belikova NA, Tyurina YY, Zhao Q, Tungekar MA, Kapralova V, Huang Z, Mintz AH, Greenberger JS, et al. A Mitochondria-Targeted Triphenylphosphonium-Conjugated Nitroxide Functions as a Radioprotector/Mitigator. Radiat Res. 2009; 172:706–717. [PubMed: 19929417]
420. Dickey JS, Gonzalez Y, Aryal B, Mog S, Nakamura AJ, Redon CE, Baxa U, Rosen E, Cheng G, Zielonka J, et al. Mito-Tempol and Dexrazoxane Exhibit Cardioprotective and Chemotherapeutic Effects through Specific Protein Oxidation and Autophagy in a Syngeneic Breast Tumor Preclinical Model. PLoS One. 2013; 8:e70575. [PubMed: 23940596]
421. Huang Z, Jiang J, Belikova NA, Stoyanovsky DA, Kagan VE, Mintz AH. Protection of Normal Brain Cells from Gamma-Irradiation-Induced Apoptosis by a Mitochondria-Targeted Triphenyl-Phosphonium-Nitroxide: A Possible Utility in Glioblastoma Therapy. J Neurooncol. 2010; 100:1–8. [PubMed: 20835910]
422. Dikalova AE, Bikineyeva AT, Budzyn K, Nazarewicz RR, McCann L, Lewis W, Harrison DG, Dikalov SI. Therapeutic Targeting of Mitochondrial Superoxide in Hypertension. Circ Res. 2010; 107:106–116. [PubMed: 20448215]
423. Galli F, Azzi A, Birringer M, Cook-Mills JM, Eggersdorfer M, Frank J, Cruciani G, Lorkowski S, Ozer NK. Vitamin E: Emerging Aspects and New Directions. Free Radic Biol Med. 2017; 102:16–36. [PubMed: 27816611]
424. Jiang Q. Natural Forms of Vitamin E: Metabolism, Antioxidant, and Anti-Inflammatory Activities and Their Role in Disease Prevention and Therapy. Free Radic Biol Med. 2014; 72:76–90. [PubMed: 24704972]
425. Dhanasekaran A, Kotamraju S, Kalivendi SV, Matsunaga T, Shang T, Keszler A, Joseph J, Kalyanaraman B. Supplementation of Endothelial Cells with Mitochondria-Targeted Antioxidants Inhibit Peroxide-Induced Mitochondrial Iron Uptake, Oxidative Damage, and Apoptosis. J Biol Chem. 2004; 279:37575–37587. [PubMed: 15220329]
426. Dong LF, Jameson VJ, Tilly D, Cerny J, Mahdavian E, Marin-Hernandez A, Hernandez-Esquivel L, Rodriguez-Enriquez S, Stursa J, Witting PK, et al. Mitochondrial Targeting of Vitamin E Succinate Enhances Its Pro-Apoptotic and Anti-Cancer Activity Via Mitochondrial Complex II. J Biol Chem. 2011; 286:3717–3728. [PubMed: 21059645]
427. Dong LF, Jameson VJ, Tilly D, Prochazka L, Rohlena J, Valis K, Truksa J, Zobalova R, Mahdavian E, Kluckova K, et al. Mitochondrial Targeting of Alpha-Tocopheryl Succinate Enhances Its Pro-Apoptotic Efficacy: A New Paradigm for Effective Cancer Therapy. Free Radic Biol Med. 2011; 50:1546–1555. [PubMed: 21402148]
428. Rodriguez-Enriquez S, Hernandez-Esquivel L, Marin-Hernandez A, Dong LF, Akporiaye ET, Neuzil J, Ralph SJ, Moreno-Sanchez R. Molecular Mechanism for the Selective Impairment of Cancer Mitochondrial Function by a Mitochondrially Targeted Vitamin E Analogue. Biochim Biophys Acta. 2012; 1817:1597–1607. [PubMed: 22627082]

429. Rohlena J, Dong LF, Kluckova K, Zobalova R, Goodwin J, Tilly D, Stursa J, Pecinova A, Philimonenko A, Hozak P, et al. Mitochondrially Targeted Alpha Tocopheryl Succinate Is Antiangiogenic: Potential Benefit against Tumor Angiogenesis but Caution against Wound Healing. Antioxid Redox Signal. 2011; 15:2923–2935. [PubMed: 21902599]

430. Truksa J, Dong LF, Rohlena J, Stursa J, Vondrusova M, Goodwin J, Nguyen M, Kluckova K, Rychtarcikova Z, Lettlova S, et al. Mitochondrially Targeted Vitamin E Succinate Modulates Expression of Mitochondrial DNA Transcripts and Mitochondrial Biogenesis. Antioxid Redox Signal. 2015; 22:883–900. [PubMed: 25578105]

431. Prochazka L, Koudelka S, Dong LF, Stursa J, Goodwin J, Neca J, Slavik J, Ciganek M, Masek J, Kluckova K, et al. Mitochondrial Targeting Overcomes ABCA1-Dependent Resistance of Lung Carcinoma to Alpha-Tocopheryl Succinate. Apoptosis. 2013; 18:286–299. [PubMed: 23299931]

432. Cheng G, Zielonka J, McAllister DM, Mackinnon AC Jr, Joseph J, Dwinell MB, Kalyanaraman B. Mitochondria-Targeted Vitamin E Analogs Inhibit Breast Cancer Cell Energy Metabolism and Promote Cell Death. BMC Cancer. 2013; 13:285. [PubMed: 23764021]

433. Mossalam M, Soto J, Lim CS, Abel ED. Solid Phase Synthesis of Mitochondrial Triphenylphosphonium-Vitamin E Metabolite Using a Lysine Linker for Reversal of Oxidative Stress. PLoS One. 2013; 8:e53272. [PubMed: 23341934]

434. Jameson VJ, Cocheme HM, Logan A, Hanton LR, Smith RA, Murphy MP. Synthesis of Triphenylphosphonium Vitamin E Derivatives as Mitochondria-Targeted Antioxidants. Tetrahedron. 2015; 71:8444–8453. [PubMed: 26549895]

435. Goldgof M, Xiao C, Chanturiya T, Jou W, Gavrilova O, Reitman ML. The Chemical Uncoupler 2,4-Dinitrophenol (DNP) Protects against Diet-Induced Obesity and Improves Energy Homeostasis in Mice at Thermoneutrality. J Biol Chem. 2014; 289:19341–19350. [PubMed: 24872412]

436. Tseng YH, Cypess AM, Kahn CR. Cellular Bioenergetics as a Target for Obesity Therapy. Nat Rev Drug Discov. 2010; 9:465–482. [PubMed: 20514071]

437. Antonenko YN, Khailova LS, Knorre DA, Markova OV, Rokitskaya TI, Ilyasova TM, Severina, Kotova EA, Karavaeva YE, Prikhodko AS, et al. Penetrating Cations Enhance Uncoupling Activity of Anionic Protonophores in Mitochondria. PLoS One. 2013; 8:e61902. [PubMed: 23626747]

438. Severin FF, Severina, Antonenko YN, Rokitskaya TI, Cherepanov DA, Mokhova EN, Vyssokikh MY, Pustovidko AV, Markova OV, Yaguzhinsky LS, et al. Penetrating Cation/Fatty Acid Anion Pair as a Mitochondria-Targeted Protonophore. Proc Natl Acad Sci U S A. 2010; 107:663–668. [PubMed: 20080732]

439. Pustovidko AV, Rokitskaya TI, Severina, Simonyan RA, Trendeleva TA, Lyamzaev KG, Antonenko YN, Rogov AG, Zvyagilskaya RA, Skulachev VP, et al. Derivatives of the Cationic Plant Alkaloids Berberine and Palmatine Amplify Protonophorous Activity of Fatty Acids in Model Membranes and Mitochondria. Mitochondrion. 2013; 13:520–525. [PubMed: 23026390]

440. Kalinovich AV, Mattsson CL, Youssef MR, Petrovic N, Ost M, Skulachev VP, Shabalina IG. Mitochondria-Targeted Dodecyltriphenylphosphonium (C12TPP) Combats High-Fat-Diet-Induced Obesity in Mice. Int J Obes (Lond). 2016; 40:1864–1874. [PubMed: 27534841]

441. Blaikie FH, Brown SE, Samuelsson LM, Brand MD, Smith RA, Murphy MP. Targeting Dinitrophenol to Mitochondria: Limitations to the Development of a Self-Limiting Mitochondrial Protonophore. Biosci Rep. 2006; 26:231–243. [PubMed: 16850251]

442. McQuaker SJ, Quinlan CL, Caldwell ST, Brand MD, Hartley RC. A Prototypical Small-Molecule Modulator Uncouples Mitochondria in Response to Endogenous Hydrogen Peroxide Production. Chem Bio Chem. 2013; 14:993–1000.

443. Chalmers S, Caldwell ST, Quin C, Prime TA, James AM, Cairns AG, Murphy MP, McCarron JG, Hartley RC. Selective Uncoupling of Individual Mitochondria within a Cell Using a Mitochondria-Targeted Photoactivated Protonophore. J Am Chem Soc. 2012; 134:758–761. [PubMed: 22239373]

444. Denisov SS, Kotova EA, Plotnikov EY, Tikhonov AA, Zorov DB, Korshunova GA, Antonenko YN. A Mitochondria-Targeted Protonophoric Uncoupler Derived from Fluorescein. Chem Commun (Camb). 2014; 50:15366–15369. [PubMed: 25349923]

445. Shchepinova MM, Denisov SS, Kotova EA, Khailova LS, Knorre DA, Korshunova GA, Tashlitsky VN, Severin FF, Antonenko YN. Dodecyl and Octyl Esters of Fluorescein as Protonophores and Uncouplers of Oxidative Phosphorylation in Mitochondria at Submicromolar Concentrations. Biochim Biophys Acta. 2014; 1837:149–158. [PubMed: 24076107]

446. Antonenko YN, Denisov SS, Silachev DN, Khailova LS, Jankauskas SS, Rokitskaya TI, Danilina TI, Kotova EA, Korshunova GA, Plotnikov EY, et al. A Long-Linker Conjugate of Fluorescein and Triphenylphosphonium as Mitochondria-Targeted Uncoupler and Fluorescent Neuro- and Nephroprotector. Biochim Biophys Acta. 2016; 1860:2463–2473. [PubMed: 27450891]

447. Michelakis ED, Webster L, Mackey JR. Dichloroacetate (DCA) as a Potential Metabolic-Targeting Therapy for Cancer. Br J Cancer. 2008; 99:989–994. [PubMed: 18766181]

448. Kankotia S, Stacpoole PW. Dichloroacetate and Cancer: New Home for an Orphan Drug? Biochim Biophys Acta. 2014; 1846:617–629. [PubMed: 25157892]

449. Pathak RK, Marrache S, Harn DA, Dhar S. Mito-DCA: A Mitochondria Targeted Molecular Scaffold for Efficacious Delivery of Metabolic Modulator Dichloroacetate. ACS Chem Biol. 2014; 9:1178–1187. [PubMed: 24617941]

450. Miles JM, Rule AD, Borlaug BA. Use of Metformin in Diseases of Aging. Curr Diab Rep. 2014; 14:490. [PubMed: 24752835]

451. Emami Riedmaier A, Fisel P, Nies AT, Schaeffeler E, Schwab M. Metformin and Cancer: From the Old Medicine Cabinet to Pharmacological Pitfalls and Prospects. Trends Pharmacol Sci. 2013; 34:126–135. [PubMed: 23277337]

452. Pryor R, Cabreiro F. Repurposing Metformin: An Old Drug with New Tricks in Its Binding Pockets. Biochem J. 2015; 471:307–322. [PubMed: 26475449]

453. Jara JA, Lopez-Munoz R. Metformin and Cancer: Between the Bioenergetic Disturbances and the Antifolate Activity. Pharmacol Res. 2015; 101:102–108. [PubMed: 26277279]

454. Foretz M, Guigas B, Bertrand L, Pollak M, Viollet B. Metformin: From Mechanisms of Action to Therapies. Cell Metab. 2014; 20:953–966. [PubMed: 25456737]

455. Evans JM, Donnelly LA, Emslie-Smith AM, Alessi DR, Morris AD. Metformin and Reduced Risk of Cancer in Diabetic Patients. BMJ. 2005; 330:1304–1305. [PubMed: 15849206]

456. Gandini S, Puntoni M, Heckman-Stoddard BM, Dunn BK, Ford L, DeCensi A, Szabo E. Metformin and Cancer Risk and Mortality: A Systematic Review and Meta-Analysis Taking into Account Biases and Confounders. Cancer Prev Res (Phila). 2014; 7:867–885. [PubMed: 24985407]

457. Heckman-Stoddard BM, Gandini S, Puntoni M, Dunn BK, DeCensi A, Szabo E. Repurposing Old Drugs to Chemoprevention: The Case of Metformin. Semin Oncol. 2016; 43:123–133. [PubMed: 26970131]

458. Eurich DT, Weir DL, Majumdar SR, Tsuyuki RT, Johnson JA, Tjosvold L, Vanderloo SE, McAlister FA. Comparative Safety and Effectiveness of Metformin in Patients with Diabetes Mellitus and Heart Failure: Systematic Review of Observational Studies Involving 34,000 Patients. Circ Heart Fail. 2013; 6:395–402. [PubMed: 23508758]

459. Bridges HR, Jones AJ, Pollak MN, Hirst J. Effects of Metformin and Other Biguanides on Oxidative Phosphorylation in Mitochondria. Biochem J. 2014; 462:475–487. [PubMed: 25017630]

460. Liu X, Romero IL, Litchfield LM, Lengyel E, Locasale JW. Metformin Targets Central Carbon Metabolism and Reveals Mitochondrial Requirements in Human Cancers. Cell Metab. 2016; 24:728–739. [PubMed: 27746051]

461. Boukalova S, Stursa J, Werner L, Ezrova Z, Cerny J, Bezawork-Geleta A, Pecinova A, Dong L, Drahota Z, Neuzil J. Mitochondrial Targeting of Metformin Enhances Its Activity against Pancreatic Cancer. Mol Cancer Ther. 2016; 15:2875–2886. [PubMed: 27765848]

462. Pearl LH. Review: The Hsp90 Molecular Chaperone-an Enigmatic ATPase. Biopolymers. 2016; 105:594–607. [PubMed: 26991466]

463. Verma S, Goyal S, Jamal S, Singh A, Grover A. Hsp90: Friends, Clients and Natural Foes. Biochimie. 2016; 127:227–240. [PubMed: 27295069]

464. Garcia-Carbonero R, Carnero A, Paz-Ares L. Inhibition of Hsp90 Molecular Chaperones: Moving into the Clinic. Lancet Oncol. 2013; 14:e358–e369. [PubMed: 23896275]

465. Kang BH, Siegelin MD, Plescia J, Raskett CM, Garlick DS, Dohi T, Lian JB, Stein GS, Languino LR, Altieri DC. Preclinical Characterization of Mitochondria-Targeted Small Molecule Hsp90 Inhibitors, Gamitrinibs, in Advanced Prostate Cancer. Clin Cancer Res. 2010; 16:4779–4788. [PubMed: 20876793]

466. Amoroso MR, Matassa DS, Sisinni L, Lettini G, Landriscina M, Esposito F. TRAP1 Revisited: Novel Localizations and Functions of a 'Next-Generation' Biomarker (Review). Int J Oncol. 2014; 45:969–977. [PubMed: 24990602]

467. Lee C, Park HK, Jeong H, Lim J, Lee AJ, Cheon KY, Kim CS, Thomas AP, Bae B, Kim ND, et al. Development of a Mitochondria-Targeted Hsp90 Inhibitor Based on the Crystal Structures of Human TRAP1. J Am Chem Soc. 2015; 137:4358–4367. [PubMed: 25785725]

468. Gorlach S, Fichna J, Lewandowska U. Polyphenols as Mitochondria-Targeted Anticancer Drugs. Cancer Lett. 2015; 366:141–149. [PubMed: 26185003]

469. Sandoval-Acuna C, Ferreira J, Speisky H. Polyphenols and Mitochondria: An Update on Their Increasingly Emerging ROS-Scavenging Independent Actions. Arch Biochem Biophys. 2014; 559:75–90. [PubMed: 24875147]

470. Biasutto L, Mattarei A, Marotta E, Bradaschia A, Sassi N, Garbisa S, Zoratti M, Paradisi C. Development of Mitochondria-Targeted Derivatives of Resveratrol. Bioorg Med Chem Lett. 2008; 18:5594–5597. [PubMed: 18823777]

471. Sassi N, Mattarei A, Azzolini M, Bernardi P, Szabo I, Paradisi C, Zoratti M, Biasutto L. Mitochondria-Targeted Resveratrol Derivatives Act as Cytotoxic Pro-Oxidants. Curr Pharm Des. 2014; 20:172–179. [PubMed: 23701548]

472. Wang XX, Li YB, Yao HJ, Ju RJ, Zhang Y, Li RJ, Yu Y, Zhang L, Lu WL. The Use of Mitochondrial Targeting Resveratrol Liposomes Modified with a Dequalinium Polyethylene Glycol-Distearoylphosphatidyl Ethanolamine Conjugate to Induce Apoptosis in Resistant Lung Cancer Cells. Biomaterials. 2011; 32:5673–5687. [PubMed: 21550109]

473. Mattarei A, Biasutto L, Marotta E, De Marchi U, Sassi N, Garbisa S, Zoratti M, Paradisi C. A Mitochondriotropic Derivative of Quercetin: A Strategy to Increase the Effectiveness of Polyphenols. Chem Bio Chem. 2008; 9:2633–2642.

474. Biasutto L, Sassi N, Mattarei A, Marotta E, Cattelan P, Toninello A, Garbisa S, Zoratti M, Paradisi C. Impact of Mitochondriotropic Quercetin Derivatives on Mitochondria. Biochim Biophys Acta. 2010; 1797:189–196. [PubMed: 19835835]

475. Mattarei A, Sassi N, Durante C, Biasutto L, Sandonà G, Marotta E, Garbisa S, Gennaro A, Paradisi C, Zoratti M. Redox Properties and Cytotoxicity of Synthetic Isomeric Mitochondriotropic Derivatives of the Natural Polyphenol Quercetin. European J Org Chem. 2011; 2011:5577–5586.

476. Sassi N, Biasutto L, Mattarei A, Carraro M, Giorgio V, Citta A, Bernardi P, Garbisa S, Szabo I, Paradisi C, et al. Cytotoxicity of a Mitochondriotropic Quercetin Derivative: Mechanisms. Biochim Biophys Acta. 2012; 1817:1095–1106. [PubMed: 22433608]

477. Reddy CA, Somepalli V, Golakoti T, Kanugula AK, Karnewar S, Rajendiran K, Vasagiri N, Prabhakar S, Kuppusamy P, Kotamraju S, et al. Mitochondrial-Targeted Curcuminoids: A Strategy to Enhance Bioavailability and Anticancer Efficacy of Curcumin. PLoS One. 2014; 9:e89351. [PubMed: 24622734]

478. Banik B, Somyajit K, Nagaraju G, Chakravarty AR. Oxovanadium(IV) Complexes of Curcumin for Cellular Imaging and Mitochondria Targeted Photocytotoxicity. Dalton Trans. 2014; 43:13358–13369. [PubMed: 25069796]

479. Madar I, Anderson JH, Szabo Z, Scheffel U, Kao PF, Ravert HT, Dannals RF. Enhanced Uptake of [11C]TPMP in Canine Brain Tumor: A PET Study. J Nucl Med. 1999; 40:1180–1185. [PubMed: 10405140]

480. Rodriguez-Cuenca S, Cocheme HM, Logan A, Abakumova I, Prime TA, Rose C, Vidal-Puig A, Smith AC, Rubinsztein DC, Fearnley IM, et al. Consequences of Long-Term Oral Administration of the Mitochondria-Targeted Antioxidant MitoQ to Wild-Type Mice. Free Radic Biol Med. 2010; 48:161–172. [PubMed: 19854266]

481. Madar I, Weiss L, Izbicki G. Preferential Accumulation of 3H-Tetraphenylphosphonium in Non-Small Cell Lung Carcinoma in Mice: Comparison with 99mtc-Mibi. J Nucl Med. 2002; 43:234–238. [PubMed: 11850490]

482. Swed A, Eyal S, Madar I, Zohar-Kontante H, Weiss L, Hoffman A. The Role of P-Glycoprotein in Intestinal Transport Versus the BBB Transport of Tetraphenylphosphonium. Mol Pharm. 2009; 6:1883–1890. [PubMed: 19722701]

483. Madar I, Ravert HT, Du Y, Hilton J, Volokh L, Dannals RF, Frost JJ, Hare JM. Characterization of Uptake of the New PET Imaging Compound 18F-Fluorobenzyl Triphenyl Phosphonium in Dog Myocardium. J Nucl Med. 2006; 47:1359–1366. [PubMed: 16883017]

484. Madar I, Ravert H, Nelkin B, Abro M, Pomper M, Dannals R, Frost JJ. Characterization of Membrane Potential-Dependent Uptake of the Novel PET Tracer 18F-Fluorobenzyl Triphenylphosphonium Cation. Eur J Nucl Med Mol Imaging. 2007; 34:2057–2065. [PubMed: 17786439]

485. Shoup TM, Elmaleh DR, Brownell AL, Zhu A, Guerrero JL, Fischman AJ. Evaluation of (4-[18F]Fluorophenyl)Triphenylphosphonium Ion. A Potential Myocardial Blood Flow Agent for PET. Mol Imaging Biol. 2011; 13:511–517. [PubMed: 20563755]

486. Porteous CM, Logan A, Evans C, Ledgerwood EC, Menon DK, Aigbirhio F, Smith RA, Murphy MP. Rapid Uptake of Lipophilic Triphenylphosphonium Cations by Mitochondria in Vivo Following Intravenous Injection: Implications for Mitochondria-Specific Therapies and Probes. Biochim Biophys Acta. 2010; 1800:1009–1017. [PubMed: 20621583]

487. Gane EJ, Weilert F, Orr DW, Keogh GF, Gibson M, Lockhart MM, Frampton CM, Taylor KM, Smith RA, Murphy MP. The Mitochondria-Targeted Anti-Oxidant Mitoquinone Decreases Liver Damage in a Phase II Study of Hepatitis C Patients. Liver Int. 2010; 30:1019–1026. [PubMed: 20492507]

488. Snow BJ, Rolfe FL, Lockhart MM, Frampton CM, O'Sullivan JD, Fung V, Smith RA, Murphy MP, Taylor KM. Protect Study G. A Double-Blind, Placebo-Controlled Study to Assess the Mitochondria-Targeted Antioxidant MitoQ as a Disease-Modifying Therapy in Parkinson's Disease. Mov Disord. 2010; 25:1670–1674. [PubMed: 20568096]

489. Prah D, Paulson E, Wagner-Schuman M, Zielonka J, Lopez M, Hardy M, Joseph J, Kalyanaraman B, Schmainda K. In Vivo Mitochondrial Labeling Using Mito-Carboxy Proxyl (Mito-CP) Enhanced Magnetic Resonance Imaging. Proc Intl Soc Mag Reson Med. 2008; 16:1690.

490. Mukhopadhyay P, Horvath B, Zsengeller Z, Zielonka J, Tanchian G, Holovac E, Kechrid M, Patel V, Stillman IE, Parikh SM, et al. Mitochondrial-Targeted Antioxidants Represent a Promising Approach for Prevention of Cisplatin-Induced Nephropathy. Free Radic Biol Med. 2012; 52:497–506. [PubMed: 22120494]

491. Smith RAJ, Murphy MP. Animal and Human Studies with the Mitochondria-Targeted Antioxidant MitoQ. Ann N Y Acad Sci. 2010; 1201:96–103. [PubMed: 20649545]

492. Lowes DA, Thottakam BM, Webster NR, Murphy MP, Galley HF. The Mitochondria-Targeted Antioxidant MitoQ Protects against Organ Damage in a Lipopolysaccharide-Peptidoglycan Model of Sepsis. Free Radic Biol Med. 2008; 45:1559–1565. [PubMed: 18845241]

493. Dranka BP, Gifford A, McAllister D, Zielonka J, Joseph J, O'Hara CL, Stucky CL, Kanthasamy AG, Kalyanaraman B. A Novel Mitochondrially-Targeted Apocynin Derivative Prevents Hyposmia and Loss of Motor Function in the Leucine-Rich Repeat Kinase 2 (LRRK2(R1441g)) Transgenic Mouse Model of Parkinson's Disease. Neurosci Lett. 2014; 583:159–164. [PubMed: 25263790]

494. Langley M, Ghosh A, Charli A, Sarkar S, Ay M, Luo J, Zielonka J, Brenza T, Bennett B, Jin H, et al. Mito-Apocynin Prevents Mitochondrial Dysfunction, Microglial Activation, Oxidative Damage, and Progressive Neurodegeneration in Mitopark Transgenic Mice. Antioxid Redox Signal. 2017; doi: 10.1089/ars.2016.6905

495. Ghosh A, Langley MR, Harischandra DS, Neal ML, Jin H, Anantharam V, Joseph J, Brenza T, Narasimhan B, Kanthasamy A, et al. Mitoapocynin Treatment Protects against Neuroinflammation and Dopaminergic Neurodegeneration in a Preclinical Animal Model of Parkinson's Disease. J Neuroimmune Pharmacol. 2016; 11:259–278. [PubMed: 26838361]

496. Bernal SD, Lampidis TJ, McIsaac RM, Chen LB. Anticarcinoma Activity in Vivo of Rhodamine 123, a Mitochondrial-Specific Dye. Science. 1983; 222:169–172. [PubMed: 6623064]

497. Manetta A, Gamboa G, Nasseri A, Podnos YD, Emma D, Dorion G, Rawlings L, Carpenter PM, Bustamante A, Patel J, et al. Novel Phosphonium Salts Display in Vitro and in Vivo Cytotoxic Activity against Human Ovarian Cancer Cell Lines. Gynecol Oncol. 1996; 60:203–212. [PubMed: 8631539]

498. Ward PS, Thompson CB. Metabolic Reprogramming: A Cancer Hallmark Even Warburg Did Not Anticipate. Cancer Cell. 2012; 21:297–308. [PubMed: 22439925]

499. Liberti MV, Locasale JW. The Warburg Effect: How Does It Benefit Cancer Cells? Trends Biochem Sci. 2016; 41:211–218. [PubMed: 26778478]

500. Pavlova NN, Thompson CB. The Emerging Hallmarks of Cancer Metabolism. Cell Metab. 2016; 23:27–47. [PubMed: 26771115]

501. DeBerardinis RJ, Chandel NS. Fundamentals of Cancer Metabolism. Sci Adv. 2016; 2:e1600200. [PubMed: 27386546]

502. Vyas S, Zaganjor E, Haigis MC. Mitochondria and Cancer. Cell. 2016; 166:555–566. [PubMed: 27471965]

503. Zong WX, Rabinowitz JD, White E. Mitochondria and Cancer. Mol Cell. 2016; 61:667–676. [PubMed: 26942671]

504. Weinberg SE, Chandel NS. Targeting Mitochondria Metabolism for Cancer Therapy. Nat Chem Biol. 2015; 11:9–15. [PubMed: 25517383]

505. Sullivan LB, Chandel NS. Mitochondrial Reactive Oxygen Species and Cancer. Cancer Metab. 2014; 2:17. [PubMed: 25671107]

506. Diebold L, Chandel NS. Mitochondrial ROS Regulation of Proliferating Cells. Free Radic Biol Med. 2016; 100:86–93. [PubMed: 27154978]

507. Zhang YK, Wang YJ, Gupta P, Chen ZS. Multidrug Resistance Proteins (MRPs) and Cancer Therapy. AAPS J. 2015; 17:802–812. [PubMed: 25840885]

508. Deeley RG, Westlake C, Cole SP. Transmembrane Transport of Endo- and Xenobiotics by Mammalian ATP-Binding Cassette Multidrug Resistance Proteins. Physiol Rev. 2006; 86:849–899. [PubMed: 16816140]

509. Porteous CM, Menon DK, Aigbirhio FI, Smith RA, Murphy MP. P-Glycoprotein (Mdr1a/1b) and Breast Cancer Resistance Protein (Bcrp) Decrease the Uptake of Hydrophobic Alkyl Triphenylphosphonium Cations by the Brain. Biochim Biophys Acta. 2013; 1830:3458–3465. [PubMed: 23454352]

510. Fetisova EK, Antoschina MM, Cherepanynets VD, Izumov DS, Kireev II, Kireev RI, Lyamzaev KG, Riabchenko NI, Chernyak BV, Skulachev VP. Radioprotective Effects of Mitochondria-Targeted Antioxidant SkQR1. Radiat Res. 2015; 183:64–71. [PubMed: 25496313]

511. Fetisova EK, Antoschina MM, Cherepanynets VD, Izumov DS, Kireev II, Kireev RI, Lyamzaev KG, Riabchenko NI, Chernyak BV, Skulachev VP. Mitochondria-Targeted Antioxidant SkQR1 Selectively Protects MDR-Negative Cells from Ionizing Radiation. Cell Tiss Biol. 2015; 9:87–95.

512. Agapova LS, Chernyak BV, Domnina LV, Dugina VB, Efimenko AY, Fetisova EK, Ivanova OY, Kalinina NI, Khromova NV, Kopnin BP, et al. Mitochondria-Targeted Plastoquinone Derivatives as Tools to Interrupt Execution of the Aging Program. 3. Inhibitory Effect of SkQ1 on Tumor Development from P53-Deficient Cells. Biochemistry (Mosc). 2008; 73:1300–1316. [PubMed: 19120016]

513. Fetisova EK, Avetisian AV, Iziumov DS, Korotetskaia MV, Tashlitskii VN, Skulachev VP, Cherniak BV. Multidrug Resistance P-Glycoprotein Inhibits the Antiapoptotic Action of Mitochondria-Targeted Antioxidant SkQR1. Tsitologiia. 2011; 53:488–497. [PubMed: 21870505]

514. Zhou Y, Tozzi F, Chen J, Fan F, Xia L, Wang J, Gao G, Zhang A, Xia X, Brasher H, et al. Intracellular ATP Levels Are a Pivotal Determinant of Chemoresistance in Colon Cancer Cells. Cancer Res. 2012; 72:304–314. [PubMed: 22084398]

515. Han M, Vakili MR, Soleymani Abyaneh H, Molavi O, Lai R, Lavasanifar A. Mitochondrial Delivery of Doxorubicin Via Triphenylphosphine Modification for Overcoming Drug Resistance in MDA-MB-435/DOX Cells. Mol Pharm. 2014; 11:2640–2649. [PubMed: 24811541]

516. Solomon MA, Shah AA, D'Souza GG. In Vitro Assessment of the Utility of Stearyl Triphenyl Phosphonium Modified Liposomes in Overcoming the Resistance of Ovarian Carcinoma Ovcar-3 Cells to Paclitaxel. Mitochondrion. 2013; 13:464–472. [PubMed: 23123917]
517. Nakazawa MS, Keith B, Simon MC. Oxygen Availability and Metabolic Adaptations. Nat Rev Cancer. 2016; 16:663–673. [PubMed: 27658636]
518. Denko NC. Hypoxia, HIF1 and Glucose Metabolism in the Solid Tumour. Nat Rev Cancer. 2008; 8:705–713. [PubMed: 19143055]
519. Yeom CJ, Goto Y, Zhu Y, Hiraoka M, Harada H. Microenvironments and Cellular Characteristics in the Micro Tumor Cords of Malignant Solid Tumors. Int J Mol Sci. 2012; 13:13949–13965. [PubMed: 23203043]
520. Raghunand N, Gatenby RA, Gillies RJ. Microenvironmental and Cellular Consequences of Altered Blood Flow in Tumours. Br J Radiol. 2003; 76(Spec No 1):S11–22. [PubMed: 15456710]
521. Rideout DC, Calogeropoulou T, Jaworski JS, Dagnino R Jr, McCarthy MR. Phosphonium Salts Exhibiting Selective Anti-Carcinoma Activity in Vitro. Anticancer Drug Des. 1989; 4:265–280. [PubMed: 2619865]
522. Rideout D, Bustamante A, Patel J. Mechanism of Inhibition of FaDu Hypopharyngeal Carcinoma Cell Growth by Tetraphenylphosphonium Chloride. Int J Cancer. 1994; 57:247–253. [PubMed: 8157363]
523. Wang F, Ogasawara MA, Huang P. Small Mitochondria-Targeting Molecules as Anti-Cancer Agents. Mol Aspects Med. 2010; 31:75–92. [PubMed: 19995573]
524. Lampidis TJ, Hasin Y, Weiss MJ, Chen LB. Selective Killing of Carcinoma Cells "in Vitro" by Lipophilic-Cationic Compounds: A Cellular Basis. Biomed Pharmacother. 1985; 39:220–226. [PubMed: 3936557]
525. Modica-Napolitano JS, Aprille JR. Delocalized Lipophilic Cations Selectively Target the Mitochondria of Carcinoma Cells. Adv Drug Deliv Rev. 2001; 49:63–70. [PubMed: 11377803]
526. Summerhayes IC, Lampidis TJ, Bernal SD, Nadakavukaren JJ, Nadakavukaren KK, Shepherd EL, Chen LB. Unusual Retention of Rhodamine 123 by Mitochondria in Muscle and Carcinoma Cells. Proc Natl Acad Sci U S A. 1982; 79:5292–5296. [PubMed: 6752944]
527. Nadakavukaren KK, Nadakavukaren JJ, Chen LB. Increased Rhodamine 123 Uptake by Carcinoma Cells. Cancer Res. 1985; 45:6093–6099. [PubMed: 4063967]
528. Christman JE, Miller DS, Coward P, Smith LH, Teng NN. Study of the Selective Cytotoxic Properties of Cationic, Lipophilic Mitochondrial-Specific Compounds in Gynecologic Malignancies. Gynecol Oncol. 1990; 39:72–79. [PubMed: 2227576]
529. Beckman WC Jr, Powers SK, Brown JT, Gillespie GY, Bigner DD, Camps JL Jr. Differential Retention of Rhodamine 123 by Avian Sarcoma Virus-Induced Glioma and Normal Brain Tissue of the Rat in Vivo. Cancer. 1987; 59:266–270. [PubMed: 3026604]
530. Lampidis TJ, Bernal SD, Summerhayes IC, Chen LB. Selective Toxicity of Rhodamine 123 in Carcinoma Cells in Vitro. Cancer Res. 1983; 43:716–720. [PubMed: 6848187]
531. Bernal SD, Lampidis TJ, Summerhayes IC, Chen LB. Rhodamine-123 Selectively Reduces Clonal Growth of Carcinoma Cells in Vitro. Science. 1982; 218:1117–1119. [PubMed: 7146897]
532. Sehy DW, Shao LE, Rideout D, Yu J. Sensitivity of Committed Hematopoietic Progenitor Cells in Vitro (BFU-E, CFU-E, CFU-GM) and Two Human Carcinoma Cell Lines toward Rhodamine-123 and Phosphonium Salt II-41. Leuk Res. 1993; 17:247–253. [PubMed: 8450673]
533. Lampidis TJ, Salet C, Moreno G, Chen LB. Effects of the Mitochondrial Probe Rhodamine 123 and Related Analogs on the Function and Viability of Pulsating Myocardial Cells in Culture. Agents Actions. 1984; 14:751–757. [PubMed: 6475672]
534. Higuti T, Niimi S, Saito R, Nakasima S, Ohe T, Tani I, Yoshimura T. Rhodamine 6G, Inhibitor of Both H+-Ejections from Mitochondria Energized with ATP and with Respiratory Substrates. Biochim Biophys Acta. 1980; 593:463–467. [PubMed: 7236646]
535. Sun X, Wong JR, Song K, Hu J, Garlid KD, Chen LB. AA1, a Newly Synthesized Monovalent Lipophilic Cation, Expresses Potent in Vivo Antitumor Activity. Cancer Res. 1994; 54:1465–1471. [PubMed: 8137249]

536. Emaus RK, Grunwald R, Lemasters JJ. Rhodamine 123 as a Probe of Transmembrane Potential in Isolated Rat-Liver Mitochondria: Spectral and Metabolic Properties. Biochim Biophys Acta. 1986; 850:436–448. [PubMed: 2873836]

537. Modica-Napolitano JS, Weiss MJ, Chen LB, Aprille JR. Rhodamine 123 Inhibits Bioenergetic Function in Isolated Rat Liver Mitochondria. Biochem Biophys Res Commun. 1984; 118:717–723. [PubMed: 6200108]

538. ModicaNapolitano JS, Koya K, Weisberg E, Brunelli BT, Li Y, Chen LB. Selective Damage to Carcinoma Mitochondria by the Rhodacyanine MKT-077. Cancer Res. 1996; 56:544–550. [PubMed: 8564969]

539. Koya K, Li Y, Wang H, Ukai T, Tatsuta N, Kawakami M, Shishido, Chen LB. MKT-077, a Novel Rhodacyanine Dye in Clinical Trials, Exhibits Anticarcinoma Activity in Preclinical Studies Based on Selective Mitochondrial Accumulation. Cancer Res. 1996; 56:538–543. [PubMed: 8564968]

540. Weisberg EL, Koya K, Modica-Napolitano J, Li Y, Chen LB. In Vivo Administration of MKT-077 Causes Partial yet Reversible Impairment of Mitochondrial Function. Cancer Res. 1996; 56:551–555. [PubMed: 8564970]

541. Bleday R, Weiss MJ, Salem RR, Wilson RE, Chen LB, Steele G Jr. Inhibition of Rat Colon Tumor Isograft Growth with Dequalinium Chloride. Arch Surg. 1986; 121:1272–1275. [PubMed: 3778199]

542. Anderson WM, Patheja HS, Delinck DL, Baldwin WW, Smiley ST, Chen LB. Inhibition of Bovine Heart Mitochondrial and Paracoccus Denitrificans NADH-Ubiquinone Reductase by Dequalinium Chloride and Three Structurally Related Quinolinium Compounds. Biochem Int. 1989; 19:673–685. [PubMed: 2515858]

543. Anderson WM, Delinck DL, Benninger L, Wood JM, Smiley ST, Chen LB. Cytotoxic Effect of Thiacarbocyanine Dyes on Human Colon Carcinoma Cells and Inhibition of Bovine Heart Mitochondrial NADH-Ubiquinone Reductase Activity Via a Rotenone-Type Mechanism by Two of the Dyes. Biochem Pharmacol. 1993; 45:691–696. [PubMed: 8442768]

544. Fantin VR, Berardi MJ, Scorrano L, Korsmeyer SJ, Leder P. A Novel Mitochondriotoxic Small Molecule That Selectively Inhibits Tumor Cell Growth. Cancer Cell. 2002; 2:29–42. [PubMed: 12150823]

545. He H, Li DW, Yang LY, Fu L, Zhu XJ, Wong WK, Jiang FL, Liu Y. A Novel Bifunctional Mitochondria-Targeted Anticancer Agent with High Selectivity for Cancer Cells. Sci Rep. 2015; 5:13543. [PubMed: 26337336]

546. Millard M, Pathania D, Shabaik Y, Taheri L, Deng J, Neamati N. Preclinical Evaluation of Novel Triphenylphosphonium Salts with Broad-Spectrum Activity. PLoS One. 2010; 5:e13131. [PubMed: 20957228]

547. Reily C, Mitchell T, Chacko BK, Benavides G, Murphy MP, Darley-Usmar V. Mitochondrially Targeted Compounds and Their Impact on Cellular Bioenergetics. Redox Biol. 2013; 1:86–93. [PubMed: 23667828]

548. Ju J, Picinich SC, Yang Z, Zhao Y, Suh N, Kong AN, Yang CS. Cancer-Preventive Activities of Tocopherols and Tocotrienols. Carcinogenesis. 2010; 31:533–542. [PubMed: 19748925]

549. Anso E, Mullen AR, Felsher DW, Mates JM, Deberardinis RJ, Chandel NS. Metabolic Changes in Cancer Cells Upon Suppression of MYC. Cancer Metab. 2013; 1:7. [PubMed: 24280108]

550. Yan B, Stantic M, Zobalova R, Bezawork-Geleta A, Stapelberg M, Stursa J, Prokopova K, Dong L, Neuzil J. Mitochondrially Targeted Vitamin E Succinate Efficiently Kills Breast Tumour-Initiating Cells in a Complex II-Dependent Manner. BMC Cancer. 2015; 15:401. [PubMed: 25967547]

551. Kovarova J, Bajzikova M, Vondrusova M, Stursa J, Goodwin J, Nguyen M, Zobalova R, Pesdar EA, Truksa J, Tomasetti M, et al. Mitochondrial Targeting of Alpha-Tocopheryl Succinate Enhances Its Anti-Mesothelioma Efficacy. Redox Rep. 2014; 19:16–25. [PubMed: 24225203]

552. Wang ZD, Wei SQ, Wang QY. Targeting Oncogenic Kras in Non-Small Cell Lung Cancer Cells by Phenformin Inhibits Growth and Angiogenesis. Am J Cancer Res. 2015; 5:3339–3349. [PubMed: 26807315]

553. Caraci F, Chisari M, Frasca G, Chiechio S, Salomone S, Pinto A, Sortino MA, Bianchi A. Effects of Phenformin on the Proliferation of Human Tumor Cell Lines. Life Sci. 2003; 74:643–650. [PubMed: 14623034]

554. Jiang W, Finniss S, Cazacu S, Xiang C, Brodie Z, Mikkelsen T, Poisson L, Shackelford DB, Brodie C. Repurposing Phenformin for the Targeting of Glioma Stem Cells and the Treatment of Glioblastoma. Oncotarget. 2016; 7:56456–56470. [PubMed: 27486821]

555. Kwong SC, Brubacher J. Phenformin and Lactic Acidosis: A Case Report and Review. J Emerg Med. 1998; 16:881–886. [PubMed: 9848705]

556. Dykens JA, Jamieson J, Marroquin L, Nadanaciva S, Billis PA, Will Y. Biguanide-Induced Mitochondrial Dysfunction Yields Increased Lactate Production and Cytotoxicity of Aerobically-Poised HepG2 Cells and Human Hepatocytes in Vitro. Toxicol Appl Pharmacol. 2008; 233:203–210. [PubMed: 18817800]

557. Wheaton WW, Weinberg SE, Hamanaka RB, Soberanes S, Sullivan LB, Anso E, Glasauer A, Dufour E, Mutlu GM, Budigner GS, et al. Metformin Inhibits Mitochondrial Complex I of Cancer Cells to Reduce Tumorigenesis. Elife. 2014; 3:e02242. [PubMed: 24843020]

558. Brand MD. Mitochondrial Generation of Superoxide and Hydrogen Peroxide as the Source of Mitochondrial Redox Signaling. Free Radic Biol Med. 2016; 100:14–31. [PubMed: 27085844]

559. Tormos KV, Anso E, Hamanaka RB, Eisenbart J, Joseph J, Kalyanaraman B, Chandel NS. Mitochondrial Complex III ROS Regulate Adipocyte Differentiation. Cell Metab. 2011; 14:537–544. [PubMed: 21982713]

560. Starenki D, Park JI. Mitochondria-Targeted Nitroxide, Mito-CP, Suppresses Medullary Thyroid Carcinoma Cell Survival in Vitro and in Vivo. J Clin Endocrinol Metab. 2013; 98:1529–1540. [PubMed: 23509102]

561. Cunniff B, Benson K, Stumpff J, Newick K, Held P, Taatjes D, Joseph J, Kalyanaraman B, Heintz NH. Mitochondrial-Targeted Nitroxides Disrupt Mitochondrial Architecture and Inhibit Expression of Peroxiredoxin 3 and FOXM1 in Malignant Mesothelioma Cells. J Cell Physiol. 2013; 228:835–845. [PubMed: 23018647]

562. Kang BH. TRAP1 Regulation of Mitochondrial Life or Death Decision in Cancer Cells and Mitochondria-Targeted TRAP1 Inhibitors. BMB Rep. 2012; 45:1–6. [PubMed: 22281005]

563. Fulda S. Betulinic Acid for Cancer Treatment and Prevention. Int J Mol Sci. 2008; 9:1096–1107. [PubMed: 19325847]

564. Fulda S, Scaffidi C, Susin SA, Krammer PH, Kroemer G, Peter ME, Debatin KM. Activation of Mitochondria and Release of Mitochondrial Apoptogenic Factors by Betulinic Acid. J Biol Chem. 1998; 273:33942–33948. [PubMed: 9852046]

565. Spivak AY, Nedopekina DA, Shakurova ER, Khalitova RR, Gubaidullin RR, Odinokov VN, Dzhemilev UM, Bel'skii YP, Bel'skaya NV, Stankevich SA, et al. Synthesis of Lupane Triterpenoids with Triphenylphosphonium Substituents and Studies of Their Antitumor Activity. Russ Chem Bull, Int Ed. 2014; 62:188–198.

566. Strobykina IY, Belenok MG, Semenova MN, Semenov VV, Babaev VM, Rizvanov I, Mironov VF, Kataev VE. Triphenylphosphonium Cations of the Diterpenoid Isosteviol: Synthesis and Antimitotic Activity in a Sea Urchin Embryo Model. J Nat Prod. 2015; 78:1300–1308. [PubMed: 26042548]

567. Weissig V. Mitochondria-Specific Nanocarriers for Improving the Proapoptotic Activity of Small Molecules. Methods Enzymol. 2012; 508:131–155. [PubMed: 22449924]

568. Boddapati SV, D'Souza GG, Erdogan S, Torchilin VP, Weissig V. Organelle-Targeted Nanocarriers: Specific Delivery of Liposomal Ceramide to Mitochondria Enhances Its Cytotoxicity in Vitro and in Vivo. Nano Lett. 2008; 8:2559–2563. [PubMed: 18611058]

569. Marrache S, Dhar S. The Energy Blocker inside the Power House: Mitochondria Targeted Delivery of 3-Bromopyruvate. Chem Sci. 2015; 6:1832–1845. [PubMed: 25709804]

570. Kumar BS, Raghuvanshi DS, Hasanain M, Alam S, Sarkar J, Mitra K, Khan F, Negi AS. Recent Advances in Chemistry and Pharmacology of 2-Methoxyestradiol: An Anticancer Investigational Drug. Steroids. 2016; 110:9–34. [PubMed: 27020471]

571. Zhang Y, Hu Z, Xu G, Gao C, Wu Ra, Zou H. Elevating Mitochondrial Reactive Oxygen Species by Mitochondria-Targeted Inhibition of Superoxide Dismutase with a Mesoporous Silica Nanocarrier for Cancer Therapy. Nano Res. 2014; 7:1103–1115.

572. Hickey JL, Ruhayel RA, Barnard PJ, Baker MV, Berners-Price SJ, Filipovska A. Mitochondria-Targeted Chemotherapeutics: The Rational Design of Gold(I) N-Heterocyclic Carbene Complexes That Are Selectively Toxic to Cancer Cells and Target Protein Selenols in Preference to Thiols. J Am Chem Soc. 2008; 130:12570–12571. [PubMed: 18729360]

573. Malhi SS, Budhiraja A, Arora S, Chaudhari KR, Nepali K, Kumar R, Sohi H, Murthy RS. Intracellular Delivery of Redox Cycler-Doxorubicin to the Mitochondria of Cancer Cell by Folate Receptor Targeted Mitocancerotropic Liposomes. Int J Pharm. 2012; 432:63–74. [PubMed: 22531856]

574. Theodossiou TA, Sideratou Z, Katsarou ME, Tsiourvas D. Mitochondrial Delivery of Doxorubicin by Triphenylphosphonium-Functionalized Hyperbranched Nanocarriers Results in Rapid and Severe Cytotoxicity. Pharm Res. 2013; 30:2832–2842. [PubMed: 23921486]

575. Qu Q, Ma X, Zhao Y. Targeted Delivery of Doxorubicin to Mitochondria Using Mesoporous Silica Nanoparticle Nanocarriers. Nanoscale. 2015; 7:16677–16686. [PubMed: 26400067]

576. Cho DY, Cho H, Kwon K, Yu M, Lee E, Huh KM, Lee DH, Kang HC. Triphenylphosphonium-Conjugated Poly(ε-caprolactone)-Based Self-Assembled Nanostructures as Nanosized Drugs and Drug Delivery Carriers for Mitochondria-Targeting Synergistic Anticancer Drug Delivery. Adv Funct Mater. 2015; 25:5479–5491.

577. Wang Y, Wang B, Liao H, Song X, Wu H, Wang H, Shen H, Ma X, Tan M. Liposomal Nanohybrid Cerasomes for Mitochondria-Targeted Drug Delivery. J Mater Chem B. 2015; 3:7291–7299.

578. Kulkarni PS, Haldar MK, Confeld MI, Langaas CJ, Yang X, Qian SY, Mallik S. Mitochondria-Targeted Fluorescent Polymersomes for Drug Delivery to Cancer Cells. Polym Chem. 2016; 7:4151–4154. [PubMed: 27833665]

579. Alexeyev M, Shokolenko I, Wilson G, LeDoux S. The Maintenance of Mitochondrial DNA Integrity - Critical Analysis and Update. Cold Spring Harb Perspect Biol. 2013; 5:a012641. [PubMed: 23637283]

580. Wisnovsky SP, Wilson JJ, Radford RJ, Pereira MP, Chan MR, Laposa RR, Lippard SJ, Kelley SO. Targeting Mitochondrial DNA with a Platinum-Based Anticancer Agent. Chem Biol. 2013; 20:1323–1328. [PubMed: 24183971]

581. Marrache S, Pathak RK, Dhar S. Detouring of Cisplatin to Access Mitochondrial Genome for Overcoming Resistance. Proc Natl Acad Sci U S A. 2014; 111:10444–10449. [PubMed: 25002500]

582. Fonseca SB, Pereira MP, Mourtada R, Gronda M, Horton KL, Hurren R, Minden MD, Schimmer AD, Kelley SO. Rerouting Chlorambucil to Mitochondria Combats Drug Deactivation and Resistance in Cancer Cells. Chem Biol. 2011; 18:445–453. [PubMed: 21513881]

583. Jean SR, Pereira MP, Kelley SO. Structural Modifications of Mitochondria-Targeted Chlorambucil Alter Cell Death Mechanism but Preserve MDR Evasion. Mol Pharm. 2014; 11:2675–2682. [PubMed: 24922525]

584. Millard M, Gallagher JD, Olenyuk BZ, Neamati N. A Selective Mitochondrial-Targeted Chlorambucil with Remarkable Cytotoxicity in Breast and Pancreatic Cancers. J Med Chem. 2013; 56:9170–9179. [PubMed: 24147900]

585. Mourtada R, Fonseca SB, Wisnovsky SP, Pereira MP, Wang X, Hurren R, Parfitt J, Larsen L, Smith RA, Murphy MP, et al. Re-Directing an Alkylating Agent to Mitochondria Alters Drug Target and Cell Death Mechanism. PLoS One. 2013; 8:e60253. [PubMed: 23585833]

586. Biswas S, Dodwadkar NS, Sawant RR, Koshkaryev A, Torchilin VP. Surface Modification of Liposomes with Rhodamine-123-Conjugated Polymer Results in Enhanced Mitochondrial Targeting. J Drug Target. 2011; 19:552–561. [PubMed: 21348804]

587. Xie C, Chang J, Hao XD, Yu JM, Liu HR, Sun X. Mitochondrial-Targeted Prodrug Cancer Therapy Using a Rhodamine B Labeled Fluorinated Docetaxel. Eur J Pharm Biopharm. 2013; 85:541–549. [PubMed: 23791719]

588. Durand RE, Biaglow JE. Radiosensitization of Hypoxic Cells of an in Vitro Tumor Model by Respiratory Inhibitors. Radiat Res. 1977; 69:359–366. [PubMed: 14354]

589. Lin A, Maity A. Molecular Pathways: A Novel Approach to Targeting Hypoxia and Improving Radiotherapy Efficacy Via Reduction in Oxygen Demand. Clin Cancer Res. 2015; 21:1995–2000. [PubMed: 25934887]

590. Zhang X, Zhou X, Chen R, Zhang H. Radiosensitization by Inhibiting Complex I Activity in Human Hepatoma HepG2 Cells to X-Ray Radiation. J Radiat Res. 2012; 53:257–263. [PubMed: 22510598]

591. Kim EH, Kim MS, Furusawa Y, Uzawa A, Han S, Jung WG, Sai S. Metformin Enhances the Radiosensitivity of Human Liver Cancer Cells to Gamma-Rays and Carbon Ion Beams. Oncotarget. 2016; 7:80568–80578. [PubMed: 27802188]

592. Song CW, Lee H, Dings RP, Williams B, Powers J, Santos TD, Choi BH, Park HJ. Metformin Kills and Radiosensitizes Cancer Cells and Preferentially Kills Cancer Stem Cells. Sci Rep. 2012; 2:362. [PubMed: 22500211]

593. Fasih A, Elbaz HA, Huttemann M, Konski AA, Zielske SP. Radiosensitization of Pancreatic Cancer Cells by Metformin through the AMPK Pathway. Radiat Res. 2014; 182:50–59. [PubMed: 24909911]

594. Wang Z, Lai ST, Ma NY, Deng Y, Liu Y, Wei DP, Zhao JD, Jiang GL. Radiosensitization of Metformin in Pancreatic Cancer Cells Via Abrogating the G2 Checkpoint and Inhibiting DNA Damage Repair. Cancer Lett. 2015; 369:192–201. [PubMed: 26304716]

595. Yang Y, Pan W, Zhang S, Cao Y, Cheng H, Chen J, Sun X. Metformin Can Enhance the Radiosensitivity of Cholangiocarcinoma through AMPK-FOXO3a Axis. Int J Clin Exp Med. 2016; 9:13539–13550.

596. Sanli T, Rashid A, Liu C, Harding S, Bristow RG, Cutz JC, Singh G, Wright J, Tsakiridis T. Ionizing Radiation Activates AMP-Activated Kinase (AMPK): A Target for Radiosensitization of Human Cancer Cells. Int J Radiat Oncol Biol Phys. 2010; 78:221–229. [PubMed: 20615625]

597. Maachani UB, Shankavaram U, Kramp T, Tofilon PJ, Camphausen K, Tandle AT. FOXM1 and STAT3 Interaction Confers Radioresistance in Glioblastoma Cells. Oncotarget. 2016; 7:77365–77377. [PubMed: 27764801]

598. Nagel R, Stigter-van Walsum M, Buijze M, van den Berg J, van der Meulen IH, Hodzic J, Piersma SR, Pham TV, Jimenez CR, van Beusechem VW, et al. Genome-Wide Sirna Screen Identifies the Radiosensitizing Effect of Downregulation of MASTL and FOXM1 in NSCLC. Mol Cancer Ther. 2015; 14:1434–1444. [PubMed: 25808837]

599. Chunta JL, Vistisen KS, Yazdi Z, Braun RD. Uptake Rate of Cationic Mitochondrial Inhibitor MKT-077 Determines Cellular Oxygen Consumption Change in Carcinoma Cells. PLoS One. 2012; 7:e37471. [PubMed: 22616013]

600. Chilakamarthi U, Giribabu L. Photodynamic Therapy: Past, Present and Future. Chem Rec. 2017; n/a-n/a. doi: 10.1002/tcr.201600121

601. Morgan J, Oseroff AR. Mitochondria-Based Photodynamic Anti-Cancer Therapy. Adv Drug Deliv Rev. 2001; 49:71–86. [PubMed: 11377804]

602. Sibrian-Vazquez M, Nesterova IV, Jensen TJ, Vicente MG. Mitochondria Targeting by Guanidine- and Biguanidine-Porphyrin Photosensitizers. Bioconjug Chem. 2008; 19:705–713. [PubMed: 18269224]

603. Lei W, Xie J, Hou Y, Jiang G, Zhang H, Wang P, Wang X, Zhang B. Mitochondria-Targeting Properties and Photodynamic Activities of Porphyrin Derivatives Bearing Cationic Pendant. J Photochem Photobiol B. 2010; 98:167–171. [PubMed: 20060312]

604. Han K, Lei Q, Wang SB, Hu JJ, Qiu WX, Zhu JY, Yin WN, Luo X, Zhang XZ. Dual-Stage-Light-Guided Tumor Inhibition by Mitochondria-Targeted Photodynamic Therapy. Adv Funct Mater. 2015; 25:2961–2971.

605. Han K, Zhu JY, Jia HZ, Wang SB, Li SY, Zhang XZ, Han HY. Mitochondria-Targeted Chimeric Peptide for Trinitarian Overcoming of Drug Resistance. ACS Appl Mater Interfaces. 2016; 8:25060–25068. [PubMed: 27595983]

606. Wang XH, Peng HS, Yang W, Ren ZD, Liu YA. Mitochondria-Targeted Theranostic Nanoparticles For optical Sensing of Oxygen, Photodynamic Cancer Therapy, and Assessment of Therapeutic Efficacy. Microchim Acta. 2016; 183:2723–2731.

607. Ge Y, Weng X, Tian T, Ding F, Huang R, Yuan L, Wu J, Wang T, Guo P, Zhou X. A Mitochondria-Targeted Zinc(II) Phthalocyanine for Photodynamic Therapy. RSC Adv. 2013; 3:12839.

608. Marrache S, Tundup S, Harn DA, Dhar S. Ex Vivo Programming of Dendritic Cells by Mitochondria-Targeted Nanoparticles to Produce Interferon-Gamma for Cancer Immunotherapy. ACS Nano. 2013; 7:7392–7402. [PubMed: 23899410]

609. Marrache S, Tundup S, Harn DA, Dhar S. Ex Vivo Generation of Functional Immune Cells by Mitochondria-Targeted Photosensitization of Cancer Cells. Methods Mol Biol. 2015; 1265:113–122. [PubMed: 25634271]

610. Guo F, Yu M, Wang J, Tan F, Li N. The Mitochondria-Targeted and IR780-Regulated Theranosomes for Imaging and Enhanced Photodynamic/Photothermal Therapy. RSC Adv. 2016; 6:11070–11076.

611. Lv W, Zhang Z, Zhang KY, Yang H, Liu S, Xu A, Guo S, Zhao Q, Huang W. A Mitochondria-Targeted Photosensitizer Showing Improved Photodynamic Therapy Effects under Hypoxia. Angew Chem Int Ed Engl. 2016; 55:9947–9951. [PubMed: 27381490]

612. Liu J, Chen Y, Li G, Zhang P, Jin C, Zeng L, Ji L, Chao H. Ruthenium(II) Polypyridyl Complexes as Mitochondria-Targeted Two-Photon Photodynamic Anticancer Agents. Biomaterials. 2015; 56:140–153. [PubMed: 25934287]

613. Luo S, Tan X, Fang S, Wang Y, Liu T, Wang X, Yuan Y, Sun H, Qi Q, Shi C. Mitochondria-Targeted Small-Molecule Fluorophores for Dual Modal Cancer Phototherapy. Adv Funct Mater. 2016; 26:2826–2835.

614. Chennoufi R, Bougherara H, Gagey-Eilstein N, Dumat B, Henry E, Subra F, Bury-Mone S, Mahuteau-Betzer F, Tauc P, Teulade-Fichou MP, et al. Mitochondria-Targeted Triphenylamine Derivatives Activatable by Two-Photon Excitation for Triggering and Imaging Cell Apoptosis. Sci Rep. 2016; 6:21458. [PubMed: 26947258]

615. Zhang X, Ai F, Sun T, Wang F, Zhu G. Multimodal Upconversion Nanoplatform with a Mitochondria-Targeted Property for Improved Photodynamic Therapy of Cancer Cells. Inorg Chem. 2016; 55:3872–3880. [PubMed: 27049165]

616. Curigliano G, Mayer EL, Burstein HJ, Winer EP, Goldhirsch A. Cardiac Toxicity from Systemic Cancer Therapy: A Comprehensive Review. Prog Cardiovasc Dis. 2010; 53:94–104. [PubMed: 20728696]

617. Sioka C, Kyritsis AP. Central and Peripheral Nervous System Toxicity of Common Chemotherapeutic Agents. Cancer Chemother Pharmacol. 2009; 63:761–767. [PubMed: 19034447]

618. Perazella MA, Moeckel GW. Nephrotoxicity from Chemotherapeutic Agents: Clinical Manifestations, Pathobiology, and Prevention/Therapy. Semin Nephrol. 2010; 30:570–581. [PubMed: 21146122]

619. Liu H, Hu YP, Savaraj N, Priebe W, Lampidis TJ. Hypersensitization of Tumor Cells to Glycolytic Inhibitors. Biochemistry. 2001; 40:5542–5547. [PubMed: 11331019]

620. Dilip A, Cheng G, Joseph J, Kunnimalaiyaan S, Kalyanaraman B, Kunnimalaiyaan M, Gamblin TC. Mitochondria-Targeted Antioxidant and Glycolysis Inhibition: Synergistic Therapy in Hepatocellular Carcinoma. Anticancer Drugs. 2013; 24:881–888. [PubMed: 23872912]

621. Cheng G, Lopez M, Zielonka J, Hauser AD, Joseph J, McAllister D, Rowe JJ, Sugg SL, Williams CL, Kalyanaraman B. Mitochondria-Targeted Nitroxides Exacerbate Fluvastatin-Mediated Cytostatic and Cytotoxic Effects in Breast Cancer Cells. Cancer Biol Ther. 2011; 12:707–717. [PubMed: 21799303]

622. Modica-Napolitano JS, Nalbandian R, Kidd ME, Nalbandian A, Nguyen CC. The Selective in Vitro Cytotoxicity of Carcinoma Cells by AZT Is Enhanced by Concurrent Treatment with Delocalized Lipophilic Cations. Cancer Lett. 2003; 198:59–68. [PubMed: 12893431]

623. Tacar O, Sriamornsak P, Dass CR. Doxorubicin: An Update on Anticancer Molecular Action, Toxicity and Novel Drug Delivery Systems. J Pharm Pharmacol. 2013; 65:157–170. [PubMed: 23278683]

624. Meredith AM, Dass CR. Increasing Role of the Cancer Chemotherapeutic Doxorubicin in Cellular Metabolism. J Pharm Pharmacol. 2016; 68:729–741. [PubMed: 26989862]

625. Minotti G, Menna P, Salvatorelli E, Cairo G, Gianni L. Anthracyclines: Molecular Advances and Pharmacologic Developments in Antitumor Activity and Cardiotoxicity. Pharmacol Rev. 2004; 56:185–229. [PubMed: 15169927]

626. Hortobagyi GN. Anthracyclines in the Treatment of Cancer. An Overview. Drugs. 1997; 54(Suppl 4):1–7.

627. Lipshultz SE. Exposure to Anthracyclines During Childhood Causes Cardiac Injury. Semin Oncol. 2006; 33:S8–14.

628. Bryant J, Picot J, Levitt G, Sullivan I, Baxter L, Clegg A. Cardioprotection against the Toxic Effects of Anthracyclines Given to Children with Cancer: A Systematic Review. Health Technol Assess. 2007; 11:102.

629. Lipshultz SE, Lipsitz SR, Sallan SE, Dalton VM, Mone SM, Gelber RD, Colan SD. Chronic Progressive Cardiac Dysfunction Years after Doxorubicin Therapy for Childhood Acute Lymphoblastic Leukemia. J Clin Oncol. 2005; 23:2629–2636. [PubMed: 15837978]

630. Octavia Y, Tocchetti CG, Gabrielson KL, Janssens S, Crijns HJ, Moens AL. Doxorubicin-Induced Cardiomyopathy: From Molecular Mechanisms to Therapeutic Strategies. J Mol Cell Cardiol. 2012; 52:1213–1225. [PubMed: 22465037]

631. Chatterjee K, Zhang J, Honbo N, Karliner JS. Doxorubicin Cardiomyopathy. Cardiology. 2010; 115:155–162. [PubMed: 20016174]

632. Wallace KB. Doxorubicin-Induced Cardiac Mitochondrionopathy. Pharmacol Toxicol. 2003; 93:105–115. [PubMed: 12969434]

633. Conklin KA. Coenzyme Q10 for Prevention of Anthracycline-Induced Cardiotoxicity. Integr Cancer Ther. 2005; 4:110–130. [PubMed: 15911925]

634. Simunek T, Sterba M, Popelova O, Adamcova M, Hrdina R, Gersl V. Anthracycline-Induced Cardiotoxicity: Overview of Studies Examining the Roles of Oxidative Stress and Free Cellular Iron. Pharmacol Rep. 2009; 61:154–171. [PubMed: 19307704]

635. Varga ZV, Ferdinandy P, Liaudet L, Pacher P. Drug-Induced Mitochondrial Dysfunction and Cardiotoxicity. Am J Physiol Heart Circ Physiol. 2015; 309:H1453–1467. [PubMed: 26386112]

636. Carvalho FS, Burgeiro A, Garcia R, Moreno AJ, Carvalho RA, Oliveira PJ. Doxorubicin-Induced Cardiotoxicity: From Bioenergetic Failure and Cell Death to Cardiomyopathy. Med Res Rev. 2014; 34:106–135. [PubMed: 23494977]

637. Chandran K, Aggarwal D, Migrino RQ, Joseph J, McAllister D, Konorev EA, Antholine WE, Zielonka J, Srinivasan S, Avadhani NG, et al. Doxorubicin Inactivates Myocardial Cytochrome c Oxidase in Rats: Cardioprotection by Mito-Q. Biophys J. 2009; 96:1388–1398. [PubMed: 19217856]

638. Kalivendi SV, Konorev EA, Cunningham S, Vanamala SK, Kaji EH, Joseph J, Kalyanaraman B. Doxorubicin Activates Nuclear Factor of Activated T-Lymphocytes and Fas Ligand Transcription: Role of Mitochondrial Reactive Oxygen Species and Calcium. Biochem J. 2005; 389:527–539. [PubMed: 15799720]

639. Zhang D, Li J, Wang F, Hu J, Wang S, Sun Y. 2-Deoxy-D-Glucose Targeting of Glucose Metabolism in Cancer Cells as a Potential Therapy. Cancer Lett. 2014; 355:176–183. [PubMed: 25218591]

640. Schibler J, Tomanek-Chalkley AM, Reedy JL, Zhan F, Spitz DR, Schultz MK, Goel A. Mitochondrial-Targeted Decyl-Triphenylphosphonium Enhances 2-Deoxy-D-Glucose Mediated Oxidative Stress and Clonogenic Killing of Multiple Myeloma Cells. PLoS One. 2016; 11:e0167323. [PubMed: 27902770]

641. Cheng G, Zielonka J, McAllister D, Tsai S, Dwinell MB, Kalyanaraman B. Profiling and Targeting of Cellular Bioenergetics: Inhibition of Pancreatic Cancer Cell Proliferation. Br J Cancer. 2014; 111:85–93. [PubMed: 24867695]

642. Ghigo A, Li M, Hirsch E. New Signal Transduction Paradigms in Anthracycline-Induced Cardiotoxicity. Biochim Biophys Acta. 2016; 1863:1916–1925. [PubMed: 26828775]

643. Gratia S, Kay L, Potenza L, Seffouh A, Novel-Chate V, Schnebelen C, Sestili P, Schlattner U, Tokarska-Schlattner M. Inhibition of AMPK Signalling by Doxorubicin: At the Crossroads of the Cardiac Responses to Energetic, Oxidative, and Genotoxic Stress. Cardiovasc Res. 2012; 95:290–299. [PubMed: 22461523]

644. Dasari S, Tchounwou PB. Cisplatin in Cancer Therapy: Molecular Mechanisms of Action. Eur J Pharmacol. 2014; 740:364–378. [PubMed: 25058905]

645. Florea AM, Büsselberg D. Cisplatin as an Anti-Tumor Drug: Cellular Mechanisms of Activity, Drug Resistance and Induced Side Effects. Cancers (Basel). 2011; 3:1351. [PubMed: 24212665]

646. Ozkok A, Edelstein CL. Pathophysiology of Cisplatin-Induced Acute Kidney Injury. Bio Med Res Int. 2014; 2014:967826.

647. Peres LA, da Cunha AD Jr. Acute Nephrotoxicity of Cisplatin: Molecular Mechanisms. J Bras Nefrol. 2013; 35:332–340. [PubMed: 24402113]

648. Henchcliffe C, Beal MF. Mitochondrial Biology and Oxidative Stress in Parkinson Disease Pathogenesis. Nat Clin Pract Neurol. 2008; 4:600–609. [PubMed: 18978800]

649. Gandhi S, Abramov AY. Mechanism of Oxidative Stress in Neurodegeneration. Oxid Med Cell Longev. 2012; 2012:428010. [PubMed: 22685618]

650. Kumar H, Lim HW, More SV, Kim BW, Koppula S, Kim IS, Choi DK. The Role of Free Radicals in the Aging Brain and Parkinson's Disease: Convergence and Parallelism. Int J Mol Sci. 2012; 13:10478–10504. [PubMed: 22949875]

651. Alexander GE. Biology of Parkinson's Disease: Pathogenesis and Pathophysiology of a Multisystem Neurodegenerative Disorder. Dialogues Clin Neurosci. 2004; 6:259–280. [PubMed: 22033559]

652. Dias V, Junn E, Mouradian MM. The Role of Oxidative Stress in Parkinson's Disease. J Parkinsons Dis. 2013; 3:461–491. [PubMed: 24252804]

653. Athauda D, Foltynie T. The Ongoing Pursuit of Neuroprotective Therapies in Parkinson Disease. Nat Rev Neurol. 2015; 11:25–40. [PubMed: 25447485]

654. Mounsey RB, Teismann P. Chelators in the Treatment of Iron Accumulation in Parkinson's Disease. Int J Cell Biol. 2012; 2012:983245. [PubMed: 22754573]

655. Devos D, Moreau C, Devedjian JC, Kluza J, Petrault M, Laloux C, Jonneaux A, Ryckewaert G, Garcon G, Rouaix N, et al. Targeting Chelatable Iron as a Therapeutic Modality in Parkinson's Disease. Antioxid Redox Signal. 2014; 21:195–210. [PubMed: 24251381]

656. Ghosh A, Chandran K, Kalivendi SV, Joseph J, Antholine WE, Hillard CJ, Kanthasamy A, Kanthasamy A, Kalyanaraman B. Neuroprotection by a Mitochondria-Targeted Drug in a Parkinson's Disease Model. Free Radic Biol Med. 2010; 49:1674–1684. [PubMed: 20828611]

657. Wang Q, Qian L, Chen SH, Chu CH, Wilson B, Oyarzabal E, Ali S, Robinson B, Rao D, Hong JS. Post-Treatment with an Ultra-Low Dose of NADPH Oxidase Inhibitor Diphenyleneiodonium Attenuates Disease Progression in Multiple Parkinson's Disease Models. Brain. 2015; 138:1247–1262. [PubMed: 25716193]

658. Qian L, Gao X, Pei Z, Wu X, Block M, Wilson B, Hong JS, Flood PM. NADPH Oxidase Inhibitor DPI Is Neuroprotective at Femtomolar Concentrations through Inhibition of Microglia over-Activation. Parkinsonism Relat Disord. 2007; 13:S316–S320. [PubMed: 18267257]

659. Block ML, Zecca L, Hong JS. Microglia-Mediated Neurotoxicity: Uncovering the Molecular Mechanisms. Nat Rev Neurosci. 2007; 8:57–69. [PubMed: 17180163]

660. Qian L, Flood PM. Microglial Cells and Parkinson's Disease. Immunol Res. 2008; 41:155–164. [PubMed: 18512160]

661. Lull ME, Block ML. Microglial Activation and Chronic Neurodegeneration. Neurotherapeutics. 2010; 7:354–365. [PubMed: 20880500]

662. Nayernia Z, Jaquet V, Krause KH. New Insights on Nox Enzymes in the Central Nervous System. Antioxid Redox Signal. 2014; 20:2815–2837. [PubMed: 24206089]

663. Peterson LJ, Flood PM. Oxidative Stress and Microglial Cells in Parkinson's Disease. Mediators Inflamm. 2012; 2012:401264. [PubMed: 22544998]

664. Heumuller S, Wind S, Barbosa-Sicard E, Schmidt HH, Busse R, Schroder K, Brandes RP. Apocynin Is Not an Inhibitor of Vascular NADPH Oxidases but an Antioxidant. Hypertension. 2008; 51:211–217. [PubMed: 18086956]

665. Simons JM, t Hart BA, Ip Vai Ching TRAM, Van Dijk H, Labadie RP. Metabolic Activation of Natural Phenols into Selective Oxidative Burst Agonists by Activated Human Neutrophils. Free Radic Biol Med. 1990; 8:251–258. [PubMed: 2160411]

666. Dranka BP, Gifford A, Ghosh A, Zielonka J, Joseph J, Kanthasamy AG, Kalyanaraman B. Diapocynin Prevents Early Parkinson's Disease Symptoms in the Leucine-Rich Repeat Kinase 2 (LRRK2(R1441g)) Transgenic Mouse. Neurosci Lett. 2013; 549:57–62. [PubMed: 23721786]

667. Ghosh A, Kanthasamy A, Joseph J, Anantharam V, Srivastava P, Dranka BP, Kalyanaraman B, Kanthasamy AG. Anti-Inflammatory and Neuroprotective Effects of an Orally Active Apocynin Derivative in Pre-Clinical Models of Parkinson's Disease. J Neuroinflammation. 2012; 9:241. [PubMed: 23092448]

668. t Hart BA, Copray S, Philippens I. Apocynin, a Low Molecular Oral Treatment for Neurodegenerative Disease. Bio Med Res Int. 2014; 2014:298020.

669. Brenza TM, Ghaisas S, Ramirez JEV, Harischandra D, Anantharam V, Kalyanaraman B, Kanthasamy AG, Narasimhan B. Neuronal Protection against Oxidative Insult by Polyanhydride Nanoparticle-Based Mitochondria-Targeted Antioxidant Therapy. Nanomedicine. 2017; 13:809–820. [PubMed: 27771430]

670. Bushong, SC., Clarke, G. Magnetic Resonance Imaging: Physical and Biological Principles. 4. Elsevier Mosby; St. Louis, MO, USA: 2015.

671. Jaklovsky, J. NMR Imaging: A Comprehensive Bibliography. Addison-Wesley; Reading, PA, USA: 1983.

672. Davis RM, Mitchell JB, Krishna MC. Nitroxides as Cancer Imaging Agents. Anticancer Agents Med Chem. 2011; 11:347–358. [PubMed: 21434855]

673. Keana JF, Pou S. Nitroxide-Doped Liposomes Containing Entrapped Oxidant: An Approach to the "Reduction Problem" of Nitroxides as MRI Contrast Agents. Physiol Chem Phys Med NMR. 1985; 17:235–240. [PubMed: 3001795]

674. Hyodo F, Chuang KH, Goloshevsky AG, Sulima A, Griffiths GL, Mitchell JB, Koretsky AP, Krishna MC. Brain Redox Imaging Using Blood-Brain Barrier-Permeable Nitroxide MRI Contrast Agent. J Cereb Blood Flow Metab. 2008; 28:1165–1174. [PubMed: 18270519]

675. Hyodo F, Matsumoto K, Matsumoto A, Mitchell JB, Krishna MC. Probing the Intracellular Redox Status of Tumors with Magnetic Resonance Imaging and Redox-Sensitive Contrast Agents. Cancer Res. 2006; 66:9921–9928. [PubMed: 17047054]

676. Matsumoto K, Hyodo F, Anzai K, Utsumi H, Mitchell JB, Krishna MC. Brain Redox Imaging. Methods Mol Biol. 2011; 711:397–419. [PubMed: 21279614]

677. Matsumoto K, Hyodo F, Matsumoto A, Koretsky AP, Sowers AL, Mitchell JB, Krishna MC. High-Resolution Mapping of Tumor Redox Status by Magnetic Resonance Imaging Using Nitroxides as Redox-Sensitive Contrast Agents. Clin Cancer Res. 2006; 12:2455–2462. [PubMed: 16638852]

678. Prah D, Paulson E, Zielonka J, Hardy M, Joseph J, Kalyanaraman B, Schmainda K. In Vitro Mitochondrial Labeling Using Mito-Carboxy Proxyl (Mito-CP) Enhanced Magnetic Resonance Imaging. Proc Intl Soc Mag Reson Med. 2007; 15:1162.

679. Kalyanaraman, B., Joseph, J., Schmainda, KM., Prah, DE., Lopez, M., Hardy, MJ. In Vivo Mitochondrial Labeling Using Positively-Charged Nitroxide Enhanced and Gadolinum Chelate Enhanced Magnetic Resonance Imaging. Patent US. 8388936. 2013.

680. Lopez M, Prah DE, Hardy MJ, Zielonka J, Paulson ES, Schmainda KM, Joseph J, Kalyanaraman B. Mitochondria-Targeted Nitroxides as MRI Contrast Agents and Chemotherapeutics. Free Radic Biol Med. 2008; 45:S55–S55.

681. Davis RM, Matsumoto S, Bernardo M, Sowers A, Matsumoto K, Krishna MC, Mitchell JB. Magnetic Resonance Imaging of Organic Contrast Agents in Mice: Capturing the Whole-Body Redox Landscape. Free Radic Biol Med. 2011; 50:459–468. [PubMed: 21130158]

682. Hyodo F, Soule BP, Matsumoto K, Matusmoto S, Cook JA, Hyodo E, Sowers AL, Krishna MC, Mitchell JB. Assessment of Tissue Redox Status Using Metabolic Responsive Contrast Agents

and Magnetic Resonance Imaging. J Pharm Pharmacol. 2008; 60:1049–1060. [PubMed: 18644197]

683. Hahn SM, Krishna MC, DeLuca AM, Coffin D, Mitchell JB. Evaluation of the Hydroxylamine Tempol-H as an in Vivo Radioprotector. Free Radic Biol Med. 2000; 28:953–958. [PubMed: 10802227]
684. Kuppusamy P, Chzhan M, Wang P, Zweier JL. Three-Dimensional Gated EPR Imaging of the Beating Heart: Time-Resolved Measurements of Free Radical Distribution During the Cardiac Contractile Cycle. Magn Reson Med. 1996; 35:323–328. [PubMed: 8699943]
685. Kuppusamy P, Li H, Ilangovan G, Cardounel AJ, Zweier JL, Yamada K, Krishna MC, Mitchell JB. Noninvasive Imaging of Tumor Redox Status and Its Modification by Tissue Glutathione Levels. Cancer Res. 2002; 62:307–312. [PubMed: 11782393]
686. Bakalova R, Georgieva E, Ivanova D, Zhelev Z, Aoki I, Saga T. Magnetic Resonance Imaging of Mitochondrial Dysfunction and Metabolic Activity, Accompanied by Overproduction of Superoxide. ACS Chem Neurosci. 2015; 6:1922–1929. [PubMed: 26367059]
687. Zhelev Z, Bakalova R, Aoki I, Lazarova D, Saga T. Imaging of Superoxide Generation in the Dopaminergic Area of the Brain in Parkinson's Disease, Using Mito-Tempo. ACS Chem Neurosci. 2013; 4:1439–1445. [PubMed: 24024751]
688. Zhou Z, Lu ZR. Gadolinium-Based Contrast Agents for Magnetic Resonance Cancer Imaging. Wiley Interdiscip Rev Nanomed Nanobiotechnol. 2013; 5:1–18. [PubMed: 23047730]
689. Prah, DE. PhD Thesis. Medical College of Wisconsin; Milwaukee, WI, USA: 2008. The Development of Diffusion and Contrast Agent MRI Biomarkers for the Evaluation of Neoplasms.
690. Chandrasekharan P, Yong CX, Poh Z, He T, He Z, Liu S, Robins EG, Chuang KH, Yang CT. Gadolinium Chelate with DO3A Conjugated 2-(Diphenylphosphoryl)-Ethyldiphenylphosphonium Cation as Potential Tumor-Selective MRI Contrast Agent. Biomaterials. 2012; 33:9225–9231. [PubMed: 23026708]
691. Wang J, Yang CT, Kim YS, Sreerama SG, Cao Q, Li ZB, He Z, Chen X, Liu S. 64Cu-Labeled Triphenylphosphonium and Triphenylarsonium Cations as Highly Tumor-Selective Imaging Agents. J Med Chem. 2007; 50:5057–5069. [PubMed: 17867662]
692. Yang CT, Li Y, Liu S. Synthesis and Structural Characterization of Complexes of a DO3A-Conjugated Triphenylphosphonium Cation with Diagnostically Important Metal Ions. Inorg Chem. 2007; 46:8988–8997. [PubMed: 17784751]
693. Kim YS, Yang CT, Wang J, Wang L, Li ZB, Chen X, Liu S. Effects of Targeting Moiety, Linker, Bifunctional Chelator, and Molecular Charge on Biological Properties of 64Cu-Labeled Triphenylphosphonium Cations. J Med Chem. 2008; 51:2971–2984. [PubMed: 18419113]
694. Yang CT, Kim YS, Wang J, Wang L, Shi J, Li ZB, Chen X, Fan M, Li JJ, Liu S. 64Cu-Labeled 2-(Diphenylphosphoryl)Ethyldiphenylphosphonium Cations as Highly Selective Tumor Imaging Agents: Effects of Linkers and Chelates on Radiotracer Biodistribution Characteristics. Bioconjug Chem. 2008; 19:2008–2022. [PubMed: 18763821]
695. Morrison DE, Aitken JB, de Jonge MD, Ioppolo JA, Harris HH, Rendina LM. High Mitochondrial Accumulation of New Gadolinium(III) Agents within Tumour Cells. Chem Commun (Camb). 2014; 50:2252–2254. [PubMed: 24352097]
696. Morrison DE, Aitken JB, de Jonge MD, Issa F, Harris HH, Rendina LM. Synthesis and Biological Evaluation of a Class of Mitochondrially-Targeted Gadolinium(III) Agents. Chemistry (Easton). 2014; 20:16602–16612.
697. Joseph J, Lopez M, Cheng G, Zielonka JM, Ramadoss JS, McAllister DM, Chandel NS, Kalyanaraman B. Mitochondria-Targeted Nitroxide Mitigates Doxorubicin Toxicity in Cardiomyocites but Exacerbates Breast Tumor Cell Cytotoxicity. Free Radic Biol Med. 2009; 47:S170–S171.
698. Sanabria-Barrera SM, Avila-Rojas GC, Hardy M, Ouari O, Lopez M. Cytotoxic Effects of Mitochondria-Targeted Nitroxide Mito-SG1 on Hepatic Cancer Cells. Free Radic Biol Med. 2012; 53:S50.
699. Sanabria-Barrera SM, Sanchez-Aranguren LC, Espinosa-Gonzalez CT, Gonzalez-Ortiz LM, Hardy M, Ouari O, Lopez M. Targeting Triple-Negative Breast Cancer Metabolism and

Bioenergetics by Mitochondria-Targeted SG-1 Nitroxide (Mito-SG1). Free Radic Biol Med. 2015:S72.

700. Milligan G, Strange PG. Reduction in Accumulation of [3H]Triphenylmethylphosphonium Cation in Neuroblastoma Cells Caused by Optical Probes of Membrane Potential. Biochim Biophys Acta. 1983; 762:585–592. [PubMed: 6871253]
701. Hansson E, Jacobson I, Venema R, Sellstrom A. Measurement of the Membrane Potential of Isolated Nerve Terminals by the Lipophilic Cation [3H]Triphenylmethylphosphonium Bromide. J Neurochem. 1980; 34:569–573. [PubMed: 7354332]
702. Hirota N, Matsuura S, Mochizuki N, Mutoh N, Imae Y. Use of Lipophilic Cation-Permeable Mutants for Measurement of Transmembrane Electrical Potential in Metabolizing Cells of Escherichia Coli. J Bacteriol. 1981; 148:399–405. [PubMed: 6795176]
703. Sehlin J, Taljedal IB. Triphenylmethylphosphonium Uptake by Pancreatic Islet Cells. Exp Cell Res. 1981; 136:147–156. [PubMed: 7028493]
704. Lauffer L, Hucho F. Triphenylmethylphosphonium Is an Ion Channel Ligand of the Nicotinic Acetylcholine Receptor. Proc Natl Acad Sci U S A. 1982; 79:2406–2409. [PubMed: 6285383]
705. Goldinger JM, Duffey ME, Hong SK. Triphenylmethylphosphonium (TPMP+) as a Probe for Peritubular Membrane Potential in the Kidney Slice. Proc Soc Exp Biol Med. 1983; 173:281–287. [PubMed: 6867006]
706. Kauppinen RA, Hiltunen JK, Hassinen IE. Mitochondrial Membrane Potential, Transmembrane Difference in the NAD+ Redox Potential and the Equilibrium of the Glutamate-Aspartate Translocase in the Isolated Perfused Rat Heart. Biochim Biophys Acta. 1983; 725:425–433. [PubMed: 6652078]
707. Hillard CJ, Pounds JJ. [3H]Tetraphenylphosphonium Accumulation in Cerebral Cortical Synaptosomes as a Measure of Nicotine-Induced Changes in Membrane Potential. J Pharmacol Exp Ther. 1991; 259:1118–1123. [PubMed: 1762066]
708. Steichen JD, Weiss MJ, Elmaleh DR, Martuza RL. Enhanced in Vitro Uptake and Retention of 3H-Tetraphenylphosphonium by Nervous System Tumor Cells. J Neurosurg. 1991; 74:116–122. [PubMed: 1984490]
709. Srivastava PC, Knapp FF Jr. [(E)-1-[123i]Iodo-1-Penten-5-Yl]Triphenylphosphonium Iodide: Convenient Preparation of a Potentially Useful Myocardial Perfusion Agent. J Med Chem. 1984; 27:978–981. [PubMed: 6747996]
710. Counsell RE, Yu T, Ranade VV, Buswink AA, Carr EA Jr, Carroll M. Radioiodinated Bretylium Analogs for Myocardial Scanning. J Nucl Med. 1974; 15:991–996. [PubMed: 4422832]
711. Korn N, Buswink A, Yu T, Carr EA, Carroll M, Counsell RE. A Radioiodinated Bretylium Analog as a Potential Agent for Scanning the Adrenal Medulla. J Nucl Med. 1977; 18:87–89. [PubMed: 830836]
712. Huang CC, Friedman AM, Rayudu GV, Clark P, Fordham EW. In Vivo Stability and Distribution of [131I]Iodomethyl Trimethylammonium Chloride: Concise Communication. J Nucl Med. 1980; 21:679–681. [PubMed: 7391844]
713. Burns HD, Marzilli LG, Dannals RF, Dannals TE, Trageser TC, Conti P, Wagner HN. 4-[125I] Iodophenyltrimethylammonium Ion, an Iodinated Acetylcholinesterase Inhibitor with Potential as a Myocardial Imaging Agent. J Nucl Med. 1980; 21:875–879. [PubMed: 7411220]
714. Srivastava PC, Hay HG, Knapp FF Jr. Effects of Alkyl and Aryl Substitution on the Myocardial Specificity of Radioiodinated Phosphonium, Arsonium and Ammonium Cations. J Med Chem. 1985; 28:901–904. [PubMed: 4009613]
715. Fukuda H, Syrota A, Charbonneau P, Vallois J, Crouzel M, Prenant C, Sastre J, Crouzel C. Use of 11C-Triphenylmethylphosphonium for the Evaluation of Membrane Potential in the Heart by Positron-Emission Tomography. Eur J Nucl Med. 1986; 11:478–483. [PubMed: 3488216]
716. Krause BJ, Szabo Z, Becker LC, Dannals RF, Scheffel U, Seki C, Ravert HT, Dipaola AF Jr, Wagner HN Jr. Myocardial Perfusion with [11C]Methyl Triphenyl Phosphonium: Measurements of the Extraction Fraction and Myocardial Uptake. J Nucl Biol Med. 1994; 38:521–526. [PubMed: 7865551]
717. Ravert HT, Madar I, Dannals RF. Radiosynthesis of 3-[18F]Fluoropropyl and 4-[18F]Fluorobenzyl Triarylphosphonium Ions. J Labelled Comp Radiopharm. 2004; 47:469–476.

718. Cheng Z, Subbarayan M, Chen X, Gambhir SS. Synthesis of (4-[18F]Fluorophenyl)Triphenylphosphonium as a Potential Imaging Agent for Mitochondrial Dysfunction. J Labelled Comp Radiopharm. 2005; 48:131–137.

719. Kim DY, Yu KH, Bom HS, Min JJ. Synthesis of (4-[18F] Fluorophenyl) Triphenylphosphonium as a Mitochondrial Voltage Sensor for PET. Nucl Med Mol Imaging (2010). 2007; 41:561–565.

720. Kim DY, Kim HJ, Yu KH, Min JJ. Synthesis of [18F]-Labeled (2-(2-Fluoroethoxy)Ethyl)Tris(4-Methoxyphenyl)Phosphonium Cation as a Potential Agent for Positron Emission Tomography Myocardial Imaging. Nucl Med Biol. 2012; 39:1093–1098. [PubMed: 22575270]

721. Kim DY, Kim HJ, Yu KH, Min JJ. Synthesis of [18F]-Labeled (2-(2-Fluoroethoxy)Ethyl)Triphenylphosphonium Cation as a Potential Agent for Myocardial Imaging Using Positron Emission Tomography. Bioorg Med Chem Lett. 2012; 22:319–322. [PubMed: 22133630]

722. Kim DY, Kim HS, Le UN, Jiang SN, Kim HJ, Lee KC, Woo SK, Chung J, Kim HS, Bom HS, et al. Evaluation of a Mitochondrial Voltage Sensor, (18F-Fluoropentyl) Triphenylphosphonium Cation, in a Rat Myocardial Infarction Model. J Nucl Med. 2012; 53:1779–1785. [PubMed: 23038748]

723. Li L, Brichard L, Larsen L, Menon DK, Smith RA, Murphy MP, Aigbirhio FI. Radiosynthesis of 11-[18F]Fluoroundecyltriphenylphosphonium (MitoF) as a Potential Mitochondria-Specific Positron Emission Tomography Radiotracer. J Labelled Comp Radiopharm. 2013; 56:717–721. [PubMed: 24339010]

724. Yuan H, Cho H, Chen HH, Panagia M, Sosnovik DE, Josephson L. Fluorescent and Radiolabeled Triphenylphosphonium Probes for Imaging Mitochondria. Chem Commun (Camb). 2013; 49:10361–10363. [PubMed: 24072060]

725. Zhao G, Yu YM, Shoup TM, Elmaleh DR, Bonab AA, Tompkins RG, Fischman AJ. Membrane Potential-Dependent Uptake of 18F-Triphenylphosphonium - a New Voltage Sensor as an Imaging Agent for Detecting Burn-Induced Apoptosis. J Surg Res. 2014; 188:473–479. [PubMed: 24582214]

726. Zhao Z, Yu Q, Mou T, Liu C, Yang W, Fang W, Peng C, Lu J, Liu Y, Zhang X. Highly Efficient One-Pot Labeling of New Phosphonium Cations with Fluorine-18 as Potential PET Agents for Myocardial Perfusion Imaging. Mol Pharm. 2014; 11:3823–3831. [PubMed: 24852080]

727. Kim DY, Kim HS, Min JJ. Radiosynthesis and Evaluation of 18F-Labeled Aliphatic Phosphonium Cations as a Myocardial Imaging Agent for Positron Emission Tomography. Nucl Med Commun. 2015; 36:747–754. [PubMed: 25850717]

728. Kim DY, Min JJ. Synthesis and Evaluation of 18F-Labeled Fluoroalkyl Triphenylphosphonium Salts as Mitochondrial Voltage Sensors in PET Myocardial Imaging. Methods Mol Biol. 2015; 1265:59–72. [PubMed: 25634267]

729. Kim DY, Min JJ. Radiolabeled Phosphonium Salts as Mitochondrial Voltage Sensors for Positron Emission Tomography Myocardial Imaging Agents. Nucl Med Mol Imaging. 2016; 50:185–195. [PubMed: 27540422]

730. Zhou Y, Liu S. 64Cu-Labeled Phosphonium Cations as PET Radiotracers for Tumor Imaging. Bioconjug Chem. 2011; 22:1459–1472. [PubMed: 21696200]

731. Liu S, Kim YS, Zhai S, Shi J, Hou G. Evaluation of 64Cu(DO3A-Xy-Tpep) as a Potential PET Radiotracer for Monitoring Tumor Multidrug Resistance. Bioconjug Chem. 2009; 20:790–798. [PubMed: 19284752]

732. Zhou Y, Kim YS, Shi J, Jacobson O, Chen X, Liu S. Evaluation of 64Cu-Labeled Acridinium Cation: A PET Radiotracer Targeting Tumor Mitochondria. Bioconjug Chem. 2011; 22:700–708. [PubMed: 21413736]

733. Fritzberg AR, Kasina S, Eshima D, Johnson DL. Synthesis and Biological Evaluation of Technetium-99m MAG3 as a Hippuran Replacement. J Nucl Med. 1986; 27:111–116. [PubMed: 2934521]

734. Wang Y, Liu X, Hnatowich DJ. An Improved Synthesis of NHS-MAG3 for Conjugation and Radiolabeling of Biomolecules with (99m)Tc at Room Temperature. Nat Protoc. 2007; 2:972–978. [PubMed: 17446896]

Biographies

Jacek Zielonka

Jacek Zielonka graduated from the Lodz University of Technology with an MSc in Chemistry in 1998. He started his research on the chemistry of reactive radical intermediates generated from biologically relevant compounds under the guidance of Professor Jerzy Gebicki and received his PhD in 2002. In 2004, he joined the lab of Dr. Kalyanaraman and has been working ever since on the development of new probes and methods for the detection of short-lived reactive oxidants in biological systems. He is currently a research director in the Free Radical Research Center at the Medical College of Wisconsin.

Adam Sikora

Adam Sikora obtained an MSc degree in Chemistry from Lodz University of Technology in 2002. He subsequently carried out his doctoral research at the Institute of Applied Radiation Chemistry (Lodz University of Technology) on the chemistry of nitrenium cations and the processes of their generation. In 2008, he joined the laboratory of Dr. Kalyanaraman at the Medical College of Wisconsin as a postdoctoral fellow and investigated the mechanism of peroxynitrite-derived oxidation of boronic acids and boronate-based fluorogenic probes. He is currently an assistant professor at the Lodz University of Technology, and his research focuses on the development of the methodology of reactive oxygen and nitrogen species detection and the chemistry of HNO (azanone).

Micael Hardy

Micael Hardy obtained his PhD in Organic Chemistry from Université de Provence in 2005. He started his research on the synthesis of phosphorous-containing nitrone spin traps for detecting reactive oxygen species. In 2006, he joined Dr. Kalyanaraman's laboratory and worked on the preparation of mitochondria-targeted probes. In 2008, he obtained the position of Maître de Conference at Aix Marseille Université. The relationship between the design and synthesis of new probes for free radical detection and their application for a better understanding of the implication of free radicals in biological processes is the core of its research activity.

Olivier Ouari

Olivier Ouari is an associate professor (Maître de Conférences, 2005) at the Institute of Free Radical Chemistry at the University of Aix-Marseille. After receiving his PhD in Chemistry (1999), he undertook postdoctoral stays in the groups of Professor A. Laschewsky (UCL, Belgium), Professor P. Ballesteros (UNED, Spain), and Professor A.D. Sherry (UTD, Dallas, TX). His research interests concern organic free radicals (synthesis, magneto-structural studies, and EPR characterization) with applications in dynamic nuclear polarization combined with NMR detection, the detection of transient free radicals and mitochondria targeted methods, and paramagnetic supramolecular assemblies.

Jeannette Vasquez-Vivar

Jeannette Vasquez-Vivar, PhD, is a professor in the Department of Biophysics at the Medical College of Wisconsin. Her work on eNOS and nNOS led to the characterization of the role of the tetrahydrobiopterin (BH4) cofactor in enzyme uncoupling mechanisms. BH4 redox mechanisms in heart and immature brain tissue and possible therapeutic intervention are her major research interest. More recently, she has focused on mitochondrial biochemistry in the phenotypical changes in the heart and hematopoietic stem cell phenotype.

Gang Cheng

Gang Cheng received his BSc in Pharmacy at Shandong University and his PhD in Pharmacology at Shenyang Pharmaceutical University. He joined Dr. Kalyanaraman's research group at the Medical College of Wisconsin in 2009 has been investigating mitochondria-targeted compounds for anticancer applications.

Marcos Lopez

Marcos Lopez completed a BS in Industrial Chemistry at the University of Puerto Rico at Humacao under the guidance of Dr. Antonio E. Alegría in 2000. In 2005, he was awarded a PhD in Biochemistry from the University of Akron. His doctoral research was carried out under the mentorship Dr. Daniel J. Smith in biocompatible nanofibers and nitric oxide donors. In 2006, he joined Dr. Kalyanaraman's research group, as a postdoctoral fellow, at the Department of Biophysics in the Medical College of Wisconsin. As part of his research, he synthesized and tested the efficacy of various mitochondria-targeted compounds in cancer cell models. In 2010, he started his independent research group at the Fundación Cardiovascular de Colombia in Bucaramanga, Colombia. His current research efforts are aimed at understanding and exploiting the early metabolic and immunological perturbations in pathologies like cancer and preeclampsia, and in infectious and rare metabolic diseases.

Balaraman Kalyanaraman

Balaraman Kalyanaraman received his BS in Chemistry from the University of Madras, India, and his MS from the Indian Institute of Technology, Bombay. In 1978, he received his PhD in Chemistry from the University of Alabama, Tuscaloosa, and received postdoctoral training at the NIEHS in Research Triangle Park, NC. In 1981, he joined the Medical College of Wisconsin, Milwaukee, where he serves as Chair and Professor of Biophysics. In 2000, he founded the Medical College of Wisconsin's Free Radical Research Center. He codirects the Medical College of Wisconsin Cancer Center's Cancer Biology Program, and directs the Redox and Bioenergetics Shared Resource. He received the International EPR Society Silver Medal for Outstanding Research in the Application of EPR in Biology and Medicine and the Lifetime Achievement Award from the Society for Free Radical Biology and Medicine, and he was named the Harry R. & Angeline E. Quadracci Professor in Parkinson's Research, and an Honorary Professor of Medicine by the School of Medicine, University of the Republic in Montevideo, Uruguay. Dr. Kalyanaraman has served on the editorial boards for *Biochemical Journal*, *Free Radical Research*, and *Free Radical Biology and Medicine*.

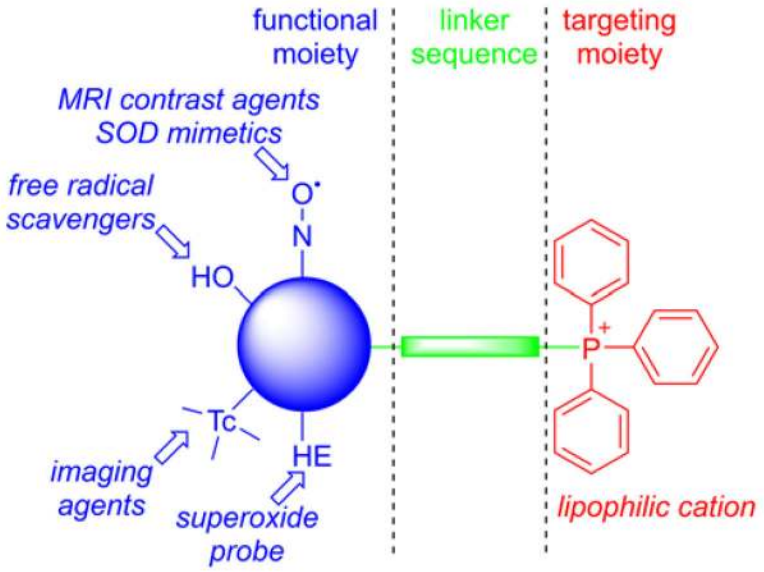

Figure 1.
Anatomy of TPP^+-Based MTA

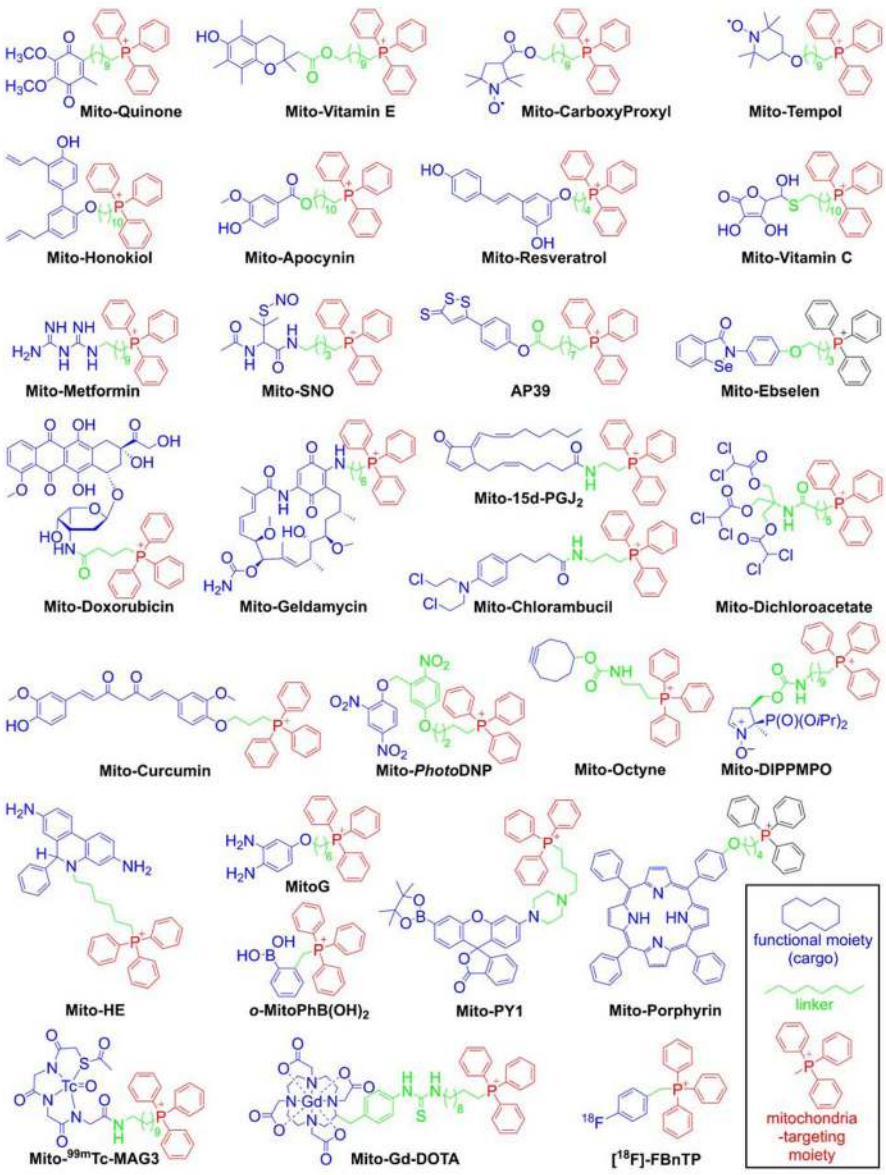

Figure 2.

Examples of the TPP^+-conjugated Compounds for Their Mitochondrial Delivery. Color coding represents the three parts of the mitochondria-targeted molecules: functional moiety (blue), linker (green), and targeting moiety (red).

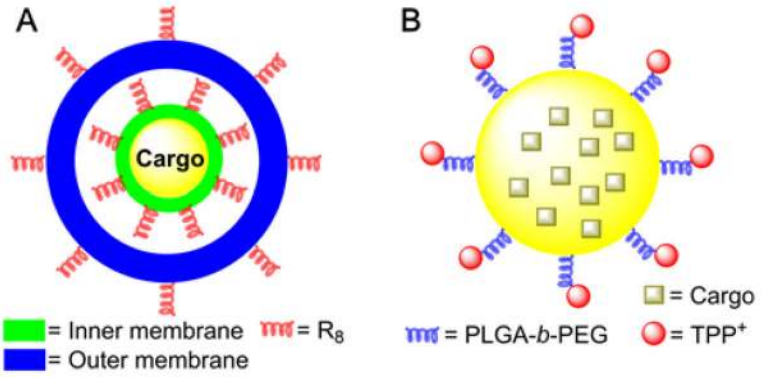

Figure 3.
Structure of the MITO-Porter (A) and PLGA-b-PEG-TPP^+-Containing (B) Mitochondria-Targeting Particles

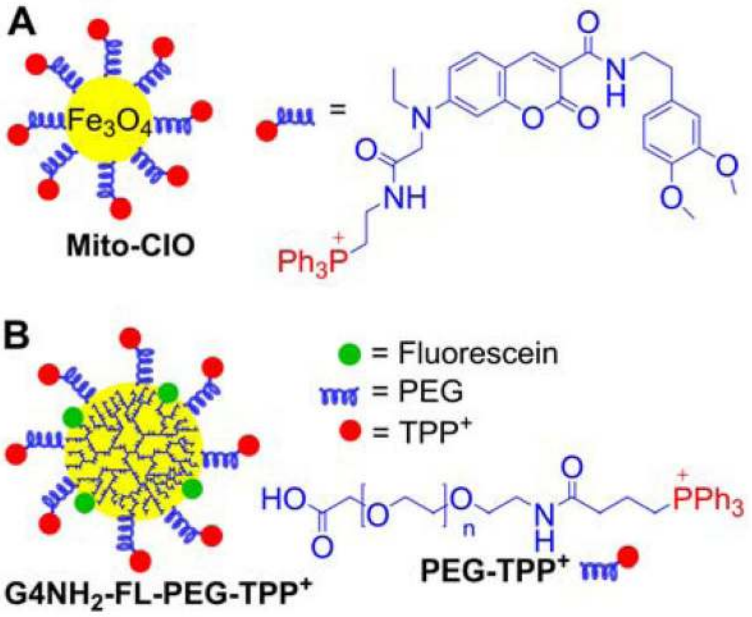

Figure 4.

Anatomy of the Mito-CIO Particle (A) and the PAMAM-G4-NH_2-Based TPP^+-Conjugated Mitochondria-Targeted Dendrimer (B)

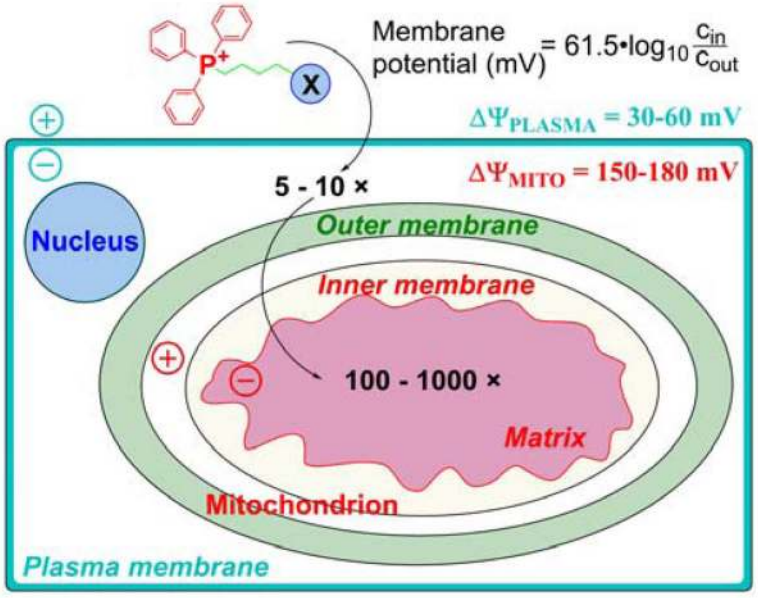

Figure 5.

Cellular Uptake of TPP^+-Linked Compounds Driven by Plasma Membrane and Mitochondrial Membrane Potentials (Adapted with permission from Ref.[159]. Copyright 2003 National Academy of Sciences)

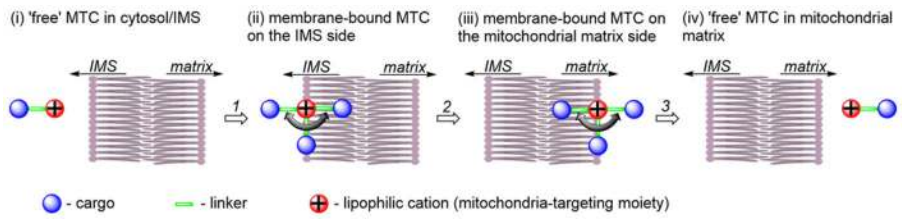

Figure 6.

Schematic Representation of the Transport of an MTC From the Mitochondrial IMS to the Matrix through the Mitochondrial Inner Membrane

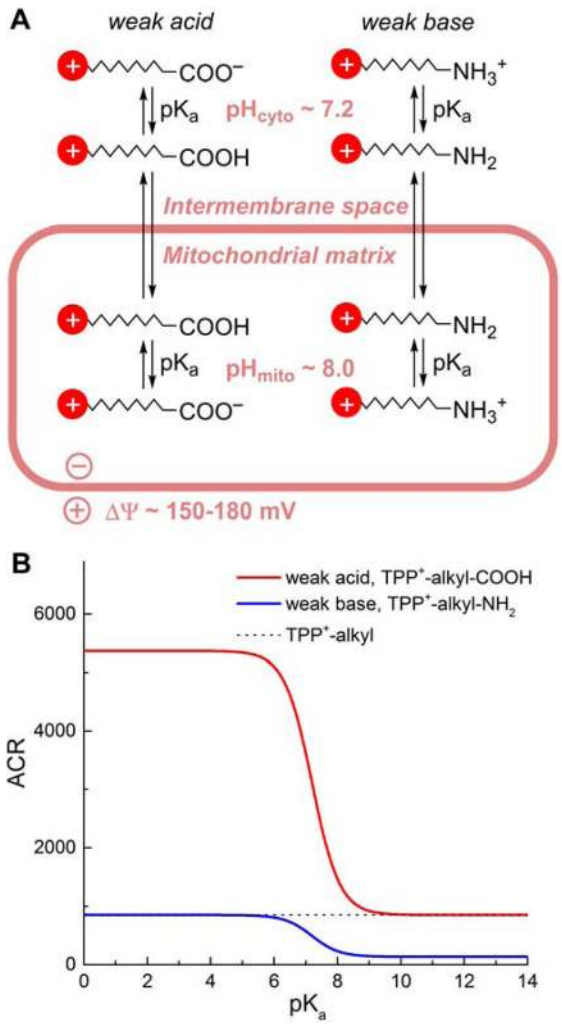

Figure 7.

Comparison of the Mitochondria to Cytosol ACR for TPP^+-Linked Weak Acids and Bases, as a Function of Their pK_a Values. (A) Scheme of the Transport of Weak Acids and Bases Conjugated to a Lipophilic Cation; (B) Calculated Equilibrium ACR Values as a Function of pK_a of Acids and Bases.

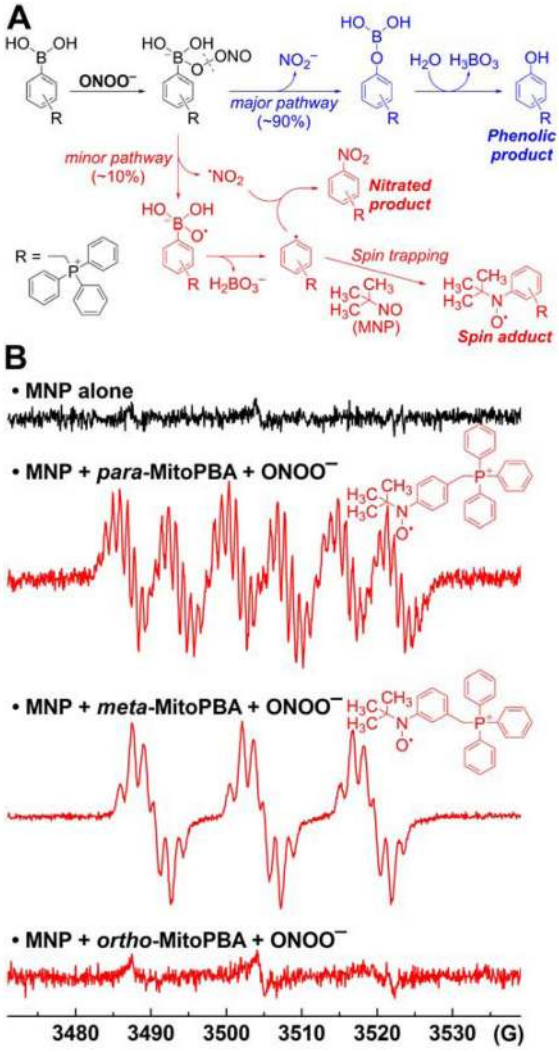

Figure 8.

Formation of Phenyl Radicals During the Reaction of Mitochondria-Targeted Phenylboronates (MitoPhB(OH)$_2$) with ONOO$^-$. (A) Chemical scheme showing the two pathways of the reaction of MitoPhB(OH)$_2$ isomers with ONOO$^-$: major nonradical pathway (blue) and minor, radical-mediated pathway (red). (B) EPR spectra detected after reacting three MitoPhB(OH)$_2$ isomers with ONOO$^-$ in the presence of the MNP spin trap. (Adapted with permission from Ref.[295]. This research was originally published in The Journal of Biological Chemistry. Zielonka J, Zielonka M, VerPlank L, Cheng G, Hardy M, Ouari O, Ayhan MM, Podsiadly R, Sikora A, Lambeth JD. Mitigation of NADPH Oxidase 2 Activity as a Strategy to Inhibit Peroxynitrite Formation. The Journal of Biological Chemistry. 2016; 291:7029–7044. © the American Society for Biochemistry and Molecular Biology.)

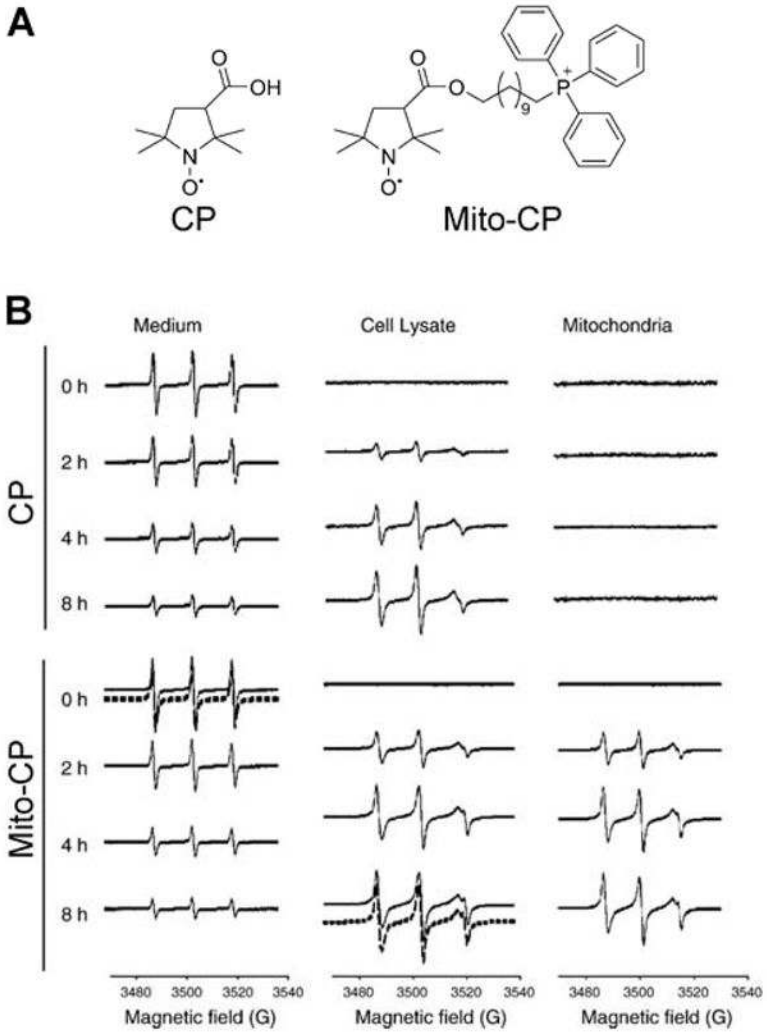

Figure 9.

Cellular Uptake and Mitochondrial Accumulation of CP and Mito-CP in Endothelial Cells. (A) Chemical structures of CP and Mito-CP. (B) EPR spectra of the medium, cell lysates, and mitochondrial fractions of cells treated with CP or Mito-CP (1 μM each) for different periods of time. Dashed lines show nonlinear least squares fit to the spectra. (Adapted with permission from Ref.[164]. Reprinted from Free Radical Biology and Medicine, 39/5, Dhanasekaran A, Kotamraju S, Karunakaran C, Kalivendi SV, Thomas S, Joseph J, Kalyanaraman B, Mitochondria superoxide dismutase mimetic inhibits peroxide-induced oxidative damage and apoptosis: Role of mitochondrial superoxide, 567–583, Copyright 2005, with permission from Elsevier.)

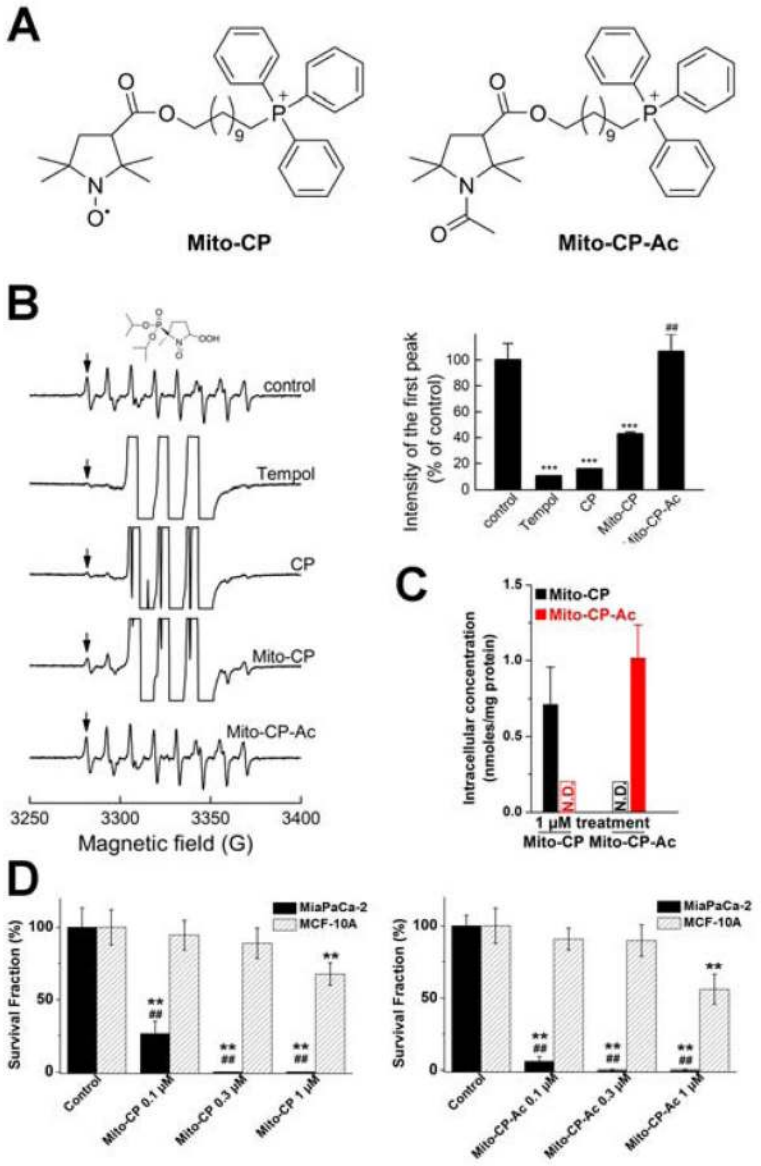

Figure 10.

Superoxide-Scavenging and Antiproliferative Activities of Mito-CP and Mito-CP-Ac. (A) Chemical structures of Mito-CP and Mito-CP-Ac. (B) EPR spectra collected during EPR spin trapping of superoxide radical anion. Control incubations containing DIPPMPO (25 mM) and the solution of KO_2 in DMSO were slowly infused over 10 min into the aqueous phosphate buffer (50 mM, pH 7.4) containing dtpa (100 μM). Where indicated, incubations contained Mito-CP (1 mM), Mito-CP-Ac (1 mM), TEMPOL (1 mM), or CP (1 mM). The bar graph shows the quantitative analyses of the DIPPMPO– •OOH adduct formed in various incubations, using the EPR intensity of the low field line, as indicated by the arrows in the EPR spectra. (C) Intracellular concentrations of Mito-CP and Mito-CP-Ac in MiaPaCa-2 cells treated with 1 μM Mito-CP or Mito-CP-Ac for 24 h. (D) Effects of Mito-CP or Mito-CP-Ac on colony formation by MiaPaCa-2 and MCF-10A cells. Cells were treated with

Mito-CP (left panel) or Mito-CP-Ac (right panel) for 24 h, and the colonies formed were counted after additional incubation. (Adapted with permission from Ref.[17]. Reprinted from Cancer Letters, 365/1, Cheng G, Zielonka J, McAllister D, Hardy M, Ouari O, Joseph J, Dwinell MB, Kalyanaraman B, Antiproliferative effects of mitochondria-targeted cationic antioxidants and analogs: Role of mitochondrial bioenergetics and energy-sensing mechanism, 96–106, Copyright 2015, with permission from Elsevier.)

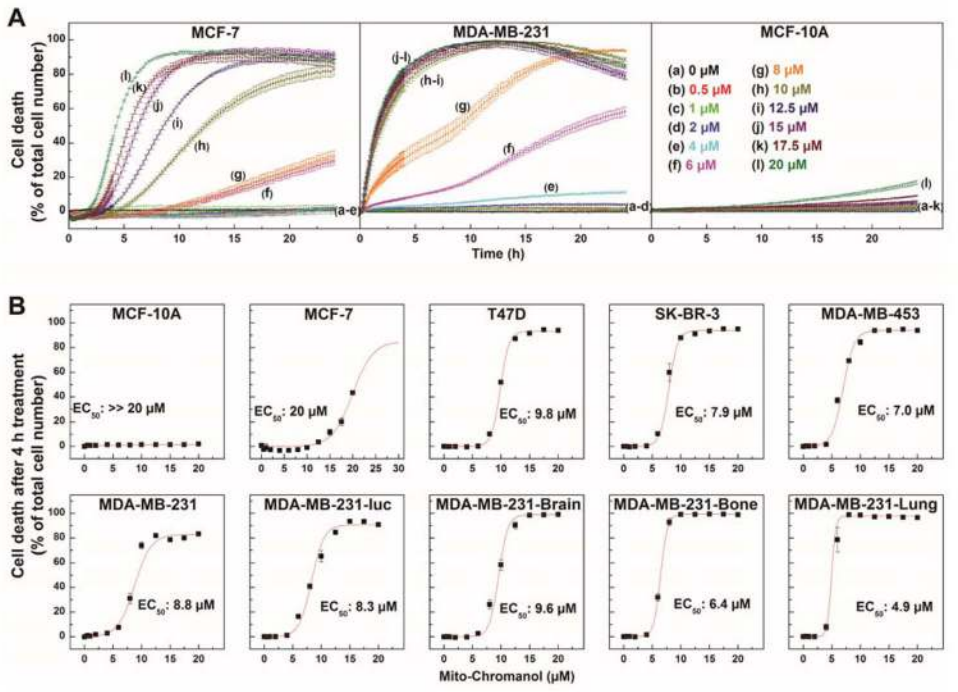

Figure 11.

Cytotoxicity of Mito-ChM Toward Breast Cancer Cells and Nontumorigenic MCF-10A Cells. Nine different breast cancer cells and MCF-10A cells were treated with Mito-ChM at the indicated concentrations (0.5–20 μM) for 24 h, and cell death was monitored in real time by Sytox Green staining. Data shown are the means ± SEM for n = 4. Real-time cell death curves were plotted in Panel A for MCF-7 (left), MDA-MB-231 (middle), and MCF-10A cells (right). Panel B shows the titration of breast cancer and noncancerous cells with Mito-ChM, and the extent of cell death observed after four h of treatment is plotted against Mito-ChM concentration. Solid lines represent the fitting curves used to determine the EC_{50} values indicated in each panel. (Adapted with permission from Ref.[432]. This research was originally published by BioMed Central in BMC Cancer. Cheng G, Zielonka J, McAllister DM, Mackinnon AC, Joseph J, Dwinell MB, Kalyanaraman B. (2013) Mitochondria-Targeted Vitamin E Analogs Inhibit Breast Cancer Cell Energy Metabolism and Promote Cell Death. BMC Cancer. 13:285. © BioMed Central.)

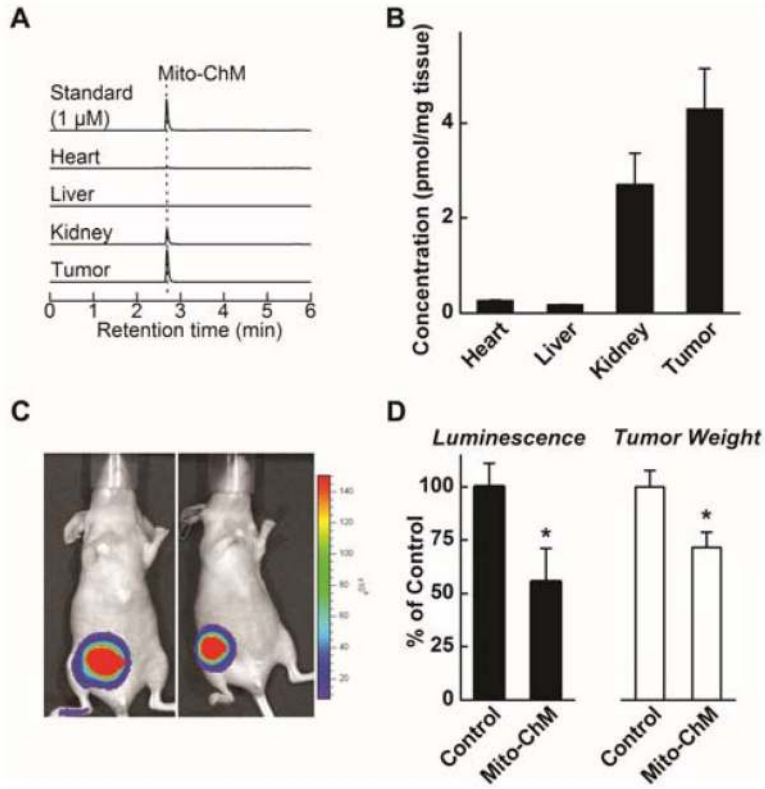

Figure 12.

Antitumor Effects of Mito-ChM in Mice Xenograft Model of Breast Cancer. (A) HPLC-MS/MS chromatograms (MRM transition: 679.1→515.0) of the Mito-ChM standard (1 μM) and of indicated tissue extracts from MDA-MB-231-luc tumor xenograft mice treated with Mito-ChM. Quantitative data on concentrations of Mito-ChM after normalization to tissue wet weight are shown in Panel B. Tumor growth was determined by both bioluminescence signal intensity and tumor wet weight after four weeks of treatment. Representative bioluminescent images are show in (C). Quantitative data were plotted in Panel D on bioluminescence signal intensity (left) and wet tumor weight (right). Data are represented as a percentage of control mice, mean ± SEM (n = 10, control group, and n= 9, Mito-ChM treated group). *, $P < 0.05$ vs. control group. (Adapted with permission from Ref.[432]. This research was originally published by BioMed Central in BMC Cancer. Cheng G, Zielonka J, McAllister DM, Mackinnon AC, Joseph J, Dwinell MB, Kalyanaraman B. (2013) Mitochondria-Targeted Vitamin E Analogs Inhibit Breast Cancer Cell Energy Metabolism and Promote Cell Death. BMC Cancer. 13:285. © BioMed Central.)

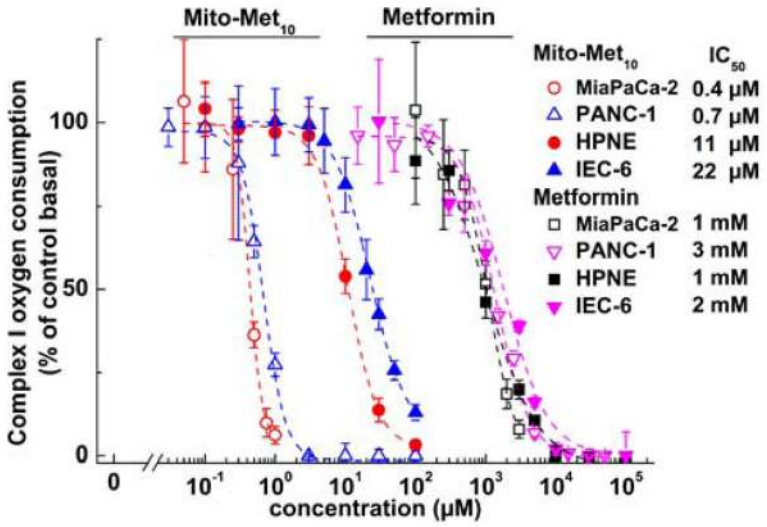

Figure 13.

Inhibition of Mitochondrial Complex I by Mito-Met_{10} in Pancreatic Cancer versus Noncancerous Cells. Pancreatic cancer cells or normal nonmalignant cells were pretreated with Met or Mito-Met_{10} for 24 h. Mitochondrial complex I oxygen consumption is plotted against concentration of Met or Mito-Met_{10}. Dashed lines represent the fitting curves used for determination of the IC_{50} values. (Adapted with permission from Ref.[21]. This research was originally published in Cancer Research. Cheng G, Zielonka J, Ouari O, Lopez M, McAllister D, Boyle K, Barrios CS, Weber JJ, Johnson BD, Hardy M, Dwinnell MB, Kalyanaraman B. (2016) Mitochondria superoxide dismutase mimetic inhibits peroxide-induced oxidative damage and apoptosis: Role of mitochondrial superoxide. Cancer Research 76(13):3904–3915. doi: 10.1158/0008-5472.CAN-15-2534.)

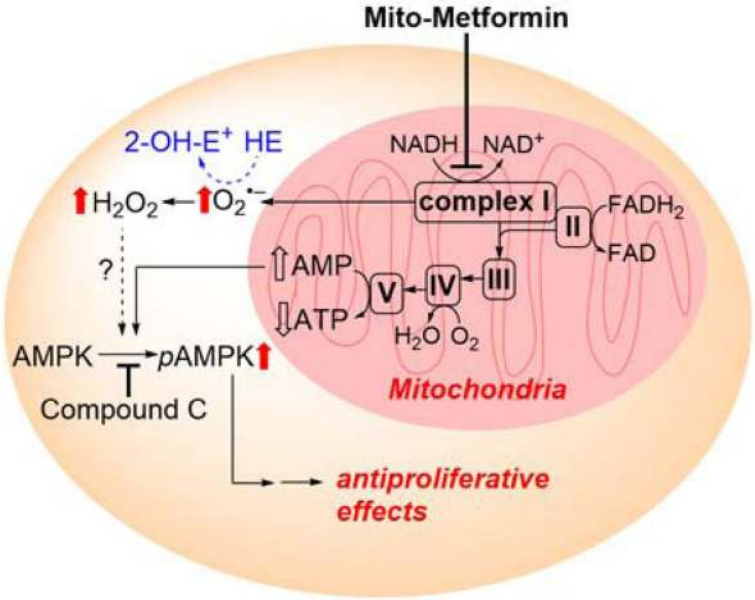

Figure 14.

Proposed Mechanism of Antiproliferative Effects of Mito-Met_{10} in Pancreatic Cancer Cells. Mito-Met_{10} inhibits complex I, stimulates ROS production, and activates AMPK phosphorylation, leading to antiproliferative effects. Changes due to the treatment with Mito-Met10 are shown by red block arrows. HE conversion to 2-OH-E^+ is used for specific detection of superoxide. (Adapted with permission from Ref.[21]. This research was originally published in Cancer Research. Cheng G, Zielonka J, Ouari O, Lopez M, McAllister D, Boyle K, Barrios CS, Weber JJ, Johnson BD, Hardy M, Dwinnell MB, Kalyanaraman B. (2016) Mitochondria superoxide dismutase mimetic inhibits peroxide-induced oxidative damage and apoptosis: Role of mitochondrial superoxide. Cancer Research 76(13):3904–3915. doi: 10.1158/0008-5472.CAN-15-2534.)

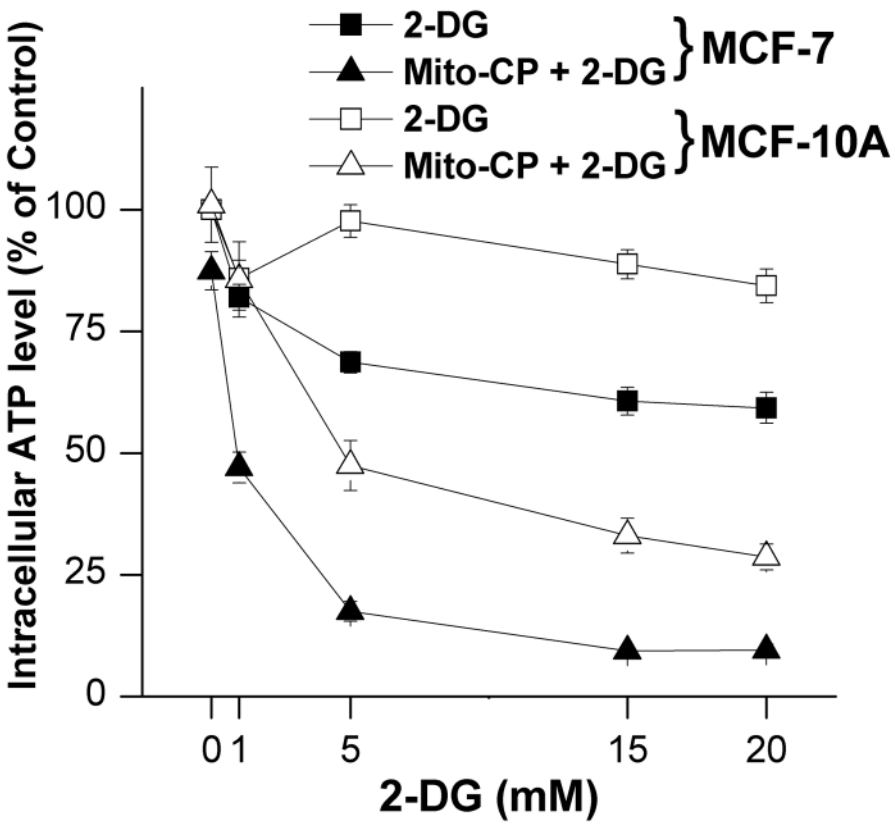

Figure 15.

Synergistic Effects of 2-DG and Mito-CP on the Intracellular ATP Level in Breast Cancer MCF-7 and Nontumorigenic MCF-10A Cells. MCF-7 and MCF-10A cells were treated with 2-DG in the presence and absence of 1 μM of Mito-CP for six h. Intracellular ATP levels were monitored using a luciferase-based assay. Data are represented as a percentage of control (nontreated) cells after normalization to total protein for each well. The calculated absolute values of ATP (nmol ATP/μg protein) for MCF-7 and MCF-10A control cells were 20.6 ± 1.9 and 28.0 ± 2.0, respectively. Data shown are the means ± SEM, n = 4. (Adapted with permission from Ref.[16]. This research was originally published in Cancer Research. Cheng G, Zielonka J, Dranka BP, McAllister D, Mackinnon Jr AC, Joseph J, Kalyanaraman B. (2012) Mitochondria-targeted drugs synergize with 2-deoxyglucose to trigger breast cancer cell death. Cancer Research 72(10):2634–2644. doi: 10.1158/0008-5472.CAN-11-3928.)

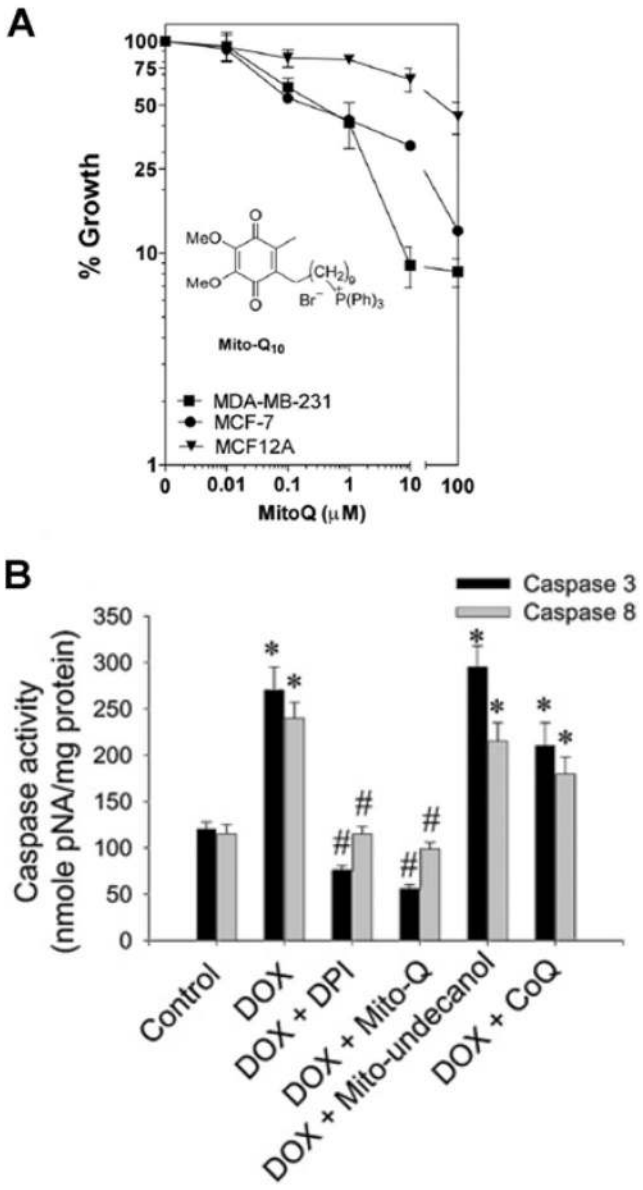

Figure 16.

Differential Toxicity of MitoQ in Cancer Cells and Noncancerous Cells. (A) An SRB dye-based assay was used to measure cell viability following increasing concentrations of MitoQ after 72 h in breast cancer cell lines (MDA-MB-231 or MCF-7) or healthy breast epithelial cells (MCF-12A). (B) H9c2 cells were treated with 1 μM DOX in the presence and absence of DPI (5 μM), MitoQ (1 μM), Mito-undecanol (1 μM), or CoQ (1 μM) for eight h and caspase-3 and -8 activities were determined. (Adapted with permission from Ref.[19,638]. A portion of this research was originally published in The Journal of Biological Chemistry. Rao VA, Klein SR, Bonar SJ, Zielonka J, Mizuno N, Dickey JS, Keller PW, Joseph J, Kalyanaraman B, Shacter E. The antioxidant transcription factor Nrf2 negatively regulates autophagy and growth arrest induced by the anticancer redox agent mitoquinone. The Journal of Biological Chemistry. 2010; 285:34447–59. © the American Society for

Biochemistry and Molecular Biology. A version of this figure was originally published in Kalivendi SV, Konorev EA, Cunningham S, Vanamala SK, Kaji EH, Joseph J, Kalyanaraman B. Biochemical Journal. 2005.)

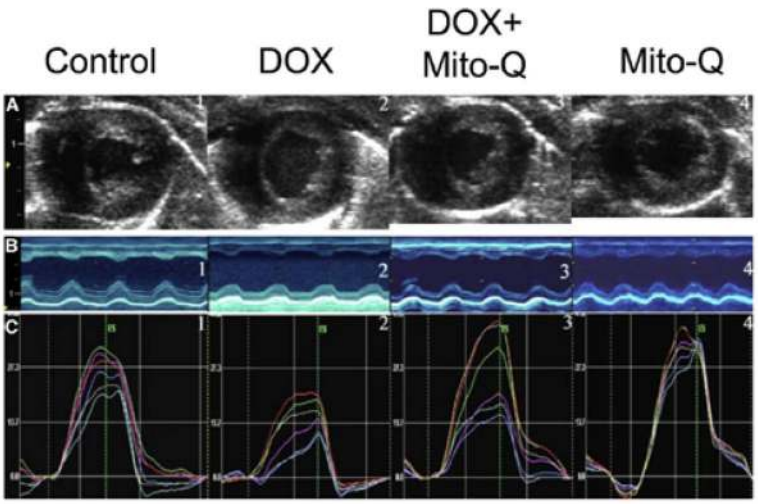

Figure 17.

Protective Effects of MitoQ Against DOX-Induced Cardiomyopathy In Vivo. (A) Endsystolic 2D B-mode images at the midventricular level: (1) Control rat, (2) DOX treatment for 12 weeks, (3) DOX plus MitoQ treatment for 12 weeks, and (4) MitoQ treatment for 12 weeks. (B) Anatomical M-mode through the anterior and interior walls. (C) Graph showing the radial strain in one cardiac cycle of six equidistant regions of the myocardium in the short-axis view. The global radial strain was computed as the average of all six segments. (Adapted with permission from Ref.[637]. Reprinted from Biophysical Journal, 94/4, Chandran K, Aggarwal D, Migrino RQ, Joseph J, McAllister D, Konorev EA, Antholine WE, Zielonka J, Srinivasan S, Avadhani NG, Kalyanaraman B, Doxorubicin inactivates myocardial cytochrome c oxidase in rats: Cardioprotection by Mito-Q, 1388–1398, Copyright 2009, with permission from Elsevier.)

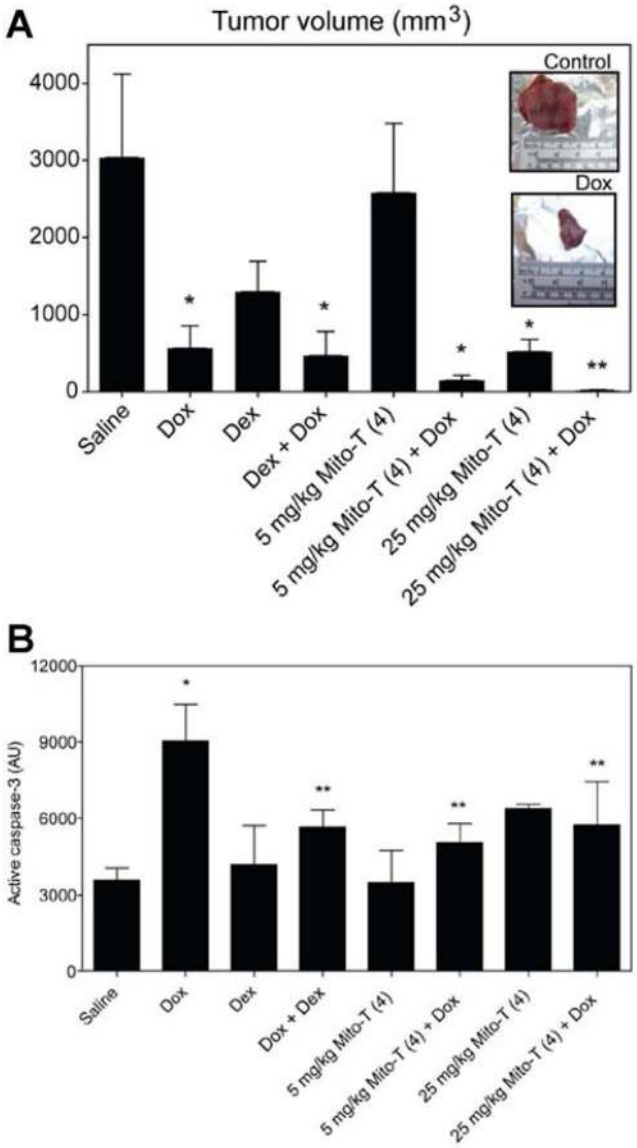

Figure 18.

Cardioprotective and Chemotherapeutic Effects of Mito-TEMPOL-C_4 in the Syngeneic Rat Breast Cancer Model. (A) Effect of Mito-TEMPOL-C_4 (Mito-T (4)) alone and in combination with DOX on the tumor size. Spontaneously hypertensive rats (SHRs) were implanted with SST-2 cells and 24 h later were administered either doxorubicin (10 mg/kg), dexrazoxane (50 mg/kg), Mito-T (4) (5 or 25 mg/kg), a combination of doxorubicin and dexrazoxane, or a combination of doxorubicin and Mito-T (4). Each treatment group consisted of 10 animals. The mean tumor volumes (mm^3) were measured 14 days after drug treatment. The two inset images show representative excised tumors from saline and doxorubicin-treated SHR/SST-2 animals. (B) Effect of Mito-TEMPOL-C_4 on DOXinduced cell apoptosis in cardiac tissues, as measured by monitoring caspase-3 activity. Paraffin-embedded cardiac tissues were stained with the anti-active caspase-3 antibody. The intensity of the HRP-tagged secondary antibody was quantified as an indication of active caspase-3

using the ScanScope software. Mean intensities are shown in the graph and derived from at least 10 images per animal (five animals per group). (Adapted with permission from Ref.[420]. This research was originally published in PLOS One. Dickey et al. (2013) Mito-TEMPOL and Dexrazoxane Exhibit Cardioprotective and Chemotherapeutic Effects through Specific Protein Oxidation and Autophagy in a Syngeneic Breast Tumor Preclinical Model. PLOS one 8(8):e70575. doi: 10.1371/journal.pone.0070575.)

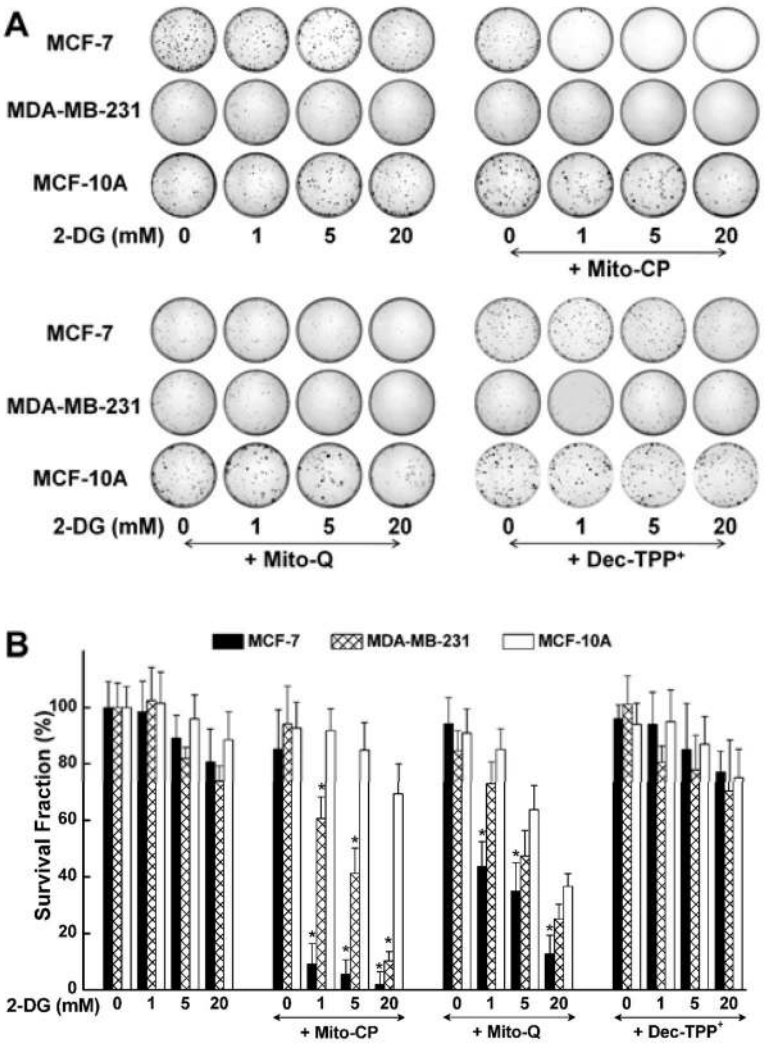

Figure 19.

Synergistic Effects of 2-DG and Mito-CP on Proliferation of Breast Cancer Cells and Nontumorigenic Cells. MTDs synergize with 2-DG to inhibit colony formation in MCF-7 and MDA-MB-231 cells but not in MCF-10A cells. (A) MCF-7, MDA-MB-231, and MCF-10A cells were treated with 2-DG only (top, left), 2-DG in the presence of Mito-CP (1 μM; top, right), 2-DG in the presence of MitoQ (1 μM) for six h (bottom, left), 2-DG in the presence of Dec-TPP$^+$ (bottom, right), and the number of colonies formed was counted. (B) The survival fraction was calculated under the same conditions as in (A). The calculated plating efficiency for MCF-7, MDA-MB-231, and MCF-10A cells was 55 ± 6, 33 ± 4, and 34 ± 8, respectively. Data shown represent the mean ± SEM. *, $P < 0.05$ ($n = 5$) comparing MCF-7 and MDA-MB-231 with MCF-10A under the same treatment conditions. (Adapted with permission from Ref.[16]. This research was originally published in Cancer Research. Cheng G, Zielonka J, Dranka BP, McAllister D, Mackinnon Jr AC, Joseph J, Kalyanaraman B. (2012) Mitochondria-targeted drugs synergize with 2-deoxyglucose to trigger breast cancer cell death. Cancer Research 72(10):2634–2644. doi: 10.1158/0008-5472.CAN-11-3928.)

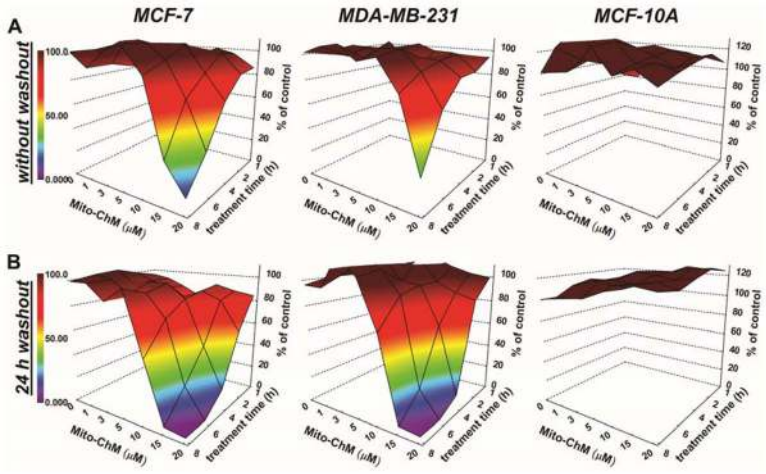

Figure 20.

Selective Depletion of Intracellular ATP Levels in Breast Cancer Cells by Mitochondria-Targeted Vitamin E Analog, Mito-ChM. The MCF-7, MDA-MB-231, and MCF-10A cells were treated with Mito-ChM (1–20 μM) as indicated for one to eight h. After treatment, cells were washed with complete media and either assayed immediately (A), or returned to cell culture incubator for 24 h (B). Intracellular ATP levels were measured using a luciferase-based assay. Data are represented as a percentage of control (nontreated) cells after normalization to total cellular protein. (Adapted with permission from Ref.[432]. This research was originally published by BioMed Central in BMC Cancer. Cheng G, Zielonka J, McAllister DM, Mackinnon AC, Joseph J, Dwinell MB, Kalyanaraman B. (2013) Mitochondria-Targeted Vitamin E Analogs Inhibit Breast Cancer Cell Energy Metabolism and Promote Cell Death. BMC Cancer. 13:285. © BioMed Central.)

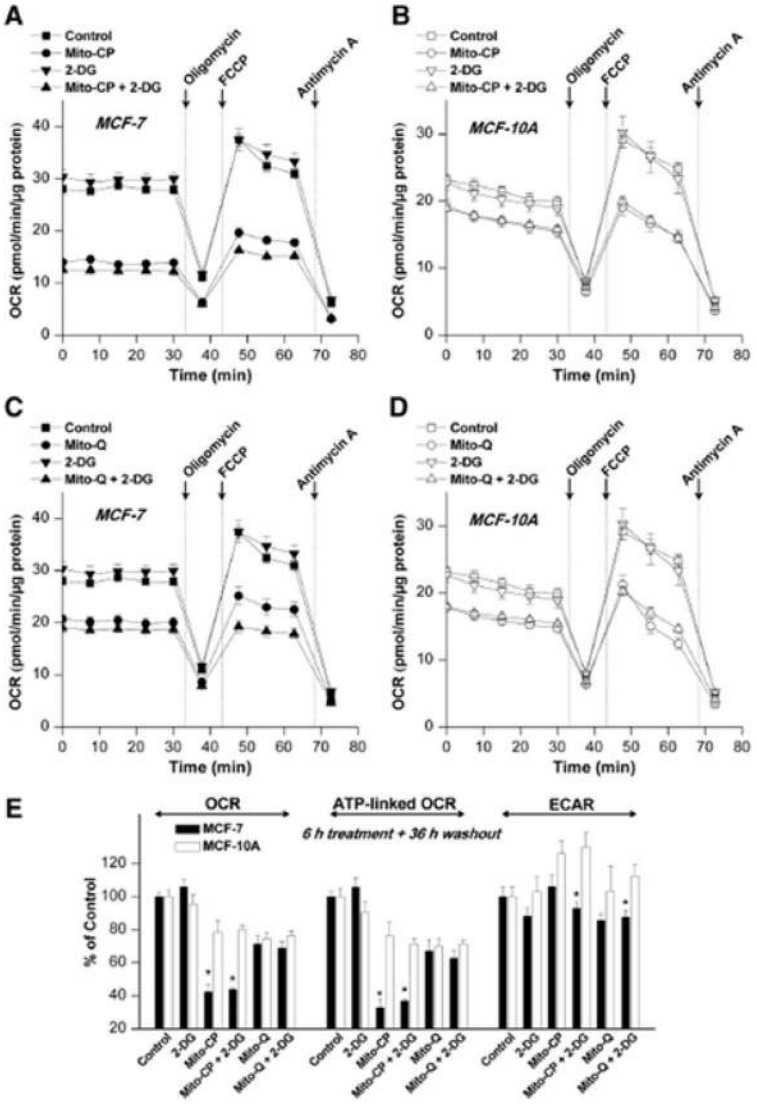

Figure 21.

Selective Retention and Irreversible Inhibition of Mitochondrial Function by MTDs in Breast Cancer Cells. (A–D) MCF-7 and MCF-10A cells (20,000 cells per well) seeded in V7 culture plates were treated with the indicated compounds for six h. The cells were then washed with complete media (MEM-a for MCF-7 and DMEM/F12 for MCF-10A) and returned to a 37 °C incubator for 36 h. The cells were then washed with unbuffered media as described. Five baseline OCR and ECAR measurements were then taken before injection of oligomycin (1 µg/mL), to inhibit ATP synthase, FCCP (1–3 µM), to uncouple the mitochondria and yield maximal OCR, and antimycin A (10 µM) to inhibit complex III and mitochondrial oxygen consumption. The effects of MTDs and 2-DG on basal OCR, ATP-linked OCR, and ECAR are shown in E. *P < 0.01 (n = 5) comparing MCF-7 with MCF-10A under the same treatment conditions. (Adapted with permission from from Ref[16]. This research was originally published in Cancer Research. Cheng G, Zielonka J, Dranka BP, McAllister D, Mackinnon Jr AC, Joseph J, Kalyanaraman B. (2012) Mitochondria-

targeted drugs synergize with 2-deoxyglucose to trigger breast cancer cell death. Cancer Research 72(10):2634–2644. doi: 10.1158/0008-5472.CAN-11-3928.)

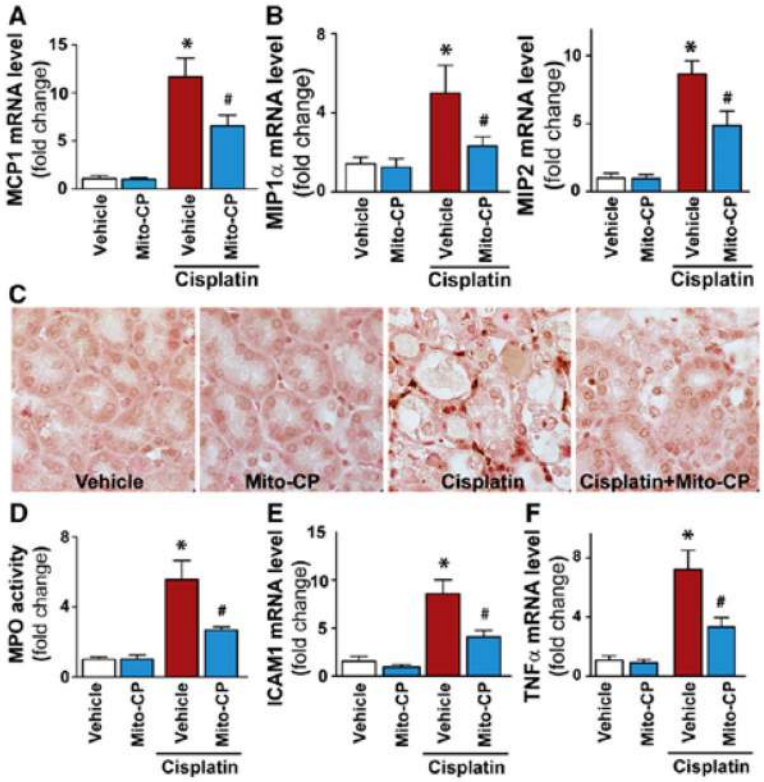

Figure 22.

Mito-CP-Induced Mitigation of the Inflammatory Response in Kidneys of Mice Treated with Cisplatin. Mito-CP attenuates cisplatin-induced inflammation. Cisplatin significantly increased mRNA expression of proinflammatory chemokines (A) MCP-1, (B) MIP1α and MIP2, (C and D) myeloperoxidase staining and activity, and (E and F) adhesion molecule ICAM-1 and proinflammatory cytokine TNF-α mRNA expression in the kidneys 72 h after its administration to mice, indicating enhanced inflammatory response. These changes could be largely prevented by treatment with Mito-CP. Results are means±SEM of 6–16/group. *P < 0.05 vs. vehicle; #P < 0.05 vs. cisplatin. (Adapted with permission from Ref.[490]. Reprinted from Free Radical Biology and Medicine, 52/2, Mukhopadhyay P, Horváth B, Zsengellér Z, Zielonka J, Tanchian G, Holovac E, Kechrid M, Patel V, Stillman IE, Parikh SM, Joseph J, Kalyanaraman B, Pacher P, Mitochondrial-targeted antioxidants represent a promising approach for prevention of cisplatin-induced nephropathy, 497–506, Copyright 2012, with permission from Elsevier.)

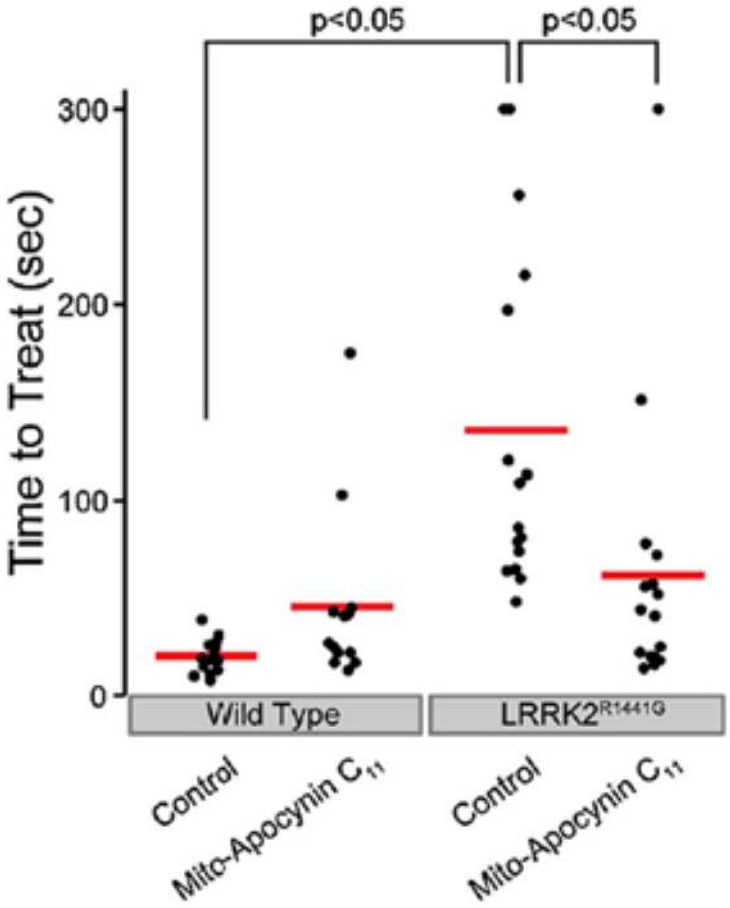

Figure 23.

Neuroprotective Effects of Mito-Apo$_{11}$. Mito-apocynin-C$_{11}$ improves time-to-treat performance in LRRK2^{R1441G} tg mice. The time required to identify either a chow pellet or a fruit cereal treat was monitored in mice in a novel cage with clean bedding. Individual mice are represented by the black dots, and the mean is shown as the red bar. (Adapted with permission from Ref.[493]. Reprinted from Neuroscience Letters, 583, Dranka BP, Gifford A, McAllister D, Zielonka J, Joseph J, O'Hara CL, Stucky CL, Kanthasamy AG, Kalyanaraman B, A novel mitochondrially-targeted apocynin derivative prevents hyposmia and loss of motor function in the leucine-rich repeat kinase 2 (LRRK2R1441G) transgenic mouse model of Parkinson's disease, 159–164., Copyright 2014, with permission from Elsevier.)

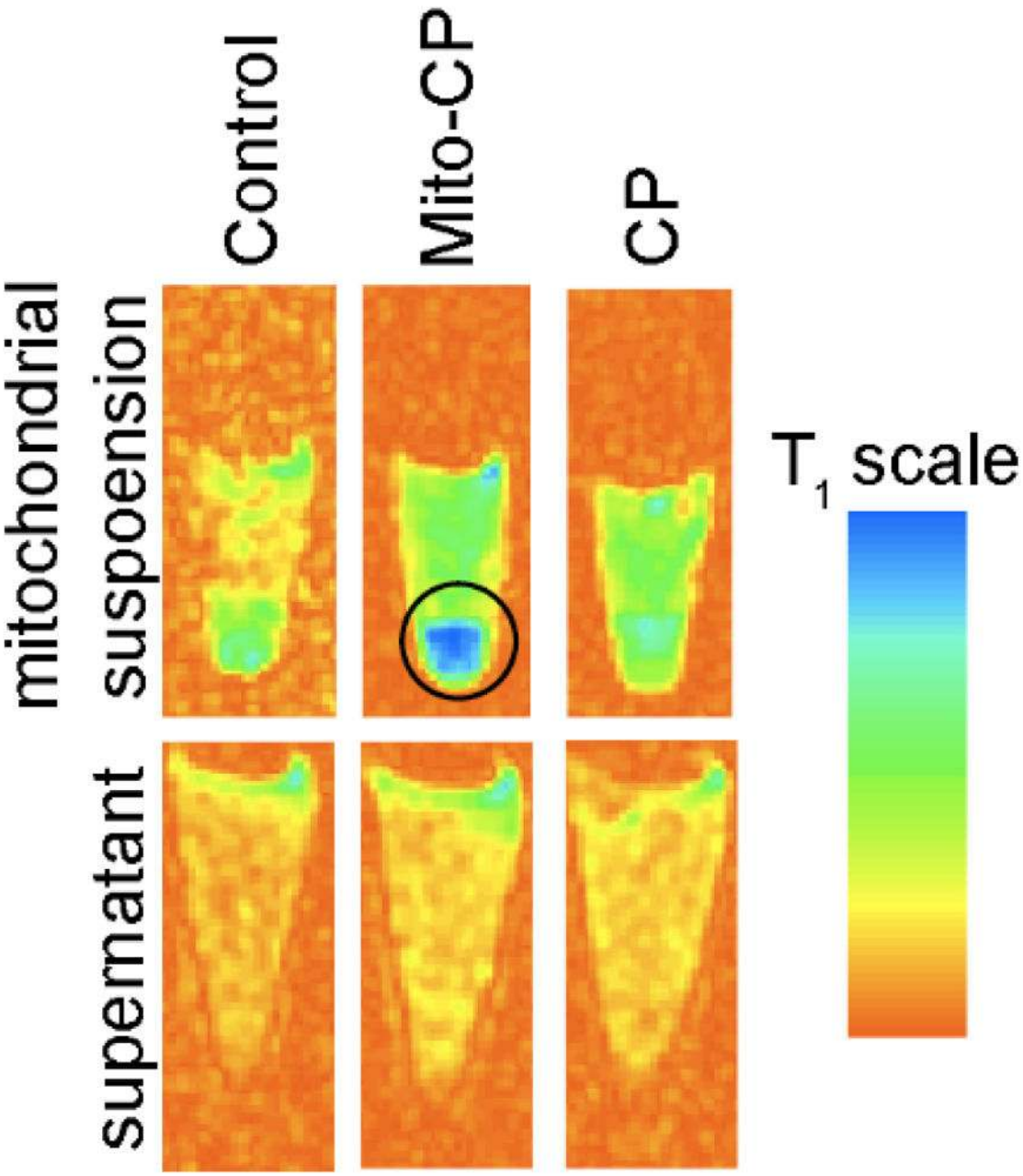

Figure 24.

Spin Echo Inversion Recovery Images (T_1=1900 ms) of the Tubes Containing Isolated Mitochondria (top) or Post-Mitochondrial Supernatant (bottom) in PBS Containing Succinate and the Nitroxides, as Indicated. (Adapted with permission from Ref.[678]. This research was originally published in Proceedings of the International Society for Magnetic Resonance in Medicine. Prah D, Paulson E, Zielonka J, Hardy M, Joseph J, Kalyanaraman B, Schmainda K. (2007) In Vitro Mitochondrial Labeling using Mito-CarboxyPROXYL (Mito-CP) Enhanced Magnetic Resonance Imaging. Proc Intl Soc Mag Reson Med 15:1162.)

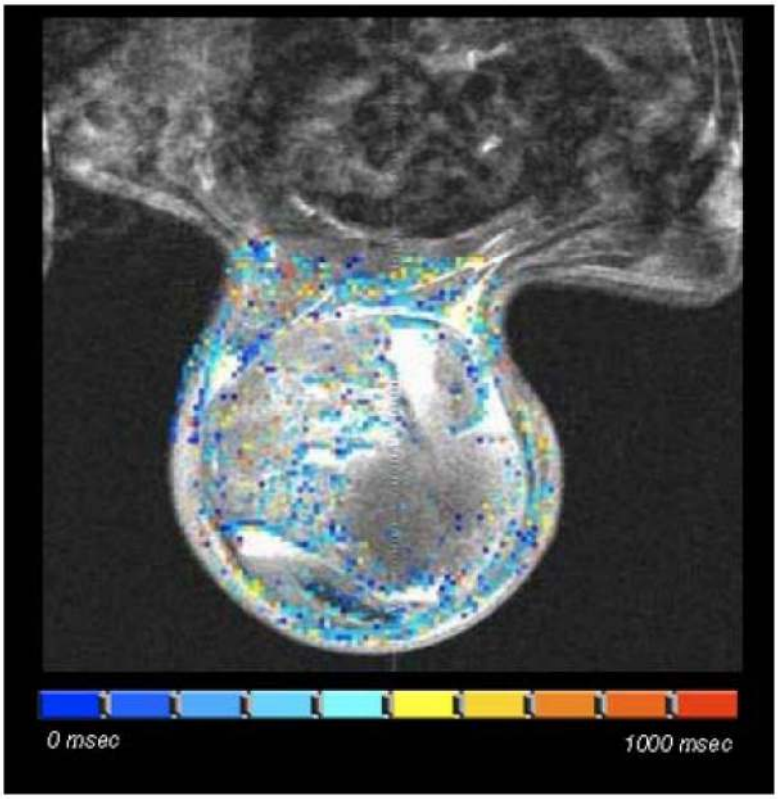

Figure 25.

Mito-CP-Based Imaging of Breast Cancer in Rats (Adapted with permission from Ref.[489]. This research was originally published in Proceedings of the International Society for Magnetic Resonance in Medicine. Prah D, Paulson E, Wagner-Schuman M, Zielonka J, Lopez M, Hardy M, Joseph J, Kalyanaraman B, Schmainda K. (2008) In Vivo Mitochondrial Labeling using Mito-CarboxyPROXYL (Mito-CP) Enhanced Magnetic Resonance Imaging. Proc Intl Soc Mag Reson Med 16:106.)

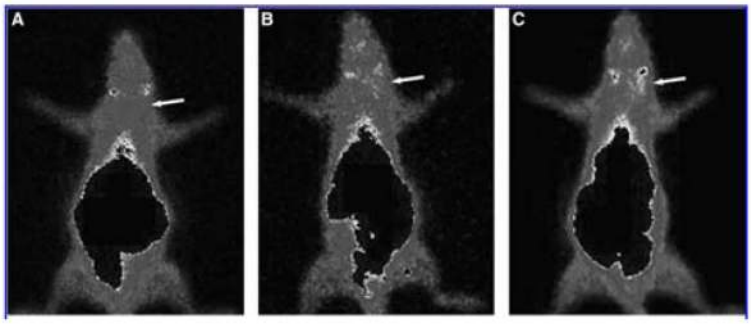

Figure 26.

Application of the Mito-^{99m}Tc-MAG$_3$ for In Vivo Tumor Imaging in Rats in Chemically Induced Breast Cancer. Anterior images of the same rat from three consecutive weeks are shown in (A–C). The site of progressive tumor growth, as detected by Mito-^{99m}Tc-MAG$_3$, is indicated with an arrow. (Adapted with permission from Ref.[235]. This research was originally published in Cancer Biotherapy and Radiopharmaceuticals. Li Z, Lopez M, Hardy M, McAllister DM, Kalyanaraman B, Zhao M. (2009) A 99mTc-Labeled Triphenylphosphonium Derivative for the Early Detection of Breast Tumors. 24(5): 579–587. doi: 10.1089/cbr.2008.0606.)

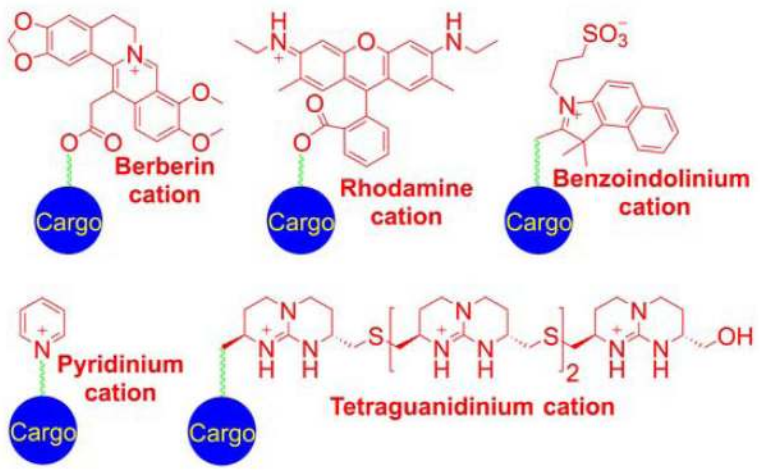

Chart 1.

Examples of Heterocyclic Cations Used as Mitochondria-Targeting Moieties. Color coding represents three parts of the mitochondria-targeted molecules: targeting moiety (red), linker (green), and functional moiety (blue).

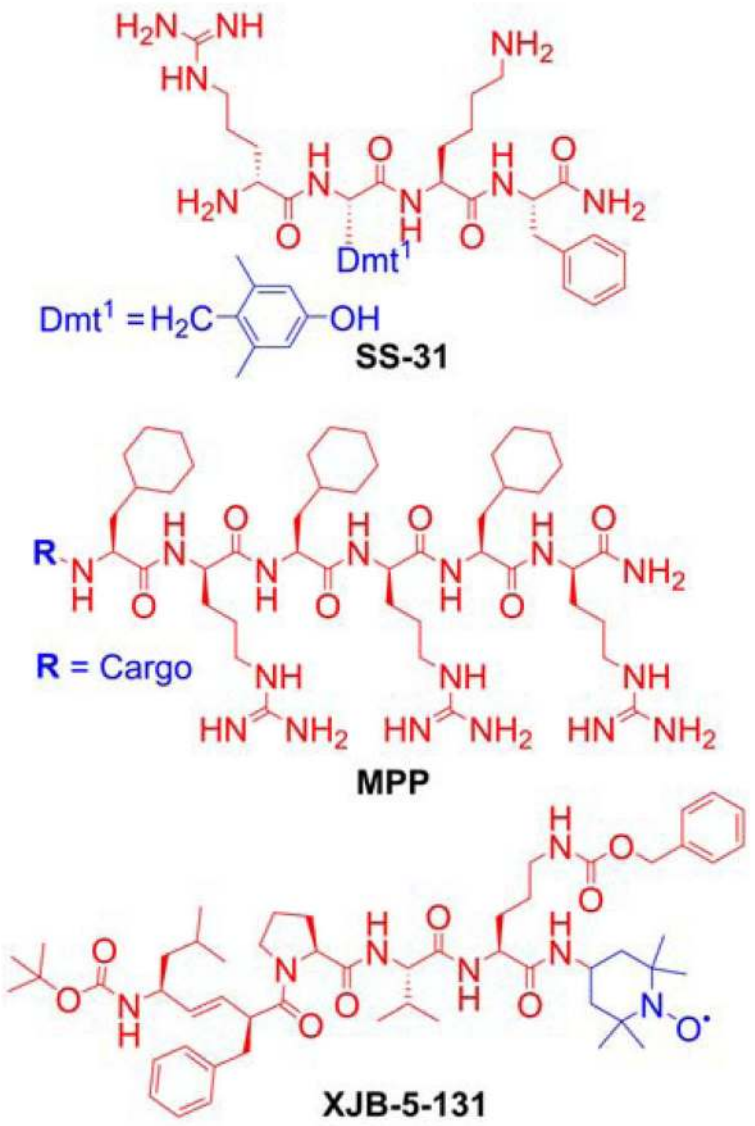

Chart 2.

Examples of Mitochondria-Targeted Peptides: SS Peptide (SS-31), MPP, and Hemigramicidin S-linked Nitroxide (XJB-5-131)

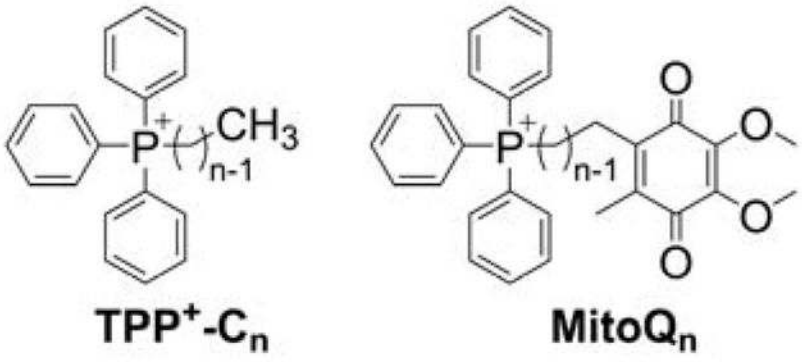

Chart 3.
Structures of TPP^{+}-C_n and $MitoQ_n$

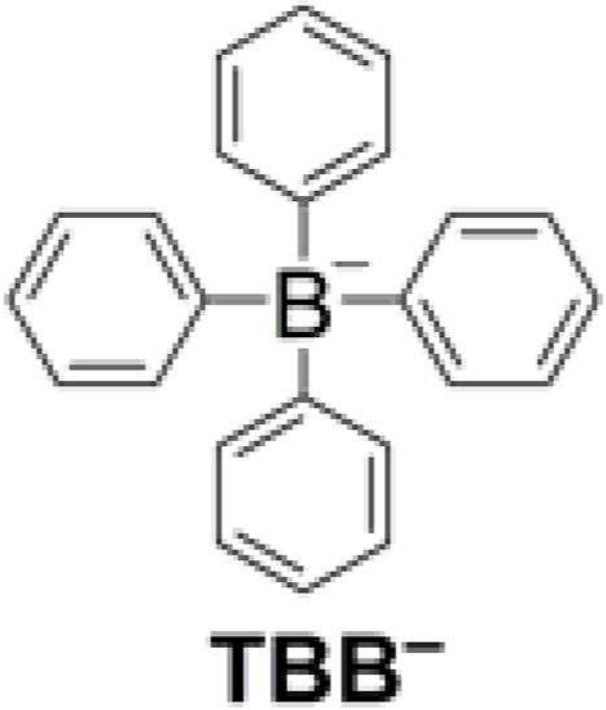

Chart 4.
Structure of the TBB^- Lipophilic Anion

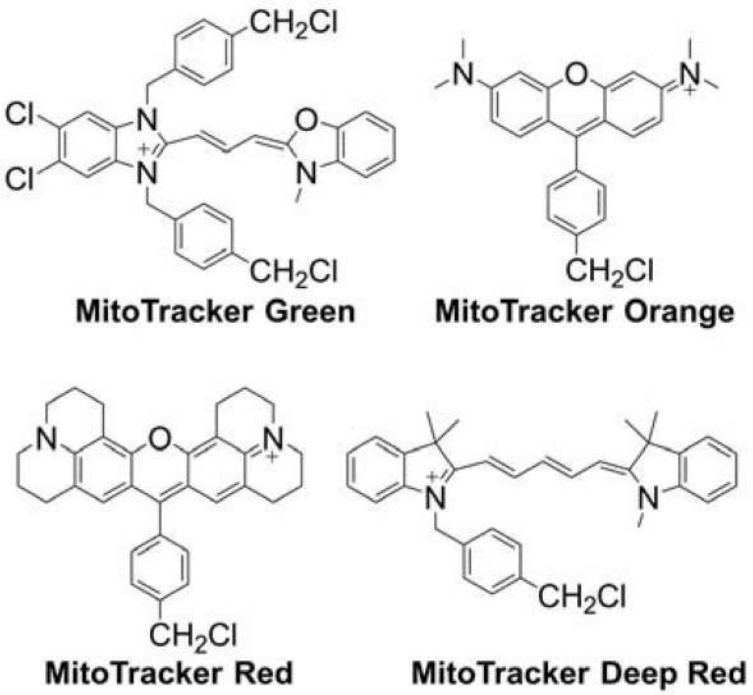

Chart 5.
Structures of Different MitoTracker Probes

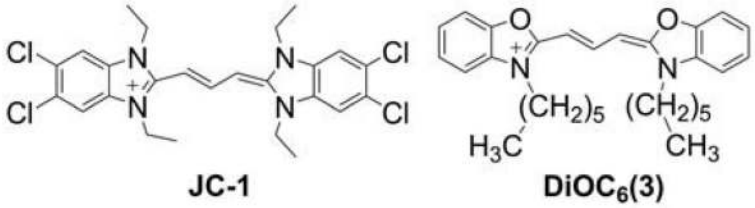

Chart 6.
Structures of JC-1 and $DiOC_6(3)$ Probes

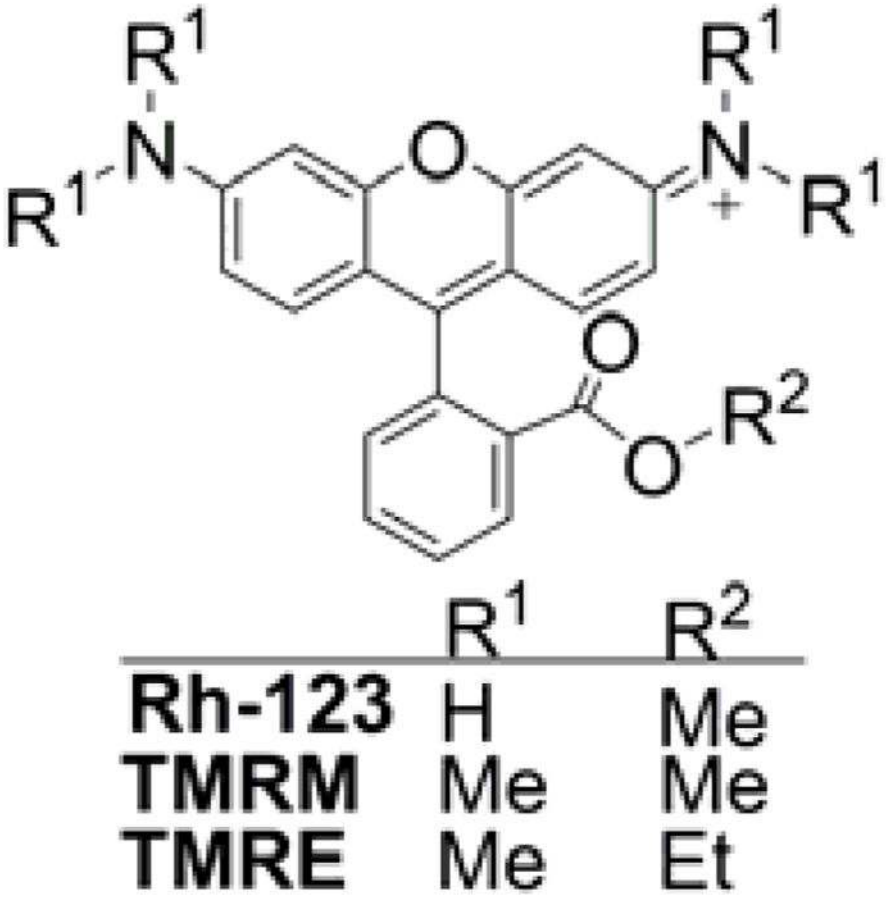

Chart 7.
Structures of Rhodamine-Based Indicators of Mitochondrial Membrane Potential

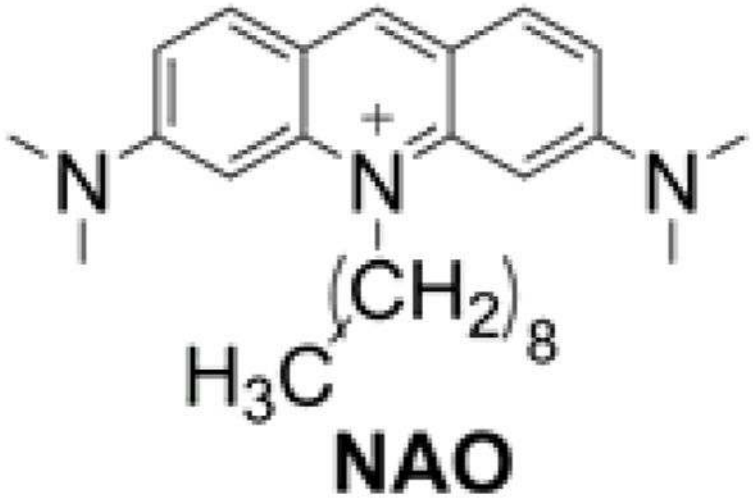

Chart 8.
Structure of NOA

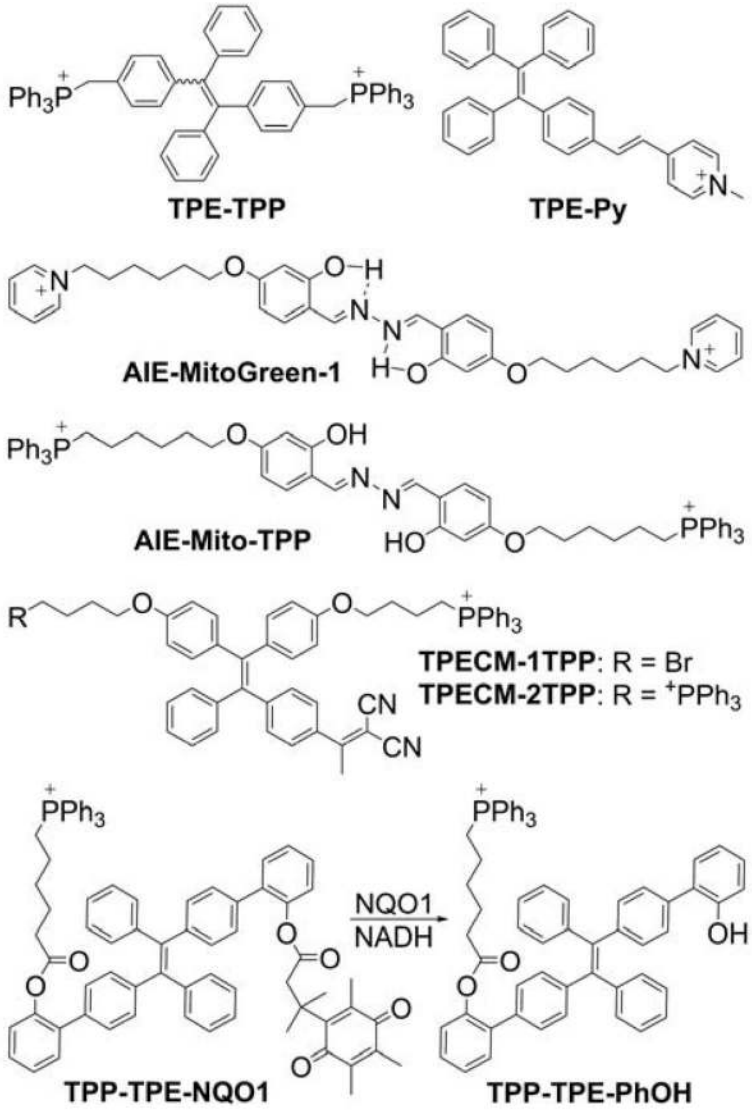

Chart 9.
Chemical Structures of Mitochondria-Targeted Probes with AIE (Mito-AIE Probes)

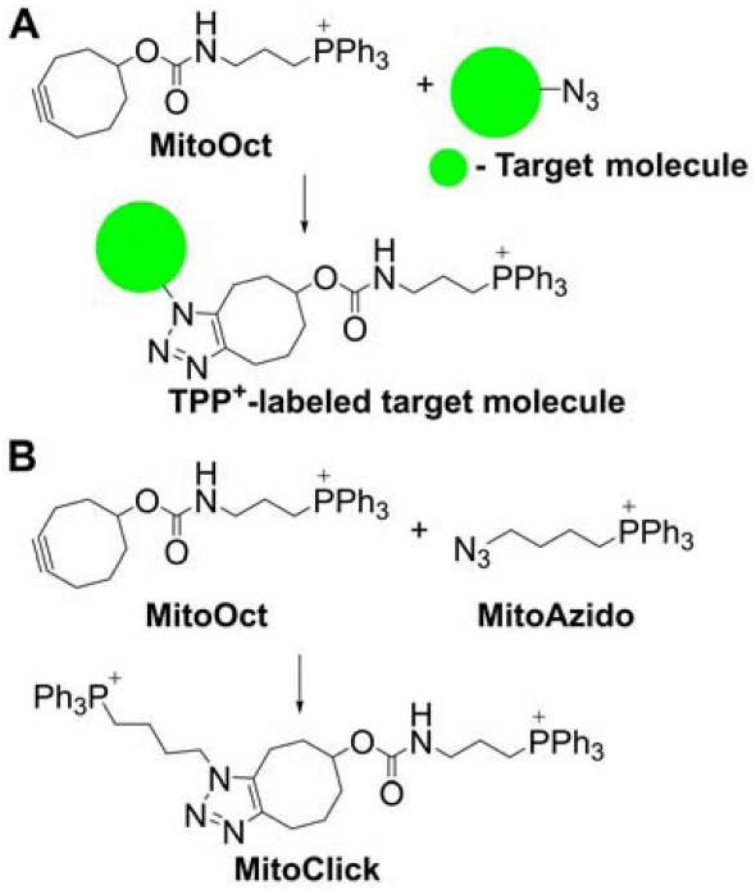

Chart 10.
Click-Chemistry-Based Mitochondrial Probes

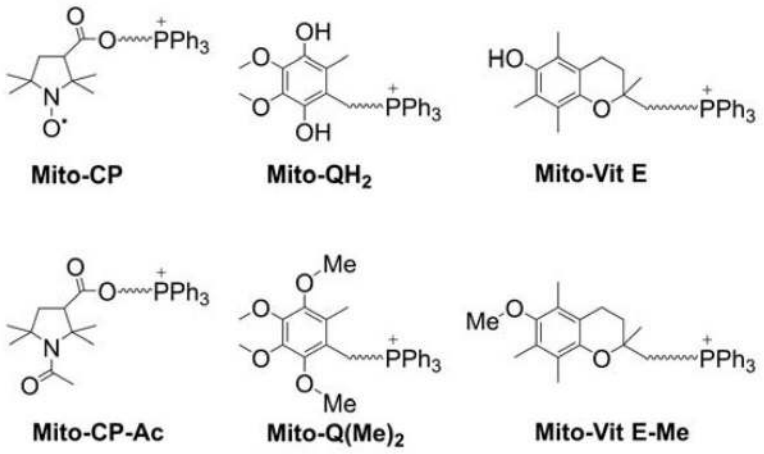

Chart 11.
Examples of "Control" Compounds for Mitochondria-Targeted Antioxidants

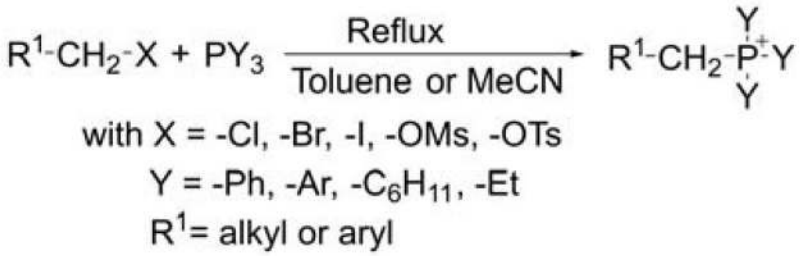

Chart 12.
Alkylation of Trisubstituted Phosphines

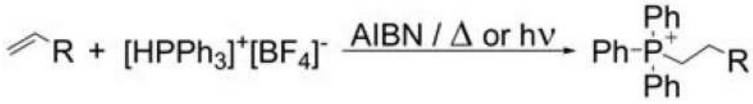

Chart 13.
Free-Radical-Mediated Hydrophosphonation of Alkenes

Chart 14.
Reaction of Triphenylphosphine with Sulfones

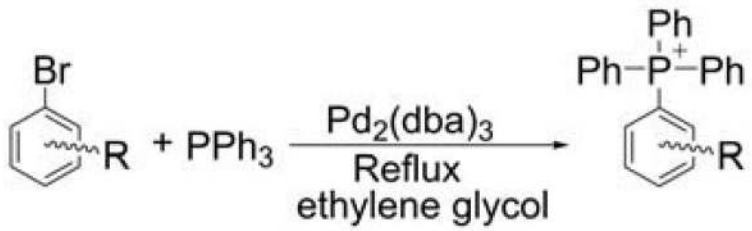

Chart 15.
Palladium-Catalyzed Arylation of Triphenylphosphine

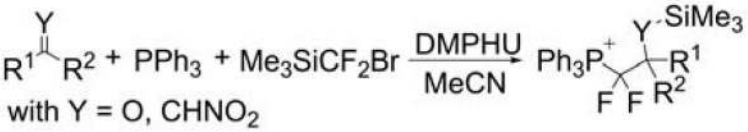

Chart 16.
Difluoromethylation Using Me_3SiCF_2Br and DMPU

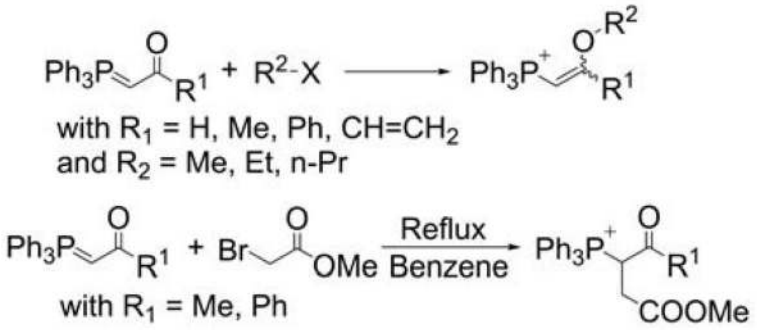

Chart 17.
O- and C-alkylation of Stabilized Ylides

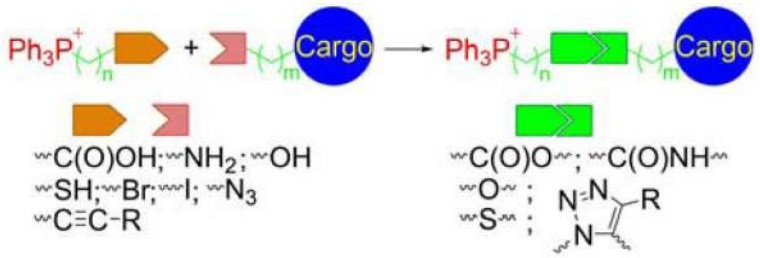

Chart 18.

Strategies for Conjugating the TPP^+ Cations with Functional Moieties (Cargo). Color coding represents three parts of the mitochondria-targeted molecules: targeting moiety (red), linker (green), and functional moiety (blue).

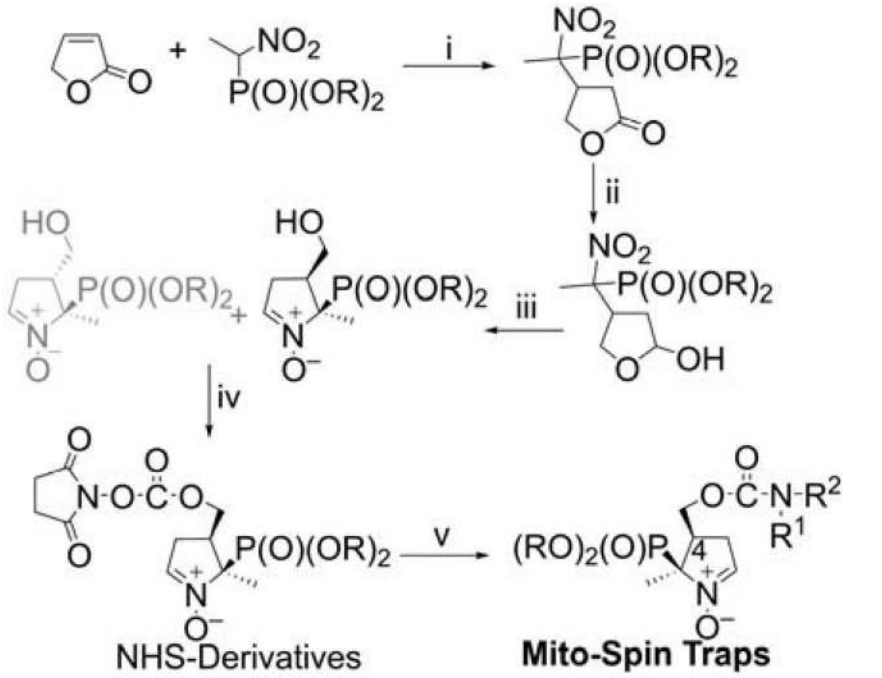

Mito$_2$-DEPMPO: R = Et, R^1 = $(CH_2)_2$-$^+PPh_3,Br^-$, R^2 = H
Mito$_2$-DIPPMPO: R = iPr, R^1 = $(CH_2)_2$-$^+PPh_3,Br^-$, R^2 = H
Mito-bis-DIPPMPO: R = iPr, R^1 = R^2 = $(CH_2)_2$-$^+PPh_3,Br^-$
Mito$_5$-DIPPMPO: R = iPr, R^1 = $(CH_2)_5$-$^+PPh_3,Br^-$, R^2 = H
Mito$_{10}$-DEPMPO: R = Et, R^1 = $(CH_2)_{10}$-$^+PPh_3,Br^-$, R^2 = H
Mito$_{10}$-DIPPMPO: R = iPr, R^1 = $(CH_2)_{10}$-$^+PPh_3,Br^-$, R^2 = H

Chart 19.
Scheme of Synthesis of Mitochondria-Targeted Spin Traps Based on

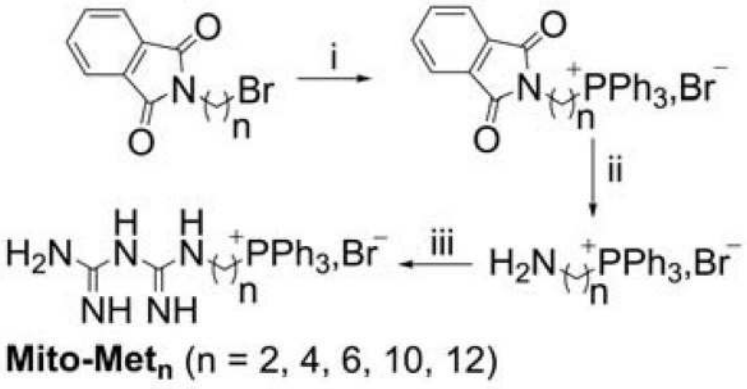

Chart 20.

Synthetic Pathway for Mitochondria-Targeted Metformins, Mito-Met_n. Reagents and conditions: i, PPh_3, ACN, reflux, 70–80%; ii, NH_2-NH_2, EtOH, reflux, 75–80%; iii, HCl, sodium dicyanamide, neat, 180°C, 25–40%.

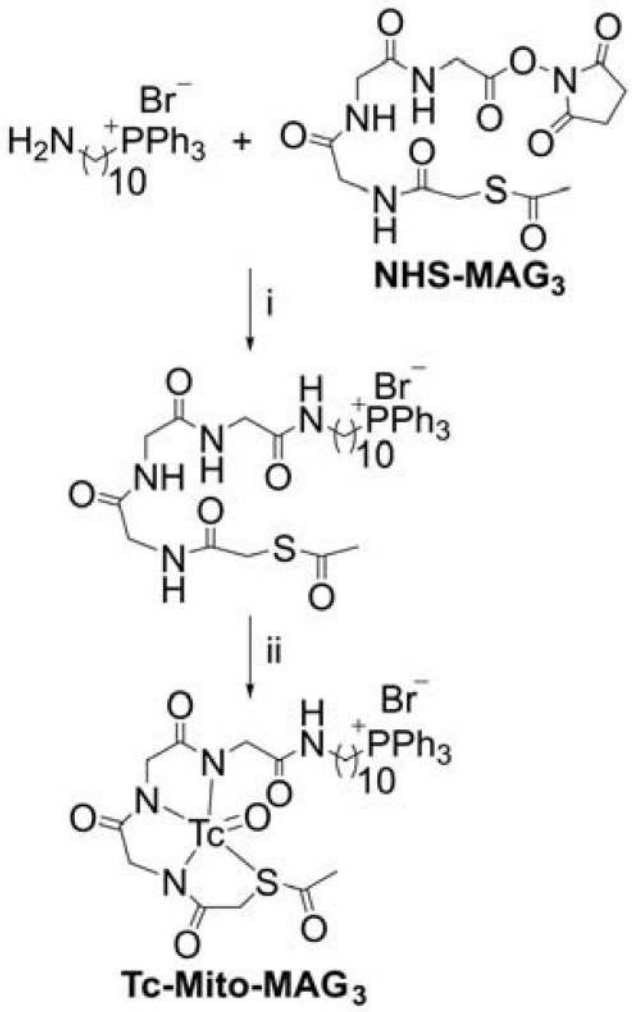

Chart 21.

Synthesis of ^{99m}Tc-Mito-MAG$_3$ Probe. Reagents and conditions: i, DMSO, TEA, rt, 50%; ii, radiolabeling with ^{99m}Tc, 92%.

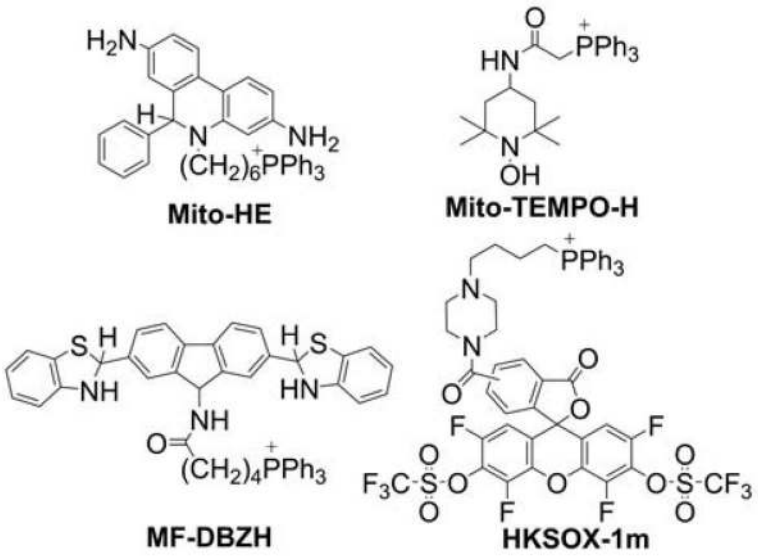

Chart 22.
Mitochondria-Targeted Probes for $O_2^{\bullet-}$

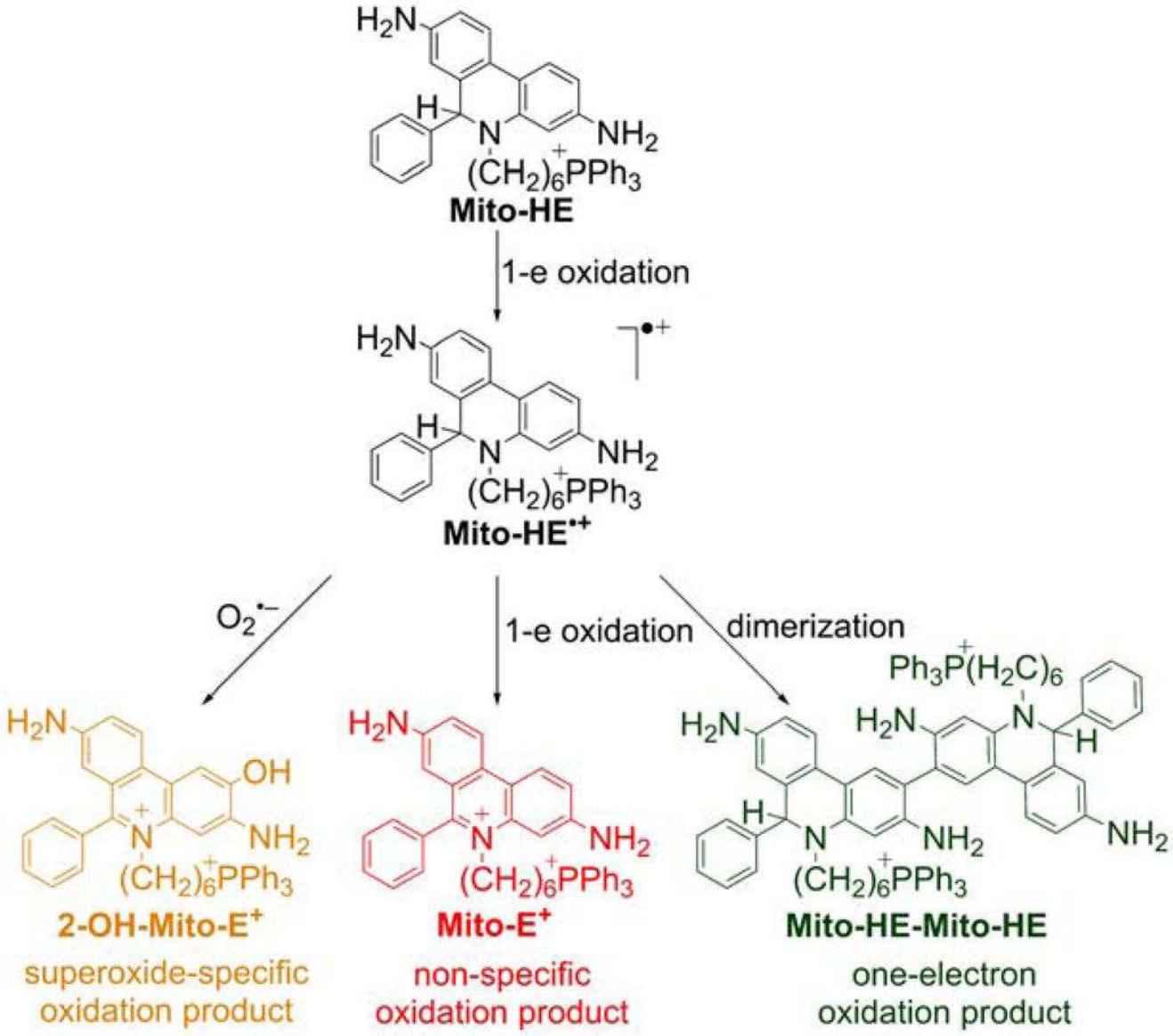

Chart 23.

Formation of Superoxide-Specific and Nonspecific Oxidation Products of Mito-HE (or MitoSOX Red)

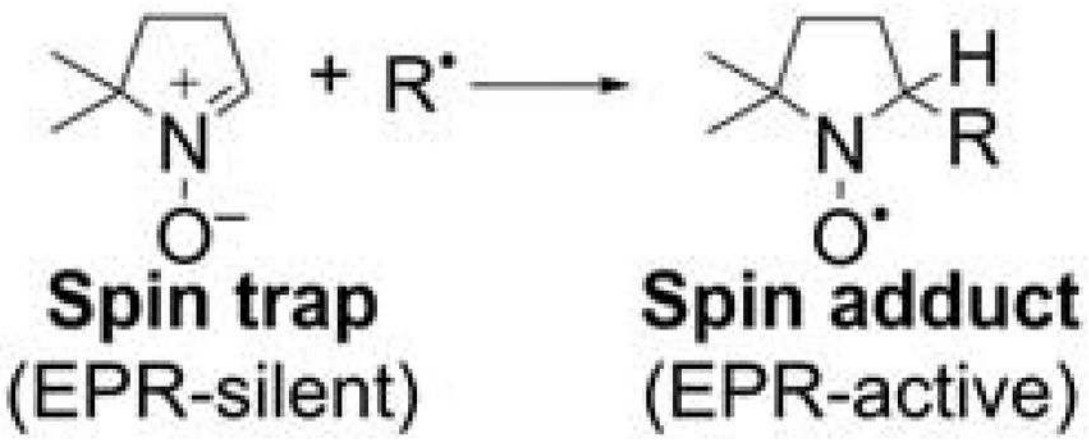

Chart 24.
EPR Spin Trapping of Short-Lived Radicals, Using a Cycling Nitrone

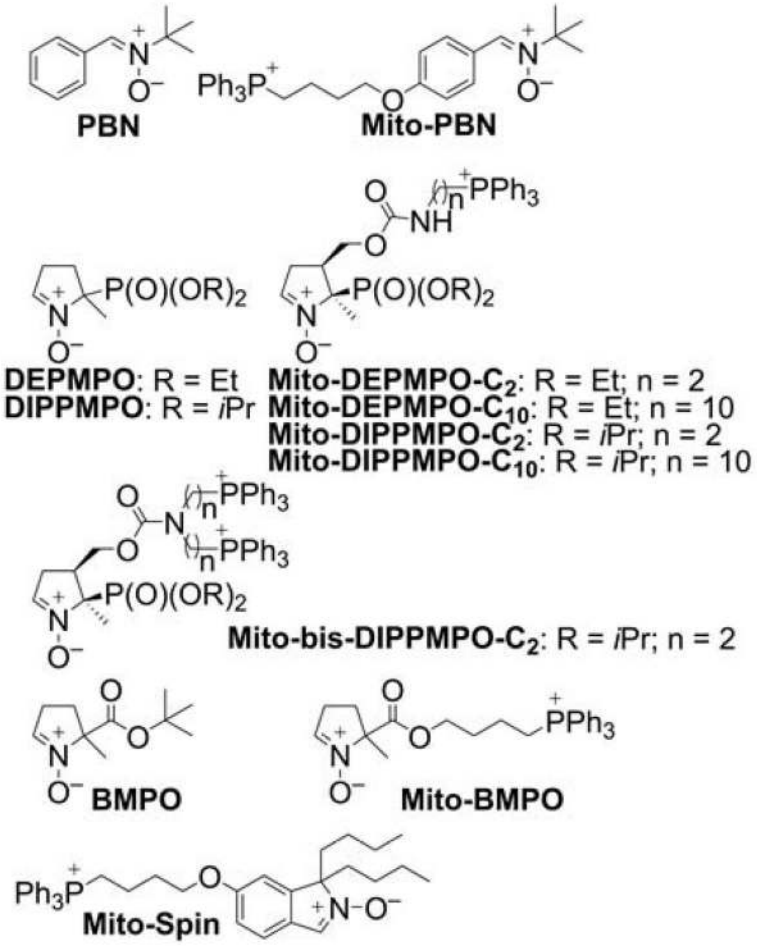

Chart 25.
Spin Traps and Their Mitochondria-Targeted Analogs

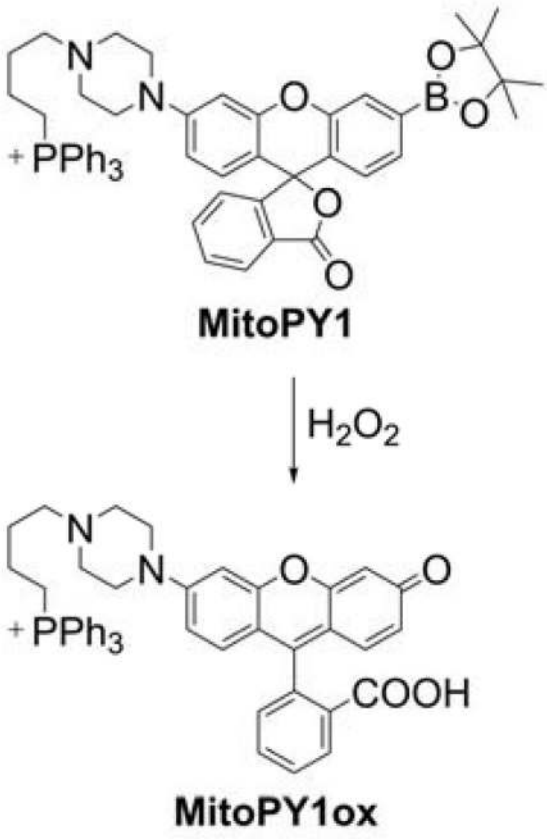

Chart 26.
Mitochondria-Targeted Boronate-Based Probe, MitoPY1

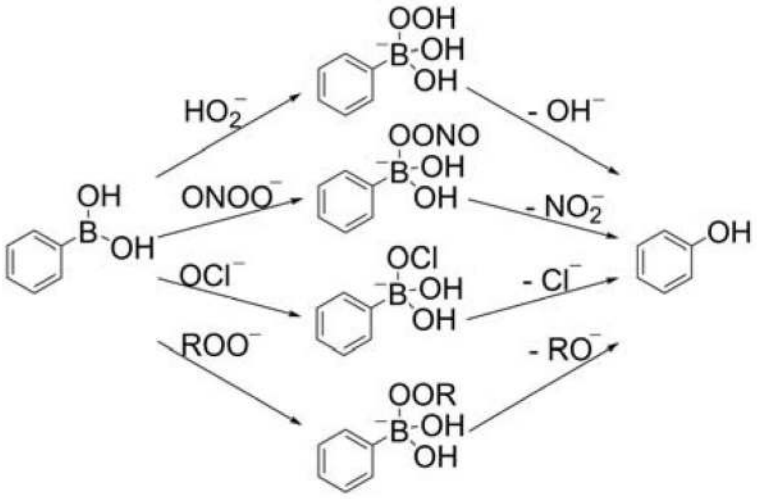

Chart 27.
Oxidation of Arylboronates by Various Oxidants

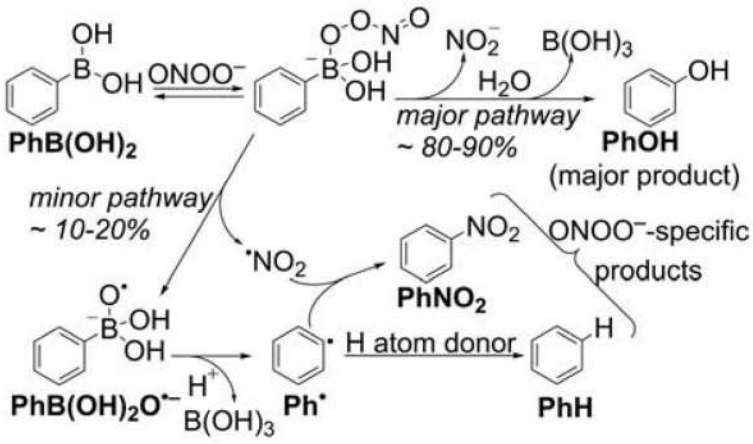

Chart 28.

Mechanism and Products of the Reaction Between Arylboronates and $ONOO^-$

***p*-MitoPhB(OH)$_2$** ***m*-MitoPhB(OH)$_2$** ***o*-MitoPhB(OH)$_2$**
(MitoB)

Chart 29.
Mitochondria-Targeted Phenylboronate Probes

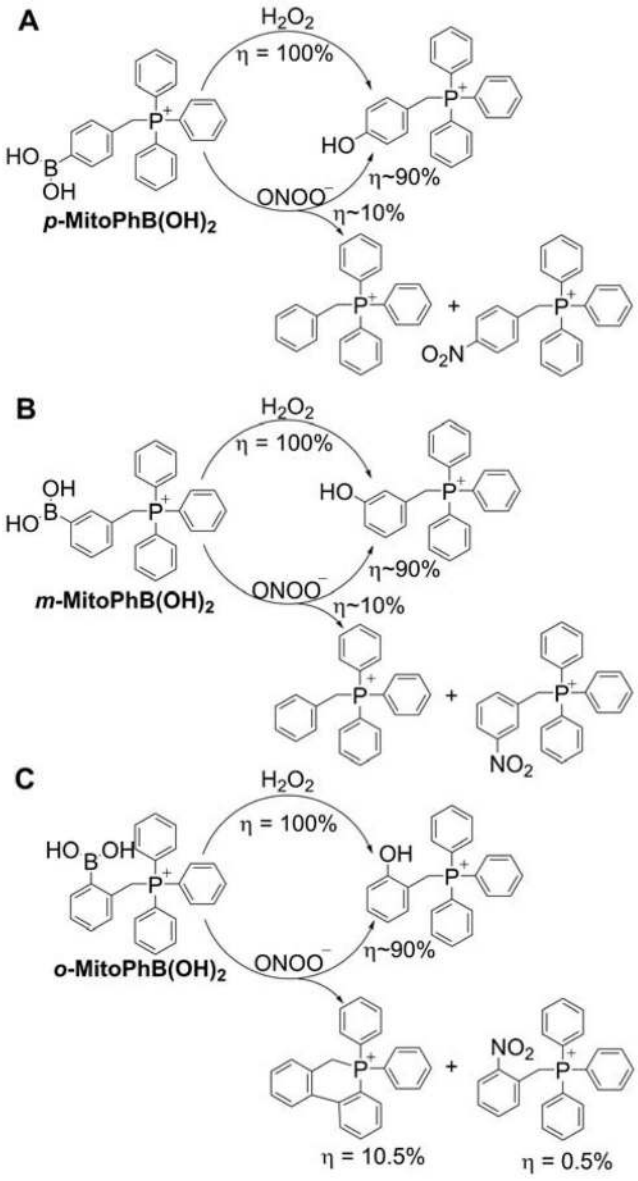

Chart 30.

Formation of Peroxynitrite-Specific Products from (A) *Para*, (B) *Meta,* and (C) *Ortho* Isomers of MitoPhB(OH)$_2$

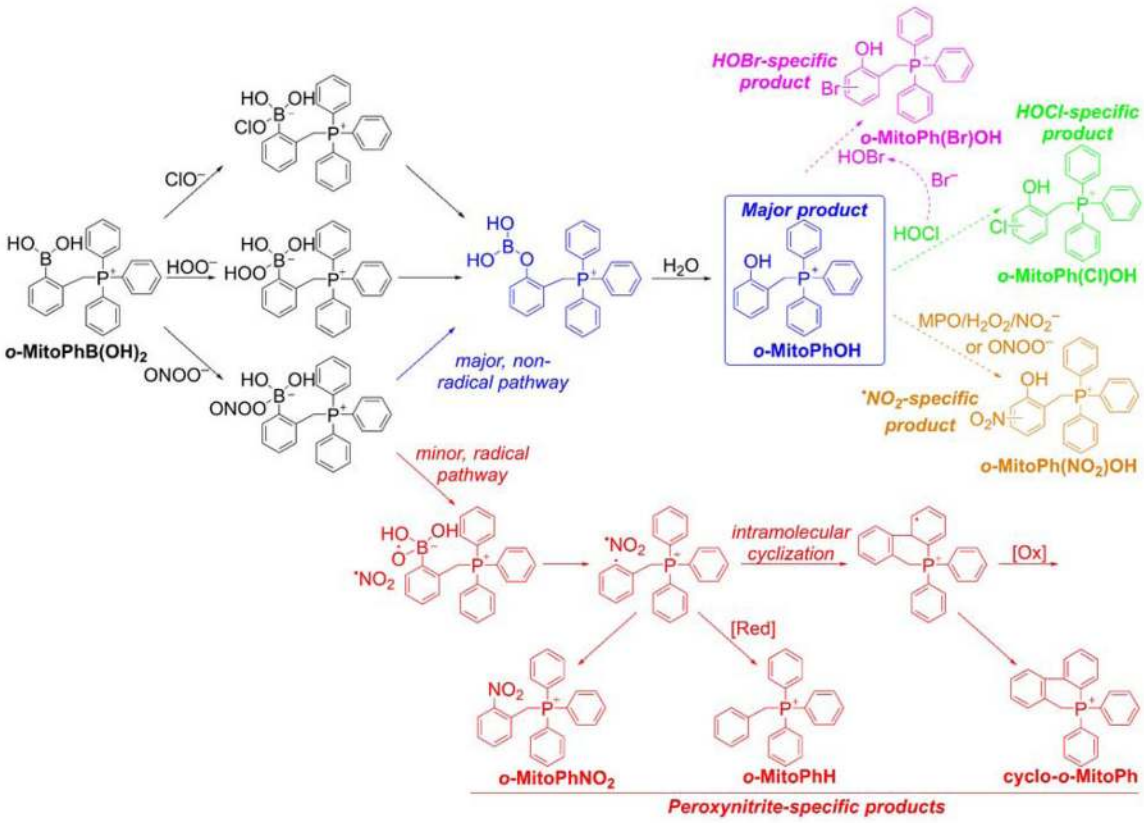

Chart 31.

Products Formed and Detected upon Oxidation of the *ortho*-MitoPhB(OH)$_2$ Probe by Different Oxidants. The peroxynitrite-specific, minor pathway and products are shown in red. (Adapted with permission from Ref.[286]. This research was originally published in The Journal of Biological Chemistry. Zielonka J, Zielonka M, VerPlank L, Cheng G, Hardy M, Ouari O, Ayhan MM, Podsiadly R, Sikora A, Lambeth JD. Mitigation of NADPH Oxidase 2 Activity as a Strategy to Inhibit Peroxynitrite Formation. The Journal of Biological Chemistry. 2016; 291:7029–7044. © the American Society for Biochemistry and Molecular Biology.)

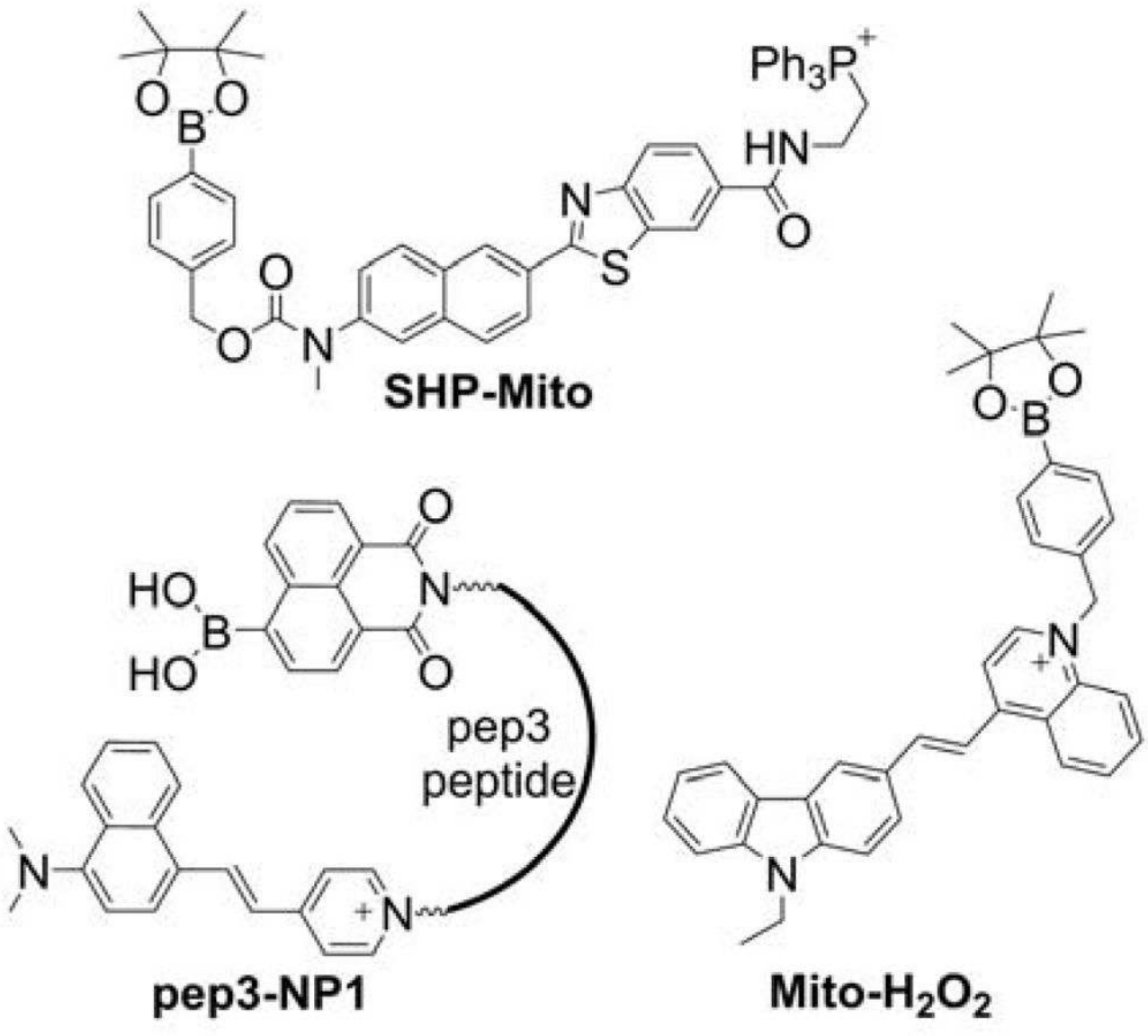

Chart 32.
Mitochondria-Targeted Boronate Probes: SHP-Mito, pep3-NP1, and Mito-H_2O_2

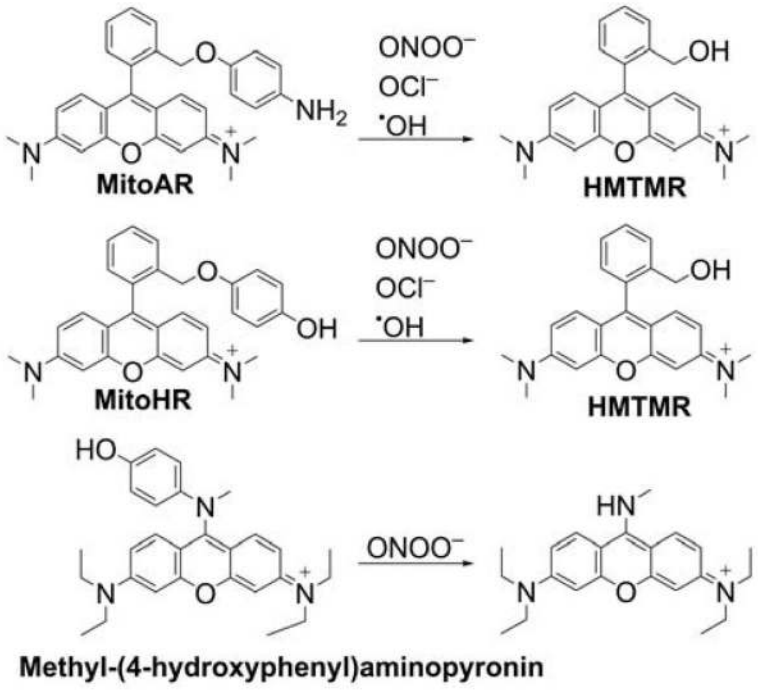

Chart 33.
Mitochondria-Accumulating Rhodamine-Based Probes for Peroxynitrite and Other Oxidants

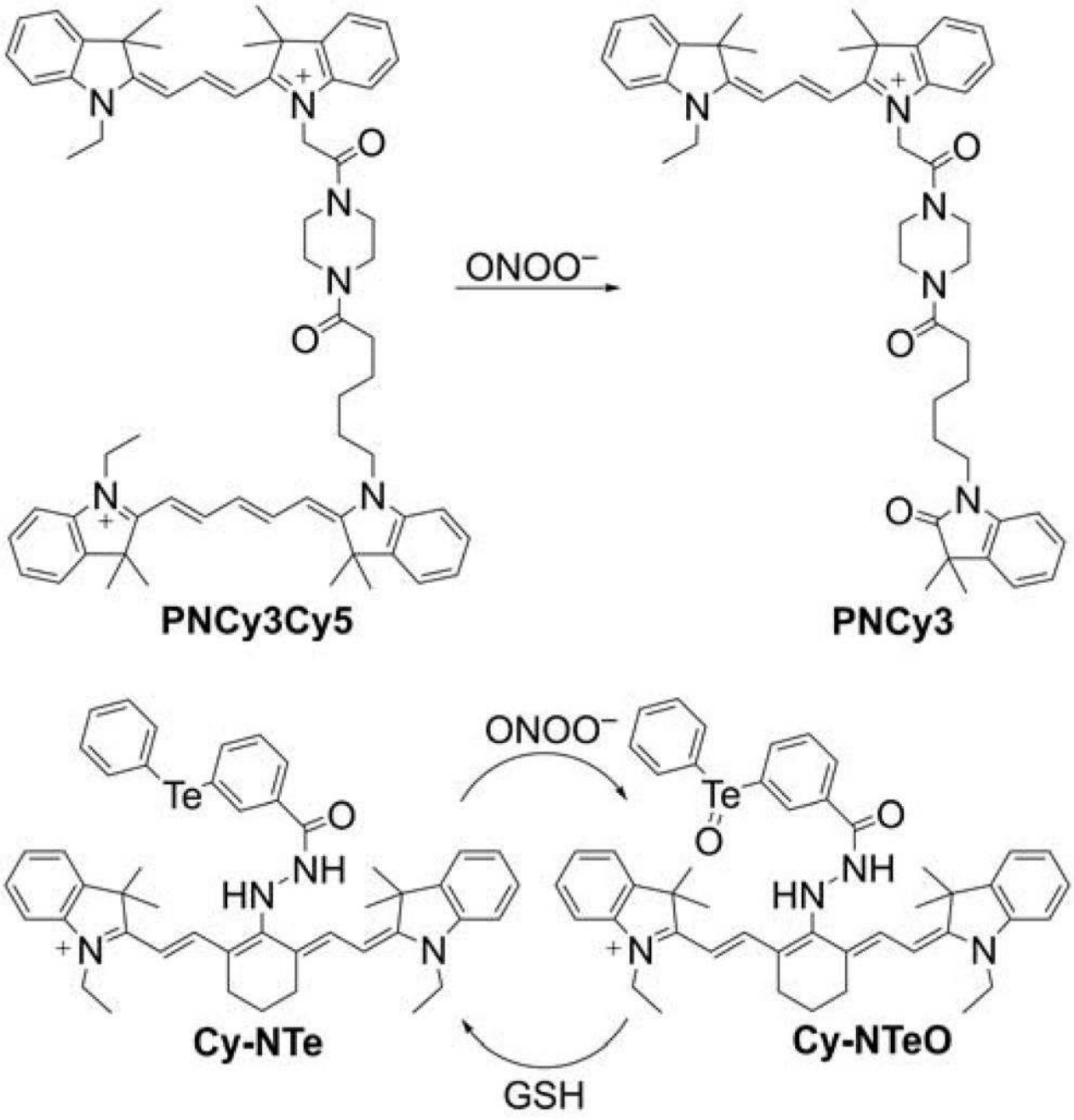

Chart 34.
Cyanine-Based Mitochondria-Targeted Probes for Peroxynitrite

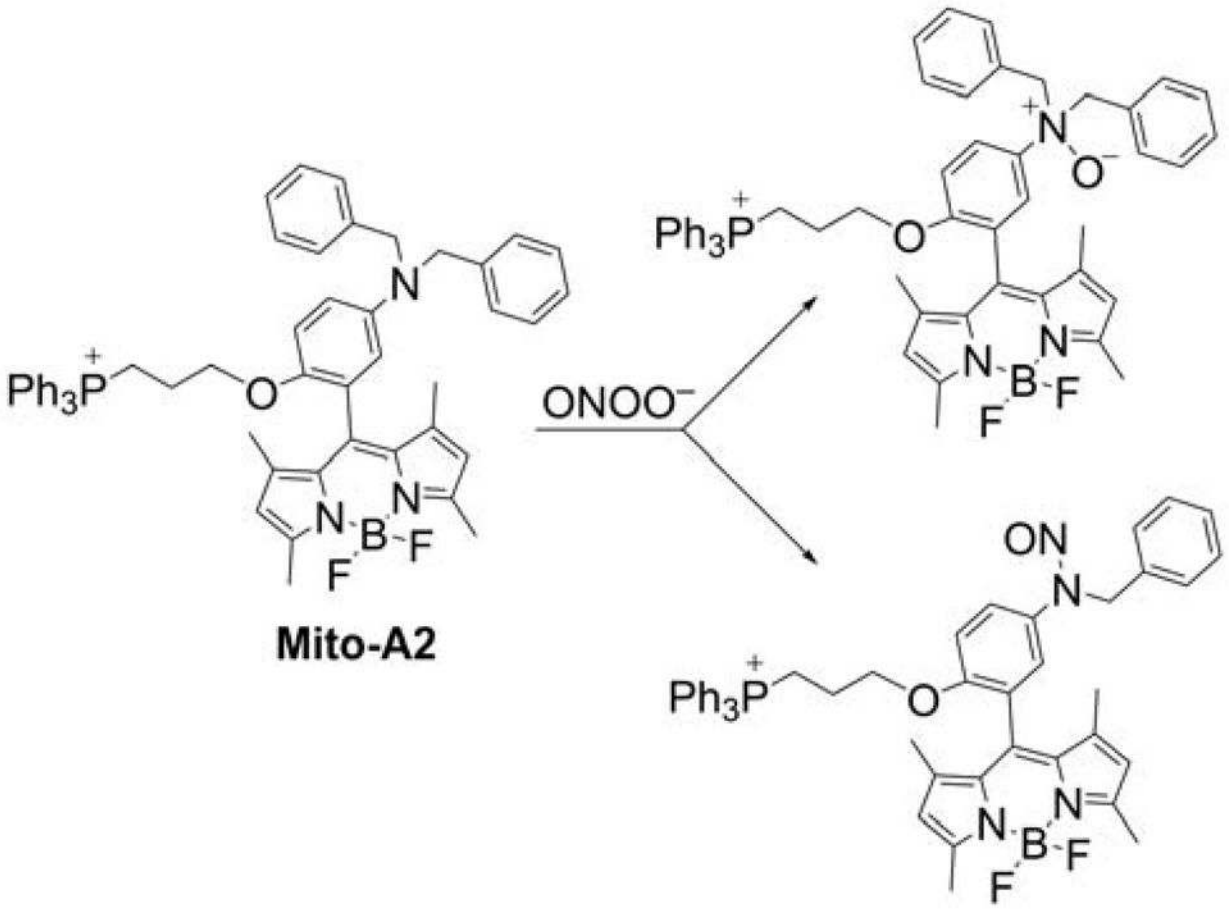

Chart 35.
Mito-A2 probe for Mitochondrial Peroxynitrite

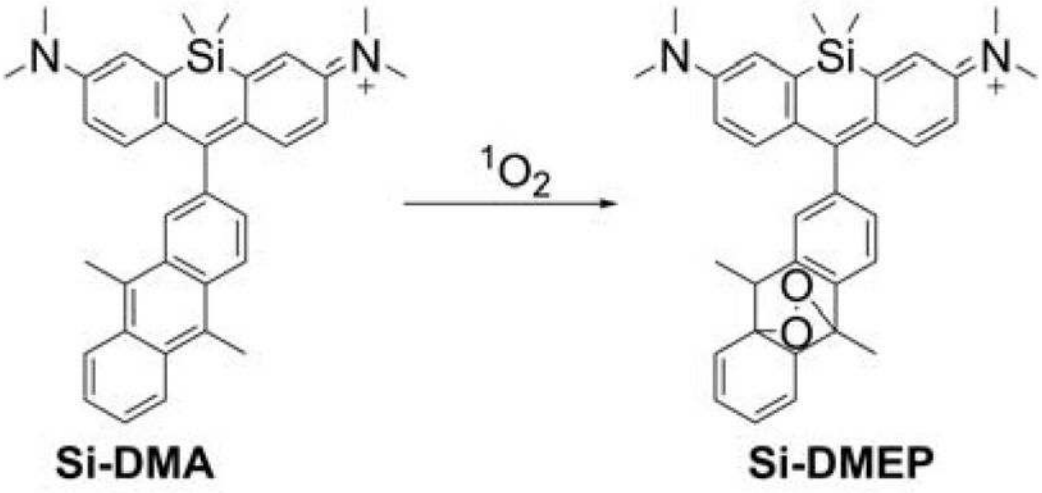

Chart 36.
Mitochondria-Targeted Probes for Singlet Oxygen

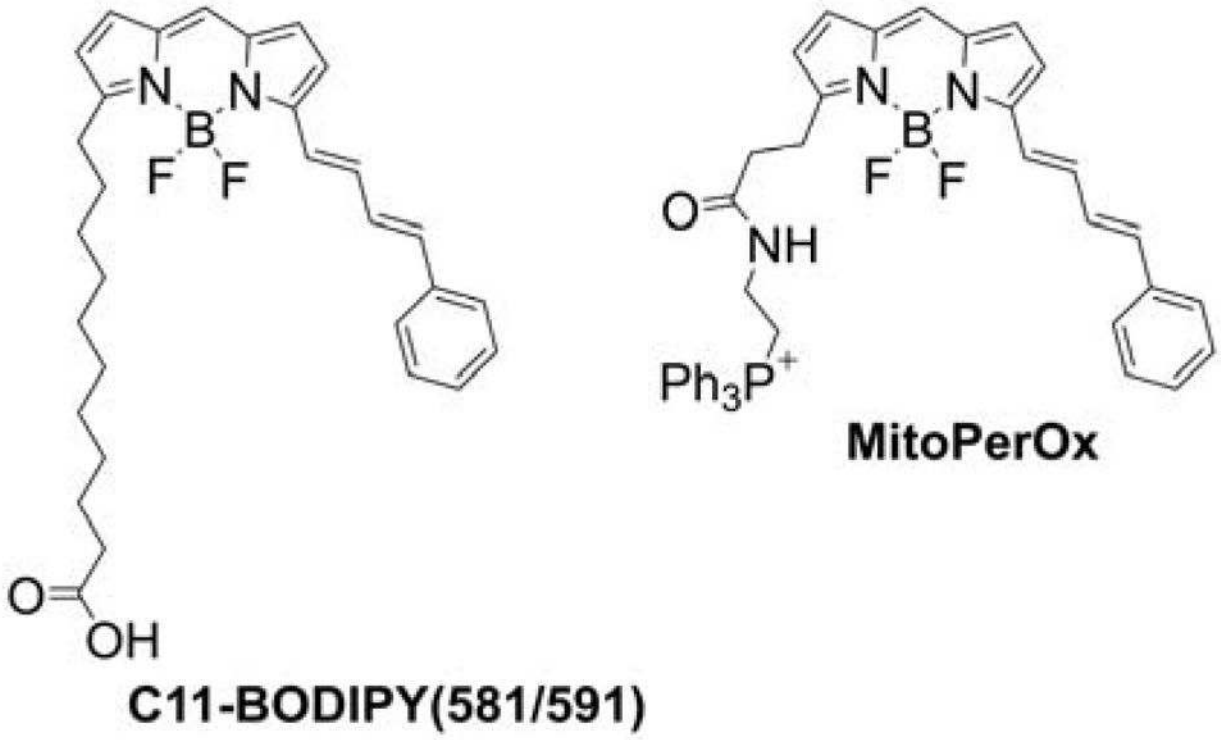

Chart 37.

C11-BODIPY(581/591) Probe and Its Mitochondria-Targeted Analog, MitoPerOx, for Reporting Lipid Peroxidation

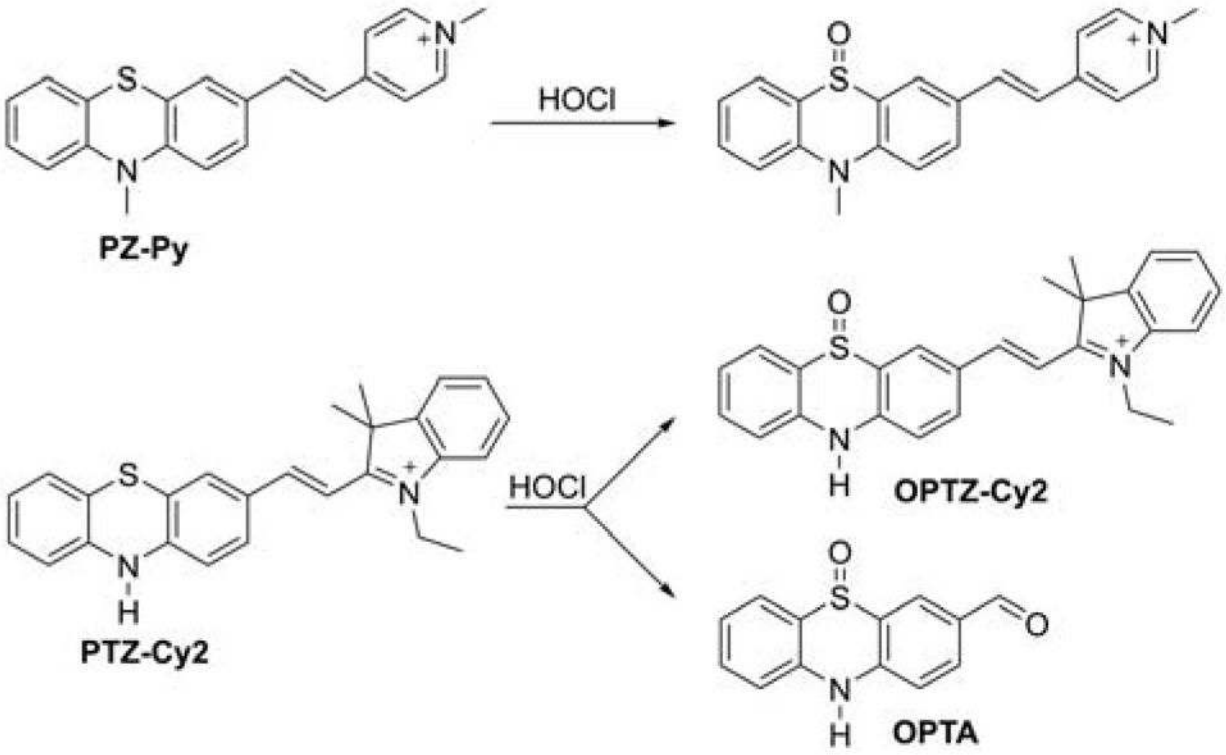

Chart 38.
Phenothiazine-Based Mitochondria-Targeted Probes Designed for HOCl

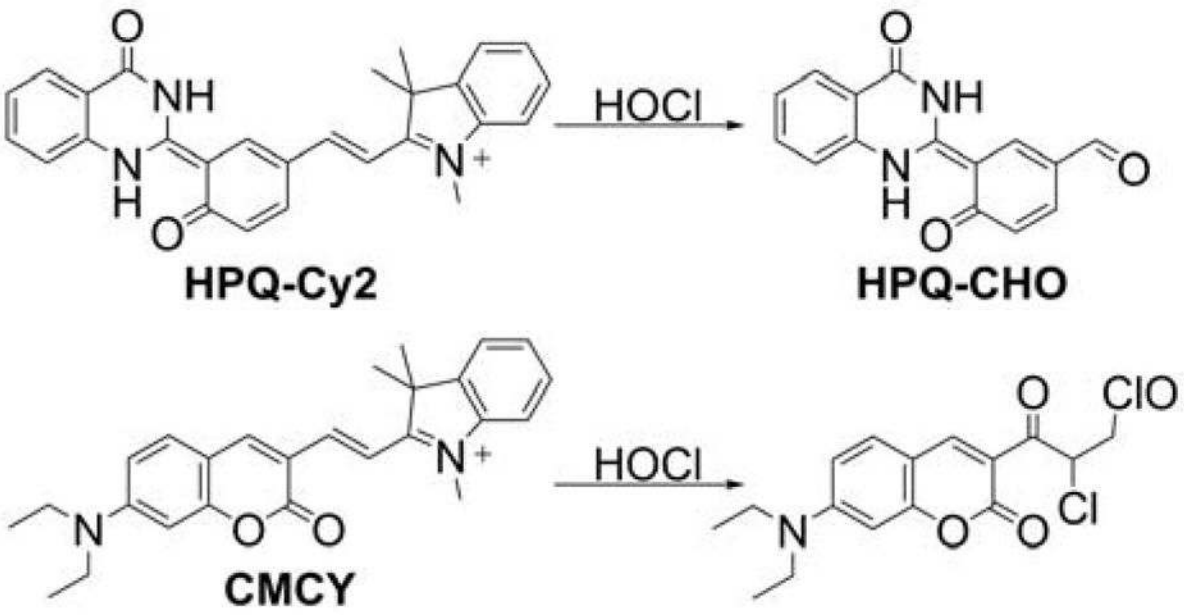

Chart 39.
Cyanine-Based Mitochondria-Targeted Probes for HOCl

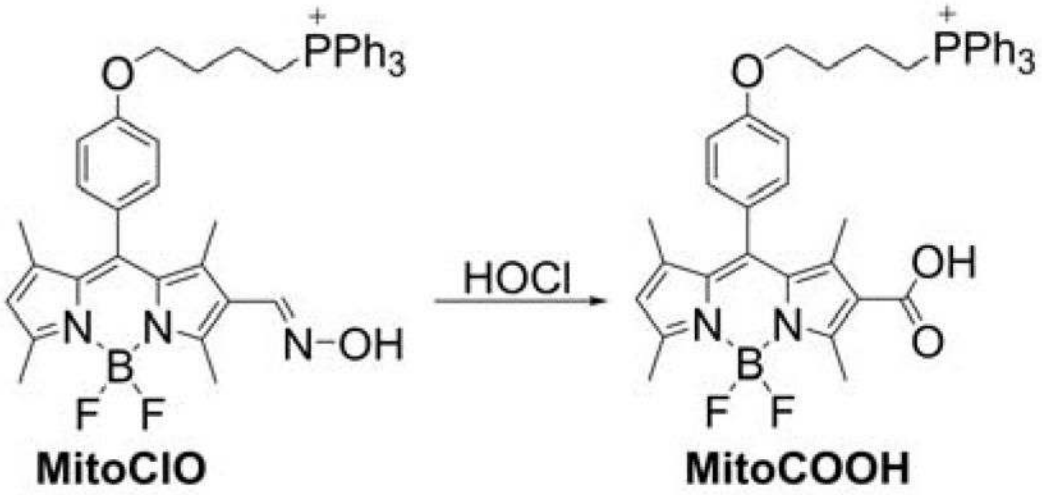

Chart 40.
MitoClO Probe for HOCl

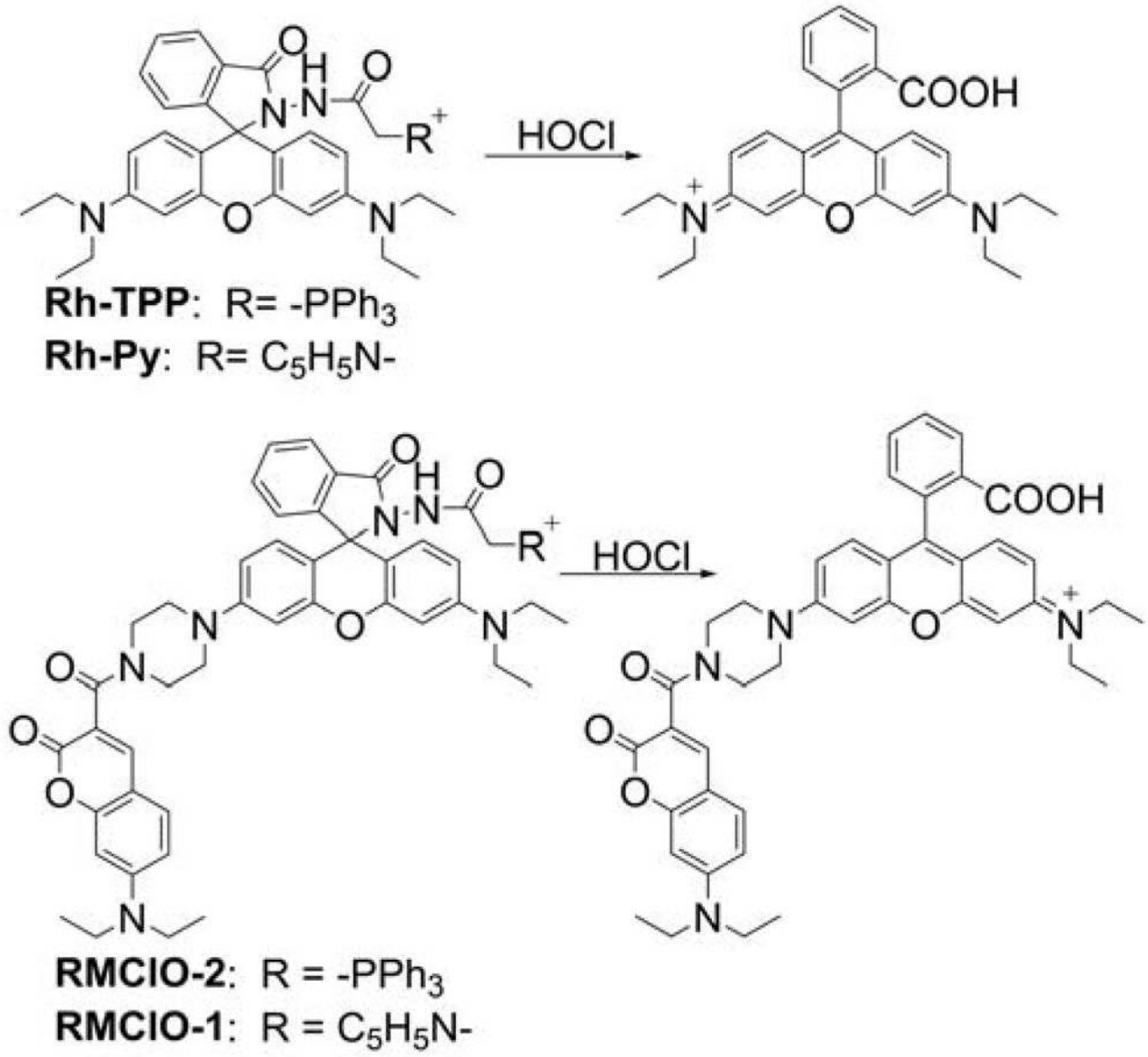

Chart 41.

Rh-TPP, Rh-Py, RMClO-1, and RMClO-2 Probes for Mitochondrial HOCl Other mitochondria-targeted probes reported for HOCl detection include MITO-TP (Chart 42), based on the acedan fluorophore and iridium(III) complexes, with the diaminomaleonitrile moiety as the HOCl-reactive reporter group.[317–319]

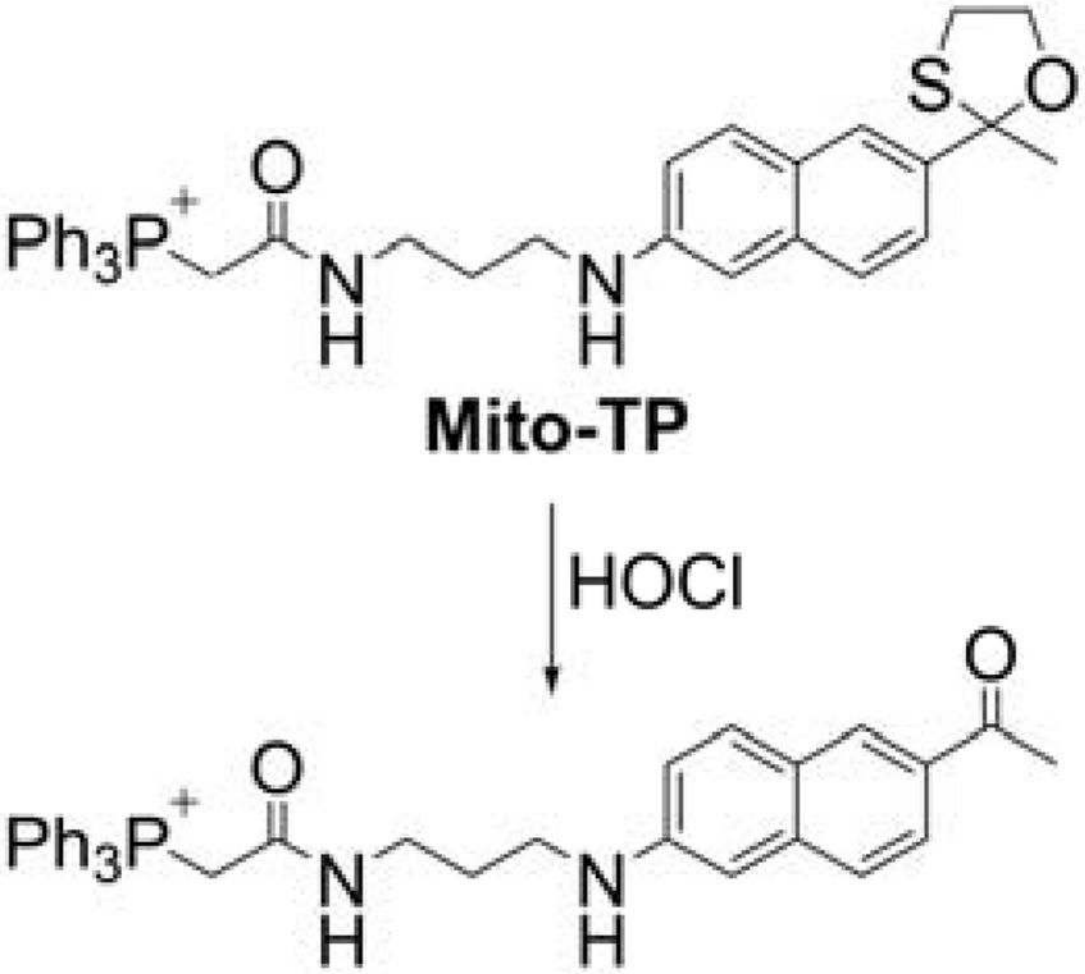

Chart 42.
Mito-TP Probe for Mitochondrial HOCl

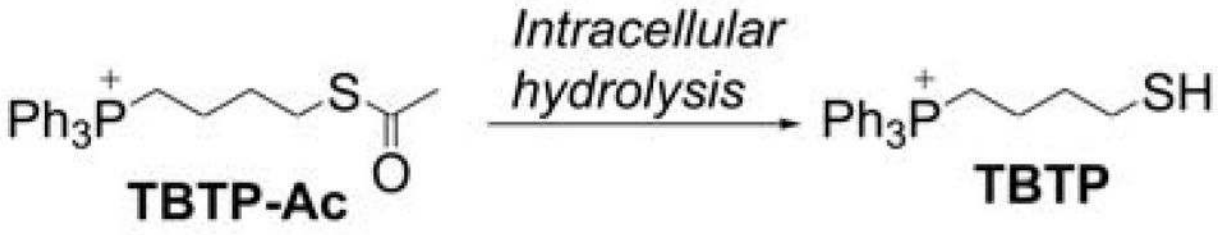

Chart 43.
TBTB Probes for Mitochondrial Thiol Redox Status

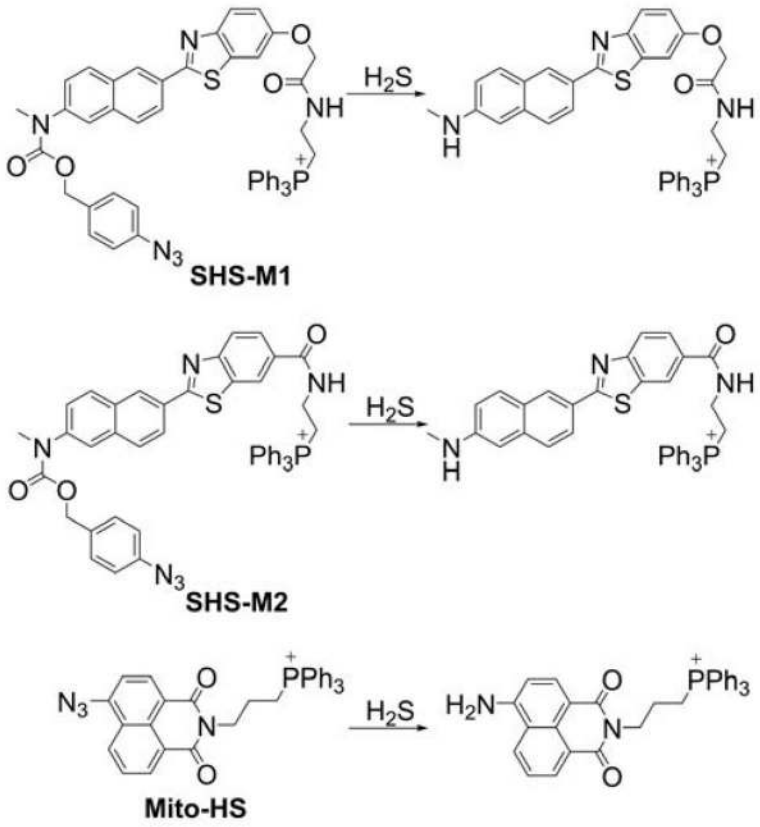

Chart 44.

Mitochondria-Targeted Probes for the Detection of H_2S, Based on Reduction of the Azidyl Group

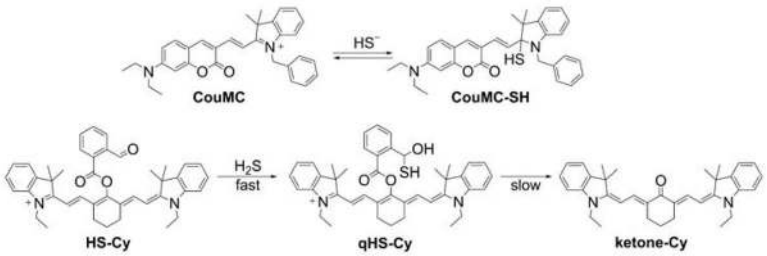

Chart 45.

Mitochondria-Targeted Probes for Detecting H_2S, Based on the Nucleophilic Addition Mechanisms

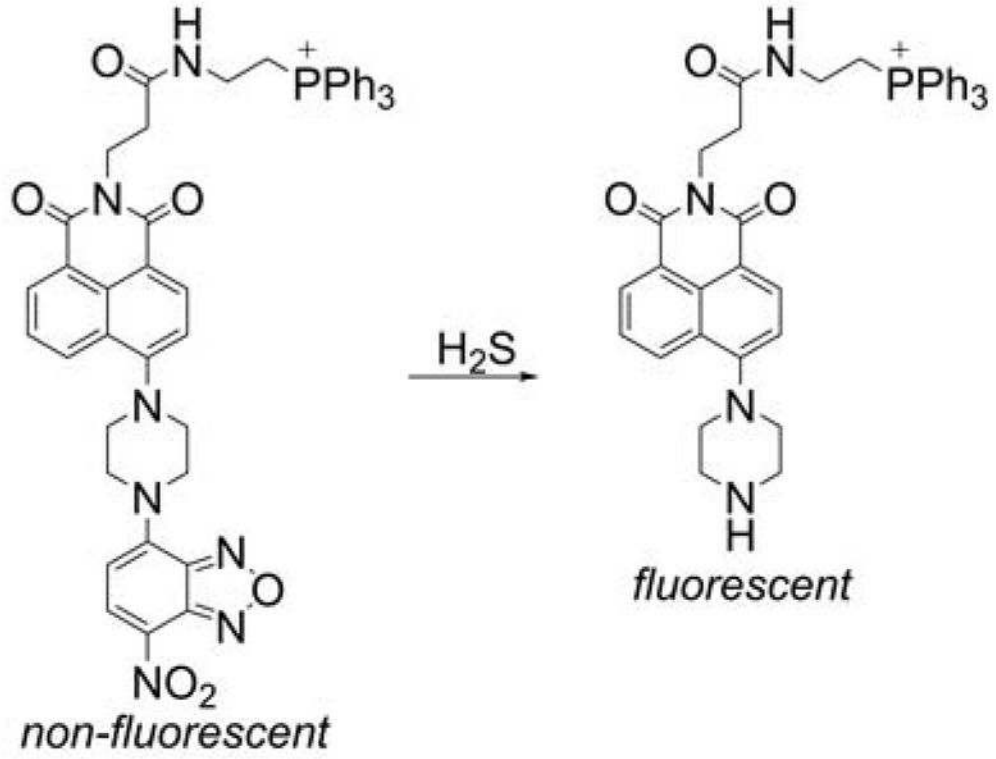

Chart 46.

Mitochondria-Targeted Probes for detecting H_2S, Based on Thiolysis of the 7-nitro-1,2,3-benzodiazole Amine Moiety

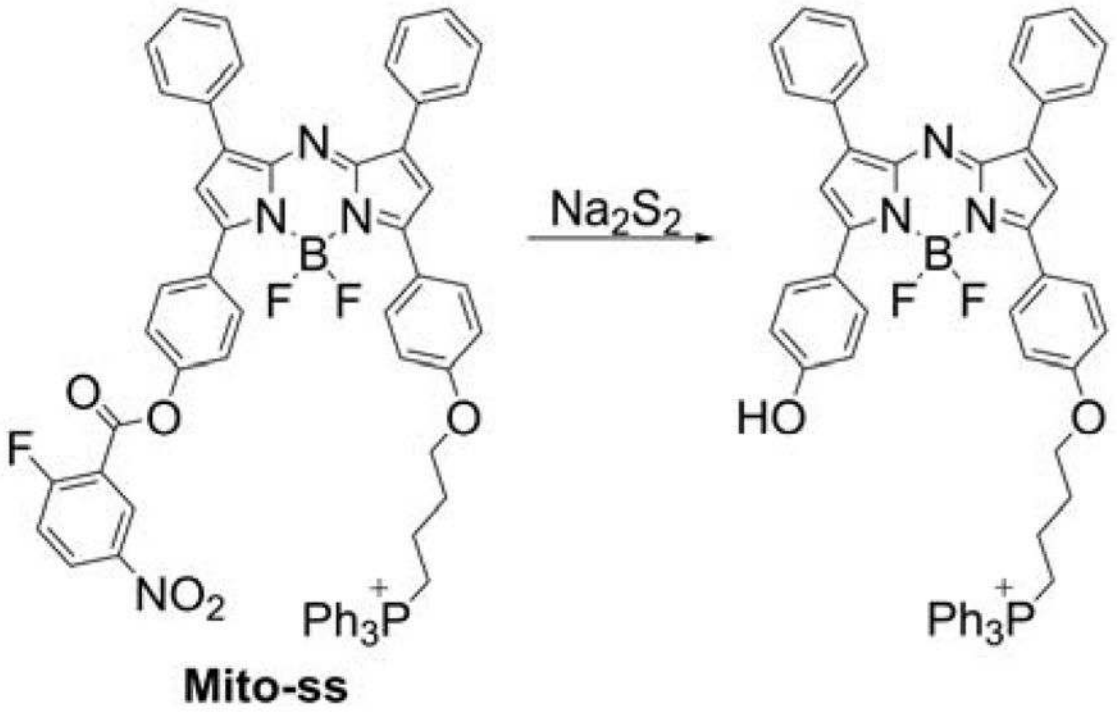

Chart 47.
Mitochondria-Targeted Probe for Polysulfides, Mito-ss.

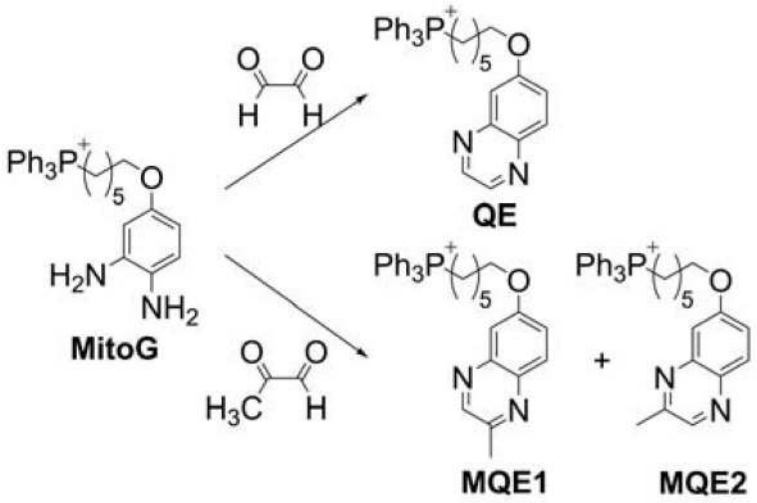

Chart 48.
Mitochondria-Targeted Probe for Glyoxals, MitoG

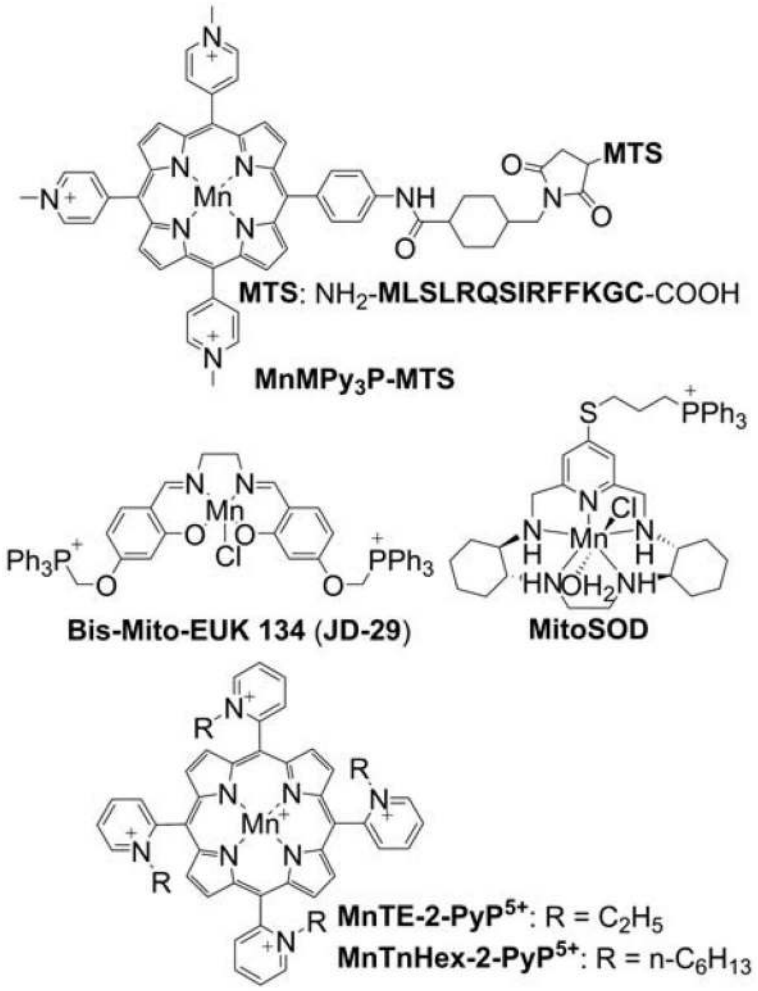

Chart 49.
Mitochondria-Targeted Macrocyclic SOD Mimetics

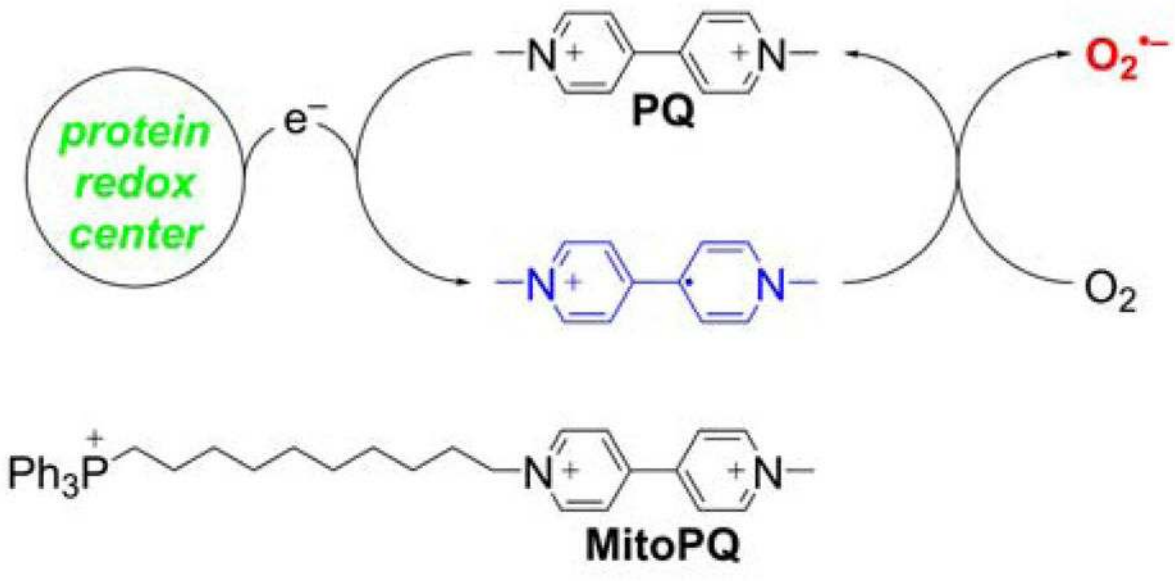

Chart 50.
Redox Cycling of PQ and Structure of MitoPQ

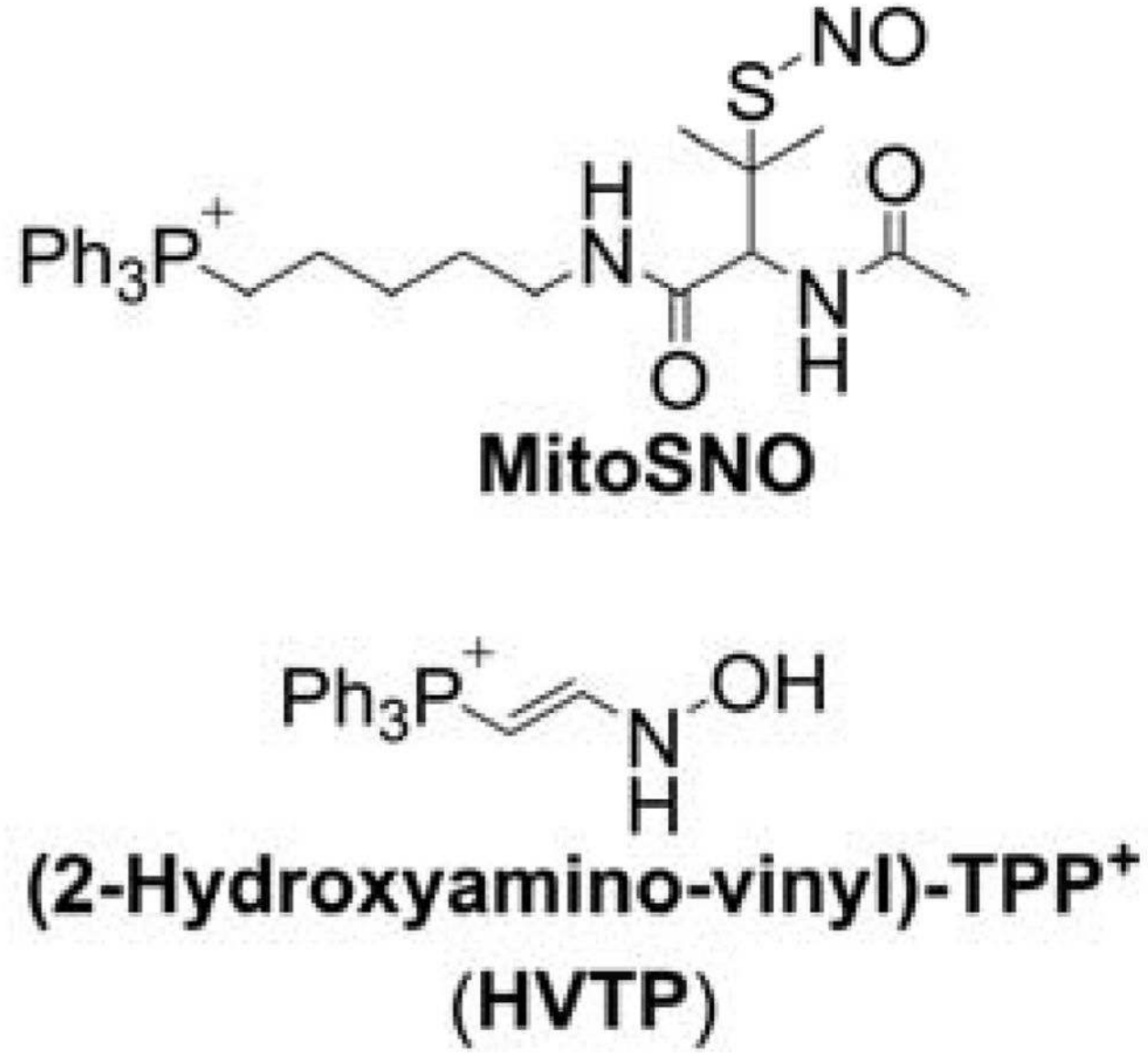

Chart 51.
Structures of MitoSNO and HVTP Donors

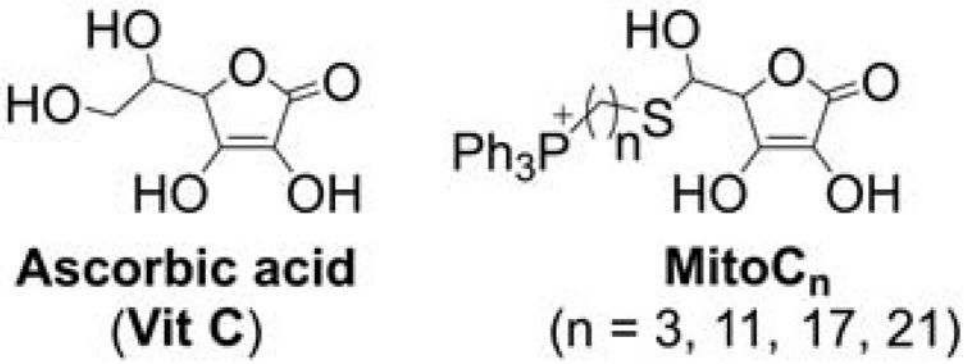

Chart 52.
Ascorbic Acid and MitoVitC

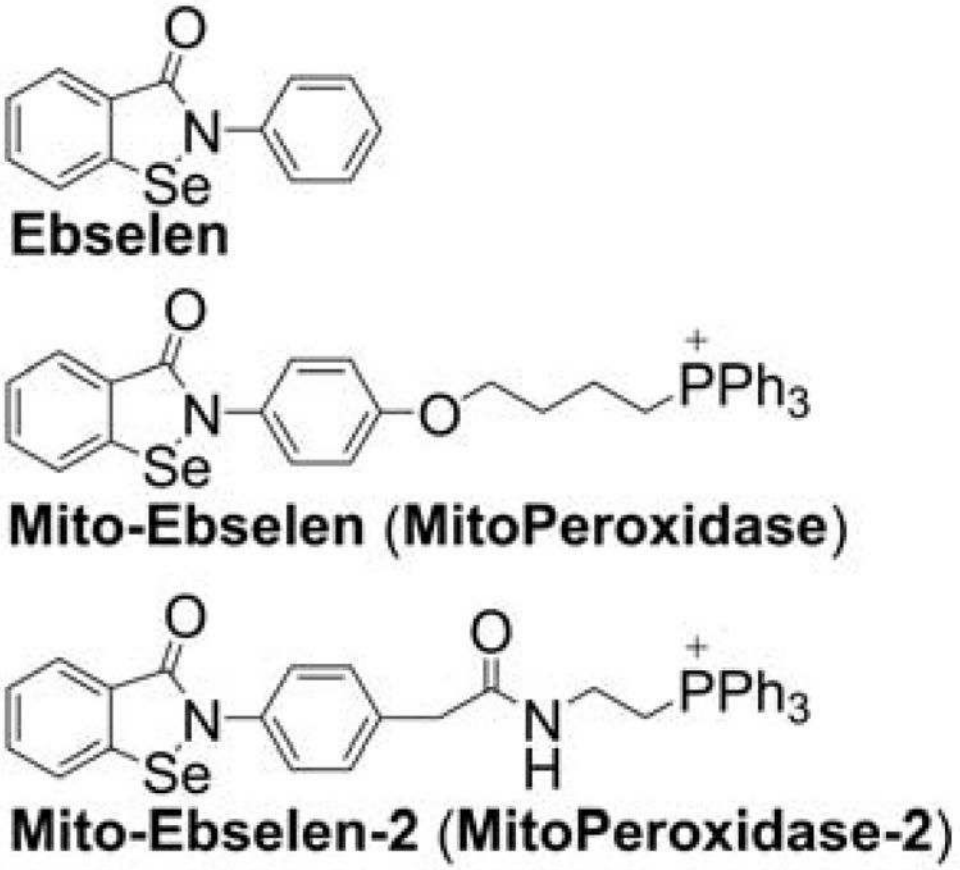

Chart 53.
Ebselen and Mito-Ebselens

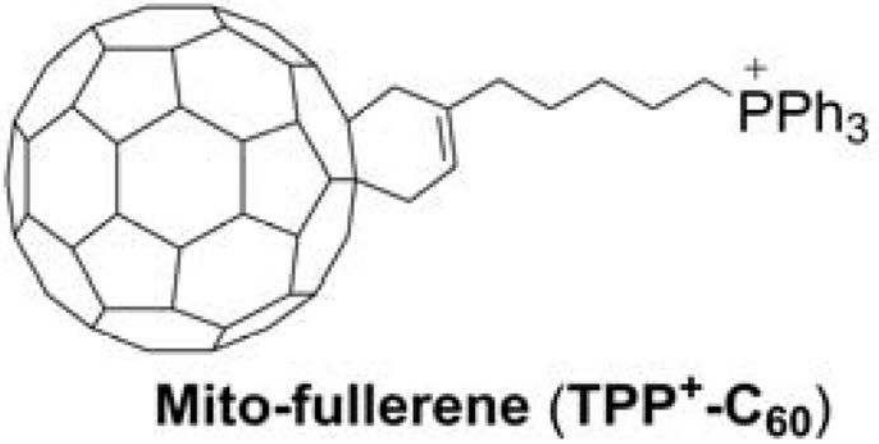

Chart 54.
Mitochondria-Targeted Fullerene

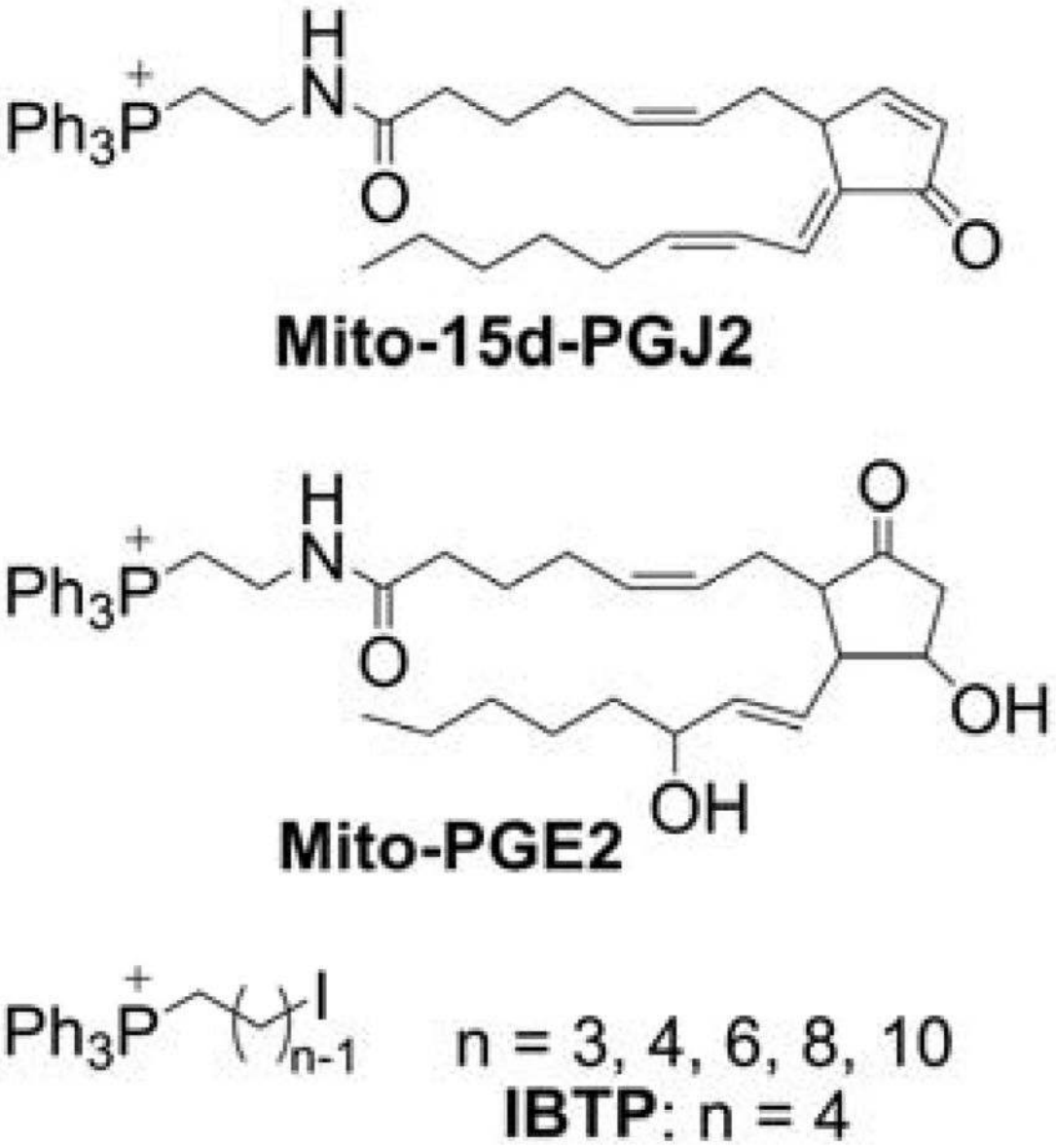

Chart 55.
Structures of Mitochondria-Targeted Electrophiles

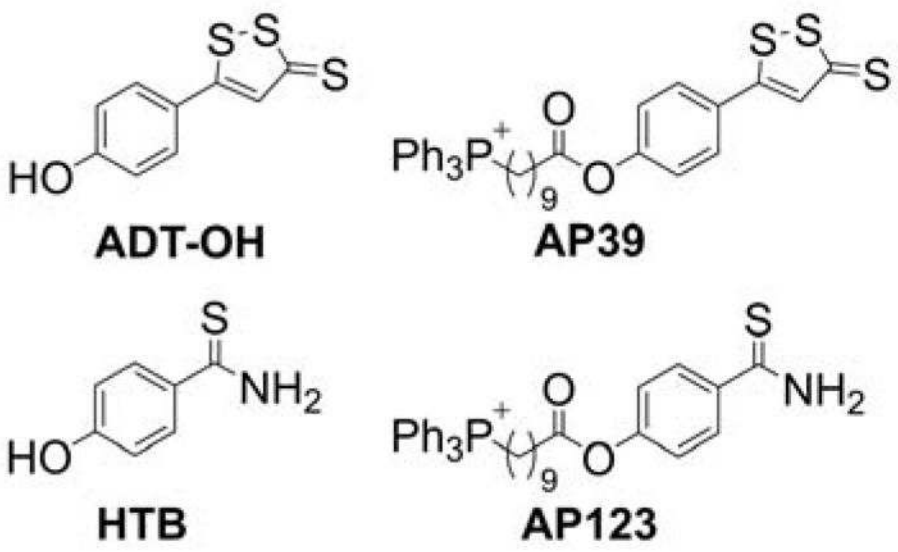

Chart 56.

H_2S Donors, ADT-OH and HTB, and Their Mitochondria-Targeted Analogs, AP39 and AP123

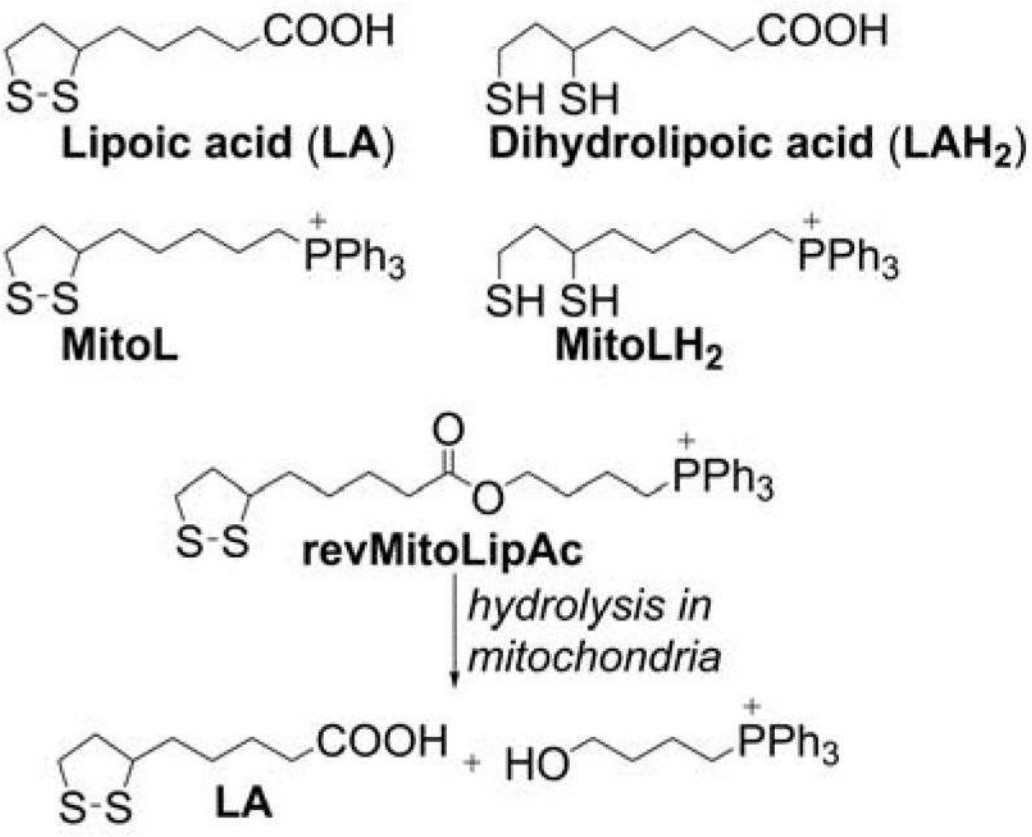

Chart 57.
Lipoic Acid and its Mitochondria-Targeted Analogs

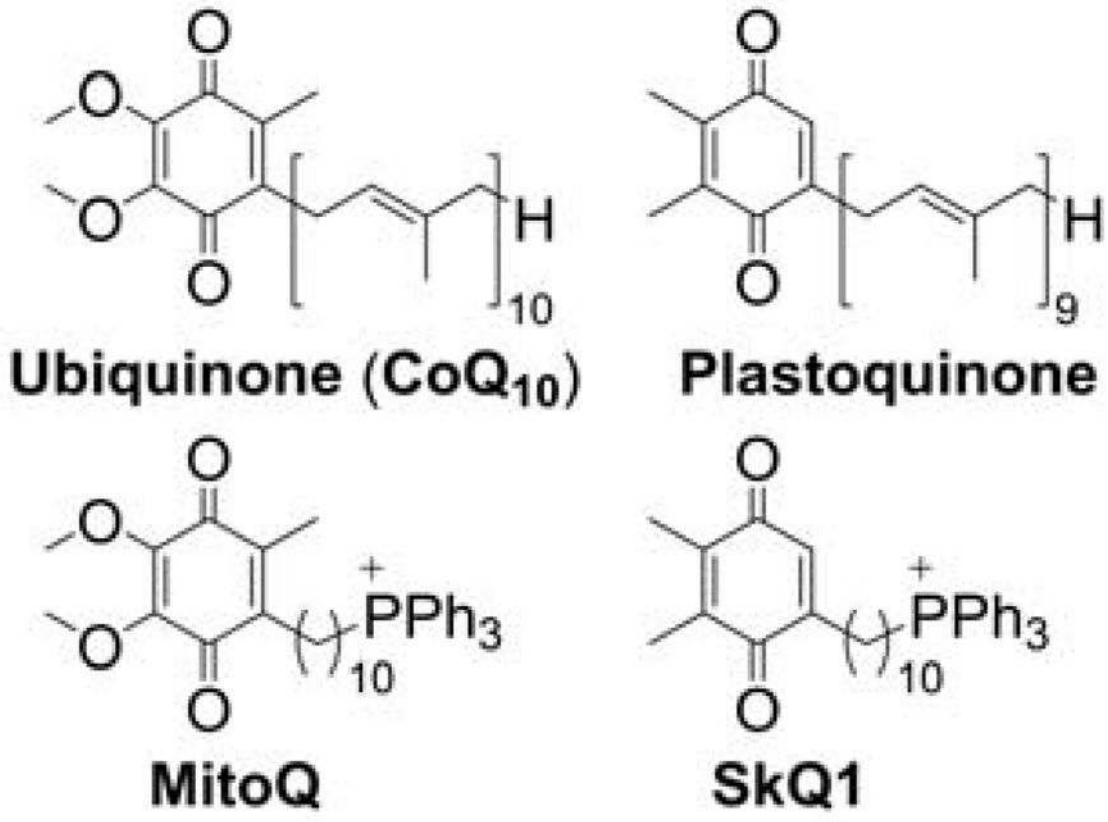

Chart 58.
Ubiquinone and Plastoquinone and Their Mitochondria-Targeted Analogs (MitoQ and SkQ1, Respectively)

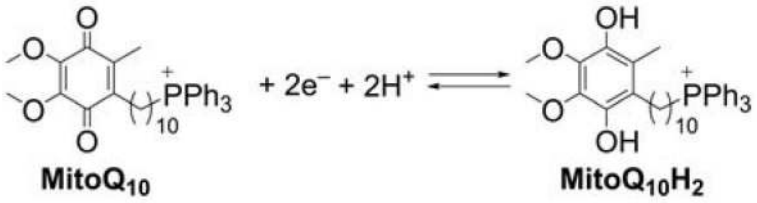

Chart 59.
Two-electron Redox Equilibrium of MitoQ/MitoQH_2 Couple

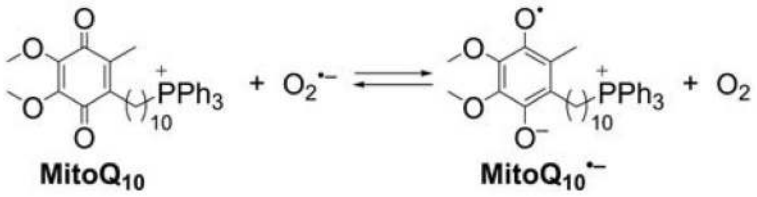

Chart 60.
Redox Equilibrium Between MitoQ and $O_2^{\bullet-}$

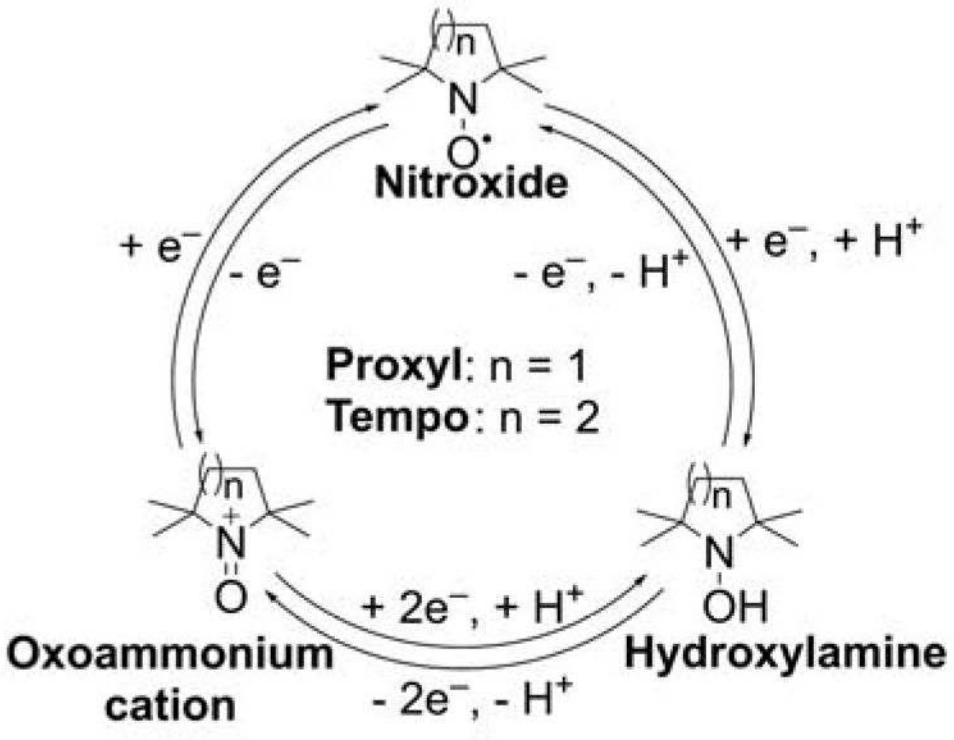

Chart 61.
Redox Cycle of Nitroxide Radicals

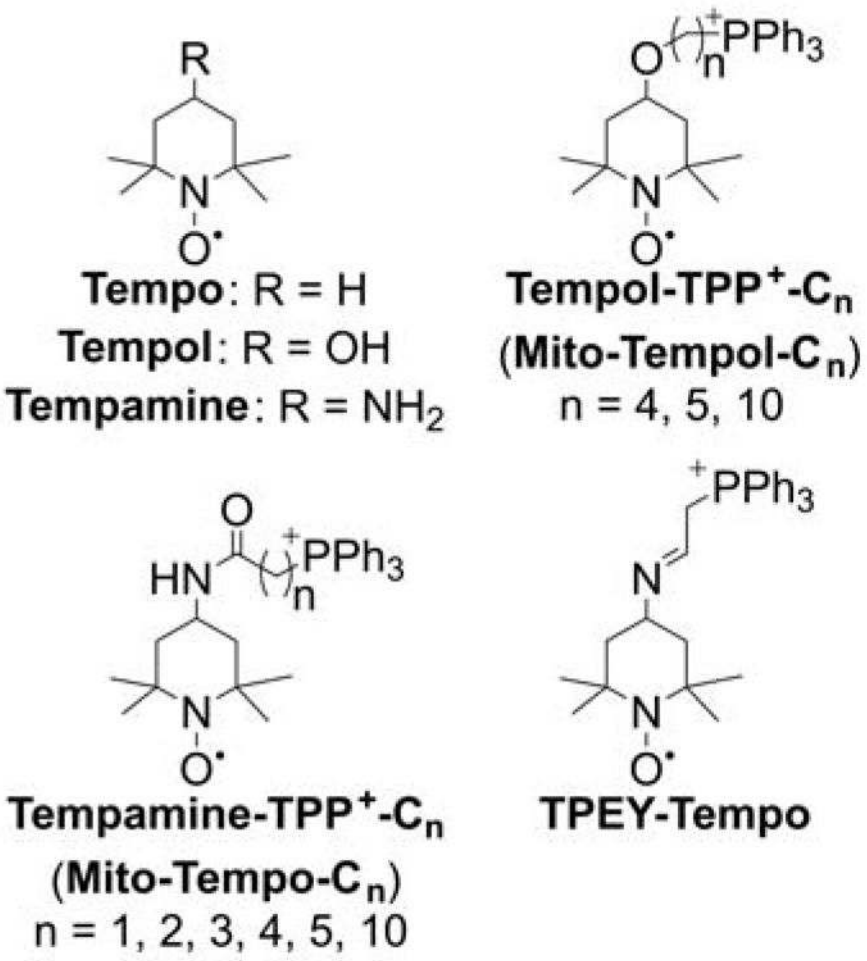

Chart 62.
Structures of Tempo and Mito-Tempo Analogs[160,265,340,418,419]

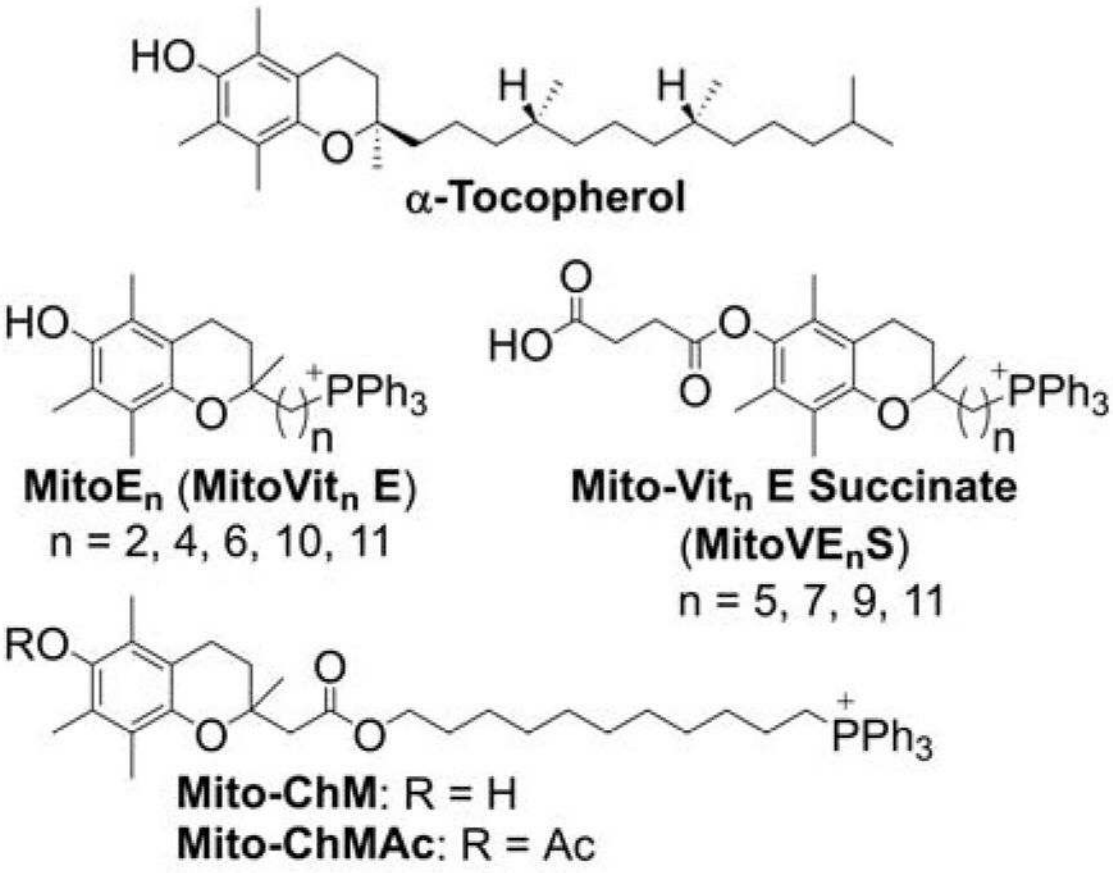

Chart 63.
α-Tocopherol, Mito-Vit E Analogs

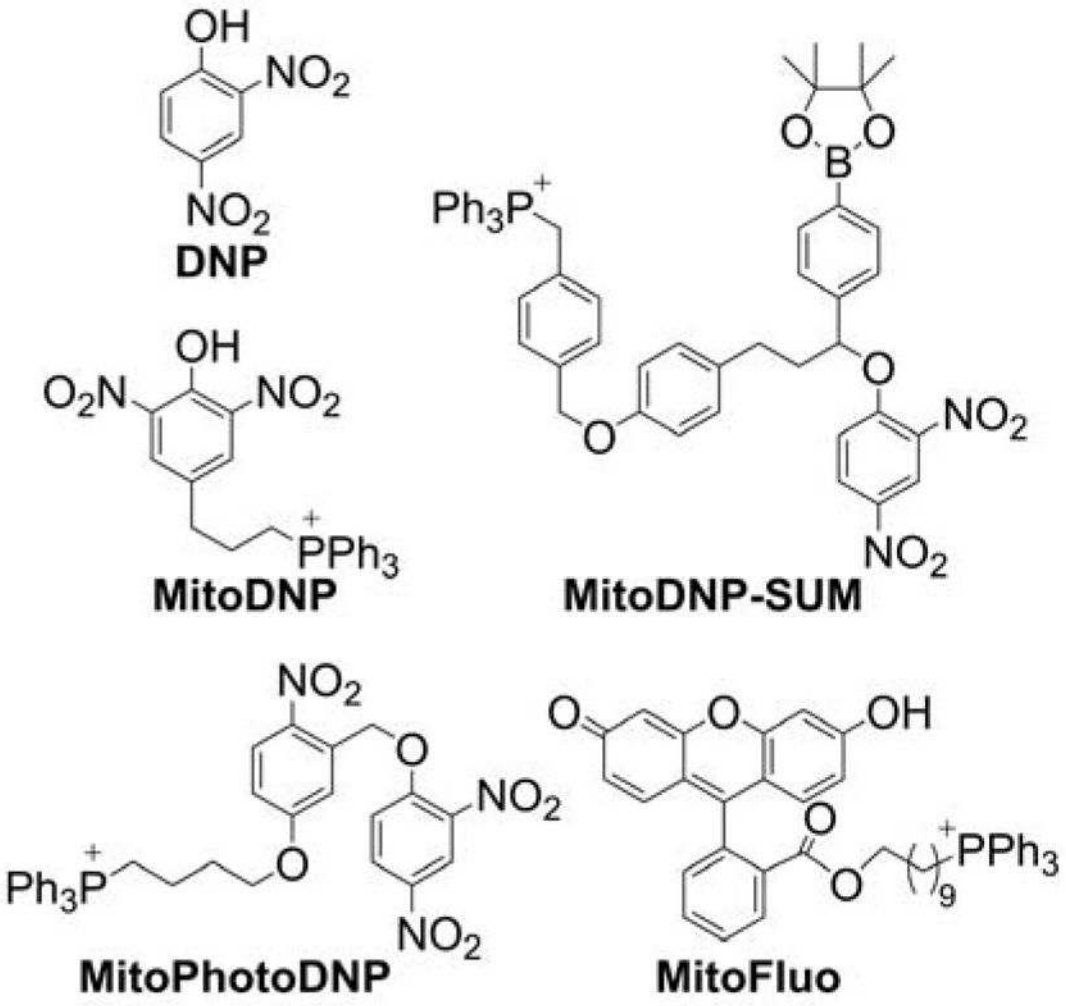

Chart 64.
Mitochondria-Targeted Uncouplers and "Caged" Uncouplers

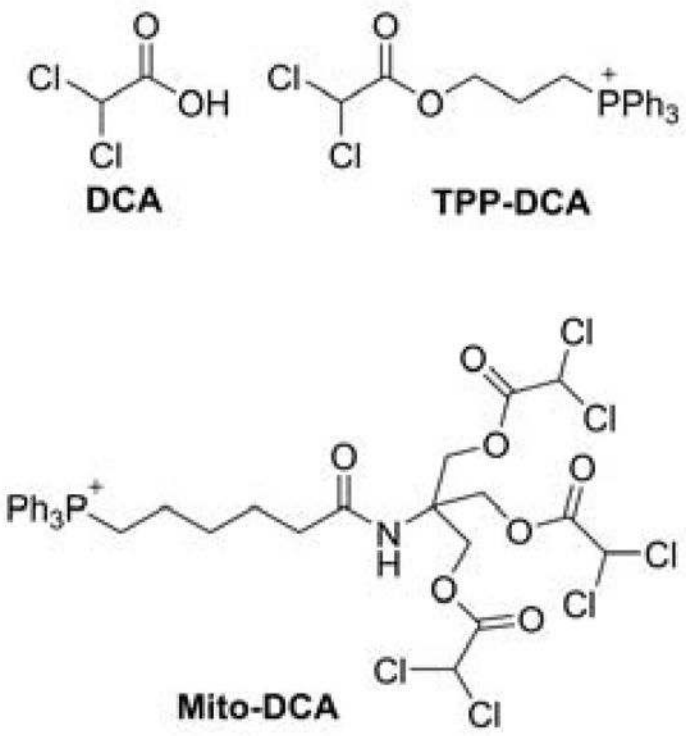

Chart 65.
DCA and Mitochondria-Targeted Analogs

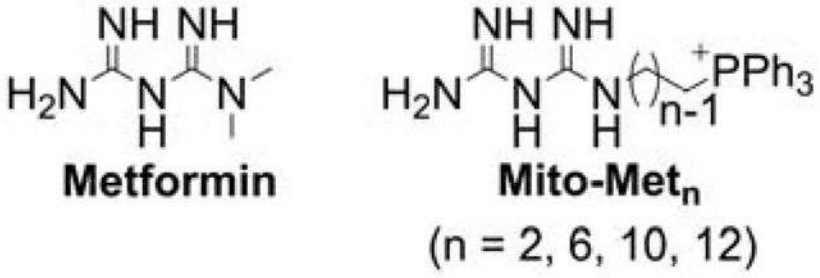

Chart 66.
Metformin and Mito-Metformins

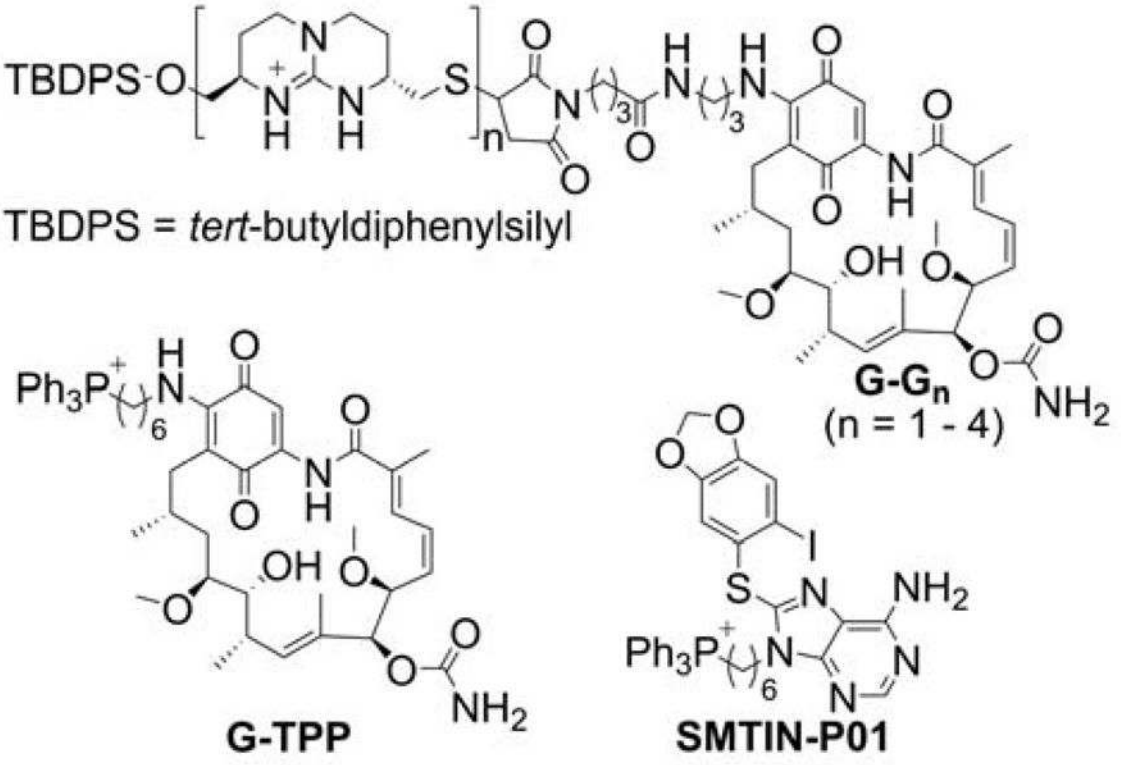

Chart 67.
Mitochondria-Targeted Hsp90 Inhibitors

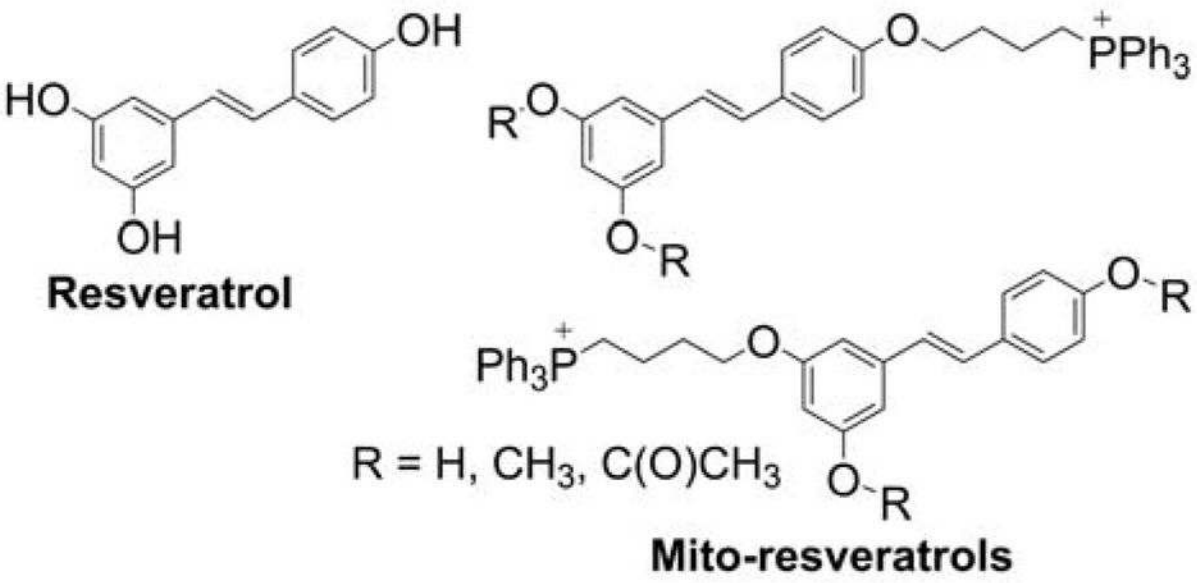

Chart 68.
Mitochondria-Targeted Resveratrols

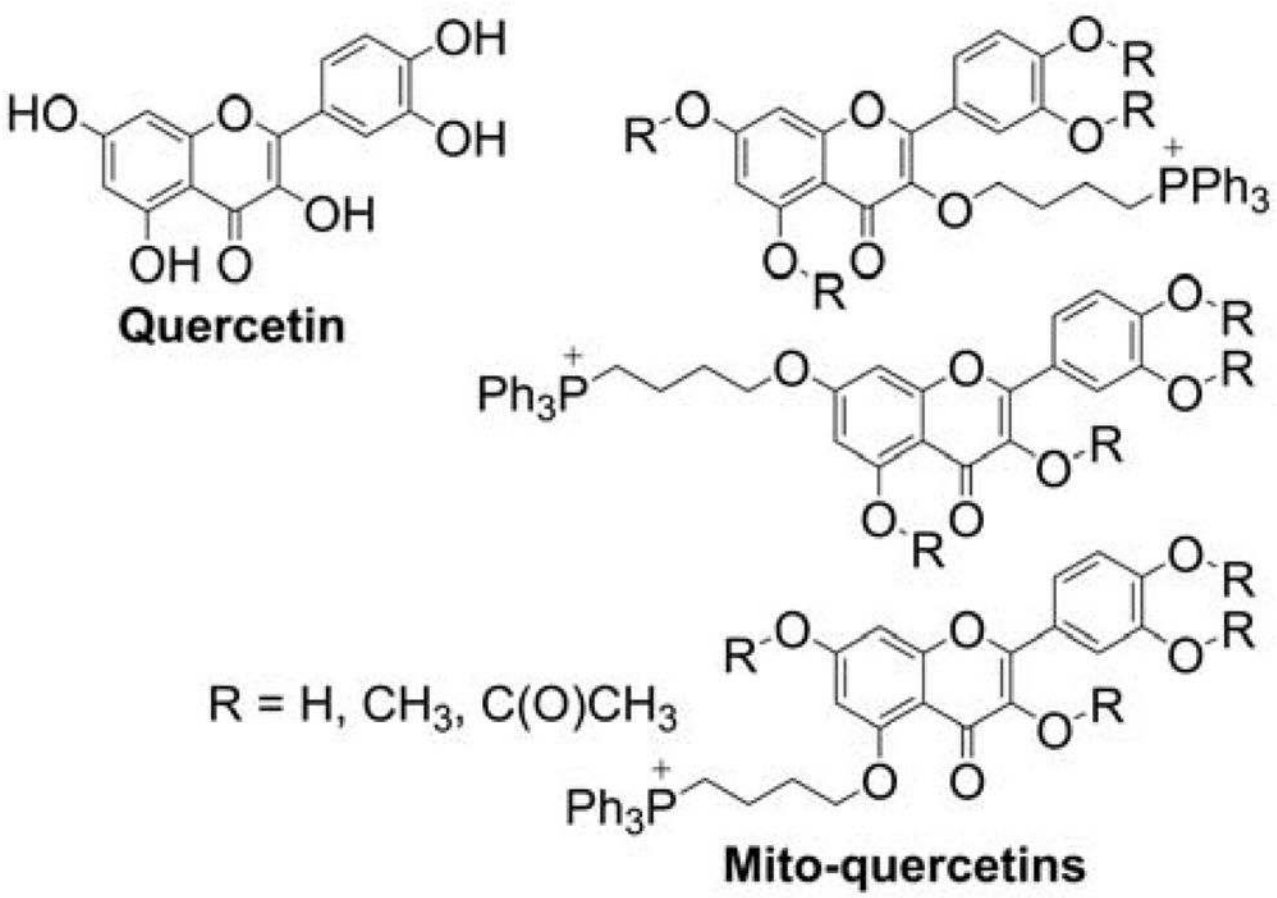

Chart 69.
Mitochondria-Targeted Quercetins

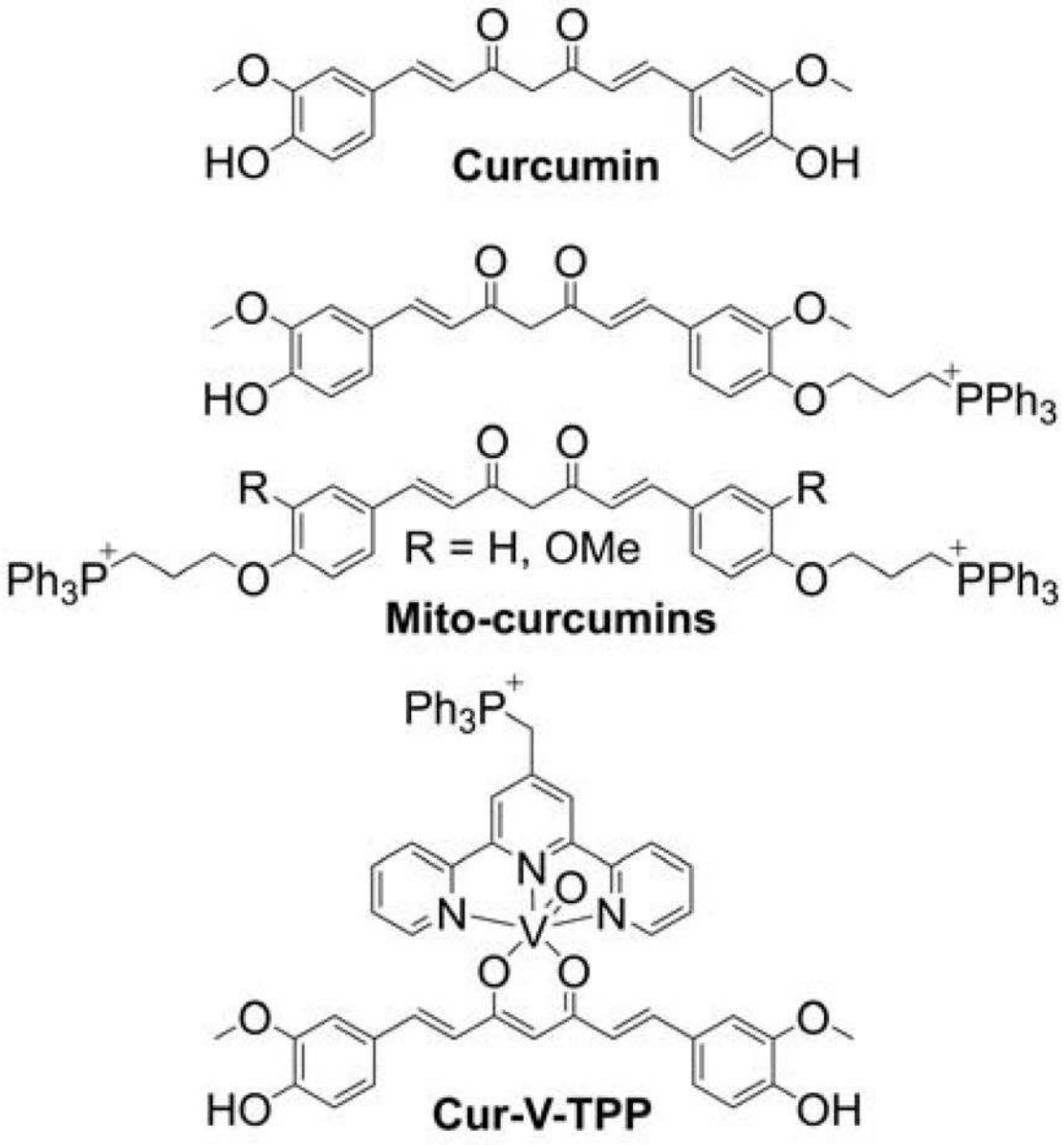

Chart 70.
Mitochondria-Targeted Derivatives of Curcumin

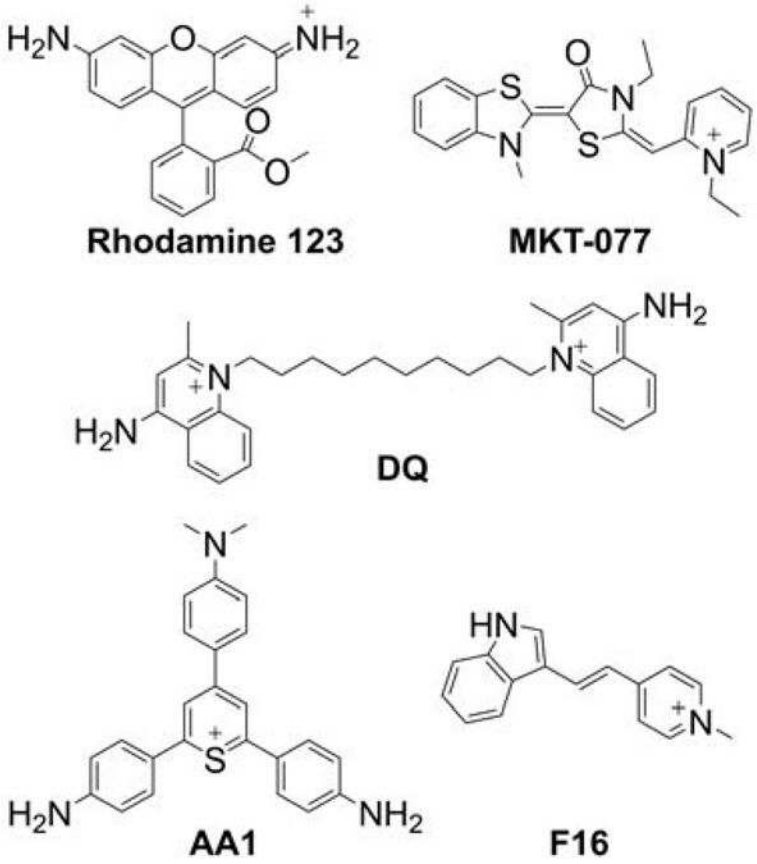

Chart 71.

Examples of Lipophilic Cationic Compounds Exhibiting Anticancer Effects (Rh-123, MKT-077, Dequalinium, AA1, F16)

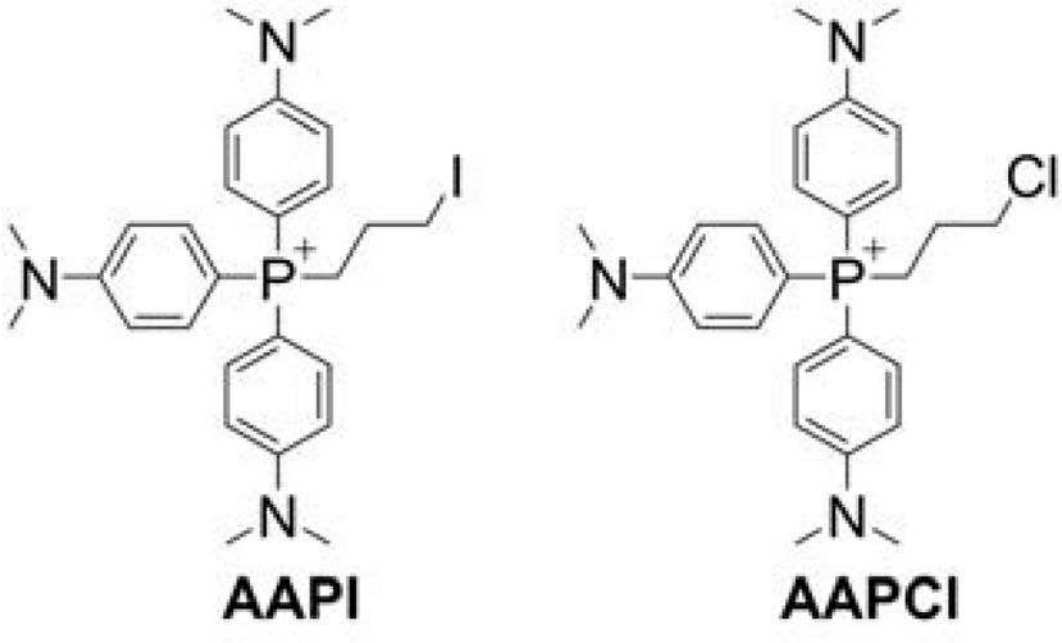

Chart 72.
Structure of APPCL and APPI Compounds

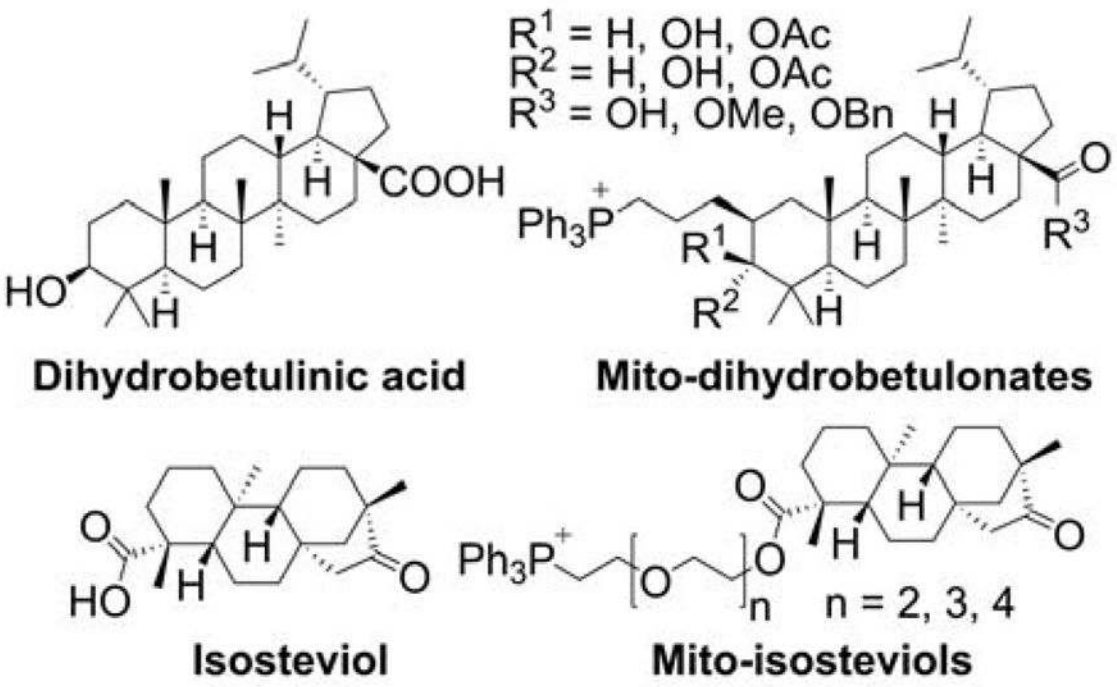

Chart 73.
Mitochondria-Targeted Terpenoids

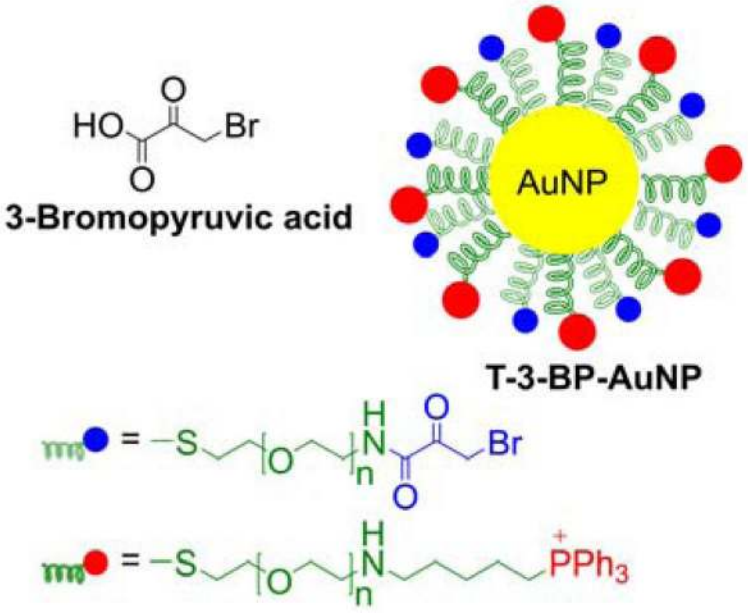

Chart 74.
3-Bromopyruvate (Free and in TPP^+-Nanoparticles)

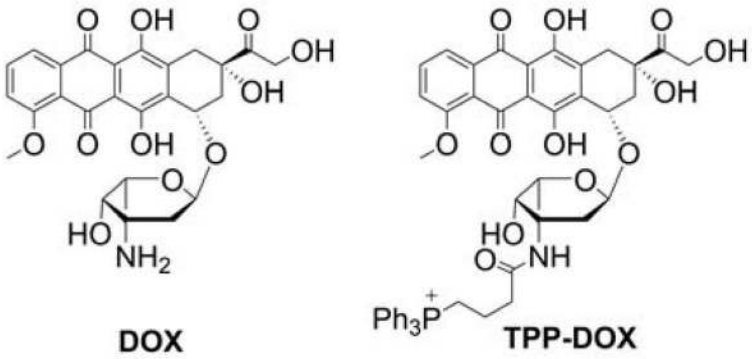

Chart 75.
DOX and TPP-DOX

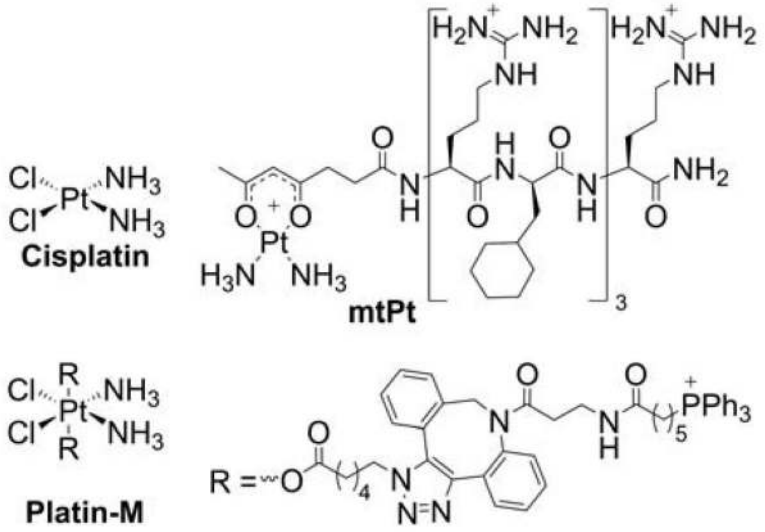

Chart 76.
Cisplatin and Its Mitochondria-Targeted Analogs

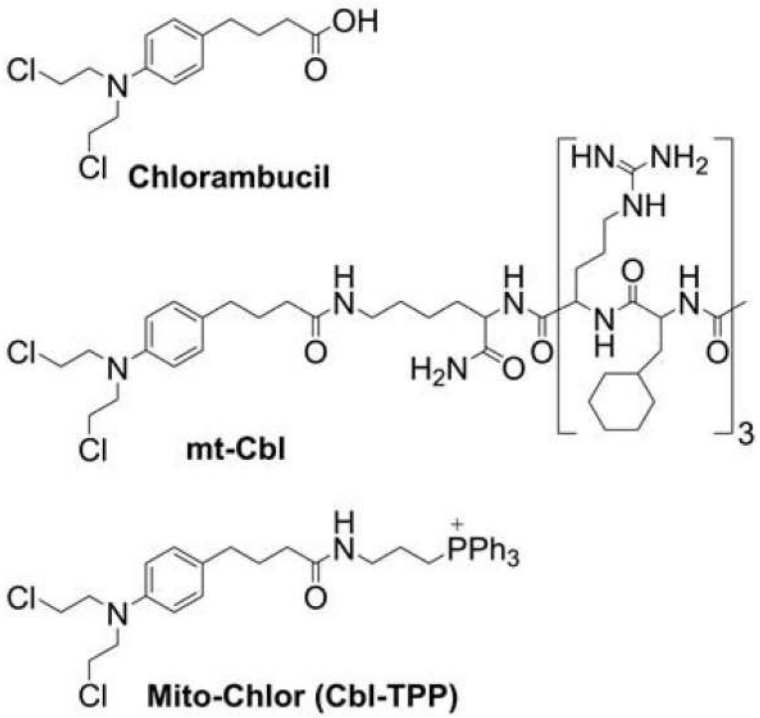

Chart 77.
Chlorambucil and Mitochondria-Targeted Analogs

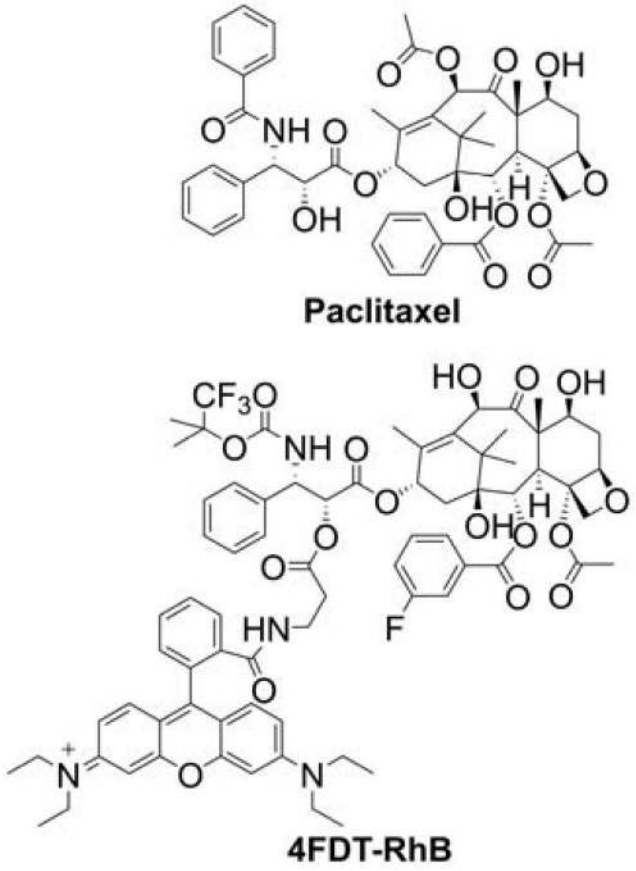

Chart 78.
Paclitaxel and Mitochondria-Targeted Analog

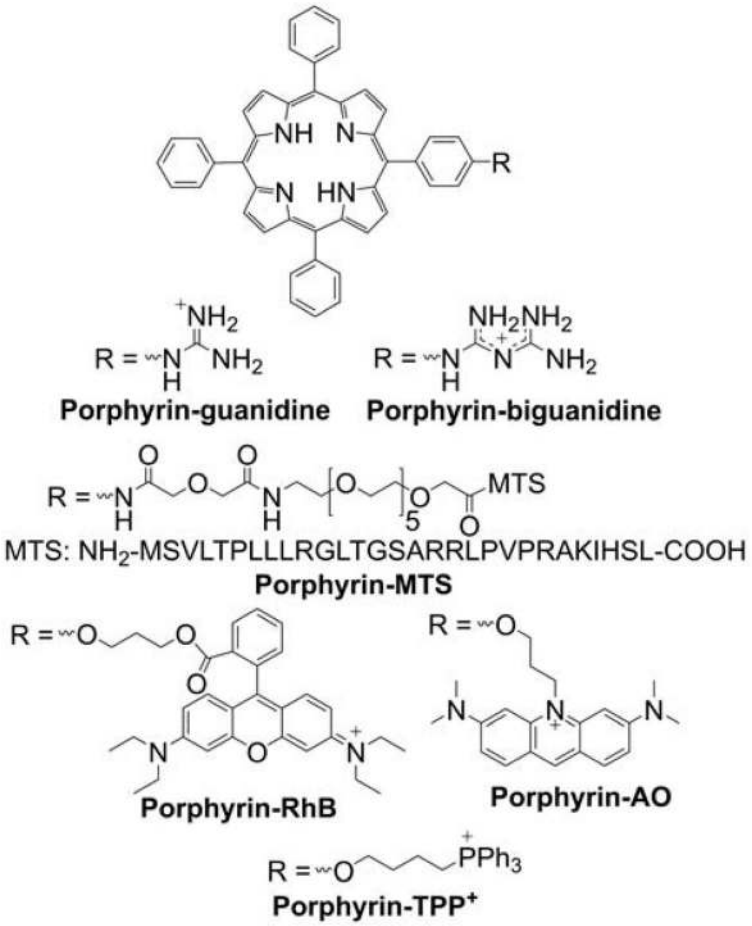

Chart 79.
Targeting Porphyrin-Based Photosensitizers to Mitochondria

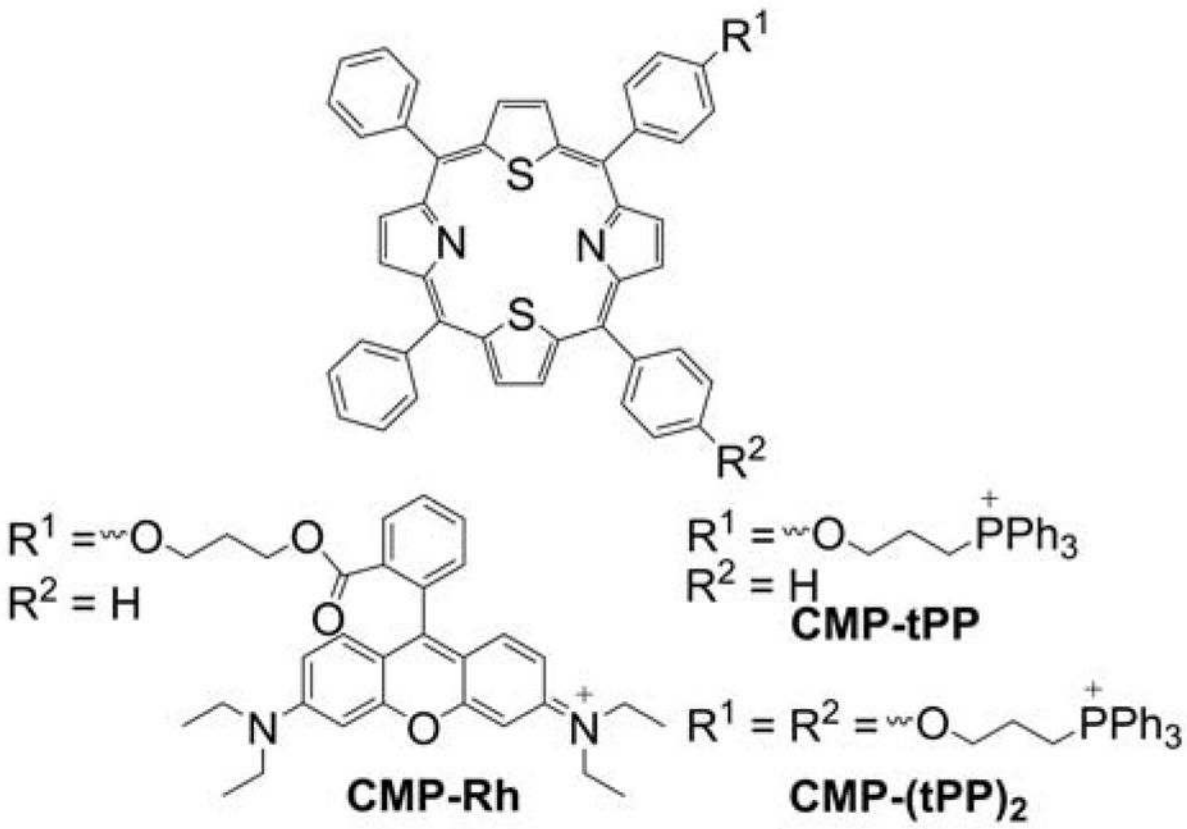

Chart 80.
Targeting Dithiaporphyrin-Based Photosensitizers to Mitochondria

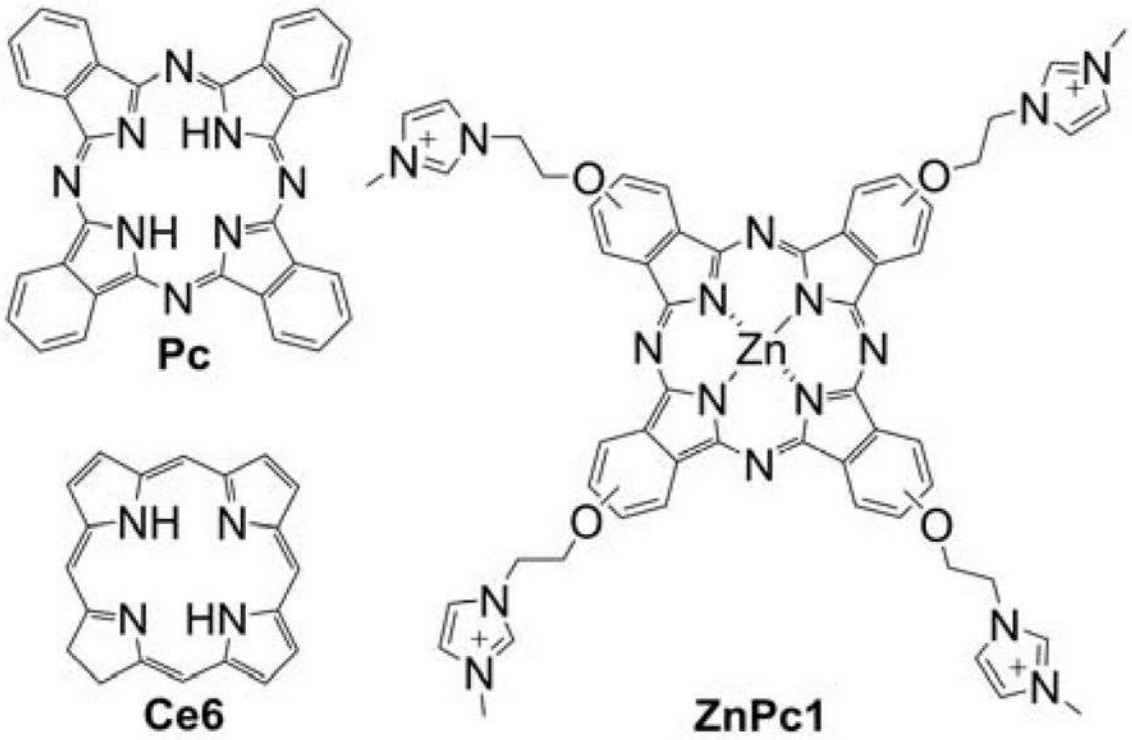

Chart 81.
Pc, Ce6, and ZnPc1 Photosensitizers

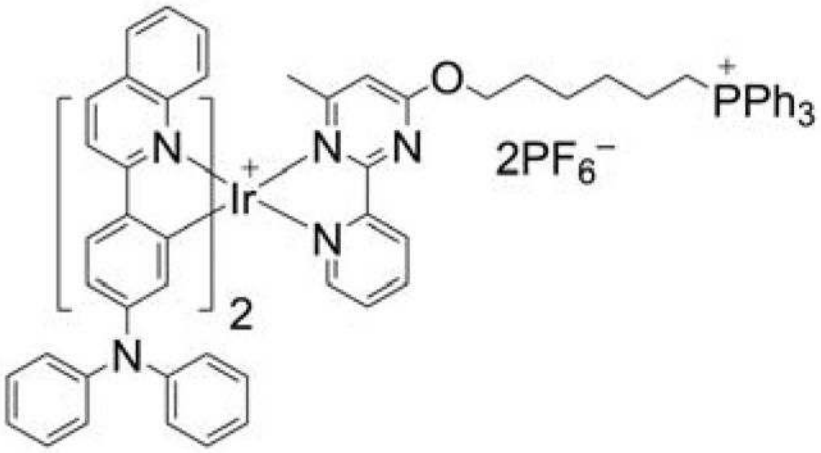

Chart 82.
Iridium-Based TPP^{+}-Linked Photosensitizer

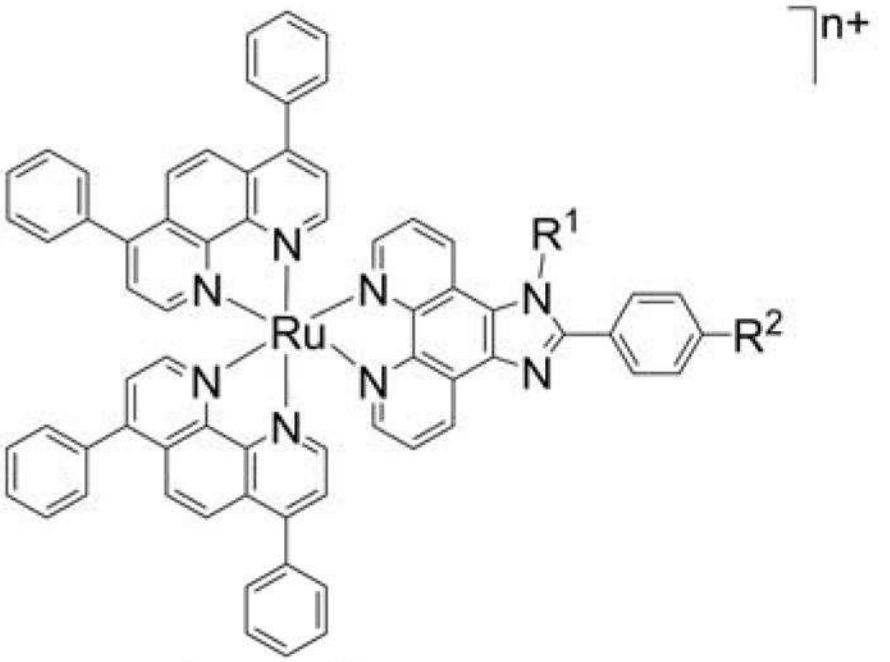

RuL1: R^1 = H; R^2 = H; n = 2
RuL2: R^1 = Ph; R^2 = H; n = 2
RuL3: R^1 = Ph; R^2 = $-CH_2-{}^+PPh_3$; n = 3
RuL4: R^1 = Ph; R^2 = $-O-(CH_2)_4-{}^+PPh_3$; n = 3

Chart 83.
Ruthenium-Based Photosensitizers

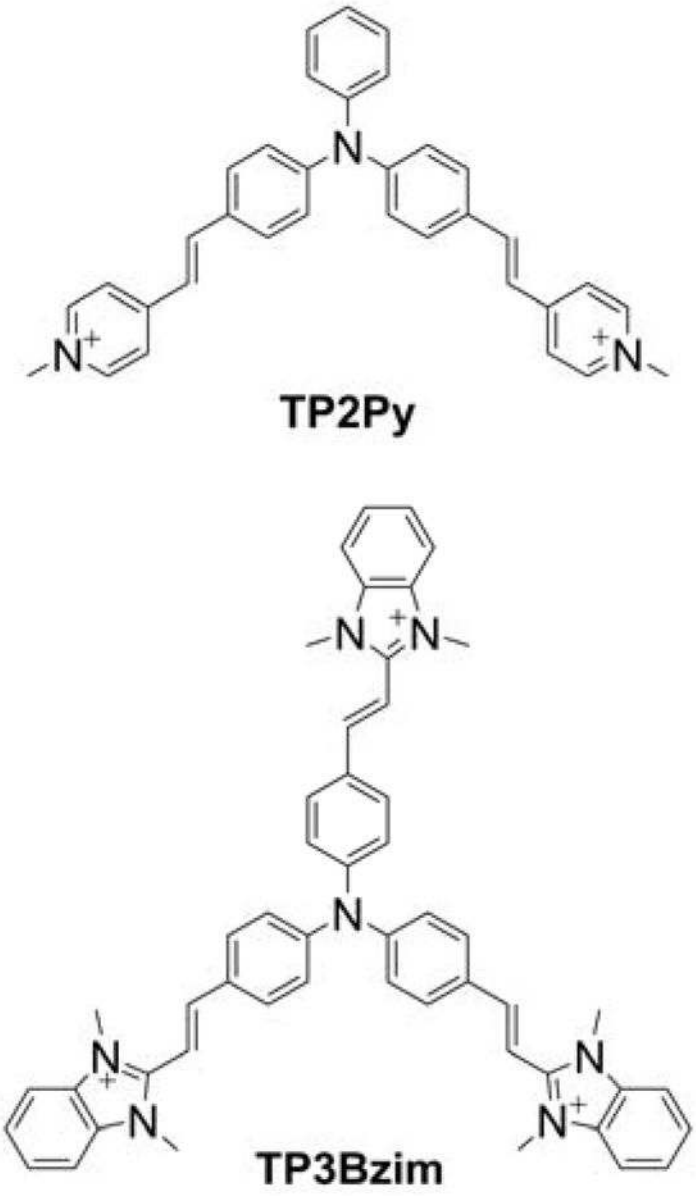

Chart 84.
Triphenylamine-Based Mitochondria-Targeted Photosensitizers

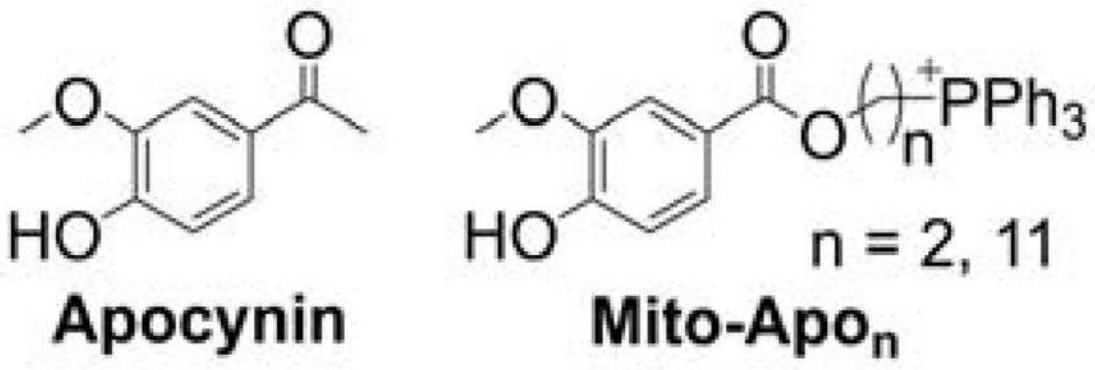

Chart 85.
Mitochondria-Targeted Apocynin Analogs

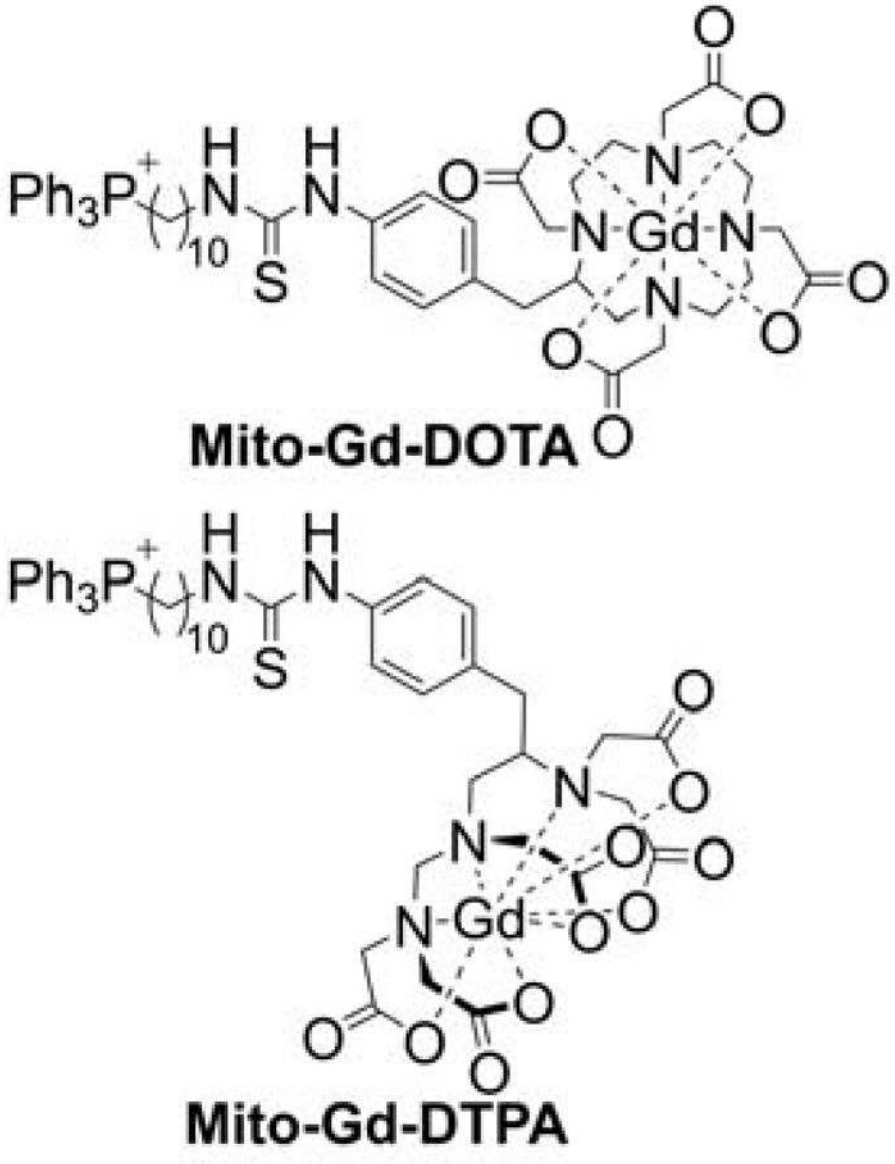

Chart 86.
Structures of Mito-Gd(III)-DOTA and Mito-Gd(III)-DTPA

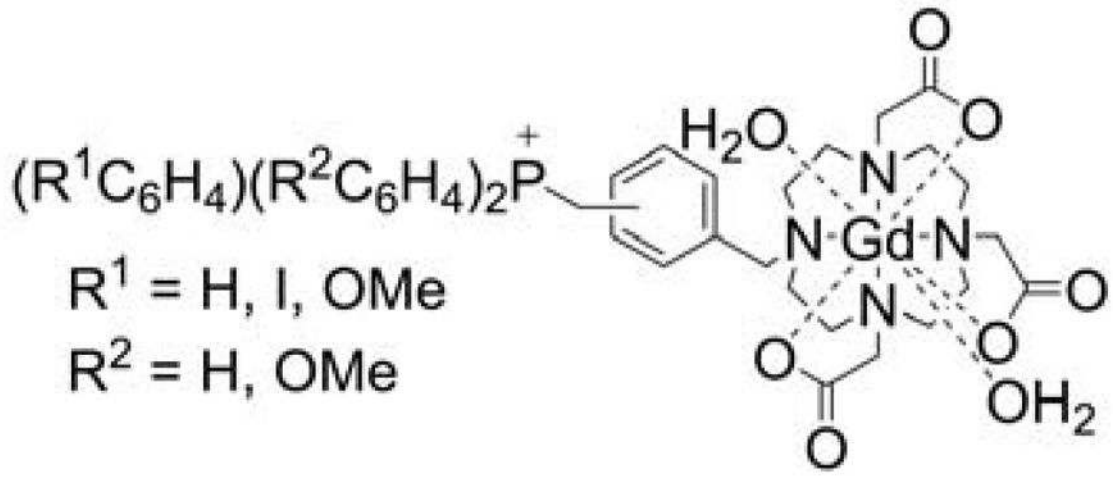

Chart 87.
Mitochondria-Targeted Gd-Based MRI Contrast Agents Carrying Arylphosphonium Cations

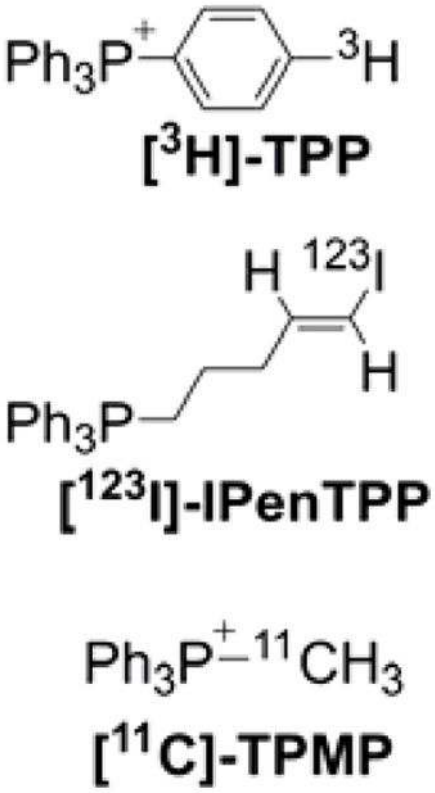

Chart 88.
Radiolabeled Triphenylphosphonium Cations for Imaging Applications

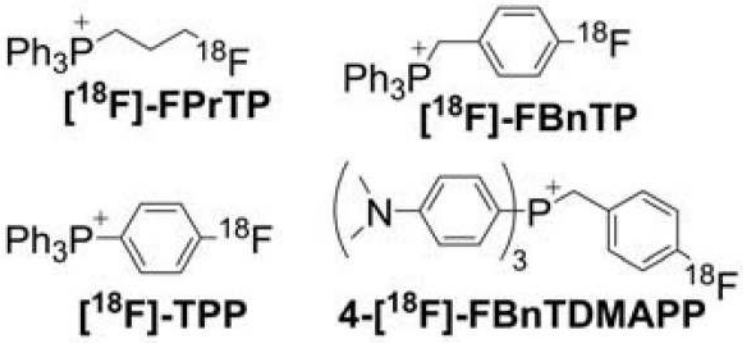

Chart 89.
^{18}F-labeled Triphenylphosphonium Cations for Imaging Applications

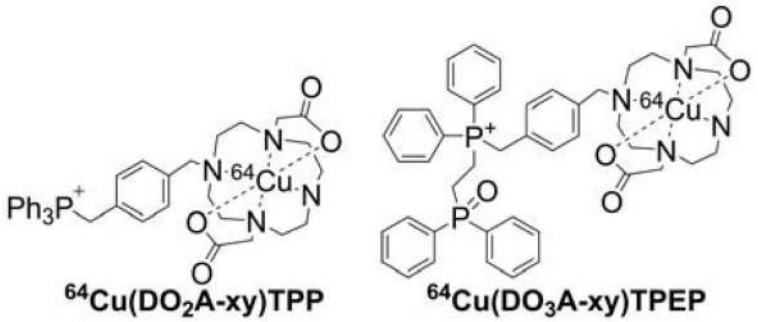

Chart 90.
^{64}Cu-Labeled Mitochondria-Targeted Imaging Agents

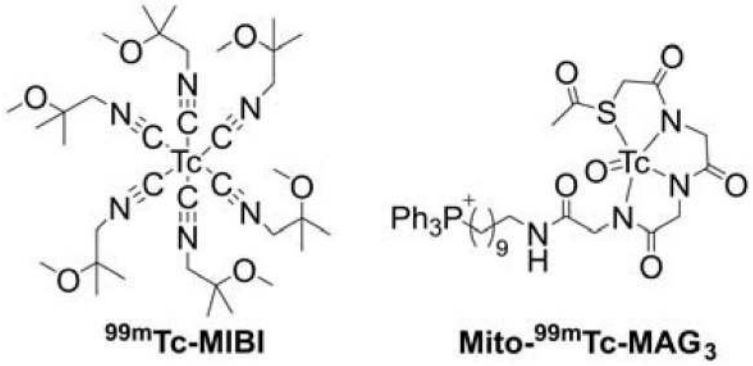

Chart 91.
^{99m}Tc-Labeled Mitochondria-Targeted Imaging Agents

Table 1

Selected granted US patents, demonstrating various applications of TPP^+-linked mitochondria targeted agents, ordered by priority date.

Priority date (YYYY-MM-DD)	Patent title and number	Compound *(see* Figure 2)
1997-11-25	Mitochondrially targeted antioxidants (US 7232809)	Mito-Quinone, Mito-Vitamin E
1998-11-25	Mitochondrially targeted antioxidants (US 6331532)	Mito-Quinone, Mito-Vitamin E
2002-08-12	Mitochondrially targeted antioxidants (US 6984636, US 7109189)	Mito-Ebselen
2003-08-22	Mitoquinone derivatives used as mitochondrially targeted antioxidants (US 7888334)	Mito-Quinone
2006-09-28	Nitric oxide donors (US 9045505)	Mito-SNO
2007-09-10	Mitochondria-targeted anti-tumor agents (US 08466140)	Mito-Geldamycin
2008-02-22	In vivo mitochondrial labeling using positively-charged nitroxide enhanced and gadolinium chelate enhanced magnetic resonance imaging (US 8388936)	Mito-CarboxyProxyl Mito-Gd-DOTA
2008-02-29	^{99m}Tc-labeled triphenylphosphonium derivative contrasting agents and molecular probes for early detection and imaging of breast tumors (US 8388931)	Mito-^{99m}Tc-MAG3
2009-04-27	Neuroprotective compounds and their use (US 89626002)	Mito-Apocynin
2009-09-04	Mitochondria targeted cationic anti-oxidant compounds for prevention, therapy or treatment of hyper-proliferative disease, neoplasias and cancers (US 8466130)	Mito-Tempol
2009-11-20	Organ cold storage composition and methods of use (US 9258995)	Mito-Quinone

Table 2

Clinical trials including TPP^+-linked compounds reported in the ClinicalTrials.gov database.

	Trial title	Condition	Compound	ClinicalTrials.gov identifier	Status
1	A Trial of MitoQ for the Treatment of People With Parkinson's Disease	Parkinson's Disease	MitoQ	NCT00329056	Completed
2	Trial of MitoQ for Raised Liver Enzymes Due to Hepatitis C	Chronic Hepatitis C	MitoQ	NCT00433108	Completed
3	A Clinical Study to Assess the Safety and Efficacy of an Ophthalmic Solution (SkQ1) in the Treatment of Dry Eye Syndrome	Keratoconjunctivitis Sicca	SkQ1	NCT02121301	Completed
4	A Study to Compare MitoQ and Placebo to Treat Non-alcoholic Fatty Liver Disease (NAFLD) (MARVEL)	Non-alcoholic Fatty Liver Disease	MitoQ	NCT01167088	Terminated
5	The Efficacy of Oral Mitoquinone (MitoQ) Supplementation for Improving Physiological in Middle-aged and Older Adults	Aging	MitoQ	NCT02597023	Recruiting
6	Vascular Function in Health and Disease	Chronic Obstructive Pulmonary Disease; Pulmonary Artery; Hypertension; Heart Failure; Hypertension	MitoQ	NCT02966665	Recruiting
7	Mitochondrial Oxidative Stress and Vascular Health in Chronic Kidney Disease	Chronic Kidney Disease	MitoQ	NCT02364648	Not Yet Recruiting